An innovative assessment of the dynamics of facial movements in surgically managed Unilateral Cleft Lip using 4D imaging

Shyam Gattani B.D.S., M.P.H.

Submitted in fulfilment of the requirement for the degree of Doctor of Philosophy

Glasgow Dental School, College of Medical, Veterinary and Life Sciences

University of Glasgow

January 2020

To my parents for always loving and supporting me. There wasn't a "how to be good parents" book in the world that could have prepared you for what was to come, but you still stood by me, no matter the eccentricity.

Summary

Introduction

Verbal and non-verbal facial expressions form an integral part of everyday social interactions among human beings. Facial expressions may be distorted and asymmetric in conditions like craniofacial anomalies, trauma and facial palsy. Cleft lip and palate is one such craniofacial anomaly, that is managed surgically early in life by means of cleft lip repair surgery, nasal reconstruction and lip revision procedures. The goal of surgical repair is to ensure the renewal of optimum form and function in these patients. Despite these surgical procedures, a certain degree of asymmetry persists in patients, which result in decreased aesthetics and function in areas associated with the poorly approximated muscle bundle or due to scar tissue around the surgically corrected muscle group. This asymmetry that ensues after surgery, affects the performance of facial expressions. It is important to quantify facial movement and facial expressions in an objective fashion, in order to be able to assess the effectiveness of surgery and decide on the need for further revision surgery. A lot of work on quantification of facial movements in cleft lip and palate patients has been carried out previously using 2D and 3D imaging modalities. 2D imaging systems do not analyse the depth of images and therefore these methods lose out on an important dimension of facial morphology that needs to be assessed. 3D systems analyse the depth of images but are unable to assess the moving face (the fourth dimension) and only quantify facial movement on still or static images (3D). The human face is rarely static in day to day life and therefore measurement of facial expressions requires that facial expressions be recorded in a dynamic way in such a way that the speed, magnitude and pattern of facial movement be recorded. Each facial expression has specific muscle groups that undergo contraction and relaxation in different phases of the movement starting from rest to peak expression and final resting position. Some of these muscle groups are surgically corrected or re-approximated during cleft lip repair whereas other muscles are relatively or completely untouched. It is therefore necessary to analyse the entire movement sequence for asymmetry as this will highlight which specific muscle groups are associated with high asymmetry scores during the movement, thereby enabling the surgeon to plan on revision procedures accordingly.

Furthermore, it is also essential that the entire facial topography be assessed. A lot of the previous work done on quantifying facial movement and assessing facial asymmetry

used individual landmarks on the face and measured the displacement of these landmarks as asymmetry scores. The disadvantage of using individual landmarks is that the remaining facial surface is not taken into consideration and therefore results obtained may not be representative of the entire facial structure. The novelty in this study is that it used a generic face mesh which undergoes elastic deformation in a process called 'conformation' in order to resemble the patient's facial morphology. This conformed face mesh is then used to assess and quantify facial movement and measure facial asymmetry. This study therefore assesses the facial surface in its entirety along with analyzing asymmetry on a moving or dynamically changing facial surface. Colour maps were used to understand the directionality of facial asymmetry and asymmetry was seen in all three spatial planes- the x, y and z directions.

Objective

To characterise and assess facial asymmetry during four facial expressions- maximum smile, cheek puff, lip purse and grimace, in patients with surgically managed Unilateral Cleft Lip (UCL), using a real time 3D imaging (Di4D) system, and compare these with asymmetry that is seen in an age and sex matched control group.

Design

Prospective two cohort comparative study. 25 surgically managed UCL cases and 75 controls at 8-10 years of age were recruited.

Methods

Facial movements during each of the four expressions were recorded using stereo-photogrammetry at a rate of 60 3D facial images per second. Each expression took approximately 3 seconds and generated 180 3D facial images for the analysis. A generic facial mesh which consists of more than 7000 quasi landmarks, was used for the assessment of facial asymmetry. This was wrapped (conformed) on the 3D image, the conformed mesh was mirror imaged, the original and mirror images were superimposed and the distances between the corresponding landmarks of the original and mirrored images of the five selected frames quantified facial asymmetry.

Results

Statistically significant differences were seen regarding the magnitude of facial asymmetry between the UCL group and the non-cleft controls in all four facial expressions.

In *maximum smile*, asymmetry was prominent in the nasal regions- the nasal tip and alar regions as well as the upper lip vermillion border, the philtrum and columella. Higher average asymmetry in the UCL group in the total face was seen in the 3D frame mid-way between maximum smile and rest (frame 4) followed by the frame at peak expression of maximum smile (frame 3).

In *cheek puff*, asymmetry in the total face was seen most pronounced in frame 2 as the face was moving into the phase of peak facial expression. In the X direction, asymmetry was most noted in the alar regions and philtrum and upper lip regions. Vertical asymmetries were minimal. Anteroposterior asymmetry was most noted in frame 2 in areas around the ala of the nose and upper lip vermillion and philtrum.

In *lip purse*, asymmetry in the UCL group was seen to be higher in the peak frame (frame 3) followed by frame 4 and 2 for the total face. Asymmetry in the total face was most pronounced in the alar regions of the nose, the philtrum and upper lip vermillion border.

In *grimace*, asymmetry in the UCL group was seen to be higher in the mid-way frame (frame 2-mid-way between initial resting frame and peak expression of cheek puff) followed by frame 3 for the total face.

Vertical asymmetries were seen to be minimal in all facial expressions except in the case of lip purse. The nasolabial region showed maximum asymmetry during facial movement.

Conclusion

This study provides a sensitive and innovative tool to assess and quantify the dynamics of facial muscle movement, which correspondingly highlights the anatomical areas of residual asymmetry. This further enables surgeons to understand where the deficiency exists and accordingly plan revision procedures to improve facial symmetry and therefore optimally revive facial form and function. This thesis identifies the limitations and inability of primary lip repair to bring about symmetrical outcomes and helps understand the modifications and refinements required during cleft lip repair which ultimately

improves the quality and efficacy of the surgery and the quality of life in patients with cleft lip and palate.

Contents

List of Appendices

List of Tables

List of Figures

ACKNOWLEDGEMENTS

"Nothing in life is to be feared, it is only to be understood. Now is the time to understand more, so that we may fear less"- Marie Curie.

Undertaking this PhD has truly been a life changing experience for me. The past 4 years have seen me grow immensely as an individual and researcher, and the curiosity that resides within me has only increased by multitudes and further inspires me to delve in to the depths of surgery and science, and ultimately, in my own little way, make the world a better place to live in, for the generations to come.

At the outset, I would like to graciously mention that this PhD would not have been possible, but for the immense support, encouragement, guidance and patience of my principal supervisor Professor Ashraf Ayoub. He inspires me in ways no one else has and will always continue to be a guiding light of knowledge in my life. I could not have asked for a better mentor than him.

My most sincere gratitude and thanks goes out to my co-supervisors, Dr Xiangyang Ju, for his remarkable and boundless knowledge in the field of medical analytics and software- his constructive feedbacks and endless patience and belief in me kept me going through some of the hardest moments during my PhD; Dr Aileen Bell for her constant feedback and assurance that I was going in the right direction and helping me achieve my required recruitment numbers for my study sample, and Mr Toby Gillgrass, for his enthusiastic support and swiftness in helping me with the Cleft Lip patients. This thesis would never have been possible without the guidance and encouragement of these inspiring individuals.

I would also like to express my sincere thanks to Mr Neil Nairn, who constantly kept making me see the light at the end of a long tunnel and was always around for all the support I could have ever asked for during some of the hardest moments in my tenure as a PhD student.

A grateful word of thanks also goes to Sandy, in the clinical photography department, for her input and experience during the 4D imaging sessions. Her lively words of encouragement and expertise in imaging helped me immensely in the course of my project.

I would like to express my gratefulness and sincere thanks to Dr Andrea Sheriff and Dr Alastair Gracie- their inputs and guidance during the entire period of my PhD helped me tremendously.

It is said that the hardships and obstacles encountered during a PhD can only be truly understood and relatable by your fellow colleagues. My heart filled thanks and gratitude goes out to my fellow colleagues Mahmoud Amir Alagha, Jamie Kidd and Noura Al-OTaibi. Their constructive criticisms, endless assurances, and simply just being around, meant that I could have peace of mind and could relate to someone during this journey.

No amount of gratitude and thanks is ever enough for my wonderful parents who watched me and comforted me from several thousand miles away during my PhD. My mother and father have been my pillars of strength, as they have always been throughout my career. Their sacrifice and support have been unparalleled and without their presence, my writing this thesis and going through this extra-ordinary journey would never have been possible.

A huge thanks to my family, my constant support and well-wishers who always ensured that they had my back throughout this project.

There are so many more individuals I feel I need to thank and am probably missing out on. I would not have done this without the help and support of each of these people. Time and space however, compels me to end my expression of thanks with a quote my father always reiterated- one that I reminded myself of, during this journey- “Impossible is just a big word thrown around by small men who find it easier to live in the world they've been given than to explore the power they have to change it. Impossible is not a fact. It's an opinion. Impossible is not a declaration. It's a dare. Impossible is potential. Impossible is temporary. Impossible is nothing”- Muhammad Ali.

Thank you one and all.

Shyam Gattani

Author's Declaration

I declare that, except where explicit reference is made to the contribution of others, this thesis is the result of my own work and has not been submitted for any other degree at the University of Glasgow or any other institution.

Signature

Printed name: Shyam Gattani

January 2020

List of abbreviations

CL/P	Cleft Lip and Palate
CLP	Cleft Lip and Palate
CL	Cleft Lip
CLA	Cleft Lip and Alveolus
CPO	Cleft Palate Only
IUCLP	Unilateral Incomplete Cleft Lip and Palate
UCLP	Unilateral complete Cleft Lip and Palate
IBCLP	Incomplete Bilateral Cleft Lip and Palate
BCLP	Bilateral complete Cleft Lip and Palate
UK	United Kingdom
EUROCAT	European Central Registry for Congenital Malformations at birth
LLS	Levator Labii Superioris
LLSAN	Levator Labii Superioris Alaeque Nasi
3D-CT	Three-Dimensional Computerized Tomography
UCL	Unilateral Cleft Lip
NAM	Naso-Alveolar Moulding
2D	Two Dimensional
3D	Three Dimensional
4D	Four Dimensional

CT	Computerized Tomography
CBCT	Cone Beam Computerized Tomography
MRI	Magnetic Resonance Imaging
TMJ	Temporomandibular Joint
Di3D	Dimensional Imaging three dimensions
Di4D	Dimensional Imaging four dimensions
ICP	Iterative Closest Point algorithm
PCA	Principal Component Analysis
RSM	Root Square Mean
REC	Research Ethics Committee
NHS	National Health Service
R&D	Research and Development
PC	Personal Computer

***Abbreviations for landmarks are defined in the respective chapter**

1 Background

Contents

1.1. Importance of facial expressions:

Social interactions depend on a variety of factors. Facial expression is one of the most important social interactions in human beings. Non-verbal expression has an equally important significance in day-to day interactions as do verbal expressions (De Gelder, 2009). Human beings communicate with each other through a variety of verbal and non-verbal expressions. Facial expressions can be distorted due to craniofacial anomaly, trauma, facial palsy and mental disorder.

Charles Darwin paved the way for research on facial expressions and the psychology of facial expressions through pioneering work in 'The Expression of the Emotions in Man and Animals' and 'The Descent of Man'. Darwin through his works looked at emotion as distinct entities and in doing so, focused on the human face in particular. Facial expressions are potentially the richest data bank of emotional information in human beings (Ekman, 2009). Darwin emphasised on the fact that the morphology of facial expressions provided vital information on the type of emotion being expressed. Ekman through his works stated that the intensity of muscular contractions occurring during facial expressions represent the intensity of emotion and not the type of emotion being expressed (Ekman,2009). Ekman further stated that facial expressions represent a phase of movement of muscles from rest to maximum or peak or the apex of contraction of the muscles and back to rest and any time slice during that apex holds information on the type of emotion being expressed (Ekman,2009).

Another important contribution of Darwin to the field of facial expressions was his claim that facial expressions were universal and facial gestures were culture-specific (for example specific movements in the face can mean one thing in certain cultures and an entirely different thing in a different culture). This universality of facial expressions was studied in depth in recent research by Ekman (1972,1973) and Izard (1971) where in it was concluded that there was cross-cultural agreement in emotions shown by human beings by means of facial movement.

Darwin also went on to explain through his works why certain facial expressions expressed particular emotions. The concept of 'serviceable habits' was mentioned

wherein it was stated that certain expressions evolved as a result of habits through life stages and an inherent tendency to perform those expressions with an intent to serve a purpose, for example exposing canine teeth to show that harm is intended as well as preparing for an attack (Ekman, 2009). Darwin through his aforementioned works delved not only into the psychology of facial expressions but also laid focus on not just the changes in facial appearance but also the muscular changes that were responsible for them. He focused on the anatomy of facial muscles and thereby the anatomic changes during each facial expression which eventually paved the path for future research on measurement of facial expressions (which Darwin himself did not focus on) including the facial action coding system or the FACS (Ekman & Friesen, 1978).

It was seen through various previous research work that facial expressions can relay information on different social entities such as identity (Gauthier et al., 1999) and attractiveness (Perrett et al., 1998) among several others. The face and the movement of its various muscles (non-verbal expressions) are crucial in understanding emotion, social context and mood. The face may be thought of as containing several different dimensions which are variable such as morphology, movement and skin colour or complexion (Jack & Schyns, 2017).

Cleft lip and palate (CL/P) is a craniofacial anomaly that is managed by means of surgical interventions including cleft lip repairs, nasal reconstruction and revision procedures. In spite of these surgical interventions, a certain level of asymmetry still persists (Seaward et al., 2015). The residual asymmetry results from the formed scar tissue, muscular pull, and relatively thinner tissues at the surgical site (Otero et al., 2012). In addition to the static facial asymmetry, the distorted facial movements after the surgical repair of cleft lip have a profound psychosocial impact on patients (Shaw et al., 1985). It was seen in previous work by Nicholls et al. (2019) that public speaking, being photographed and participation in school activities were prime areas wherein children affected by cleft lip and palate faced difficulties. Comments by children and adolescents who were treated for cleft lip and palate were associated with the impact on public speaking like “people struggle to understand me,” “too anxious,” “people stare at my scar,” and “it terrifies me” (Nicholls et al., 2019). It was also seen that higher incidences of

teasing was reported in adolescents and adults with cleft lip and palate than in children (Nicholls et al.,2019).

In this era of a high-pressured celebrity culture, where appearance is considered as a gateway to social acceptance, even minor asymmetries on the face are associated with negative social responses such as unwarranted staring and isolation at school and among peers (Bradbury, 2012). This ultimately leads to a sense of shame, anxiety, depression and more importantly a lack of ego development in the affected children (Bradbury & Hewison, 1994). Patients with clefts may experience cases of social exclusion and stigma alongside negative and demotivating responses from others (Rumsay et al., 2004). Surgical repair alters the orientation of facial muscles and the asymmetry that is a consequence of this repair reduces the ability of the facial muscles to perform optimally, and thus affects facial expressions in a direct way. Nasolabial appearance has a special consideration in the surgical repair of Cleft Lip and Palate. Asymmetry in the nasolabial region hinders day to day participation in social life. This was evident in work by Nicholls et al. (2019) wherein children and adolescents reported social situations like “not pretty enough,” “hate having my photo taken,” “I grew a beard to hide my lip scar,” “don’t like my cleft side being photographed,” “lip-shape and messy teeth affect my smile,” “I still get embarrassed because my nose is very crooked and people still look at me and ask what happened?,” “my nose is still crooked after 3 nose jobs and my lip scar is still prominent,” and “don’t like how I look in photos.” The emphasis on the lip scar (in the nasolabial region) in comments by children treated for cleft lip and palate provide evidence that asymmetry and scarring in the nasolabial region has a substantial impact on social interactions. Greater asymmetry was noted in the nasolabial region in children treated for cleft lip and palate (Bughaigis et al., 2014).

It is for this reason that revision procedures of lip scarring are carried out during childhood- to minimize the psychosocial impact caused due to scarring and consequent nasolabial asymmetry (Tan and Pigott, 1993). It was also seen in previous work that people looked at individuals with cleft lip and palate as less popular and facially unattractive, which points towards a huge social stigma and

a tendency to socially exclude (De Sousa et al., 2009). Mixed reports were seen in terms of academic achievement and cleft lip where some research provided evidence that lower academic achievement was seen in cleft patients (Knight et al., 2015) and others showed that having a cleft did not affect academic achievement (Collett et al., 2014).

A lot of prior research work pertaining to facial symmetry evaluation involving clefts and facial dysmorphology uses terminology like 'deformity' or 'abnormality'. It must be emphasised that this refers to the need for surgical correction, as the 'deformity' in such cases leads to severe psychological and physiological issues such as impediments in feeding and speech if left untreated. This is the case with 'severe asymmetry' observed in the face such as in conditions like cleft lips and palate and facial palsy. It must be noted here that deviation from a perfectly symmetric face in healthy individuals is considered natural, as long as this asymmetry is not noticeable.

There is nothing like perfect symmetry in this world. It is a mistake to consider the symmetry of the face sine qua non of its beauty as research has shown that beauty and attractiveness of the face is considered to stem from its inherent tendency to be slightly asymmetric (Zaidel and Cohen, 2005). It should be recognized therefore, that minor asymmetry of the face is considered normal. Mild asymmetry occurs during the normal development of the human face (Ferrario et al., 2001). It has been said that human form is inherently externally symmetrical but internally asymmetrical. This non-equivalence of the right and left half of the face does not result in an aesthetically unpleasant appearance (Ferrario et al., 2001). However, no agreement has been reached regarding the dominant side of the face- the left side of the face was found to be more dominant in some studies (McIntyre & Mossey, 2002) and the right side more dominant in other studies (Farkas & Cheung, 1981; Shaner et al. 2000).

Although previous research has shown minor asymmetry of the face to be normal, there is no consensus regarding the degree, side, and localization of the asymmetry (Ferrario et al., 2001). The consensus regards differences between the

most symmetric and most asymmetric groups also differs in previous works where some say the difference is less than 2.5mm (Ferrario et al., 2001) and others say variability in soft tissue asymmetry in the upper and mid face does not exceed 5mm (Shaner et al., 2000).

1.2. Definition of Cleft Lip and Palate

Cleft Lip and Palate is one of the most common congenital conditions (Vanderas, 1987). Cleft Lip and Palate in layman terms is the vertical fissuring that is characteristic of the upper lips and alveolus. The amount of fissuring shows variation among cases, ranging from an incomplete cleft which may be in the form of a small defect to a complete cleft which extends all the way to the nasal floor.

Clefts of the lip and palate can be subdivided in to the following categories- isolated cleft lip, cleft lip and alveolus, cleft palate only, unilateral incomplete cleft lip and palate, unilateral complete cleft lip and palate, incomplete bilateral cleft lip and palate and bilateral complete cleft lip and palate.

Development of oral structures commence at around week four of pregnancy- a lack of fusion of the primary palate manifests as cleft of the lip and alveolus whereas the secondary palate failing to fuse during the eighth week causes cleft of the palate (Sperber,2001). Embryonic development of facial structures begins in the fourth week in the pharyngeal or branchial arches. The palate development in turn occurs during the sixth week and is the result of the fusion of several palatine processes. Developmental deformities may manifest due to the slightest defects in fusion of various facial structures correspondingly resulting in the development of a cleft.

Orofacial clefts can be classified as syndromic or non-syndromic clefts. Syndromic clefts occur as a result of a mendelian or genetic deformity such as Van der Voude's syndrome and Pierre-Robin syndrome. Non-syndromic clefts do not involve genetic abnormalities.

1.3. Prevalence of Cleft Lip and Palate

Cleft lip and palate as a combined condition is more clinically common than isolated cleft lip and isolated cleft palate (Calzolari et al., 2007). Isolated Cleft lip has a strong male predisposition with the left side being most common as site

of cleft whereas isolated cleft palate was seen to be more predominant in females, possibly due to the fact that the palatine shelves show later closure in females than males (Noorollahian et al., 2015).

The prevalence of Cleft lip and palate globally is 1:700 (WHO, 2003). Higher prevalence, at the rate of 2 per 1000 is seen in Asian populations (Dixon et al., 2011). Lowest prevalence of Cleft lip and palate was seen among African populations (Mossey & Modell, 2012). Racial differences in cleft lip and palate have a genetic basis rather than a geographical or environmental basis (Ching & Chung, 1974).

Cleft Lip and Palate in the UK

In the UK, the incidence of cleft lip and palate is around 650 per year. Cleft Lip and palate incidence accounts for nearly 65% of craniofacial anomalies (William, Shaw & Devlin, 1994). Scotland in particular has a higher predilection of isolated cleft palate among all EUROCAT (European Central Registry for Congenital Malformations at birth) centers (Stone & Dolk,1994). The rest of the UK show a rate of 2:1 with regards cleft lip and palate to cleft palate ratio (Gregg, Boyd & Richardson, 1994).

1.4. Embryogenesis:

Facial morphogenesis occurs during embryological development when facial prominences fuse, grow and develop as a functional craniofacial unit (Brugmann et al., 2006). Craniofacial anomalies result when these developmental units fail to undergo fusion or do not develop and grow harmoniously. This consequently results in asymmetry affecting the face and skull.

Cleft lip and cleft palate (CLP) is a common craniofacial condition that affects 1 in 700 children a year (Thomason and Dixon, 2009). This anomaly occurs when the nasal and maxillary processes fail to fuse during embryological development, in turn leading to an asymmetric muscle pull on the nasal septum during development of the mid face (Hall and Precious, 2013).

The primary palate, which consists of the anterior nasal spine, the columella, the medial part of the upper lip and the premaxilla, is a result of the fusion of the maxillary process and the frontonasal prominence between the 6th and 7th week. The secondary palate, which consists of the hard and soft palate, arises from the maxillary processes which contain two palatine shelves. These palatine shelves develop and grow medially to fuse with each other as well as the primary palate. From an embryological point of view, cleft lip is formed as a result of abnormality in formation of the primary palate. This may go on to further involve the palate resulting in cleft lip and palate. Cleft palate is a result of an abnormality in formation of the secondary palate (Fraser, 1955). Development of the cleft lip and palate has been attributed to three possible theories (Senders et al., 2003). The classic theory states that failure in fusion of maxillary processes and lateral aspect of the medial nasal process during the sixth week results in abnormal development of the upper lip and consequent clefting. The merging theory states that the maxillary and medial nasal processes undergo fusion but there is a lack of mesenchymal penetration to support the fusion, resulting in an epithelial break down causing clefts to develop. The dynamic fusion theory claims that the development of cleft lip and palate occurs due to a hypoplasia of the mesenchymal tissue or due to lack of fusion of the epithelium (Senders et al., 2003).

The main objective for the surgical correction of cleft lip and palate is to reduce the stigma associated with facial appearance. Patients with CLP undergo multiple surgeries, aimed at reconstructing alveolar arch continuity, restoring facial symmetry and most importantly to restore functions of the palate, nose and lips (Talmant, 2006). However, surgery may lead to tissue distortion (scarring and muscle pull) and may even have a negative influence on craniofacial growth

(Kuijper and Long, 2000). This eventually leads to poor facial aesthetics which has a negative psychosocial impact on patients (Mette et al., 2014). Evidence has been presented that facial soft tissue development following surgery is hindered by scarring, muscle pull, nasal changes and thinner tissues around the surgical site (Otero et al., 2012). It has been shown that post-operative cleft scarring is correlated with poor psychological functioning (Millar et al., 2013). CLP is a condition associated with facial asymmetry particularly in the nasolabial regions (Bugaighis et al., 2014). Patients with unilateral cleft lip and palate (UCLP) showed greater asymmetry in vertical planes as compared to non-cleft patients (controls) (Ras et al., 1994).

1.5. Causes of Cleft Lip and Palate

The causes of cleft lip and palate in infants is not well understood but there is a genetic component, synergized by an interaction of a range of environmental and lifestyle factors such as alcohol, diet and smoking (Murray, 2002). Environmental and lifestyle factors include factors experienced by the mother during pregnancy such as food, drink and medications consumed. Genetically, cleft lip and palate occurs as a result of gene interactions (Shaw et al., 1996). Familial studies in the past show that the recurrence rate of orofacial clefting in children of affected parents varies according to various factors such as the cleft type, the severity of the cleft and number of individuals involved.

In recent times, the role of certain supplements such as Folic Acid have come to the forefront in reproductive health as this has shown protective effects on pregnant mothers with regards the birth of healthy babies. O Neil (2008) suggested that intake of folic acid up to 400 microgram a day reduces the incidence of cleft lip by one third. Interestingly, he also found that the lowest incidence of cleft occurred in women with high foliate diets and those who took satisfactory levels of folic acid supplements and multivitamins (O Neil, 2008). Association between environmental risk factors and CL/P such as maternal exposure to tobacco, alcohol, poor nutrition, infection, medicinal drugs and teratogens has been investigated, with maternal smoking and lack of folic acid being consistently linked with the risk of developing clefts (Mossey et al., 2009).

It has been studied previously that the main risk factors for cleft lip and palate are tobacco, alcohol, smoking, folic acid intake, low blood zinc, fever during pregnancy (Molina-Salana et al., 2013). Leite & Koifman (2009) in their study discussed how tobacco smoking during the first trimester was not statistically significant to the onset of orofacial clefting. However, the consumption of alcohol increased the likelihood of acquiring orofacial cleft.

Following are some examples of environmental and lifestyle factors that may predispose to cleft lip and palate:

- Women who are pregnant and smoke during pregnancy have higher chances of bearing a child with a cleft as compared to non-smokers (Little, Cardy and Mungers, 2004).

- Women who are diagnosed with diabetes before pregnancy have higher chances of bearing a baby with cleft as compared to women not diagnosed before pregnancy (Correa et al., 2008).

- Epileptic medication such as Topiramate and Valproic Acid consumed during the first trimester show an increased risk of babies being born with cleft lip and palate (Margulis et al., 2012).

- Maternal intake of alcohol is documented to have a teratogenic effect to the foetus (Ouelette et al., 1977).

- Maternal obesity has also been seen to be associated with higher risk of congenital anomalies (Sebire et al., 2001).

- Use of Folic Acid supplementation and medicine during pregnancy greatly reduces the risk of developmental deformity and neural tube defects (Pitkin, 2007).

1.6. Diagnosis of Cleft Lip and Palate

Diagnosing a congenital malformation requires its detection in the earliest (second trimester) stages of pregnancy. Usually, a transabdominal ultrasound at around 16-20 weeks is performed to rule out the presence of orofacial clefts. Isolated cleft palate poses a more difficult to diagnose situation. The upper lip may be

evaluated through ultrasound. This shows a sensitivity level of 88% in the detection of cleft lip.

1.7. Classification of Cleft Lip and Palate

Cleft lip and palate have several factors playing a role in its development and is etiologically heterogenous. The classification of cleft is crucial as different types of clefts may be associated with a specific genetic basis.

Several classification systems have been formulated and used for cleft lip and palate through the years. However, clinically only a few are used consistently. The most accepted classification system is Kernahan's classification who classified cleft lip and palate as a striped Y with the incisive foramen as a reference point (Kernahan, 1971). The anatomical region affected by the cleft is numbered 1 to 9. The system of classification is based on the ideology that the intra-oral view of the mouth is the shape of an inverted Y.

Cleft surgeons also commonly use the LAHSHAL classification for orofacial clefts, which makes it easier for computer-based coding. In this classification, L stands for lip, A for alveolus, H for hard palate and S for soft palate. This classification system splits the mouth into six parts. The coding system is indicative if the cleft is complete (capital letters) or incomplete (small letters)

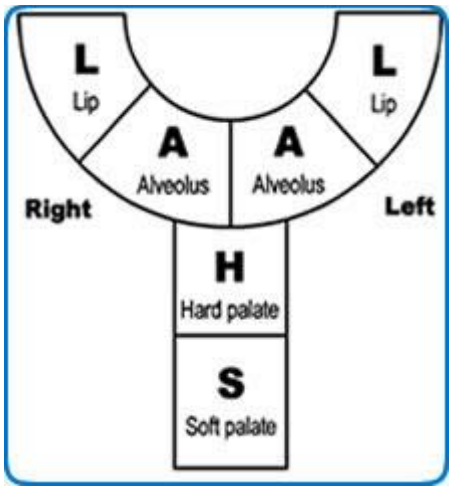

1.8. Consequences of Cleft Lip and Palate

CL/P shows visible impact on facial appearance and adversely affects the health of children associated with clefts, thereby affecting important functions such as feeding, speech, hearing, appearance and quality of life (Rumsey and Harcourt, 2005). A higher morbidity and mortality rate have been reported in children affected by CL/P in comparison to unaffected children (Mossey et al., 2009).

Cleft lip and palate is a craniofacial anomaly that varies in intensity and severity and is characterized by consequences that showcase a similar trend of severity. Children affected by cleft lip and palate tend to be affected psychosocially especially in terms of adjusting to the environment around them- self-esteem, body image, facial aesthetics, satisfaction with their speech and depression and anxiety is commonplace (Tyl et al., 1990). It has been seen in studies conducted previously that children affected by cleft lip and palate had fewer friends as compared to controls (Ramstad et al., 1995a) which signifies that socializing skills in children with cleft lip and palate is greatly reduced.

One study reported that 30-40% of children with cleft lip and palate were reported to have clinically significant behavioral and social difficulties such as shyness, reduced social competence, impulsive behavior or learning disabilities/cognitive impairments (Richman and Nopoulos, 2008).

Infants affected by cleft lip and palate may show difficulty in sucking action and therefore may not be able to feed normally due to part or whole of the roof of the mouth not being developed completely.

Dysfunction of the eustachian tube that connects the middle ear and the throat may result in recurring ear infections which correspondingly may lead to partial

or complete deafness. The failure of the fusion of the mouth and lip may result in muscle function of the mouth being compromised which in turn may lead to speech delay or abnormal speech. Due to the deformities associated with the intra-oral regions and the alveolus, teeth may not erupt normally.

Due to lack of fusion of facial plates, the facial appearance and attractiveness is compromised and is seen as varying levels of facial asymmetry depending on the severity and location of the cleft.

1.9. Anatomic Considerations- Morphology of the facial muscles

1.9.1. The Buccinator muscle

The Buccinator is found in each cheek of the face. More specifically, this muscle originates from three different locations- the alveolar process of the maxilla (the maxillary bundle), the buccal part of the alveolar process of the mandible (the mandibular bundle) and from the pterygo-mandibular raphe (the longitudinal bundle) (Baghele, 2012). The pterygo-mandibular raphe is a thick layer of connective tissue in the cheek. From these origins, the Buccinator extends and inserts into the Orbicularis Oris muscle. The Buccinator muscle is referred to as an accessory muscle of mastication due to its role in compressing the cheeks inwards towards the molars, thus ensuring that food does not accumulate in the buccal pouches. It also helps in the puffing out of cheeks and therefore called the 'trumpeter muscle'.

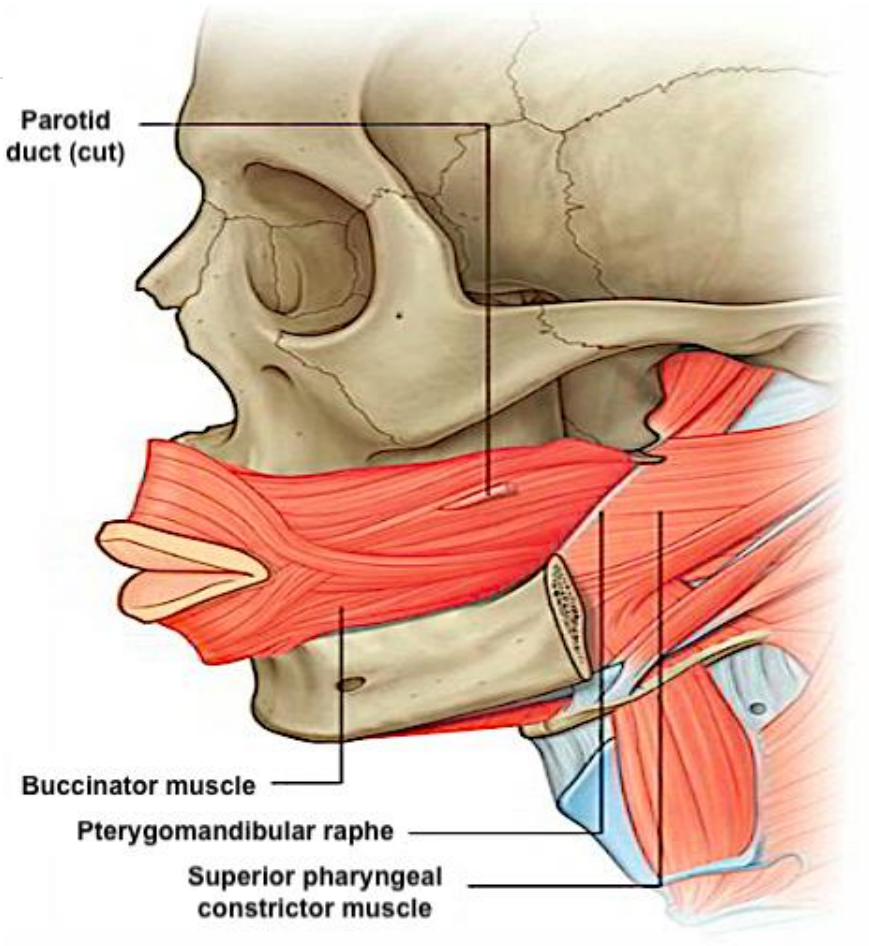

Figure 1: The Buccinator muscle showing its origin and insertion *(Source: Volker, 2018)*

1.9.2. The Orbicularis Oris Muscle

The Orbicularis Oris consists of superficial and deep layers. The deep fibres run circumferentially between the modioli and function primarily as a sphincter in feeding. The deep fibres of the Orbicularis Oris muscle originate from the modiolus on each side. These are aligned horizontally with fibres passing continuously from one commissure to the other across the midline.

The superficial fibres are further distinguished as superior fibres (Pars Peripheralis) or inferior fibres (Pars Marginalis) of the upper lip. The Pars Marginalis courses along the vermillion border, attach to the contralateral Pars Marginalis fibres at midline and inserts into the region of the vermilion tubercle. The Pars Peripheralis has a flat-fan shape diffusing out from each modiolus and

inserting into the skin of the contralateral philtral ridge, as horizontal, oblique and incisal directed fibres (Rogers et al., 2009).

Two other distinct fibres of the Pars Peripheralis have also been identified using micro-computed tomography (Wu J & Yin N, 2016). One bundle terminates at the tissue below the ipsilateral anterior nasal spine and runs its course along with the Depressor Septi. The other bundle crosses the midline and continues with the alar part of the Nasalis. The decussation of fibres results in the formation of the philtral columns, and lack of insertion at the midline results in the philtral depression.

The superficial bundle divides into an upper or nasal bundle and a lower or nasolabial bundle (Figure 2). The lower or nasolabial bundle (Pars Peripheralis) derives its fibres from the Depressor Anguli Oris muscle on each side. They insert into the skin forming the philtral ridges.

The upper fibres or the nasal bundle (Pars Marginalis) represents the common insertion of the Zygomaticus Major and Minor, the Levator muscles and the Transverse Nasi.

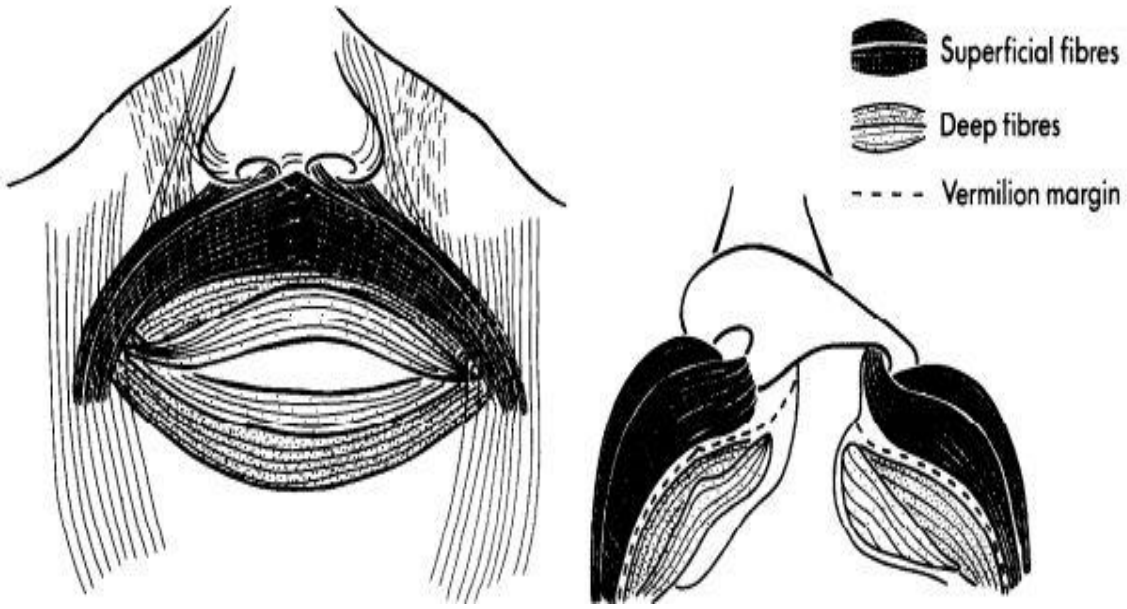

Figure 2: Deep and superficial fibers of the Orbicularis Oris *(Source: Nicolau, 1983)*

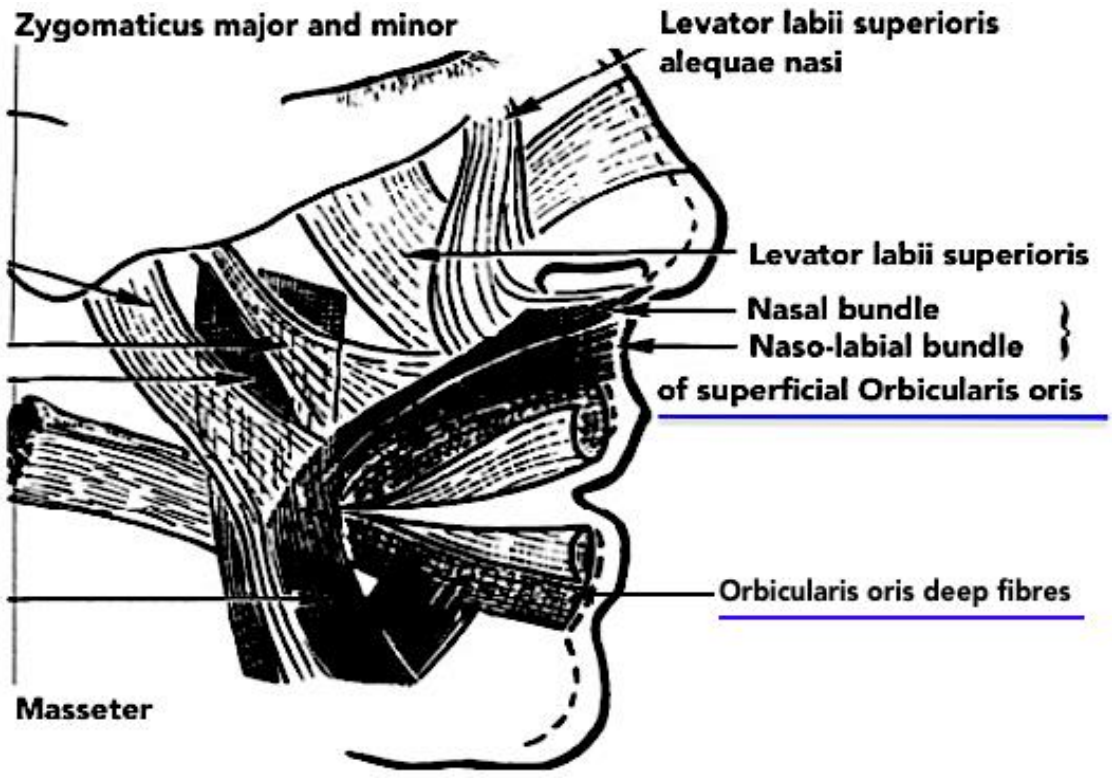

Figure 3: Transverse section showing deep and superficial bundles of the Orbicularis Oris *(Source: Nicolau, 1983)*

1.9.3. Depressor anguli oris

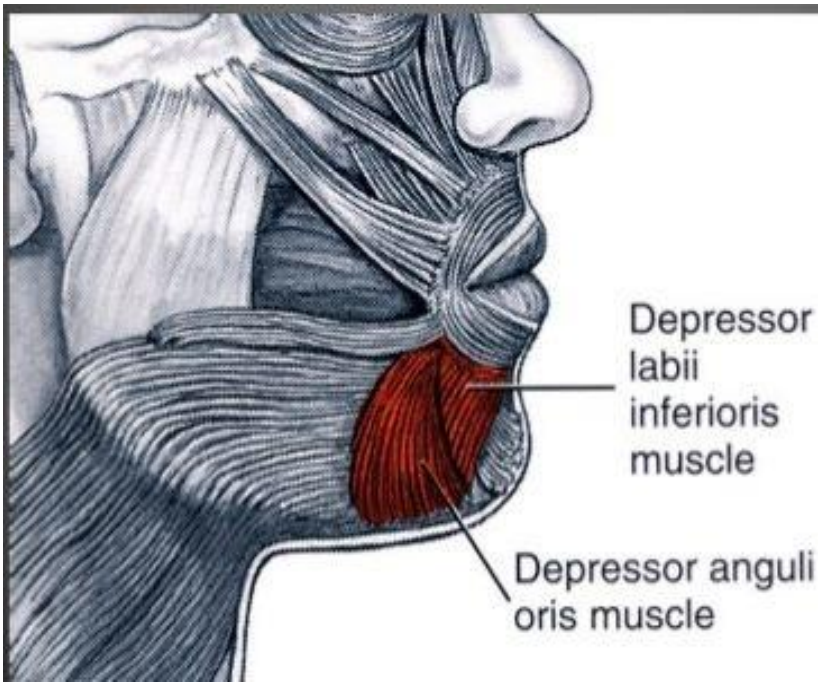

Figure 4: The Depressor muscles (Source: Kenhub*, 2019. Available from: https://www.kenhub.com/.)*

The **Depressor Anguli Oris (Figure 4)** originates from the oblique line of the mandible anteriorly, below the canines and the premolars, and inserts in to the modiolus after its fibres are directed medially.

Although it is a small muscle, its fibres are arranged in various directions because of its triangular shape. Some of its fibres may pass below the mental tubercle and cross the midline to interlace with their contralateral counterparts, thereby forming the Transversus Menti (the mental sling).

The muscle fibres of the Depressor Anguli Oris muscle may thus have several actions in the lower face depending on their orientation. The fascicles of the Levator Anguli Oris muscle and Depressor Anguli Oris cross each other at the angle

of the mouth. The fibres of the Levator muscle continue into the lower lip, and the fibres of the Depressor Anguli Oris continue into the upper lip. The function of the Depressor Anguli Oris muscle is to depress the angle of the mouth, acting as an antagonist to the Levator Anguli Oris muscle and the Zygomaticus Major muscle.

1.9.4. Depressor Labii Inferioris

The Depressor muscle originates in the lower jaw (Figure 5), near the oblique line of the mandible. Its fibres are continuous with those of the Platysma —the insertion of this muscle is the skin of the lower lip, thus bringing about the depression of the lower lip.

Figure 5: The Depressor Labii Inferioris (shown in green) *(Source: Kenhub [Internet], 2019)*

1.9.5. Platysma

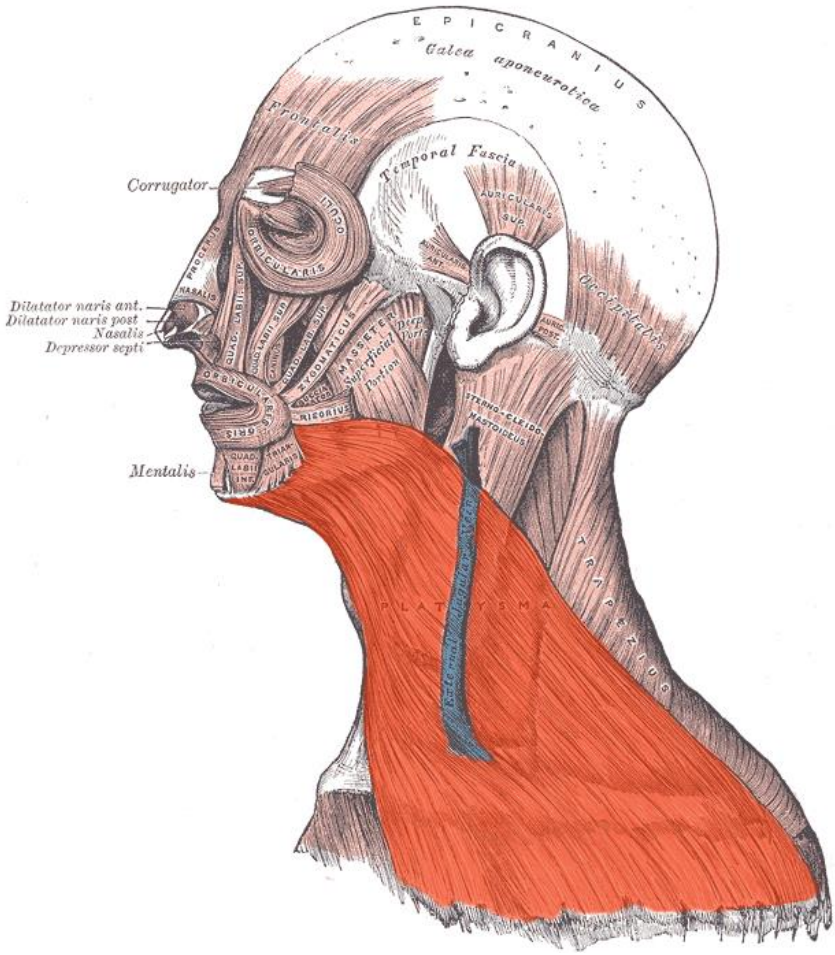

Figure 6: Platysma muscle (shown in orange) (*Source: Gray's Anatomy, 2008)*

The Platysma shows its origin in the skin of the neck and upper chest and inserts in the inferior border of mandible and the skin of the lower face (Figure 6). The function of the Platysma is one of significant controversy and debate. It helps in depression of the skin of the mandible, and in some may bring about depression of the lower lip and angle of the mouth. Its role as a lip depressor is secondary to the Depressor muscles described above (Hoerter & Patel, 2019).

1.9.6. The Levator Labii Superioris and the Levator Labiii Superiorus Alequae Nasi

The Levator Labii Superioris (LLS) muscle consists of three heads each showing different origins and insertions (figure 7). The angular head consists of the medial fibres originating from the upper part of the frontal process of the maxilla below the infraorbital foramen. These divide in to two slips of muscles, the first attaching to the greater alar cartilage and ala of the nose and the second in to the muscles of the upper lip, blending with the Orbicularis Oris. The intermediate or infraorbital head of the LLS arise from below the orbit immediately above the infraorbital foramen and attachment to the maxilla and a part of the zygomatic bone, mainly to the muscular portion of the upper lip between the Levator Anguli Oris and the angular head muscle fibres. The zygomatic head arises in the malar process of the zygomatic bone and inserts near the corner of the mouth and upper lip (Bloom & Rayi, 2019). The deep layer of the Levator Labii Superioris Alequae Nasi (LLSAN) muscle is located laterally to the Transverse Nasalis muscle (Hur *et al.*, 2010).

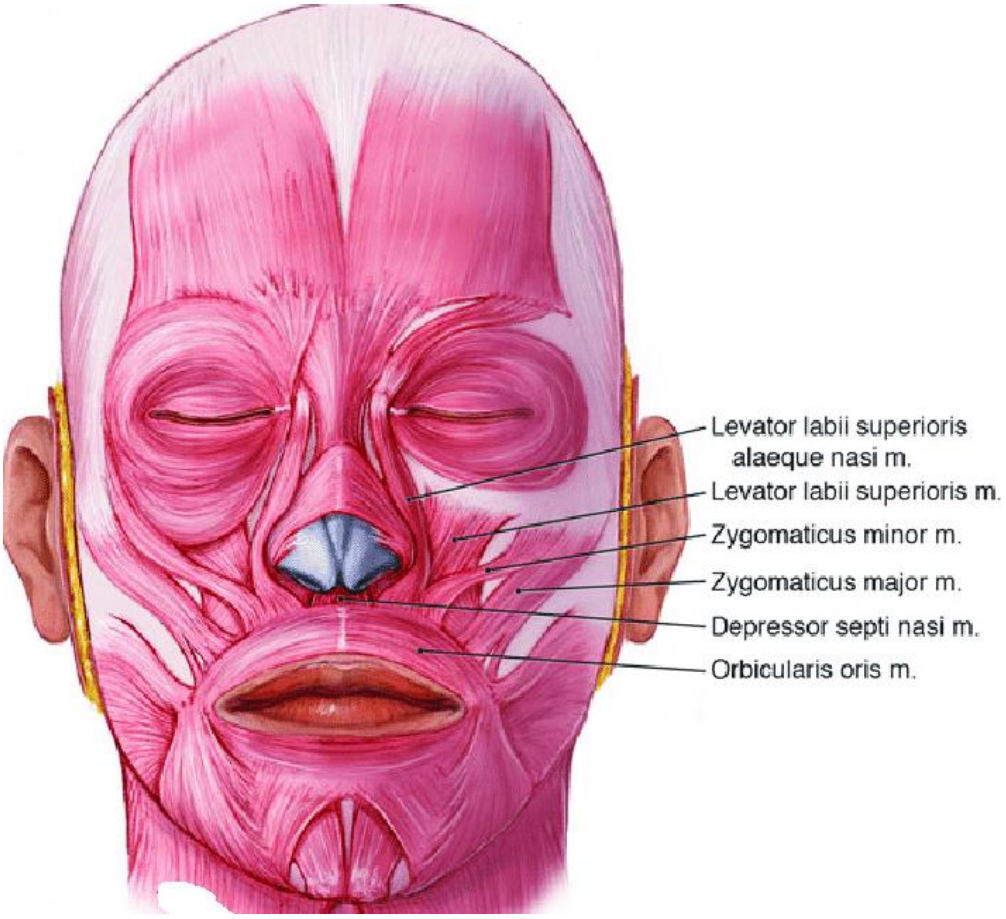

Figure 7: The Levator muscles *(Source: Nasr et al., 2015)*

1.10. The nerve supply of facial musculature

Motor neurons are neurons that enable the brain to innervate muscles, as compared to sensory neurons which transmit sensory information from sensory receptors to the brain. Motor neurons can be classified into upper motor neurons which transmit motor impulses from the motor centres of the brain to the brain stem and spinal cord and lower motor neurons which transmit motor impulses from the brain stem and spinal cord to the specific muscles eliciting movement. The lower motor neuron tract that innervate the muscles of facial expressions is the seventh cranial nerve or the facial nerve. The lower motor neuron tract also innervates the facial muscles through the fifth cranial nerve or the trigeminal nerve. The functionality of these two nerves differ significantly- the trigeminal nerve innervates the Temporalis muscle, the Masseter muscle and the Medial and Lateral Pterygoid muscles. These muscles are concerned with movements of the mandible especially during chewing and other jaw movements. The facial nerve, on the contrary, helps in the movement of muscles associated with facial expressions and does not elicit skeletal movement.

Essentially three brain stem nuclei have fibres that are linked with the facial nerve tract- i) the superior salivatory nucleus has fibres that innervate the lacrimal and salivary glands in the face, ii) the nucleus solitarius has sensory fibres that carry taste information from the anterior two-thirds of the tongue. These sensory and autonomic functions are performed by a group of fibres within the facial nerve tract called iii) the nervus intermedius. The fibres innervating the muscles of facial expression begin as a small cluster of cell bodies- the motor nucleus of the facial nerve situated in the brain stem near the pons. The lower motor neuron tract of the left and right side of the face are independent and their nuclei located in the pons are symmetrical and independent.

The intracranial course of the seventh cranial nerve is well documented and involves the fibres leaving the motor nucleus, looping around the nucleus of the sixth cranial nerve (the abducens), and then exiting the pons and joined by fibres from the superior salivatory nucleus and the nucleus solitarius. The first branch of the facial nerve intracranially is the stapedius branch which supplies the stapedius muscle in the middle ear (lesions in this branch cause hyperacusis). The facial nerve begins as two roots- the motor root and sensory root, which after coursing through the internal acoustic meatus, exit it to enter the facial canal. Within the facial canal, the two roots fuse to form the facial nerve. The nerve forms the geniculate ganglion and gives rise to the greater petrosal nerve, the nerve to the stapedius and the chorda tympani. The facial nerve then exits the facial canal via the stylomastoid foramen.

The peripheral (extracranial) portion of the facial nerve shows variation between individuals both with respect to its branches as well as muscles innervated by these branches. After exiting the skull, the first extracranial branch is the posterior auricular nerve which supplies motor innervation to the intrinsic and extrinsic muscles of the outer ear. The main trunk of the facial nerve- called the motor root, now courses into the parotid gland and terminates as five major branches- temporal, zygomatic, buccal, marginal mandibular and cervical branch. The temporal branch innervates the Frontalis muscle, Orbicularis Oculi muscle and the Corrugator Supercilii muscles. The Zygomatic branch innervates the

Orbicularis Oculi muscle. The buccal branch innervates the Orbicularis Oris muscle, Buccinator muscle and the Zygomaticus major and minor muscle. The marginal mandibular branch innervates the Mentalis muscle and the Cervical branch innervates the Platysma muscle.

1.11. Neurophysiology of facial expressions

Facial movements can be voluntary i.e. controlled by cortical pathways, reflexive, or initiated by subcortical motor pathways, located primarily in the brainstem. Specific areas in the brain are concerned with specific facial expressions. For example, the hypothalamus coordinates facial expressions related to complex behaviours such as those seen during mating and courtship (MacLean,1990).
On the one hand, where movement in limbs and extremities can be accurately measured, the facial muscles concerned with production of facial expressions modify the arrangement of facial features to express emotion. Facial expressions are not only harder to measure objectively but also have the ability to be produced with or without emotion being involved. Stroke and palsy patients involving the middle cerebral artery were seen not to be able to illicit a voluntary smile symmetrically. However, it was seen that this group of patients were able to perform a smiling movement in response to a joke (Trepel et al., 1996). These findings suggested the possibility of an alternate limbic pathway which coordinates facial expressions.

The motor areas in the cortex concerned with the production of facial expressions include the primary motor cortex, the ventrolateral premotor cortex, the supplementary motor area, and two motor areas of the dorsal midcingulate (Morecraft et al., 2007). The primary motor cortex is also concerned with the control and coordination of muscles associated with mastication and jaw movements which are innervated by fibres of the trigeminal nerve.

The primary motor cortex innervates motor neurons in the lateral segment of the contralateral facial nucleus that control the lower facial muscles (Morecraft et

al., 2001). The premotor cortex is also responsible for eliciting expressions triggered by visual cues (Mushiake et al., 2006).

The supplementary motor cortex (SMA) innervates motor neurons in the medial segment of the facial nucleus which help control upper facial movements (Morecraft et al., 2001). In comparison to the pre motor cortex which controls movements triggered by visual cues, the supplementary motor cortex takes part in self-initiated or voluntary facial expressions concerning the upper facial muscles.

The anterior and caudal face areas of the midcingulate cortex designated as M3 and M4 by Morecraft et al. (2001) are concerned with specialized movements. M3 has projections that supply the medial portions of the facial nucleus which include motor neurons that supply the upper facial musculature including muscles that move the ears. Projections from M3 also target the reticular formation of the brainstem eliciting expressions during periods of emotion. M3 is therefore in a position to control both the overt (behavioural) and covert (autonomic) expression of emotions.

M4 on the other hand contains projections that target the lateral portions of the facial nucleus especially eliciting movement in the upper lip (Morecraft et al., 2007).

Although the amygdala is not primarily concerned with the performance of facial expressions, due to its close relationship with the visual association areas of the frontal and temporal cortices, the amygdala plays an important role in evaluating facial expressions performed as well as selecting the appropriate facial expression for a specific social setting. For example, humans with bilateral lesions of the amygdala appear less shy when meeting strangers and are able to produce more friendly displays (Bliss-Moreau et al., 2013).

1.12. Anatomic Considerations- Morphology of the Cleft Lip Prior to surgery

The quantitative measurement of residual asymmetry of the face following surgical correction requires a thorough understanding of the anatomy of the cleft face including the orientation of facial muscles prior to surgery. Clinical observation and documented operative information are the main sources of anatomical information prior to corrective surgery of the cleft.

Surgery in the modern day and age is far more advanced as compared to surgeries conducted a decade ago as information and knowledge with regard to the facial muscle complex is now obtained using modern and innovative media such as microsurgical techniques, use of 3D-CT scans and advances in radiographic techniques.

The Unilateral Cleft Lip (UCL)

A complete UCL shows variability in its involvement of hard and soft tissues as this condition may range from minor notching of the vermillion border of the upper lip to a more thorough involvement that extends to the nasal floor and alveolus. The anatomical considerations of the UCL can be discussed under the following heads based on individual regions affected: -

A. The Lip

In a UCL, the fibres of the Orbicularis Oris muscle are interrupted. These muscles fibres move horizontally from the commissures towards the midline and then turn upwards along the cleft margins, where they may partly insert, or in other conditions, may extend up to the anterior nasal spine medially and alar base laterally. The vessels of the upper lip also move along the margins of the cleft.

Muscle fibres in the lateral segment end below the alar base whereas most muscle fibres in the medial segment attach to the maxillary periosteum below the columella (Malek, 2001).

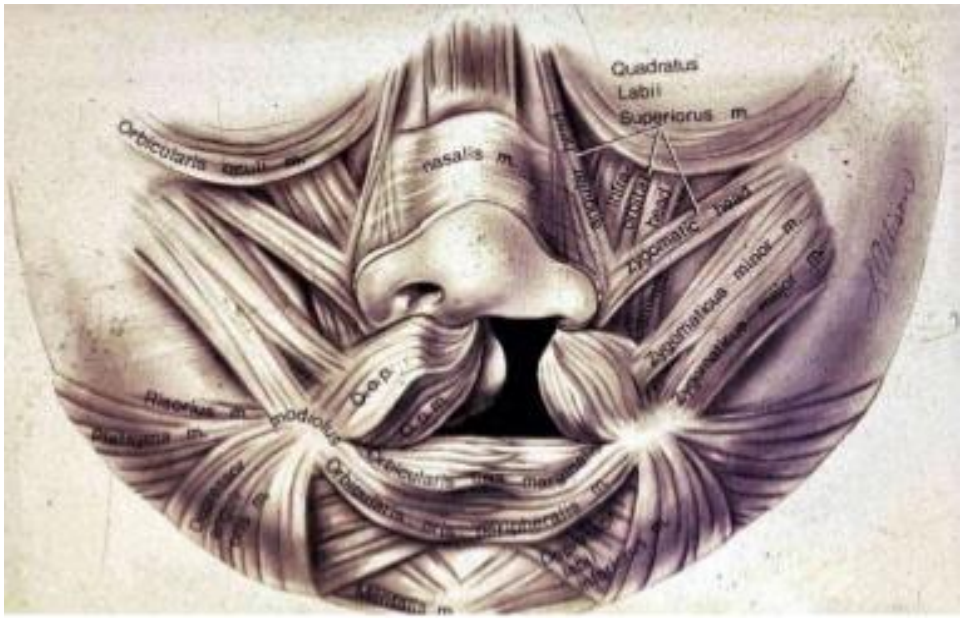

Figure 8: Muscular anatomy of the upper lip in UCL *(Source: Millard, 1976)*

In incomplete clefts, fibres of the Orbicularis Oris above the cleft region remain intact. A heaping of muscle fibres (Simonarts bands) may occur on the lateral aspect of the cleft due to accumulation of poorly or incompletely developed muscle fibres. On the medial side, muscle thinning is seen due to marked underdevelopment of muscle fibres, particularly near the philtrum adjacent to the cleft (Hood et al., 2003). In UCL, shortening of the philtrum is observed along with an abnormal philtral crest (Schendel, 2000).

On the medial aspect, a shortened lip and flattening of the philtral column is seen. On the lateral aspect, the vermillion border and red line (junction between the vermillion and mucosa) start parallel but converge towards the cleft.

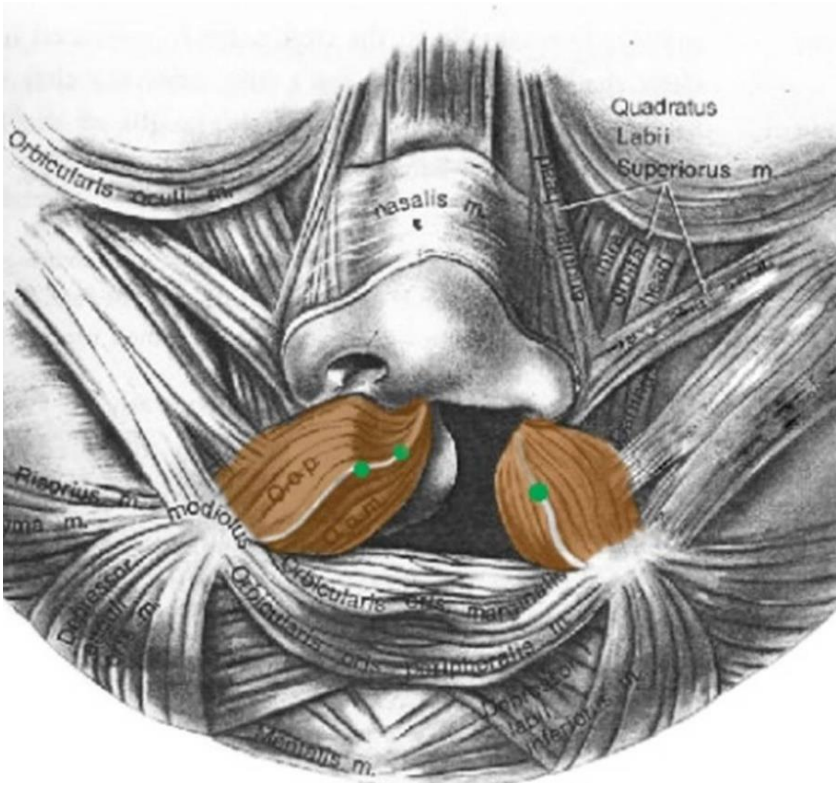

Figure 9: Differing thickness of muscles on the cleft sides (Source: *Millard, 1976*)

B. The Nose

Nasal deformity varies in intensity and may occur simultaneously with the upper lip dysmorphology. In unilateral clefts, the nasal septum shows deviation away from the midline and the lower cartilaginous septum and the vomer are about perpendicular to the vertical septum. There is also deviation of the nasal tip towards the cleft side (Figure 10B) and columella base deviation to the non-cleft side (Figure 10A)

Figure 10A: Nasal deformities in the UCL *(source: Salyer et al., 2019)*

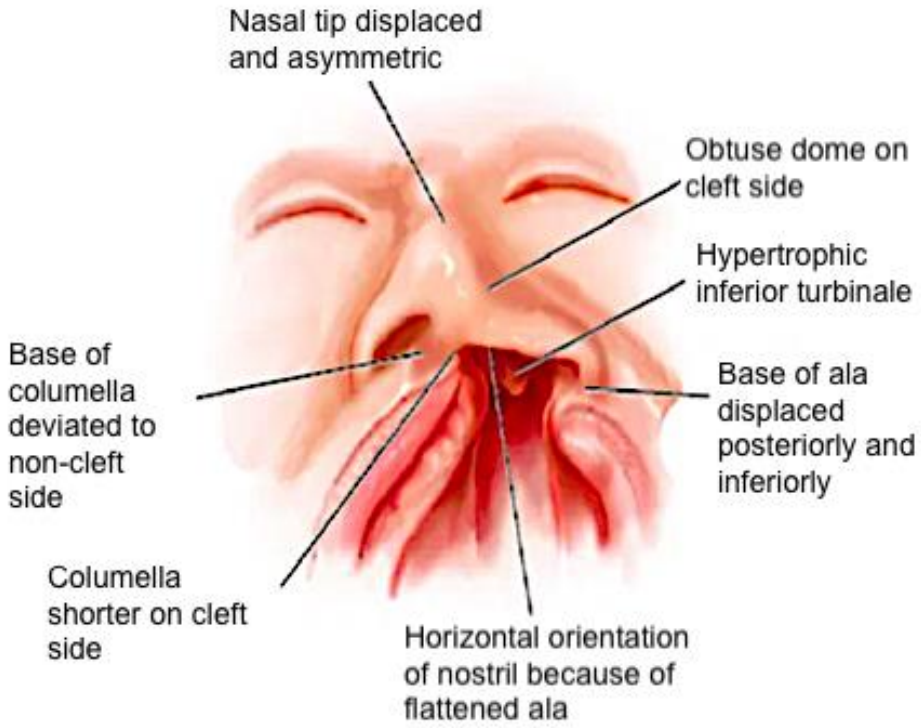

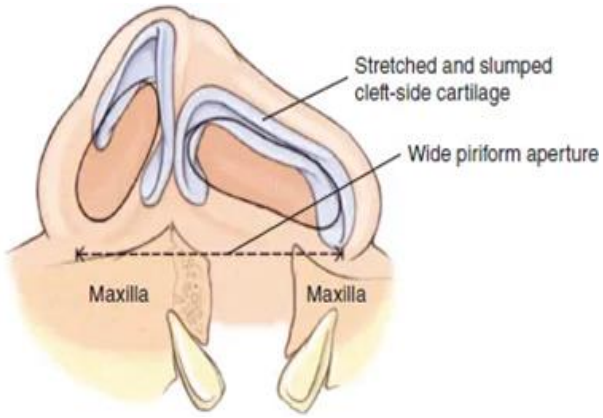

Figure 10B: Alar cartilage sitting slumped over a widened piriform aperture (source: pocketdentistry.com (online))

Figure 11: The spectrum of nasal involvement in Unilateral Cleft Lip *(source: childrens.com)*

Constriction of the nostril on the non-cleft side may occur due to the septum being deviated. The alar base on the cleft side is deviated laterally (McComb, 1990). Nasal bones may show a degree of hypertelorism.

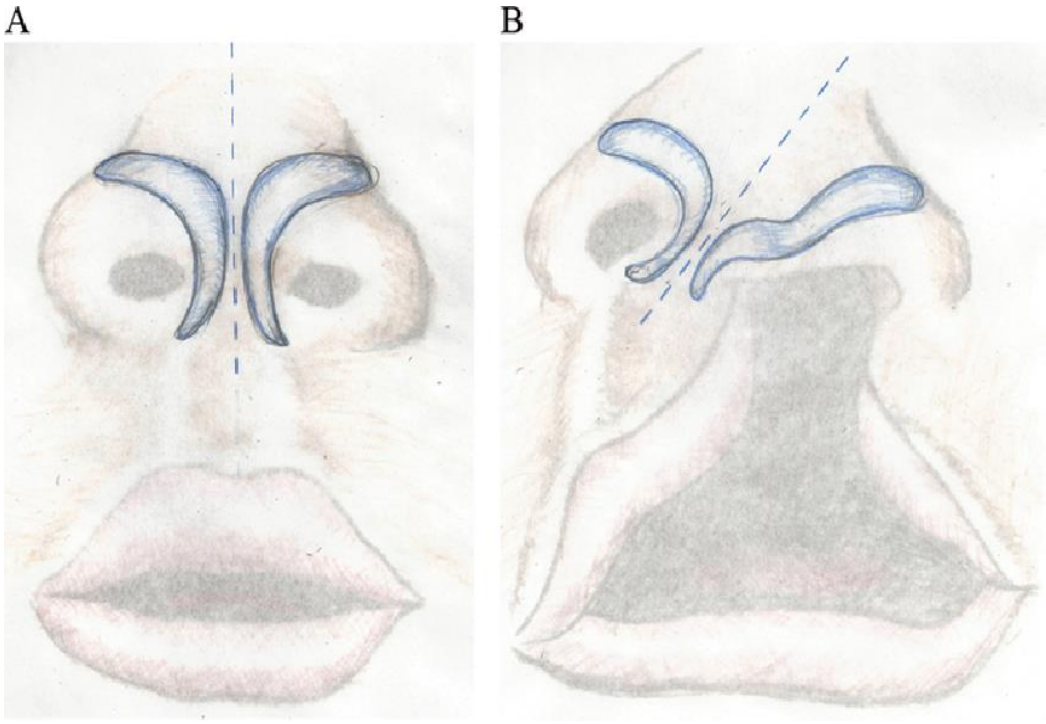

Figure 12: A. Lower lateral cartilages showing asymmetry B. Lower lateral cartilages in cleft showing asymmetry- a short medial crus, obtuse genu, and a lateral crus that

is longer and drawn into an S-shaped fold on the cleft side *(source: Chopan, M., Sayadi, L.R., & Laub, D.R., 2017)*

C. The Alveolus

The greater (medial) and lesser (lateral) segments of the alveolus show rotation in an outward direction.

Overall, the entire balance of the facial muscle complex is coordinated by muscular slings. A unilateral cleft lip causes disruption of these slings of muscle and therefore disturbs the intricate balance maintained in the facial muscle complex. This disruption of the anatomy of the muscles and corresponding disturbance in the facial muscle balance is responsible for the aesthetic and functional impediments in UCL patients.

Lip closure and correction of the deficits is important not just for regaining aesthetics and facial expression symmetry but also for appropriate optimal speech (especially bilabial sounds) and function.

1.13. Care of the Cleft Lip - Surgical and Non-Surgical Considerations

Caring for children and adolescents affected by Cleft Lip and Palate begins at birth. Treatment procedures for Cleft Lip and Palate begin from early childhood when the child is 3-6 months of age and continues until the adolescence stages. The goal of cleft lip repair is the achievement of optimum form and function. The term cleft lip is a misnomer as the nose is usually always involved and should be treated during the lip surgery. Surgical correction of the UCL can be looked at as a dynamic process as it spans the time period of an infant's facial development. This is the reason why, instead of a one-stop surgical solution, surgical management of UCL occurs over a prolonged time scale.

Time period/ age	Surgical Protocol
3 months	Primary cleft repair- lip and nose
6-9 months	Secondary flap palatoplasty
5 years	Secondary minor lip surgery
7-9 years	Cancellous Iliac bone graft to alveolus
7 years to full growth	Distraction osteogenesis in severe cleft cases
Full growth	Orthognathic Surgery
12-18 years	Rhinoplasty

Table 1: Surgical protocol at various stages in a UCL patient

The aim of surgical treatment in cleft lip and palate affected children is complete rehabilitation so that these children can live a normal life. A multidisciplinary team approach by specialists in cleft care has been recognized as the best option for treatment (Hodgkinson et al., 2005).

Surgical techniques for cleft lip repair have revolutionized in the past 25 to 30 years (Shprntzen & Bardach, 1995). The aim of cleft surgery is to attain a symmetrical cupid bow and nasal area that ensure scars are placed in less noticeable areas.

1.13.1. Non-Surgical Considerations

1.13.1.1. Emotional Support- The need to support feeding

The long-term emotional impact of a child born with a developmental condition has been well documented. Emotional support and guidance aided by counselling and psychological evaluation and care is quintessential for children with clefts (Barr and McConkey, 2007).

Feeding has been recognized as a challenge in relation to the maintenance of a child's weight and growth as well as its potential emotional impact on parents (Endriga and Kapp-Simon 1999). The all-important activities of feeding and suckling are severely compromised in cleft affected children. (Reid et al. 2006; Reid et al. 2007). Feeding difficulties have been reported amongst parents of infants with clefts in one UK survey (Oliver and Jones 1997).

1.13.1.2. Presurgical Tissue mobilisation

Its primary goal is to lessen the cleft defect before surgical treatment. Improvement in the severity of clefts pre-operatively helps achieve better results post-operatively.

A. Adhesive Tape

This presurgical technique was advised by Pool and Farmworth who stated that placing long strips of adhesive tape for 6 weeks prior to surgery tended to reduce alveolar gaps by 53% and help narrow the lip segments (between 40% and complete apposition) (Pool & Farmworth, 1994).

Figure 13: Adhesive Tape on a patient with Unilateral Cleft Lip *(Source: Chopan, M., Sayadi, L.R., & Laub, D.R., 2017)*

B. Naso-Alveolar Moulding

Naso-Alveolar moulding (NAM) is a technique carried out with the help of an intra-oral device which works to achieve the alignment of alveolar segments and correspondingly narrows the cleft defects. The appliance fits over the maxillary arch and circular elastics are attached to the face bilaterally. Every week or so, an orthodontist adjusts the appliance by adding and removing acrylic from the plate. The alveolar gap is consistently measured and once the gap reduces to less than 5mm, a nasal stent is added to this appliance using a wire. The stent is also modified in intervals by adding acrylic. This tissue expansion caused by the stent helps in shaping the alar cartilage alongside helping to achieve a lengthened columella and projected nasal tip pre-surgically.

Figure 14: A bilateral cleft lip patient with NAM device *(Source: Chopan, M., Sayadi, L.R., & Laub, D.R., 2017)*

1.13.2. Surgical Considerations

1.13.2.1. Introduction

Studies have shown that adults with un-operated complete clefts showed a smaller and more protruded maxilla with increased anterior facial height (Capelozza et al., 1993). Studies in a Brazilian cleft population have also shown that lip repair in isolated clefts of the alveolus and of the palate has no known deleterious effect on maxillofacial and maxillo-mandibular growth (Nomando.1992). The converse is said to occur when surgical repair of the lip and palate is done in complete cleft of the lip and palate, its impact was shown to be more on the antero-posterior dimension leading to downward growth rotation. However surgical repair of the lip and palate does not seem to affect mandibular growth (Semb and Shaw, 2017).

Scar tissue formation after surgical repair especially in the maxillary, palatine and pterygoid sutures have been said to prevent forward and downward translation of the maxilla, thereby impeding growth (Ross and Johnston,1972).

A few studies on cleft care in the past have concluded that the impact of surgery is more on the maxillary base and dental arches resulting in reduced maxillary antero-posterior and vertical dimension, rather than on the transverse dimensions (Dahl et al., 1981; Bergland and Sidhu,1974; Enemark et al., 1990). These studies also reported that the surgical technique used may influence the degree of scar formation and determine the extent of malocclusion. Several authors have also drawn attention to the contraction of collagen fibres that arise in granulation tissue and may restrict growth of the maxilla (Capelozza et al., 1996; Kuijpers-Jagtman and Long, 2000).

Good surgical skill of the surgeon has been reported to reduce scar tissue formation in patients with UCLP with high volume operators (surgeons performing more than 20 lip repairs a year) likely to have better surgical skill than low volume operators (surgeons performing less than 10 lip repairs a year) (Shaw et al., 1992; Ross and Johnston,1972; Prahl-Anderson & Ju,2006). Inter center comparison studies of two centers reported better treatment outcome in one center as a result of the high number of surgeries undertaken when compared to the other center that had a lower number of surgeries undertaken (Shaw et al., 1992; Ross et al., 1990). In summary, the impact of surgery in patients with UCLP, scar tissue formation and pressure on the maxilla from the lip after surgical repair are major factors that can restrict maxillary growth.

1.13.2.2. Surgical techniques of UCL Repair

Effect of Lip surgery in cleft lip and palate on facial movement and symmetry

Following cleft lip and palate surgery, muscle scarring and thinner tissues ensue around the surgical site. These factors contribute to poor mobility of facial musculature and thereby lead to increased facial asymmetry during movement. A study was conducted by CA Trotman et al. (2010) to examine the effects of lip revision on function including movement. Baseline findings in the study implied that facial movements were impaired in patients with repaired cleft lip and

palate. The most impaired was the lateral movement of the upper lip. Compensatory lower lip movement was also noted following lip repair (Trotman et al., 2005). It was also seen that in patients with cleft lip surgery, the upper lip musculature exhibited lesser force as a result of which, compensatory force was generated by the lower lip muscles which exerted high amounts of force in a faster period of time. Results showed that cheek puff and maximum smile demonstrate significant change from baseline to 12 months after surgery.

Facial muscles are striated muscles which take part in two major functions- mastication and facial expressions. There are several facial muscles that participate in facial expressions which include the Orbicularis Oris, the Zygomaticus major and Zygomaticus minor, the Levator group of muscles, the Buccinator, the Depressor Labii Inferioris, Depressor Anguli Oris, the Procerus, the Occipitofrontalis, the Risorius and Mentalis muscle. Each of these muscles contribute specifically to certain characteristic facial movements and expressions depending on their anatomic location.

- Cheek puff includes activity of Orbicularis Oris muscle followed by contraction of Buccinator, Risorius and the Zygomaticus major and Zygomaticus Minor muscles.

- Lip purse involves Orbicularis Oris contraction.

- Grimace involves movement of Depressor Anguli Oris and Depressor Labi Inferioris (with fibres intermingling with the pars fibres of the Orbicularis Oris).

- Maximal smiling involves the Levator muscles followed by the Risorius, Zygomaticus Major and Minor and Buccinator. Following surgery, scarring occurs around the Levator Labii Superioris and Levator Labii Superioris Alequae Nasi. The Levator Labii Superioris has three heads each showing different origin and insertion sites. Incomplete mobility and approximation of each of these heads could result in asymmetry following cleft lip and palate repair.

- The raising of the eyebrows involves the contraction of the Occipito-frontalis.

Following the surgical repair of cleft lip and palate, scarring around certain surgically involved muscles, or poor approximation of muscles and their individual heads may result in irregular and asymmetric facial movement thus contributing to facial asymmetry. It is therefore important to lay emphasis on both the anatomy and the surgical repair methods used during cleft lip and palate repair, in order to understand how facial asymmetry is distributed throughout the facial surface, and to thereby quantify the facial asymmetry both in the whole face and regionally.

A. Lip Adhesion

Lip adhesion developed by Randall (1965) is the first surgical step in a two-stage lip and nose reconstruction technique. It helps to improve the nasal dysmorphology and align the alveolar segments while increasing the lip height in medial and lateral segments. The drawback of this technique is the additional scarring which may occur to the primary scarring that is common following primary repair surgery. Incisions are made on the vermillion of the medial and lateral lip elements. Supraperiosteal dissection on the lateral lip element is performed with the help of an incision buccally. Subcutaneous dissection is carried out on the medial segment to the nasal tip, allowing for mobilization of the cleft-side lower lateral cartilage. With the help of mattress sutures, which pass through the medially performed incision, the buccal mucosa and Orbicularis Oris, the mucosal flaps are closed.

B. Straight Line Repairs

The Rose -Thomson Principle- This technique employs a curved incision which is concave from nostril to the vermillion at an angle of 60 degree (Rose W, 1891). Thomson, at a later stage used a diamond incision to design his procedure. These straight-line repairs may have the advantage of speed and ease of operation but

show heavy scarring and also do not show satisfactory results in terms of symmetry of the cupids bow.

C. Upper Lip Flaps

- Millard Repair- Millard proposed the rotation-advancement technique which is used most commonly by surgeons today (Millard DR, 1958). The specialty of this technique was the preservation of the cupids bow and philtral columns. The down rotation of medial lip element helps to restore vertical lip height and the advancement of the lateral lip element helps in the re-positioning of the alar base. The medial segment (rotated downward) runs from the lateral cupid's peak through the columella to the philtral column on the non-cleft side. The lateral segment (advancement in to the created defect) runs from the nasal sill and around the alar base.

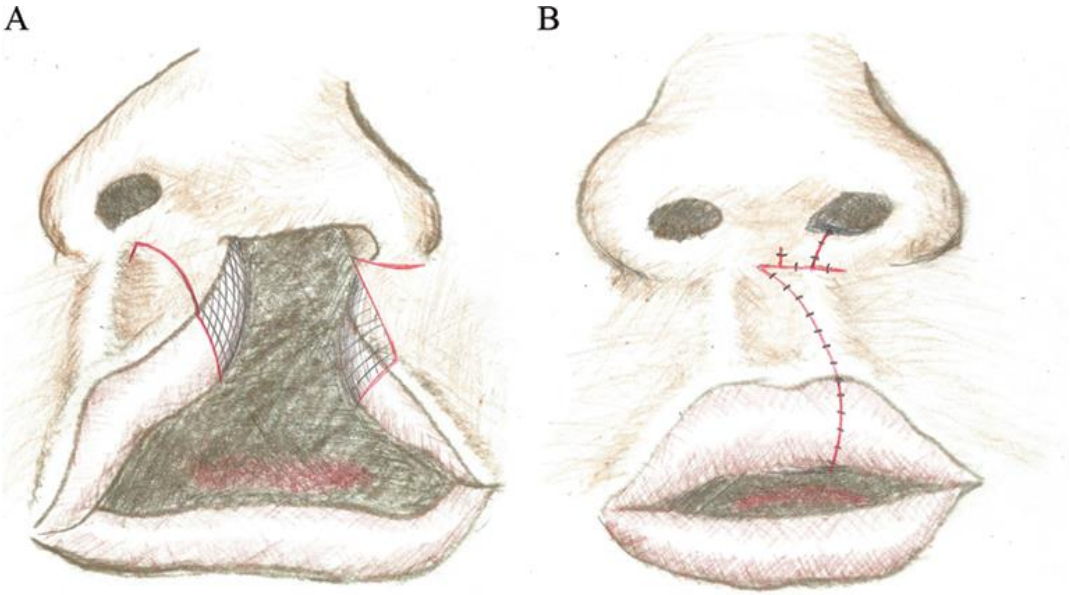

Figure 15: A. Surgical technique in Millard's repair B. Closure of Millard's repair*(Source: Chopan, M., Sayadi, L.R., & Laub, D.R., 2017)*

- Mohler's Technique- In Millard's technique, the scar runs across the philtral column. Mohler created a mirror image of the philtral column on the non-cleft side (Mohler, 1987). The lip was closed in a straight line by moving

the rotated segment till the columella and the back cut terminated at the midpoint of the philtral depression.

- Cutting's Technique- Mohler's technique was modified by Cutting. In this technique of repair, the upper incision was shifted to beyond the midline of the columella and the back cut extended down to the philtral column on the non-cleft side (Cutting, 2009). This enabled sufficient tissue in the lateral segment to fill the defect created by downward rotation.

D. Middle Lip flaps

- Le Mesurier Flaps- In this technique, a quadrilateral flap is made on the lateral aspect of the lip and rotated medially where a notch is created by making a back cut (Figure 16). This technique gives fullness to the lower lip and the scar created is a step line scar which is unlike other scars as it gives the appearance of an accidental wound to an observer (Bauer et al., 1946).

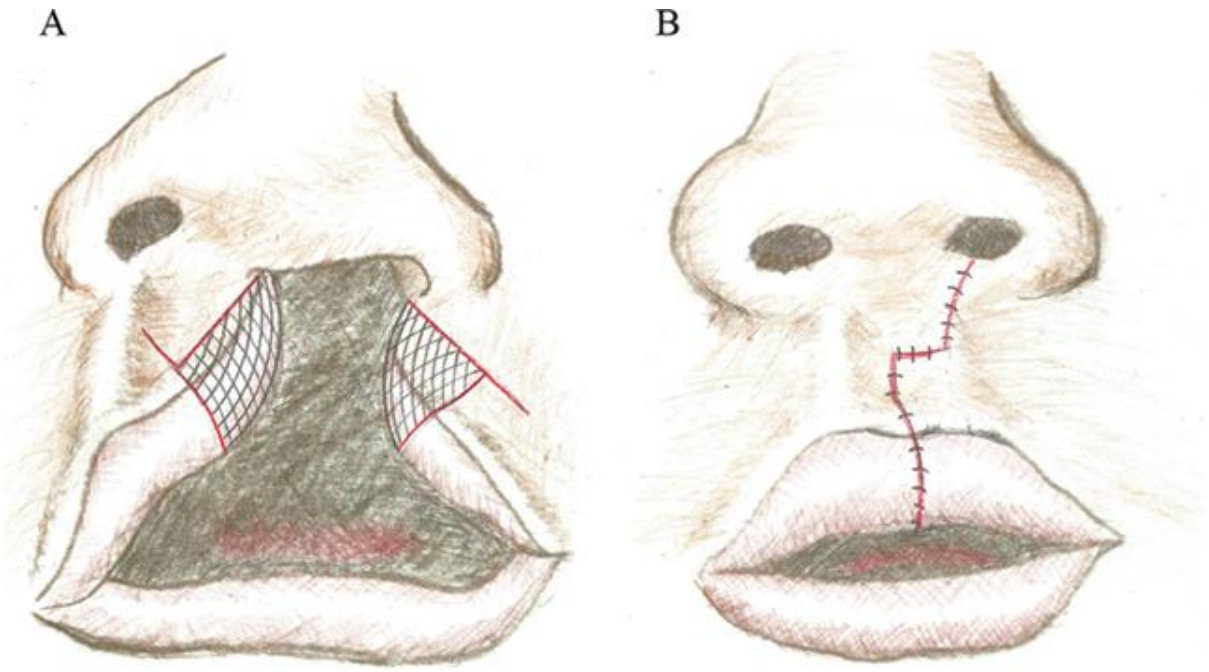

Figure 16: A. Le Mesurier technique of repair B. Closure of the repair *(Source: Chopan, M., Sayadi, L.R., & Laub, D.R., 2017)*

E. Lower Lip Flaps

- Tennison-Randall Repair-This technique of repair, especially advantageous for wide complete clefts, was proposed by Tennison, who repaired the cleft defect using the Z-plasty principle to help achieve sufficient vertical lip length (Tennison, 1946). This technique was based on a mathematical derivation, wherein the base of the triangle of the lateral element is the difference in length between the cupid's peak on non-cleft side to the base of the ala and to the columellar base (Tennison, 1959). The side length of the triangle should equal the length of the back cut in the medial element (Figure 17).

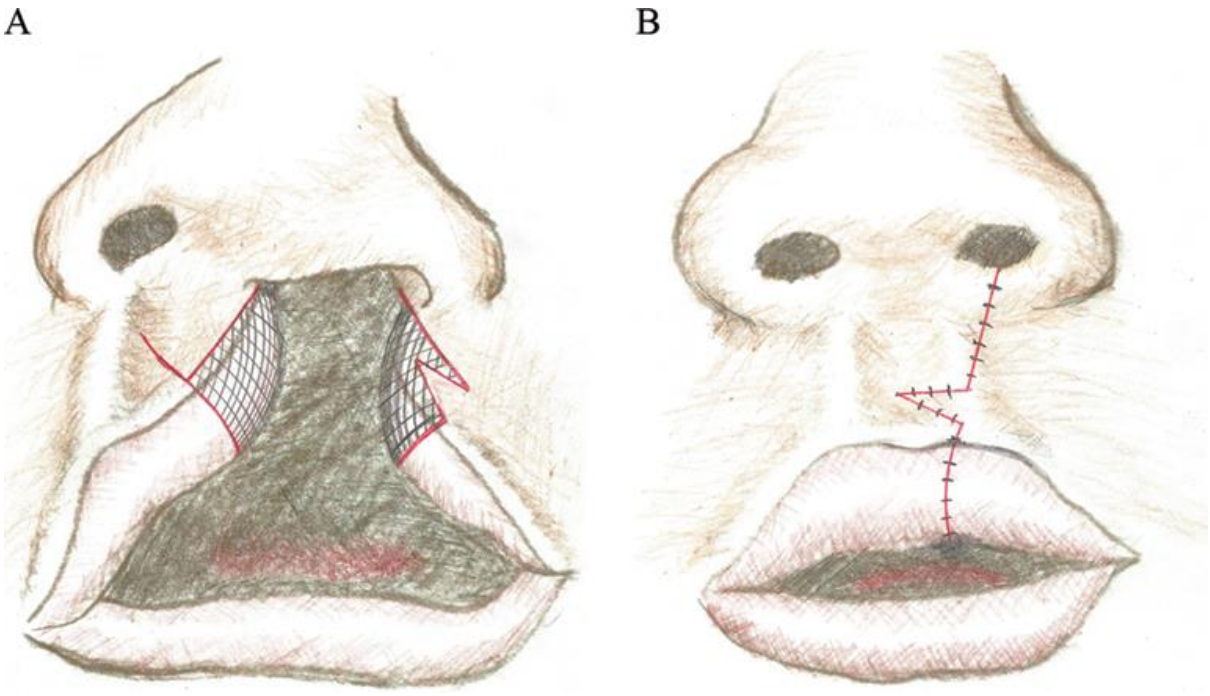

Figure 17: A. The Tennison-Randall repair incisions B. Closure of the Tennison -Randall repair technique *(Source: Chopan, M., Sayadi, L.R., & Laub, D.R., 2017)*

1.14. Adverse Consequences of Unilateral Cleft Lip Surgery

A. Dehiscence

This phenomenon is not very commonly observed during or after the repair and could be due to improper muscle approximation using sutures on the Orbicularis Oris muscle or due to excessive tension on the repair site (Narayanan & Adenwalla, 2013).

B. Scarring

Scarring observed clinically after surgical repair of the unilateral cleft lip could be controlled by the following three factors:

1. Intrinsic factors- Include sutures and their tightness and tension created thereafter.
2. Extrinsic factors- The tension at the repair site due to tissue approximation.
3. Patient factors- Response to a surgical trauma.

The upper lip techniques of surgical repair described above have a limitation in that, these result in a transverse scar along the columella-labial junction which in turn leads to hindered movement of facial muscle in that area.

The intrinsic and extrinsic factors are controllable by the surgeons. However, patient factors are not easily controlled.

In the time period immediately following surgery, scarring is observed in the cupids bow (which is pulled up) and vermillion notching is seen on the cleft side. This scarring usually settles down in most cases. However, if the initial rotation was not adequate or if the lateral lip element was too short, scarring may tend to persist. In the case where the scarring is tenacious, re-rotations may be required.

C. Notching of the Vermillion border

Discontinuity in the vermillion border is seen as a delayed response to surgical repair. This notching may be present either centrally or laterally along the scar line. In unilateral cleft lip cases, notching is seen laterally and is due to the following factors: -

1. Rotations not being adequate (Ample rotation of the medial element with enough back cut to bring down or elevate the cupids bow prevents this).
2. Inversion of suture edges (Undermining the mucosa helps prevent inversion)
3. A deficient Orbicularis Oris muscle
4. Straight line scar contracture (Can be avoided by Z-plasty technique)

D. Deformities in the nasal region

Huffman and Luerte (1949) documented the nasal deformities observed after unilateral cleft lip repair. These deformities included alar depression on the cleft side, inward rotation of the cleft side ala, increased nostril width, shortened columellar length, and deviation of septum anteriorly towards the non-cleft side.

1.15. Analysis of facial expressions- Static vs dynamic

Earlier work that was focused on facial movement was hindered by lack of suitable methods of measuring facial movements. Techniques differed from a methodological point of view, ranging from the subjective description of changes using grading scales to the analysis of movements using photographs of specific facial areas.

Direct anthropometry is a standard technique for quantifying facial dysmorphology by carrying out measurements directly on the face of an individual using measurement devices. This technique is also employed in planning treatment protocol and surgical procedures as well as assessing various treatment outcomes

of craniofacial conditions associated specifically with facial dysmorphology (Wong et al., 2008).

To offer advantages over the direct methods of anthropometry, indirect methods of anthropometry were applied, wherein measurements are carried out digitally or on photographs. 2D techniques such as photographs and videos did not accurately quantify the complexity of facial expressions. This was followed by the introduction of 3D marker-based photogrammetry, which requires the direct placement of reflective markers on the face (Trotman et al., 2013). Markers are placed in relation to corresponding muscle groups of the face and the displacement of these markers is quantified. Limitations to this technique included marker slipping (where markers placed too close to each other interfered with imaging and slipped), prolonged time for the analysis, questionable reliability as this method depended on precise landmark identification, increased patient compliance and marker occlusion (markers placed in blind spots of the cameras, e.g. the bridge of the nose).

Previous studies have shown that subjective interpretations of surgical outcomes and the need for further lip surgery are unreliable and inaccurate. It has been seen that surgeons' agreement among themselves regarding the severity of the nasolabial deformity (Asher-McDade *et al.,* 1991) or the outcomes of surgery (Trotman *et al.,* 2007; Trotman et al., 2011) were low.

The objective evaluation of facial movements in the surgically managed cleft lip and palate patients included 2D studies using photographs and video recordings. Gross *et al*. (1996), in a study comparing 2D and 3D methods of facial movement, inferred that measurements in 2D underestimated analogous 3D measurements by 43%. Several studies have been conducted using 3D images of static faces at rest and at maximum facial expressions using laser scanning (Schwenzer-Zimmerer *et al*., 2008; Djordevic *et al*., 2014) and stereo-photogrammetry (Trotman, 2007; Meyer-Marcotty *et al*., 2010; Patel *et al*., 2015; Bell *et al*., 2014). Human faces

however, are rarely static in day to day activities. The assessment of the dynamics of facial movements requires facial expressions to be recorded in real time (4D) to assess morphological characteristics at various time intervals.

The advent of 3D imaging systems ushered in an era of convenient diagnosis and accurate treatment planning (Hood et al.,2003). A systematic review on 3D imaging techniques for quantitative assessment of facial soft tissues in cleft lip and palate patients was conducted by Kuijper et al. (2014). The main 3D technique used in quantifiable assessment included CT, CBCT, MRI, stereophotogrammetry, and laser scanning. CT scanning was the most common method used for 3D imaging in patients with cleft lip and palate, primarily used for assessing results of bone grafting of the alveolar cleft. (Suzuki et al., 1999. Kawakami et al., 2003; Kim et al., 2008). CBCT was also used to assess bone grafting results whereas MRI was used for assessing speech by quantifying mobility of the lateral pharyngeal wall and the velum.

3D imaging techniques include:

1. Laser Scanning

This system works by throwing a known pattern of laser light on an object and then uses certain geometric principles to obtain a 3D model of this object (Majid et al., 2007). Digital cameras capture the light source and triangulation geometry allows depth information to be calculated using camera distances from the object. This technology generally produces facial surfaces with accuracy and resolution of ~1mm and can take up to 30s to capture (Hennessy et al., 2005). The laser scanner is a system used to capture soft tissue structure and is considered a non-invasive, reliable and reproducible imaging system (Hajeer et al., 2002). The precision of laser scanners has been tested in a few studies in the past where its accuracy was compared to digital callipers (Kau et al., 2005; Gwilliam et al., 2006). Its accuracy was less than 2 mm on the plaster model and 0.8 to 1 mm on the human face. However, it does suffer a drawback in that the time needed to capture is prolonged and requires a great deal of patient compliance (Bozic et al.,

2009). Another potentially important limitation is the fact that the laser scanners are unable to capture surface texture thus making identification of landmarks difficult. The patient's eyes must be protected, and the head kept in a stable position.

2. Cone Beam Computerized Tomogography (CBCT)

With the advent of the CBCT, the facial complex in its entirety could be viewed and assessed and with time, the CBCT has become one of the most widely used diagnostic tools in craniofacial abnormalities. However, it suffers from a limitation in that patients are exposed to dangerously high levels of radiation, which are higher than conventional X ray sources. The CBCT systems are not cost effective as compared to other 3D systems. CBCT allows the acquisition of 3D images of the skull and teeth as well as soft tissues. However, image acquisition of soft tissues is not of ideal quality. A potential limitation of the CBCT is that the field of view does not go past the cranium or the cephalometric point glabella and is therefore commonly combined with stereophotogrammetry

3. Stereophotogrammetry

Stereophotogrammetry, like laser scanning works on the triangulation principle and uses two or more pairs of cameras configured as a stereo pair to capture simultaneous images of the object (Kau et al., 2005). The cameras are kept apart from each other and the face to be imaged is placed within an area where the calibration target was imaged. The calibration ascertains the distance between the cameras, its focal lengths and the exact position of the camera with respect to the object (Majid et al., 2005). The 3D coordinates that are obtained are then used to reconstruct the face in three dimensions. Along with skeletal asymmetry, soft tissue asymmetry also leads to asymmetric faces and therefore needs to be assessed during analysis of facial asymmetry. Stereophotogrammetry (discussed in detail in the next section) is a 3D surface imaging system which is based on the principle of photogrammetry. These systems can be used to obtain exact topography of the face and help in mapping the color and texture resulting in a realistic imaging medium. As compared to laser scanning, stereophotogrammetry

does not require patient cooperation as capture time is fast and no direct contact is required (Ayoub et al.,2003). Patients are not subject to radiation and these systems are therefore advantageous in being able to be used for imaging multiple times.

4. 3D Ultrasound

Ultrasound, also referred to as sonography or ultrasonography is non-invasive diagnostic equipment that uses high frequency sound waves, produced by a transducer or a probe. These high frequency sound waves reflect off internal organs and tissues, and are detected by the transducer (Chandak et al., 2011) and create images. The differing densities of tissue, fluids and air in the internal structures cause sound waves to reflect differently and are therefore interpreted accordingly by radiologists.

Ultrasound has increasingly found application in maxillofacial surgery in procedures such as vascular malformations, osteomyelitis, space infections, and TMJ pathologies. The advantage of ultrasound is that it does not involve radiation and patient compliance is high. In addition, there are lesser occurrences of artefacts in ultrasound. However, the downside is that ultrasound is very highly operator dependent and its diagnostic success is based on the skill of the operator. Ultrasound also suffers from the drawback of anatomic noises due to the ultrasound signals bouncing back to the transducer (Sharma et al., 2014).

Other 3D techniques used in facial imaging are:

1. Morpho analysis
2. Stereolithography
3. 3D facial morphometry
4. Moirés topography
5. Contour photography

The assessment of facial muscle movements requires facial expressions to be recorded in a dynamic state, such that the speed, magnitude, pattern and symmetry of facial muscle movement can be evaluated. Static capture of expressions does not record the direction, speed and pattern of facial movement, and therefore is not a robust or accurate means of analyzing the dynamics of facial expressions. There are several issues that need consideration before the objective assessment of facial asymmetry is carried out. Whilst patient associated factors are important to consider, what is equally important is to identify appropriate facial muscle movements. Previous studies utilized facial expressions, or verbal facial actions such as words, numbers or sentences. The ideal facial motion is one that is reproducible over time, so it is performed as near to the same way on each occasion. Aside from clinical consideration, quantification of facial asymmetry (especially in 3D and 4D) poses a problem from the technical aspect. Dynamic capture of facial expressions has a technical difficulty, in that it may result in several hundred 3D images of one particular facial movement for just one patient. This results therefore, in an exponential increase in the volume of data to be processed and interpreted and a corresponding increase in the time required to process data. A thorough knowledge of computational approaches is therefore essential to ensure effective data analysis.

In general, few studies have been conducted on cleft related facial asymmetry in younger children. This is possibly due to the fact that children are not as co-operative as adults. This problem has been overcome by the development of indirect anthropometric studies, which are based on the analysis of the captured images. Dynamic Stereo photogrammetry systems capture facial images at a rate of 60 frames/second, thus generating 180 frames as each expression usually takes about 3 seconds to record. 4D imaging for analysis of facial surfaces in CLP patients has been carried out. However, the analysis of the dynamics of facial expressions in these studies was confined to a limited number of landmarks, not taking advantage of the thousands of points on the 3D captured facial surface (Hallac et al., 2017).

One of the main aims of cleft surgery is to minimize upper lip scarring. Scarring was associated with unilateral cleft lip repair using the Millard technique (Christofides et al., 2006). 2D photographs were used to assess the color, width and scar thickness. However, the details and the reproducibility of the measurement were not discussed. 3D assessment of lip scarring and dysmorphology in patients who have undergone surgical repair of CLP has been studied (Bell et al., 2014).

2 Review of Literature

Contents

2.1. INTRODUCTION

Innovation in technology in the medical world has moved in leaps and bounds as cutting edge and more sophisticated imaging devices make facial morphology analysis, diagnosis and treatment planning far easier than in earlier times. Clinical applications such as analysis of symmetry in cleft lip and cleft palate patients as well as orthognathic treatment planning, have greatly benefitted from advancements in 3D and 4D imaging technology. Imaging modalities in 3D and 4D include various techniques. Surface based measurements of the face include imaging modalities that do not penetrate the skin and include stereo photogrammetry and laser scanning.

The advantages of surface-based imaging modalities are obvious as these are radiation free. Volumetric based imaging modalities such as CT scans have an advantage in the sense that these produce detailed images in high resolution. However, there is the potential drawback in that CT scans use a higher dose of radiation than normal X-rays and hence can be the source of an increased risk of developing radiation induced cancers (Kwong and Yucel, 2003). Surface based imaging techniques such as stereo photogrammetry, do not use radiations that enter the human body. These involve photographic techniques that generate images of individuals in 3D or 4D and find varied application in diagnosis and treatment planning.

The surface-based imaging modalities can include direct and indirect anthropometric measurement methods. As the name suggests, direct anthropometric measurement methods involve placement of markers on certain fixed anatomic locations of the face and measuring the displacement of these markers on the face directly, in order to measure features objectively such as symmetry scores. These methods have been the quintessential method of measuring craniofacial dimensions since the last century (Brons et al., 2012). Direct anthropometric measurements have a major limitation in that it requires a high level of operator skill and placement of these markers should be fast, accurate and reproducible. Apart from this, patient compliance is low as it

involves staying still for a long period of time and due to the fact that these markers are stuck on the face of the individual participants. Indirect anthropometric measurement methods on the other hand involve assessing and measuring displacement of landmarks marked digitally on a static (3D) or moving (4D) image. This method overcomes the limitation of increased user skill and accuracy required in direct anthropometric methods and does not require prolonged patient waiting times (Brons et al., 2012).

Obtaining 3D surface data – Stereo-photogrammetry

Photogrammetry derives its name from the Greek word "photo" which means light and "gramma" which means writing. It is formally defined as the science of deriving accurate and reliable information about objects and the surrounding environment through assessing, measuring and interpreting images and patterns of energy derived from sensor systems (Adams & Spirakis, 1997). The fundamental characteristic of photogrammetry is that measurement and interpretation is carried out indirectly and not on the object itself (direct anthropometry and its drawbacks discussed previously). In a classical sense, the object required to be photographed is imaged from two separate locations and consequently provides a three-dimensional view to that object when viewed separately or when using a viewing device such as a stereoscope (Adams, 1974). Stereo photogrammetry involves the principle of obtaining the three-dimensional coordinates (X, Y and Z co-ordinates) of certain points on stereoscopic images. Decreasing costs have resulted in increased demands of stereo photogrammetry in clinical applications that require the objective evaluation of facial form and morphology (Honrado et al., 2004). Apart from cost factors, 3D stereo photogrammetry has the technical advantages of faster acquisition time and a more comprehensive surface coverage. There also exists the potential limitation of a considerable amount of space required to set up these systems as these include components such as tripods, an imaging device, cameras, computers and lighting sources.

Figure 18: A 3DMD stereo photogrammetry set up *(Source: Heike et al., 2010)*

Facial form and expressions also play a key role in stereo photogrammetry. Imaging sessions with children can prove particularly challenging as children generally tend to have lower levels of patience and have the tendency to move a lot during longer periods of imaging. Ideally, a neutral expression is preferred in photogrammetric imaging, wherein the participant is asked to have a relaxed face and lips gently touching (Mori et al., 2005).

2.2. WORKING PRINCIPLE OF PHOTOGRAMMETRY

Stereo photogrammetry operates on the principle of triangulation. In a layman sense of speaking, an object is photographed from two different locations, thus creating two different lines of sight- technically speaking the two side arms of a triangle. These two lines of sight can then be interpreted mathematically to obtain the three-dimensional coordinates of the object in question.

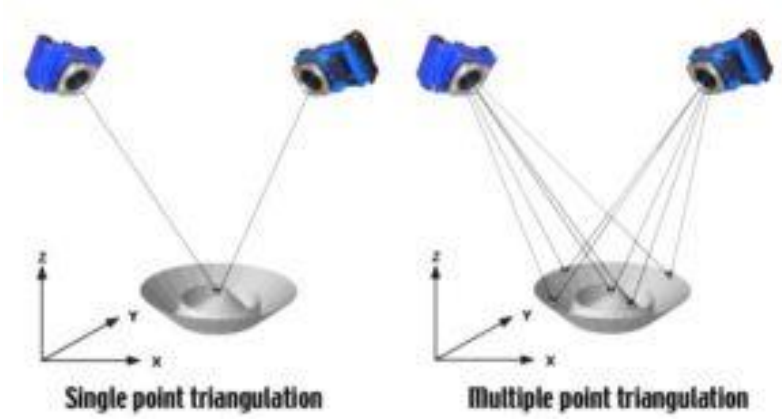

Figure 19: The Triangulation principle *(Source: GIS resources, 2013)*

The triangulation principle involves using a stereo pair of cameras to estimate the third dimension or the depth of the object. The differences between the two-dimensional location of points on the two images generated by the pair of cameras is correspondingly used to interpolate the third dimension, thereby estimating the depth of the object i.e. the third dimensional coordinate. The distance between the two cameras is fixed whereas the distance between each camera and the object varies depending on the specific point on the object to be viewed. In this way, the X1, Y1 and X2, Y2 coordinates (distance of each camera from a point on the object) of the object are known. The third or the z coordinate is calculated as z= df/ X2-X1. The 'f' is the focal length of the camera and 'd' is the length of the stereo baseline or the distance between the two camera lenses.

There are three types of photogrammetry- active, passive and hybrid photogrammetry. **Active photogrammetry** consists of projecting a light source pattern on the object and detecting the deformation of the pattern from different positions. **Passive stereo photogrammetry** involves the determination of the third dimension of an object without the use of a structured light source. As there is the lack of structured patterns, the determination of correspondences in passive photogrammetry is much more difficult than in the active type**. Hybrid stereo photogrammetry** is simply a combination of the active and passive forms and typically has higher accuracy and quality of images (Tzou et al., 2014).

In a study carried out by Van loon et al. in 2010, stereo photogrammetry was used to assess the volumetric changes in nose dimensions in cleft lip and cleft palate patients, both pre-and post-operatively. The reliability of the method was tested both intra and inter operatively and correlation tests revealed that stereo photogrammetric methods are a reliable, sensitive, fast and non-invasive method of imaging in patients with cleft lip and palate.

The most common stereophotogrammetry systems are the Di3D (Glasgow) and the 3dMD. Although based on the same principle, the two systems differ in terms of algorithms and imaging techniques. The Di3D system employs passive stereophotogrammetry wherein it relies entirely on natural skin features and generates 3D images based on these natural patterns. 3dMD systems combine active and passive stereophotogrammetry into a hybrid system. Tzou et al. (2014) compared the applicability of the Di3D and 3dMD systems and it was seen that the Di3D systems was better in terms of simplicity as regular cameras were used with flashlights, eliminating the need for the industrial sensors used in 3dMD systems. 3dMD systems on the other hand showed faster processing times and was seen to be the better system according to Tzou et al. (2014).

2.3. What is 4D imaging?

4D imaging systems enable the capture of the dynamics of facial movement by considering the movement of facial structures over time. These imaging systems can capture color textured 3D model sequences of dynamically deforming surfaces such as the moving face i.e. face movement following performing facial expressions.

Figure 20: Di4D head mounted motion capture system *(Source: Dimensional Imaging, Glasgow, 2015)*

3D motion stereophotogrammetry (4D) analysis uses two detection systems- the marker-based motion detection and marker less detection system. In the marker-based systems, camera pairs track the motion of infrared signals produced from active markers or passive reflective markers. Examples of the marker-based systems include the Vicon, C3D and the Microsoft Kinect. Marker less systems do not use markers placed on the face and instead detect motion using video recordings. Commonly available systems are the Di4D and the 3DMD systems. The 4D imaging system used in this study is the Di4D imaging systems manufactured by Dimensional imaging, Glasgow. The Di4D system consists of a pair of monochrome video cameras and a single colored video recording camera. A white light source is used as an external illuminating source and the cameras capture images at a rate of 60 frames per second. Landmarks are manually located and placed on the first frame and then automatically tracked across subsequent frames. The process of accuracy of placing landmarks was studied and evaluated by Al-Anezi et al. in 2013 and has been correspondingly used in several studies (Shujaat et al., 2014).

Figure 21: 4D imaging system used in this research study

2.4. IMAGE REGISTRATION

Image registration is defined as the process of converting different sets of data in to one coordinate system (Brown, 1992). Registration is a fundamental task in image processing used to match two or more pictures taken, for example, at different times, from different sensors, or from different viewpoints. Virtually all large systems which evaluate images require the registration of images, or a closely related operation, as an intermediate step. Specific examples of systems where image registration is a significant component include matching a target with a real-time image of a scene for target recognition, monitoring global land usage using satellite images, matching stereo images to recover shape for autonomous navigation, and aligning images from different medical modalities for diagnosis (Brown, 1992). There are three fundamental types of image registration-landmarks based registration, surface-based registration and voxel-based registration.

2.4.1. Landmark based registration

Landmark based registration procedures involve the application and identification of landmarks in order to superimpose two images onto each other. The Procrustes analysis is an example of a landmark based registration. The Procrustes analysis is a shape comparison algorithm which consists of the processes of translation of the images (such that the centroid of all the points of the images lies at the origin), scaling (changing the size of the images to correspond to each other), and rotation (rotating the images such that the sum of the squared distances of points between the two objects/images is minimised). In several applications using Procrustes analysis, the step of scaling is not carried out, thus preserving the size of the images in question to be superimposed. This is called **partial** Procrustes analysis as compared to **Full** Procrustes analysis in which scaling is carried out. The term ordinary Procrustes refers to Procrustes matching of one observation onto another. Generalized Procrustes refers to matching of at least or more than two observations onto one another (Gower, 1974).

Since the Procrustes analysis consists of manual identification of landmark points following which superimposition takes place, this registration process is prone to errors on account of operator sensitivity and accuracy.

2.4.2. Surface based registration

Surface based registration depends on the matching of surface topography between the two images to be superimposed. Although it does not require the placement of certain landmarks on the images, these can serve as a useful starting point for the matching process. An example of the surface-based registration is an algorithm called the Iterative closest point algorithm (ICP). The ICP is a matching process which considers one image as the reference image and the other as the target image. It then creates a cloud of points on both the images and carries out the processes of translation and rotation in a series of steps to bring the two images closer to each other by minimizing the sum of squared distances between corresponding points on the images (Marani et al., 2016). At each step, the algorithm assesses the local distance error and realigns and carries out

translation and rotation again (hence the term “iterative”) until the local error is a minimum and the two images are superimposed onto each other.

This study involves the novelty of using a surface-based method of analysis (Section 2.5.3.), which utilizes the entire facial surface for assessment. A generic mesh is a facial mesh which consists of several thousand vertices and undergoes elastic deformation or “conformation” (Figure 22) to resemble the underlying facial topography. The superimposition of the face meshes is done using the Procrustes analysis in this study.

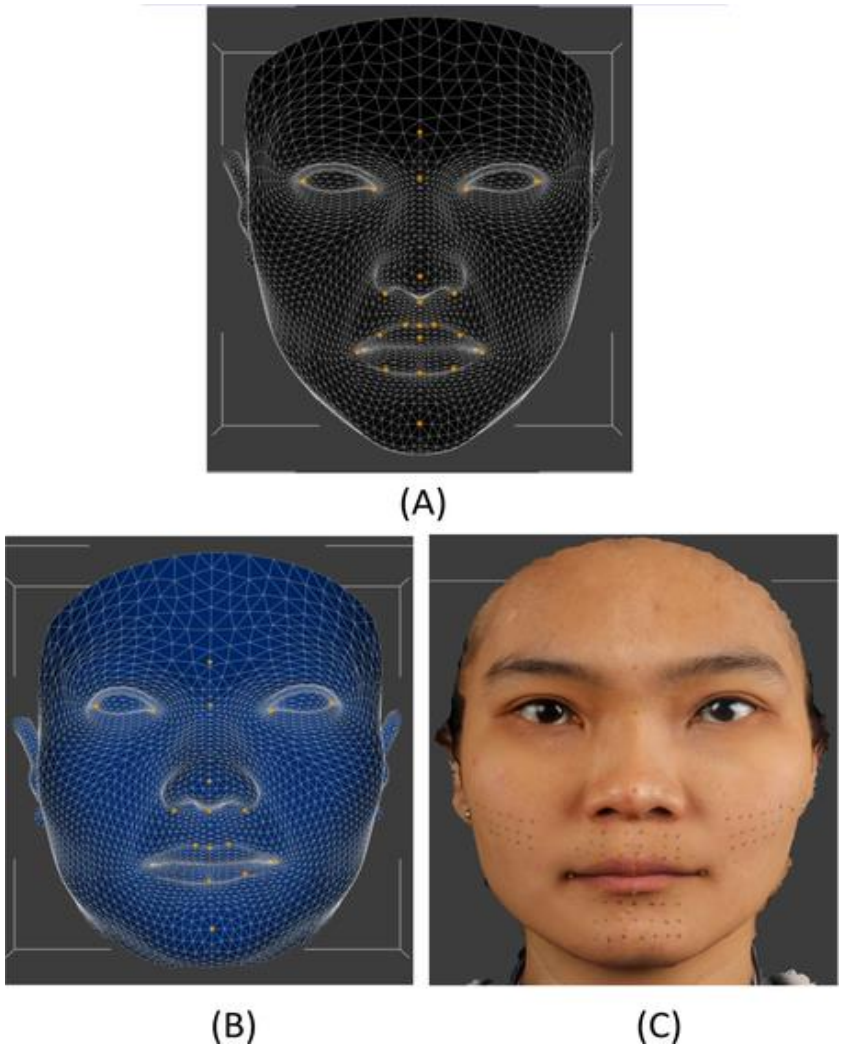

Figure 22: Generic mesh and its conformation to resemble the subjects face shape (A) Unconformed generic mesh (B) Conformed mesh with similar shape of the simulated surgical mesh (C) with the structure and topology *(Source: Cheung et al., 2016)*

2.5. Analysis of the dynamics of facial expressions:

2.5.1. Direct & Indirect Anthropometry

Analysis of facial asymmetry and facial morphology assessment in the past was carried out using direct anthropometry. This method of measurement has been mostly replaced by indirect anthropometry methods including 2D, 3D and 4D measurements of the facial complex. Direct methods of facial assessment include the measurements of facial distances and angles directly on the face of the individual using measuring devices such as vernier calipers, sliding calipers or spreading calipers. A lot of work on facial morphology assessment was carried out using direct anthropometry (Farkas, 1994). There exist several limitations of the direct method of assessment and these include poor compliance of patients due to having their face measured for prolonged times, the training required prior to analysis, and the time-consuming nature of the method (Wong et al., 2008; Aung et al.,1995).

These methods of assessment have, in recent years, been replaced by indirect methods of measurement where the measurements are carried out digitally and not on the face of an individual. This method offers the advantages of faster processing time and better patient compliance as compared to direct methods.

Indirect methods can include 2D, 3D and 4D methods of analysis of facial morphology. Until recently, two-dimensional methods of analysis of asymmetry of the face have been used wherein photographs and videos in 2D were analyzed using landmarks in a frontal view. The use of clinical photographs coupled with cephalic radiographs allow the assessment of both soft and hard tissues (Kim et al., 2014). 3D methods of assessment of facial morphology have become more common recently, as these methods measure asymmetry in all 3 spatial planes and provide for a more thorough investigation of the facial morphology, taking into consideration that the face is a 3D structure (Nkenke et al., 2006; Russel et al., 2014; Staubes et al., 2008).

More recently, 4D methods of assessment have come into the forefront with systems such as the Di4D, providing an opportunity to measure the dynamics of facial movement by focusing on asymmetry in 3 dimensions in a moving face (the 4th dimension). Previous work conducted in 2D, 3D and 4D has been discussed in the next section. This section will discuss the major types of analysis used to measure facial asymmetry.

2 main types of analysis used are the landmarks-based analysis and the surface-based analysis.

2.5.2. Landmarks based analysis

Landmarks based methods are limited to the use of certain specific landmark points on the face. Any change that occurs on the surface around these landmarks are not considered. An important drawback to this technique is the lack of comprehensiveness as this does not cover the entire facial surface. Landmarks-based analyses do however incorporate anatomic considerations in their analytical methods.

Cleft lip and palate related asymmetry have been studied previously using landmarks-based analysis (Trotman et al., 2007; Trotman et al., 2013; Hallac et al., 2017).

Following are the types of landmarks-based analysis: -

2.5.2.1. Linear and Angular measurement

A substantial amount of facial asymmetry analysis is based on measuring linear and angular distances between specific set landmark points, or in order to add comprehensiveness- adding supporting landmark points in addition to these initial landmarks and using distances and angles to determine a score for facial asymmetry in cleft patients.

Linear measurement refers to the distance between landmark points on two sides of the face. Distance between landmark points have been commonly used in a lot of cleft associated facial asymmetry research in the past. Choi et al. (2013) conducted a study to compare the soft tissue asymmetry between the unaffected and affected side in non-syndromic UCLP patients. They used linear and surface measurements to assess anteroposterior, transverse and vertical asymmetry by utilizing distances between three reference planes (Basion-perpendicular, mid-sagittal reference and horizontal planes) and the intersecting points. The study showed that soft tissue in the nasolabial and dentoalveolar region of the cleft side was inactive and posteriorly arranged as compared to the unaffected side.

Othman et al. (2016) analyzed the facial features of 20 Chinese children with repaired UCLP and compared them to a control group using linear measurements between specific facial landmarks. Landmark distances like inter-canine width, ocular width, alar base root width and nose dorsum length were used for analysis of the facial profile. Significant differences were seen in the nasolabial region. The cleft group showed a flatter nose, wider alar base root width and broader nostril width on the cleft side.

Similar landmark based linear and angular measurements were used for asymmetry assessment in several studies in the past (Zreakat et al., 2012; Bughaigis et al., 2013; Bell et al., 2014; Othman et al., 2014; Morioka et al., 2015; Trotman et al., 2000; Trotman et al., 2013; Trotman et al., 2018).

2.5.2.2. Vector analysis

The vector analysis utilizes vector maps comprising the directional features and magnification of linear displacement of landmark points. Vector analysis has been used in previous work including mandibular asymmetry and changes in facial dimensions in 3D. Verze et al. (2011) quantified facial movements using vector mapping which utilizes landmarks displacement vector for every movement.

2.5.3. Surface based analysis

The drawbacks of the landmarks-based analysis, mentioned above, are overcome using the entire facial surface for measurements. This includes color maps, absolute surface distances and dense correspondence analysis as the most commonly used surface-based measurements. The only drawback associated with surface-based analysis is the lack of anatomic correspondence associated with these methods.

1. Colour Coded Maps

The 3D colour coded distance map provides a means to assessing distance between two mesh surfaces by evaluating the distance between the vertex in one mesh and the corresponding closest vertex in the mesh to be compared. These distances between the two compared meshes are then visualized in the form of a comprehensive colour map in which colors range in a spectral scale from green to blue to yellow to red. These colors are assigned to each vertex depending on the distance between the original and adjacent (mirrored) surface mesh. Numerical values such as means, and standard deviations can also be incorporated in the scale of colours which allows the viewer to better interpret these maps and assess the disparity in the meshes being compared. Another major advantage with the colour maps is the fact that directionality can easily be assessed between the surface meshes in question. Considering the geometric centroid of the 2 meshes to be compared as a reference point for directionality, the higher the distance between the meshes in a direction away from the centroid , the greater the shift in colour scale towards the red color and the higher the distance between the meshes in a direction towards the centroid, the more the shift in colour towards the blue range.

Modifications can be made to the spectral colour ranges used in the colour-coded maps. Different colors can be used to interpret different values. For example, Kau (2006), modified the conventional spectral color range from blue to red to a threshold-based coloring pattern in which threshold points represented levels of

clinical significance. Vertices with lower distance measurements were shown as black and ones with higher distance measurements were shown in white, thus allowing the surface to be analyzed in a more objective manner as levels of clinical significance were taken as a reference point.

The use of these colour-coded surface maps is immense as they can be used to assess facial movement pre and post orthognathic surgery as well as to assess facial movement in cases of facial deformity such as cleft lip and palate and sex and age differences among the population as well. Limitations to this method include the lack of anatomical correspondence as this relies on the geometric center of the facial shells or meshes in question.

2. Dense Correspondence analysis

A limitation in the colour-coded surface maps was the fact that there was no anatomical basis of correspondence as the geometric center between the meshes compared was taken in to consideration. The dense correspondence analysis in a way overcomes the limitations of a lack of an anatomical basis. This method of analysis is a landmarks free analysis system but as a matter of fact can be considered a complete comprehensive landmarks-based analysis as it considers every single vertex on the surface mesh as a landmark. Thus, in a way, it has the objective advantages of a landmarks-based analysis and the comprehensiveness advantage of a surface-based analysis.

The method of dense correspondence analysis involves firstly the generic mesh. The generic mesh is a mathematical surface which represents the facial morphology and morphometric information of an average face and is indexed which means every vertex and distance between vertices are pre-measured. It is referred to as a generic mesh because it is universal and can be used on any facial shape for morphometric assessment. The generic mesh can be generated using 3D modelling software or it could represent an average facial model which consists of the facial morphology of the study population (Kau et al., 2010).

The next step is a process called “conformation”- the elastic deformation of the generic mesh in order to take on the facial morphology of the facial surface in question. This step brings the vertices of the generic mesh and the facial surface in question in to alignment in order to carry out the transformation of the elastic deformation of the generic mesh to resemble the underlying facial morphology. Following this step, the process of superimposition is carried out between the two meshes to be compared (in the case of this study- the conformed original mesh and its mirror image). The process of superimposition was carried out using partial Procrustes analysis

Following this step, the distance and disparity between the two facial meshes in question can be ascertained by using color maps and Procrustes or absolute mean distances.

3. Absolute surface distances

In this method, the distances between two facial meshes is measured by calculating distances between vertices on one mesh to that on the other. This method requires accurate superimposition of facial images before taking into account the disparity between two facial surfaces. (Kau & Richmond, 2008 ; Djordevic et al., 2014 ; Maal et al., 2011.)

2.6. FACIAL ASYMMETRY ANALYSIS

The surface of the face is the most visible area of the human body that both clinicians and lay individuals see and forms the key to aesthetic judgements. Symmetry is defined as “equality or correspondence in the form of parts distributed around a center or an axis, at the two extremes or poles, or in opposite sides of the body” (Patel et al., 2015). Although a mild degree of asymmetry is common in the face of normal human individuals, orthodontists and surgeons often encounter patients with severe asymmetries. Facial symmetry is historically associated with attractiveness (Grammer & Thornhill, 1994), and severe asymmetry may have a psychosocial impact (Shaw et al., 1995). Severe asymmetries combined with other skeletal deformities may require surgical intervention (Eubanks, 1957). Therefore, accurate localization and quantification

of the extent of facial asymmetry is crucial in order to facilitate diagnosis and establish treatment goals.

2.6.1. ASSESSMENT OF FACIAL ASYMMETRY USING STATIC 3D IMAGES

There are several facial deformities that lead to severe and moderate facial asymmetry. Cleft Lip and Cleft Palate is one such craniofacial anomaly that causes facial asymmetry which can be corrected by means of cleft lip repair, nasal reconstruction and revision surgeries. Following these surgeries however, a certain degree of asymmetry still persists, and it is of utmost importance that this asymmetry be assessed post-surgically and compared. An objective assessment of facial asymmetry is extremely important in this regard and forms the basis for this study. The repair of the unilateral cleft lip has now reached a level where further advances are directed to a better aesthetic result as viewed by the patients and the surgeons. The clinical decision as to whether a cleft lip requires secondary surgery may often differ between surgeons on the same patient. Trotman et al. (2007) assessed the functional outcomes of cleft lip surgery and the need for secondary corrective procedure to improve the aesthetic outcome. In part 1 of their study, the decision for lip revision was based on subjective clinical criteria where the clinicians may disagree. Their findings suggested that the agreement among surgeons was poor and they supported the need for more objective measures to assess the need for revision surgery.

Part 2 of their study was therefore aimed at objectively quantifying and evaluating nasolabial movement in patients with surgically corrected cleft lip and cleft palate. It was hypothesized that participants with repaired CLP have impairment in magnitude, direction and symmetry of nasolabial movement as compared to non-cleft volunteers. It was also hypothesized that nasolabial movement was worse in patients with bilateral cleft as compared to UCLP participants. A video-based tracking system was used to measure circum-oral movements of each participant by using 38 retro-reflective markers attached to the face. Five maximal animations of the face were recorded, and 3D images were captured and generated. As hypothesized, clear differences were seen in upper lip movement

between non cleft volunteers and participants with CLP during maximal smile and natural smiles. Also, for all facial movements, the revision group (scheduled for lip revision surgery) and non-revision group (not scheduled for any revision surgery) had restrictions in upper lip movement as compared to non-cleft volunteers. For participants who underwent surgery, the overall upper lip, vertical upper lip and lateral upper lip movements were most restricted during maximal smiling and natural smiling and least restricted during the grimace expression. Thus, this study not only objectively assessed nasolabial movement post cleft lip and cleft palate repair but also assessed which facial expressions were associated with maximum asymmetry. This study however could only provide limited information on facial movement due to only certain specific landmarks being assessed. It could have been improved by utilizing all points on the face. A major limitation in the study was the use of markers on the face. Several drawbacks such as marker slippage, time involved in the placement of these markers, correct placement of these markers and reproducibility in placement of these markers, made this objective assessment of asymmetry seemingly inaccurate. Furthermore, this study by Trotman et al. (2007) did not measure the dynamics of facial expressions. Instead it only measured changes in inter-landmark distances during five maximal expressions. There was also the time period of 3 months post-lip revision surgery which might be considered too short a time span to assess changes in mobility and symmetry.

Another study carried out by Trotman et al. (2013), aimed to determine differences in facial movement between infants with cleft lip and palate and non-cleft individuals as well as determine changes in facial movement pre and post primary lip repair surgery. A 3D video-based tracking system was used to capture dynamic facial images. This system tracked the movement of markers attached to 12 facial landmarks. Facial movements included spontaneous facial movements, movements in response to mother's voice and facial movements in response to taste stimuli of sweet and salty food (as participants were aged less than 6 months). 3D measurements of facial movements were based on changes in inter-landmark distances. It was seen in this study that infants with unilateral and bilateral CLP had 58% and 118% greater lateral upper lip movement (right inner upper lip to left inner upper lip distance) than controls. This difference became

negligible after surgery. A possible limitation in this study could have been the fact that cleft lip and palate patients may have decreased palatal taste buds or missing taste buds. This may result in no movements elicited in response to taste stimuli. A possible selection bias may be present in that, patients with cleft lip and palate exhibit higher upper lip movement and asymmetry due to the Orbicularis muscle being disrupted. The Levator muscles and the Masseter and Buccinator exhibit a pull on the lateral upper lip, resulting in hypermobility and asymmetry. The dynamics of facial movements was not discussed at all in this study. The assessment of facial expressions and facial asymmetry was carried out on static images of the face. Furthermore, information obtained on asymmetry was limited as 12 landmarks were used and such a limited range of landmarks would not give robust asymmetry measurement of the whole face. The need for more advanced objective assessments of the repaired unilateral cleft lip has resulted in complicated methods to assess facial asymmetry.

Again, there is a severe paucity of studies associated with measuring facial asymmetry in 4D. Most of the literature reviewed consists of facial asymmetry objectively assessed based on different parameters such as morphology, shape, color etc. using 3D imaging. A study in this regard by Bell et al. (2014), assessed residual asymmetry in surgically managed UCLP patients and compared this with non-cleft controls. It was seen in this study that asymmetry for the whole face was significantly higher in UCL and UCLP patients as compared with the controls. UCLP asymmetry was higher than UCL asymmetry. In cleft patients, the upper lip and the nasal rim were the most asymmetric. Control subjects also displayed a degree of facial asymmetry. Maximal smile increased the asymmetry of the vermillion border and nasal rim in all three groups. 3D static capture of facial expressions is not as comprehensive as dynamic capture of facial movement and the need arises for the capture of facial expressions while in movement (4D).

Ras et al. (1995) in a longitudinal study reported how facial asymmetry in children with clefts changed over time. It was seen that only the alar base showed change in facial asymmetry in the cleft and control populations. Stevens et al. (1999) studied nasal asymmetry as a primary outcome measure in cleft surgery in children

with unilateral cleft lip and palate, aged 9 years and compared this with a control group aged 7 to 11 years. Measurements in this case were mainly 2D as nasal outlines and nose dimensions were taken into consideration using computer assisted methods. No significant differences were seen in nasal asymmetry between the UCLP group and control group. However, sample sizes were small and 2D measurements as stated above do not accurately assess the three-dimensional morphology of the nose.

Yamada et al. (2002) conducted a study on 10 infants with UCLP who underwent rotation-advancement repair and 10 infants with UCLP who underwent triangular flap repair. A control group of 151 infants aged 4 months and 1.5 years was the comparative basis. A laser scanner was used to extract 3D facial measurements at different time points post-surgery- 2 weeks, 3 weeks, 3 months and 1.5 years. Despite the 3D data obtained, results on asymmetry of the nasal region was merely descriptive or at best showed linear differences between the cleft and non-cleft sides. It was seen that the asymmetry improved after the rotation-advancement procedure after 1.5 years.

Another such study using 3D imaging carried out by Darby et al. (2015), assessed the effect of smiling on facial asymmetry in adults with class 1 incisor relationships. This study also showed that overall facial asymmetry was greatest for maximal smile followed by the natural smile. No gender differences in asymmetry were noticed in this study. A major limitation in this study however was that areas with high levels of asymmetry (such as the lip area) could get diluted by areas with low levels of asymmetry, as mean Euclidean distances were used as a measure of facial asymmetry. These mean scores may therefore distort results. Another limitation in this study was that the participants involved in this study were completely normal with no previous history of facial deformity. The use of measuring asymmetry during facial expressions will be more to quantify facial asymmetry in craniofacial conditions rather than in normal participants.

Berssenbugge et al. (2015) in a similar study measured facial symmetry in terms of facial shape and color. A subjective (using rating on an integer scale from 0-100) and objective assessment (using colors of the face on a CIELAB color space followed by using ICP to measure the color asymmetry) was carried out for the color and 3D shape. This study had a small sample size of 30 healthy participants. Another potential limitation was the static nature of image capture. Capturing images during facial movement may have made the study more comprehensive. A major disadvantage of subjective rating is the variable internal consistency and reproducibility among raters. Also, it is very difficult to rate symmetry and attractiveness using an integer scale of 0-100, with integers in between not assigned any characteristic features of attractiveness. This was seen in a study in which visual analogue scales were used to rate attractiveness in orthodontic patients (Phillips et al., 1992). There was a significant difference between the subjective visual rating and the objective ranking scores assigned to these patients. Therefore, although visual analogue scales are convenient and rapid, it seems to be affected by personal idiosyncrasies of raters such as skill, mood at the time of rating etc.

Manyama et al. (2014) reported 3D facial shape differences to be significantly different in unrepaired non-syndromic cleft cases as compared to the controls. The cleft lip and palate group exhibited increased nasal and mouth width, increased intra-orbital distance and more prognathic premaxillary region. Within the cleft lip and palate group, facial shape analysis was carried out using PCA and showed that facial shape variation is associated with facial height, nasal cavity width, interorbital distance and midfacial prognathism. The isolated cleft lip and palate groups did not differ significantly from one another in terms of facial shape.

A recent study by Patel et al. (2015) measured facial asymmetry using 3D surface imaging. This was a landmark-independent method carried out on a group of patients with obvious facial asymmetry (requiring orthognathic treatment as ascertained by a group of orthodontists) and a group with no facial asymmetry. Quantification of facial asymmetry was done by superimposing each patient's 3D image onto its mirror image. Color maps and RMS (root mean square) mean values

were used as asymmetry indices. The root mean square values were statistically significant for the lower face in the asymmetry group as compared to the symmetrical subjects. The RMS values were statistically significant between upper and lower face in the asymmetrical subjects. Here again, the study suffered from a small sample size. Using mean values of asymmetry does not show how asymmetry is distributed over the face or the direction of asymmetry. Using mean values may result in balancing out higher asymmetry scores with lower ones and thus may distort results. This study may have been more comprehensive, had 3D images been captured during facial movement, as facial expressions and facial movement are an integral part of human facial balance and symmetry.

Very few studies on face shape and asymmetry have been conducted on children. One of the few studies by Djordjevic et al. (2014), assessed the effectiveness of facial laser scanning to quantitatively assess facial asymmetry in 5-year-old children with repaired UCLP using a surface-based 3D analysis method. Average faces were constructed for males and females in the non-cleft control group for comparison with the individual faces of cleft children. The average distance and the percentage of coincidence using color maps were used as facial asymmetry indices. The whole face asymmetry as well as individual parts of the face were considered for asymmetry measurement. Statistical differences in asymmetry were seen in UCLP cases in all measured regions except the forehead. No significant differences were noted in average distances between the cleft group and the control group. This study like several other asymmetry studies suffered from a small sample size of only 12 cases of UCLP. Laser scanning also requires longer capture time (usually about 8 seconds) and achieving co-operation with children for that period of time can be quite daunting. Impact of the gender on asymmetry was not explored due to the small sample size. A more comprehensive analysis was not considered to explore the direction of facial asymmetry.

Al-Rudainy et al. (2018) conducted a study to quantify facial asymmetry in Unilateral cleft lip and palate patients before and after surgical repair. A 3D analysis using the conformation of a generic mesh was carried out on 3D images of 30 patients (mean age of 3.7 months) acquired one to two days before surgery

and four months after surgery. The study considered the entire facial surface as it involved elastic deformation of a generic mesh in order to resemble the patients underlying facial morphology. The distance between vertices of the pre-operative and post-operative meshes and their corresponding mirror images was the basis of quantifying facial asymmetry. Asymmetry was measured in all three spatial planes and it was seen that maximum asymmetry was noticed postoperatively in the nasolabial region. Preoperatively, the philtrum and bridge of the nose showed deviation to the non-cleft side whereas vertical asymmetry was noticed at the upper lip. The study showed that facial asymmetry improved following surgery with residual antero-posterior asymmetry at the alar base and upper lip on cleft side. This study was a 3D assessment of asymmetry as this did not consider the moving face and only assessed the asymmetry on a static facial structure. 3D analysis is unable to understand the dynamics of facial movement and asymmetry on the moving face enables the understanding of how asymmetry can be reduced by laying emphasis on specific muscle groups involved in the movement. No control group was included in this study and therefore there was no comparative basis between the cleft group and a healthy population.

Wong et al. (2019) used 3D stereophotogrammetry to assess nasolabial deformity in 16 surgically repaired UCLP patients (adults) and compare this with a non-cleft control group. Linear and angular measurements between 42 landmark points were used to assess facial asymmetry. In addition, they also used a conformed average UCLP facial mesh and compared it with a conformed average control facial mesh using Procrustes analysis. Correspondingly x, y and z distances between the two average faces were depicted in color maps. The study only considered 42 landmarks and the difference in linear distances between these landmarks. The entire facial surface was also studied due to dense correspondence analysis using facial surface meshes for assessment. Furthermore, this was a 3D study and did not analyze the complexity and asymmetry of facial movement. Significant differences in asymmetry scores and linear and angular measurements were noted between the two groups.

Yilmaz & Germec (2018) conducted a 3D study to assess nasolabial morphology before and after naso-alveolar moulding in UCLP patients. This study used 3D images of facial plaster casts and then measured nasolabial linear distances to assess nasolabial dysmorphology. No differences were seen between pre and post naso-alveolar moulding except in the nasal width. This study only assessed specific landmarks and the distance between these landmarks and did not consider the entire nasolabial surface topography.

Aside from Cleft Lip and Cleft Palate, there are several other conditions which cause pronounced facial asymmetry. Condylar Hyperplasia is one such condition. Verhoeven et al. (2013) quantified objectively facial and mandibular soft tissue asymmetry in patients with unilateral condylar hyperplasia. In order to assess and quantify facial asymmetry, the 3D image of participants was superimposed onto its mirror image and the ICP was used to this regard. The registration resulted in color maps which measured the distances between two corresponding points on the original and mirrored images. These distances were used as a direct measurement of facial asymmetry. Capturing 3D images during facial movement may have explored a different pattern of asymmetry that is associated with facial expressions, as facial expressions are an integral part of human facial balance and symmetry. Using the absolute mean to quantify asymmetry may result in balancing out high asymmetry scores with lower scores. Impact of gender on facial asymmetry was not explored.

In order to eliminate the drawback of using average scores on the whole face, a study by Meyer-Marcotty et al. (2010) was aimed at measuring the degree of facial asymmetry in adults with cleft lip and palate in comparison with a control group using a landmark independent method. It also aimed to identify areas of the face which revealed asymmetry and analyze its impact on the visual perception of facial appearance. An optical 3D sensor was used to acquire facial images. Quantification of facial asymmetry was carried out by measuring the mean absolute distances of points between the original 3D data and the mirrored data. The face was divided into two parts- the midface (nasion to subnasale) and the lower face (subnasale to gnathion). For visual appearance rating, 30 volunteers

were chosen. It was seen that the entire face asymmetry was higher in CLP patients than in controls. Asymmetry of the mid-face and lower face was higher in CLP patients than in controls. The highest mean difference of asymmetry between the CLP patients and the controls was found in the mid-face followed by the lower face. In terms of the subjective assessment, CLP patients were rated more negatively in terms of appearance and symmetry than the controls. Asymmetry of the mid face was positively correlated with the rating task for symmetry and facial expression. In other words, it was seen that assessors focus on the region of the eyes, the nose and the mouth while perceiving appearance and symmetry. In this study, comprehensiveness could be more robust by using 3D dynamic data instead of static images of the face. While carrying out the picture rating task, the facial images were rated for three conditions- appearance, symmetry and facial expressions on a scale of 1-9. It is natural that such rating scales have a drawback in that the space between each grade from 1-9 cannot possibly be equidistant and defining each grade individually will make assessing easier and perhaps more standard. Therefore, it may fail to measure the true responses of the raters in an objective manner. The role of gender on asymmetry was also not assessed in this study.

As seen in the above studies, static images in 3D may not be comprehensive enough and the need of the hour is 3D dynamic imaging (4D).

2.6.2. ASSESSMENT OF FACIAL ASYMMETRY USING DYNAMIC 4D IMAGES

Very few 4D imaging related studies have been carried out. Quan et al. (2012) presented an automated method to measure the asymmetry of 3D faces not only on static but also in dynamic mode. The y-z plane was used as the reflection plane to obtain the mirror image of the original face. After superimposition of the mirror and original image using ICP, a symmetry plane was extracted after the original and mirrored faces are matched. The symmetry plane in this study was estimated by fitting the midpoints using a mathematical formula. The asymmetry of the face was measured finally by measuring the average distance between two points- one on the original face and the other on the mirror face. The face was divided into

2 regions for asymmetry measurement- an upper half and a lower half. The study described a method to measure facial asymmetry using dynamic scans of the face, considered independent of variations in facial expressions. It was also able to obtain a set of points which could be used to divide the face into local regions. This study suffered from a small sample size of just 4 patients with stroke. Intra-operator reliability was not discussed in this study despite the fact that the study was carried out at two scanning sessions, performed at a month's interval apart. Using average distances may be disadvantageous as it may result in balancing out higher asymmetry scores with lower ones. The upper and lower facial regions were not anatomically defined by the researchers. Also, dividing the face into upper and lower halves may not be anatomically accurate as asymmetry differs in as much as between the upper lip and the lower lip, as seen in previous studies. It was also not clear as to why the researchers used two different planes of symmetry. The researchers did not explain what facial expressions were examined while scanning the patients. As seen in the above study by Quan et al. (2012), defining regions of the face and measuring facial asymmetry in not only the whole face but also individual parts of the face, allows comprehensive assessment of facial asymmetry. This would also eliminate the drawback of mean asymmetry scores of the whole face measurements and avoid the disadvantages of the higher scores being balanced out by lower scores.

A 3D motion capture (4D) study to assess the reproducibility of three facial expressions was carried out by Ju et al. (2016). 23 landmarks were digitized directly on the first frame and subsequently automatically tracked for further frames. The dynamics of each landmark movement was described by landmark motion curves. Magnitude and speed of landmark displacement as well as motion curve similarity was measured. It was seen that cheek puff showed no significant difference as compared to maximal smile, but lip purse showed a significant difference with respect to landmark movement similarity. This study was carried out on healthy individuals without facial deformities. This method of assessing reproducibility of facial expressions will be applied in cases suffering from facial motion deficiencies and facial deformity. A possible limitation in this study was that certain landmarks were located in blind spots of the camera such as on either side of the eye (Exocanthion and Endocanthion) and these landmarks may get

obscured as the skin creases around it. Another possible drawback was the time period of 15 minutes between the two captures. This time period was perhaps too short to assess reproducibility of facial expressions, a time period of a month or more would have been ideal.

Previous 4D work was carried out on cleft lip and palate populations in a study by Hallac et al. (2017) used 4D imaging to record facial movement during two facial

expressions. It was seen that the cleft group showed higher magnitude of asymmetry as well as asymmetry of pattern as compared to the control group (a mean asymmetry of magnitude of the motion path of 26% in the cleft lip group vs 9% in the control group and a mean asymmetry of the shape of the motion path itself of 0.055 in the cleft lip group vs 0.039 in the control group). Differences were statistically significant. However, a major limitation in this technique was the use of only 13 specific landmarks to assess facial asymmetry. The advantages of dynamic measurement of facial movement were diluted by the fact that a comprehensive coverage of the whole facial morphology could not be taken into consideration. Also, the sample size was small and only recorded two facial expressions- the smile and the pout.

Trotman et al. (2000) conducted a study to assess nasolabial displacement during facial movement during four facial expressions in repaired cleft lip and palate patients. Their study emphasized the need for a dynamic approach to assess facial asymmetry and objectively analyze facial movement. 14 skin-based landmarks were used to measure their displacement. The sample size was small and consisted of 4 UCLP patients, 5 BCLP patients and 50 controls. After adjusting for head movement, they found that restricted movement during maximum smile, lip purse and cheek puff was noted in the nasolabial fold region whereas during grimace restricted movement occurred in the alar regions. Their study used specific landmarks to assess facial movement which does not give an accurate representation of the entire facial surface.

Trotman et al. (2007) conducted another video- based motion study to quantify nasolabial movement in cleft lip and palate patients and compare them to controls. 38 skin-based landmarks were used utilizing retro-reflective markers on the face of participants during imaging of smile, lip purse, cheek puff, grimace, and mouth opening. Results showed significant differences between non cleft participants and the cleft group (both revision surgery group and non-revision surgery group). Upper lip movement was highly restricted in cleft groups as

compared to the control group. Lateral upper lip movement was more restricted than vertical upper lip movement according to their study. This was a landmarks-based analysis and therefore could not assess the displacement of the entire facial surface during facial movement. Additionally, there are drawbacks associated with accuracy and patient compliance with regard to placing markers on a participant face.

Of note, is the paucity of articles in the literature regarding the patient's impression of the repair of his or her cleft lip. It is not uncommon that the surgeon would identify a problem which could be repaired with secondary surgery, but the patient wishes for something different to be addressed. It is obviously important that the surgeons evaluate their own results, but it is just as important to understand what the patient is dissatisfied with, as they may point out something completely different from what the surgeon has identified.

2.7. RATIONALE AND JUSTIFICATION

The main justification of the study is to improve quality of care and the treatment delivered to patients with Unilateral cleft lip. The proposed study would provide an objective assessment of asymmetry and facial dysmorphology at rest and with various facial expressions following surgical repair of unilateral cleft lip at an age range of 8-10 years. This may inform the decision of lip revision surgery to deal with the residual scarring and the associated abnormal facial muscle movements.

2.8. STUDY OBJECTIVES

i) To characterize residual facial asymmetry following surgical repair of unilateral cleft lip at rest and with various facial expressions and to compare asymmetry scores with that of controls.

ii) To identify anatomical regions which predominantly contribute to residual facial asymmetry.

2.9. HYPOTHESIS TO BE TESTED

Following are the null Hypothesis tested for: -

i) There is no significant difference in facial asymmetry scores between the UCL group and the control group

ii) There is no significant difference in facial asymmetry scores between the five frames within the UCL group.

3 Material and Methods

Contents

3.1. Study Design

The study design has two components: - a prospective evaluation of a control non-cleft group and a retrospective assessment in a cohort of UCL patients, who had their facial images captured at the Glasgow Dental School and Hospital, as part of routine data collection.

The retrospective study involved 25 patients (8-10 years of age) with Unilateral Cleft Lip (UCL) of the right side or the left side.

The prospective part of the study was conducted on 75 non cleft volunteers as controls. This control group will be age and sex matched to the study group. Participants were recruited as controls after putting up an advert in the Glasgow Dental School and Hospital, Hillhead Primary School and various after-school groups in the West End of Glasgow. An information sheet was distributed explaining to the participants and the parents of the participants the purpose of the study and the methods used. Parental consent and child assent were acquired prior to the imaging sessions. The process of recruiting participants was a laborious one and one which took a considerable amount of time as it was seen that a lot of parents were unwilling to bring their children to a hospital environment after school and work hours. Furthermore, parents of children willing to participate in the study did not find time to attend imaging sessions due to work hours as imaging sessions were held only on weekdays from 9 am to 5 pm in the Glasgow Dental Hospital and School. Children and their parents who were willing to participate, mentioned they could attend on weekends, when parents are off work, but this was not possible as the dental hospital was closed on weekends and permissions for imaging of control participants were obtained only for during hospital opening hours. To add to the issue of difficulties in recruiting participants, a small number of children that attended imaging sessions found it difficult to keep still during performance of facial expressions even though training was carried out prior to the imaging sessions. As a result of unwanted movement during imaging and the resultant noise generated in the data and poor

conformation, that participant had to either be recalled which, was a herculean task in itself, given the lack of time available for parents as mentioned above or the data completely omitted. Due to all these obstacles in the path of recruiting controls, time constraint on the research was always an issue.

The male to female ratio of the UCL group was 1.2:1 (14 males, 11 females), a mean age of 8.68 years and a median age of 9 years. In the control group the male to female ratio was 1.02:1 (38 males, 37 females), a mean age of 8.84 years and a median age of 9 years.

3.2. Inclusion Criteria

A. Patient related

- Patients with UCL who have had previous primary corrective surgery.
- Children between 8 and 10 years of age
- Patients who had their data available for analysis.

B. Control related

- Healthy non-cleft volunteers
- Volunteers aged between 8 and 10 years of age and sex matched
- No previous history of surgery involving the facial region.

3.3. Exclusion criteria

- Inadequate quality of the captured 4D images for the cleft group and the control group
- Defective images due to several varied causes
- Failure to meet the inclusion criteria

3.4. Ethical Considerations

Ethical approvals were obtained (REC reference- 16/NE/0246) and the NHS R&D (R&D Reference GN16OD291). All procedures including filing and storage of data were adhered to according to the guidelines and policies set forth by health authorities.

3.5. Sample Size Calculation

Based on information obtained from previous studies by Bughaigis *et al*. (2014) and Kuijpers *et al*. (2015), a standard deviation of 1 and an effect size of 0.7 for average asymmetry scores was observed. It was calculated that 22 participants in the UCL group and assuming a ratio of 3:1 for controls: cases (Hennessy *et al*., 1999), 66 non-cleft volunteers would need to be recruited assuming a power of 80%, in order to detect differences between the UCL group and the non-cleft control group.

3.6. Study sample

The study sample consisted of 25 Unilateral Cleft Lip patients, aged 8-10 years, and 75 age and sex matched non-cleft volunteers recruited as controls.

3.7. Materials

3.7.1. The 4D Imaging System

Each participant was imaged using a 4D video stereo-photogrammetry device (figure 23), the Di4D capture system (Dimensional Imaging, Hillington Park, Glasgow, UK). The system consisted of 2 grey-scale cameras (Model aVA 1600-65km/kc; resolution 1600x1200 pixels; sensor model KAI-02050; Kodak, Basler, Germany) and 1 color camera that captures images at a rate of 60 image frames/second using a light source (Model DIV401-DIVALITE; Kino Flo Corporation, Burbank, CA). The Di4D imaging system captures the expressions at a rate of 60 frames/second. Each expression takes about 3 seconds which generates 180 3D facial images. The imaging system is based on passive stereo-photogrammetry which allows automatic tracking of facial landmarks throughout the sequence of facial expression frames. The clinical validity of the automatic tracking of facial landmarks has been studied by Al-Anezi *et al*. (2013) and applied clinically (Shujaat *et al*. (2014) and Al-Hiyali *et al*. (2015).

Figure 23: The Di4D Imaging System

The 4D capture system was connected to a personal computer (PC) which had the following feature specifications:

- Windows 10
- Intel core
- LCD Monitor

The Di4D system was based on passive stereophotogrammetry and produced full textured 4D sequences and 3D images from ear to ear.

The Di4D system used in this study used image capturing software (Di4D Capture) and post-capture processing and viewing software (Di4D View), both running on a high-performance PC (Figures 24 and 25).

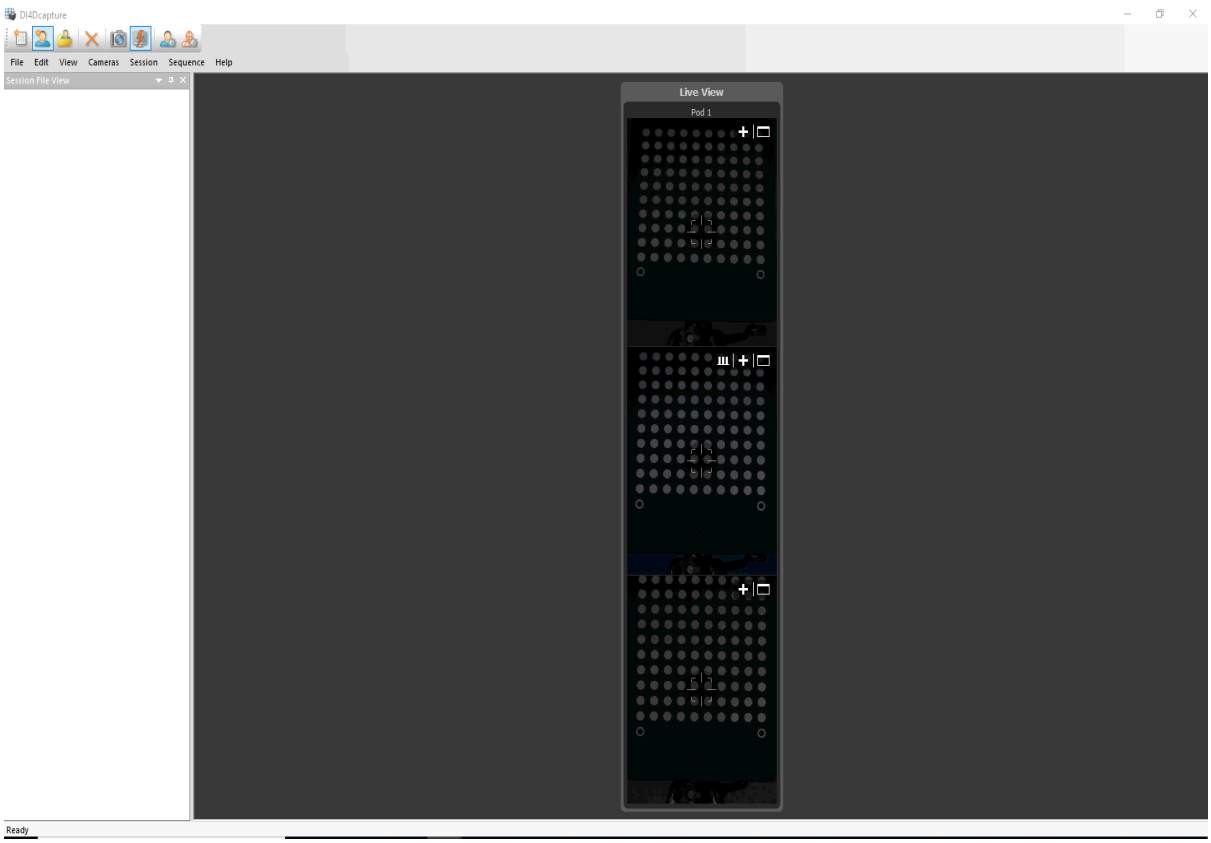

Figure 24: The Di4D Capture Software capturing the calibration target

The Di4D capture software is the user interface capture controlling panel of the Di4D system which allows the operator to calibrate, capture and build the sequences and images of facial expression in 4D. The Di4D capture software has a

"live preview" window which allows the operator to make sure the participant (patient/control) is aligned to and facing straight towards the cameras and make prior adjustments to the height of the participant in such a way that the entire facial surface is captured by the system without any cutting out of essential anatomic areas.

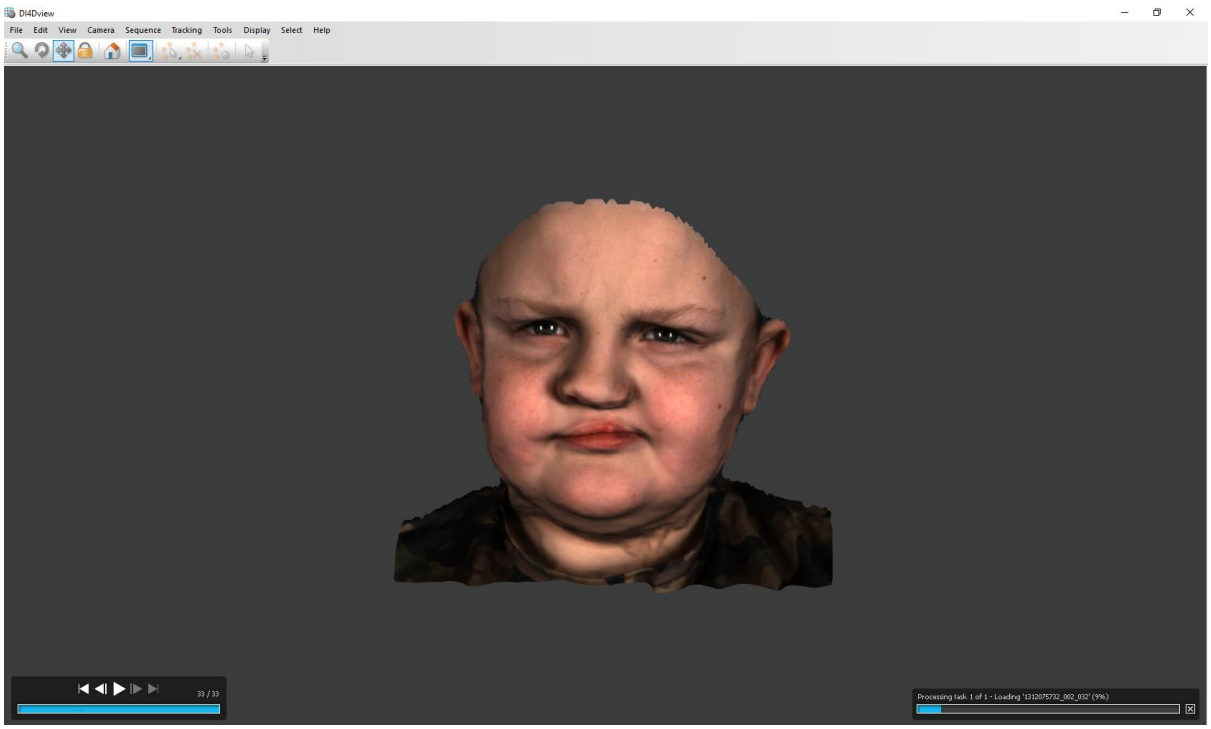

Figure 25: The Di4D View software

The Di4D View software (figure 25) allows the operator to process and manipulate the image, including magnify, translate and rotate it. The Di4D view software has user operable tools such as landmarking, superimposition of images and surface distance measurement.

The software was used in this study for the purpose of landmarking, conformation of the mesh, tracking of the conformed mesh and finally, saving the data as .dilm files (for landmarking data) or .obj files (for conformed mesh data) to the PC.

3.7.2. Calibration of the Di4D system

The Di4D system underwent a calibration process prior to the capture session each day. The calibration was performed at the start of the capture session following the instructions provided by the Di4D system manufacturers. The calibration process was automatic, and the purpose of this pre-capture calibration was to determine the intrinsic parameters and characteristics of the cameras such as the focal length, image center and the orientation of each of the cameras.

This automated process required the use of a calibration target (Figure 26). The calibration target consists of a black board with 100 white circles of specific known sizes separated by a known distance from each other. The calibration software extracted the co-ordinate distances between each of these circles on the target and could correspondingly measure the intrinsic parameters of all three cameras automatically. For this calibration process, the calibration target was captured eight times at varying angles and following this, the calibration of the system was carried out automatically (Figure 27).

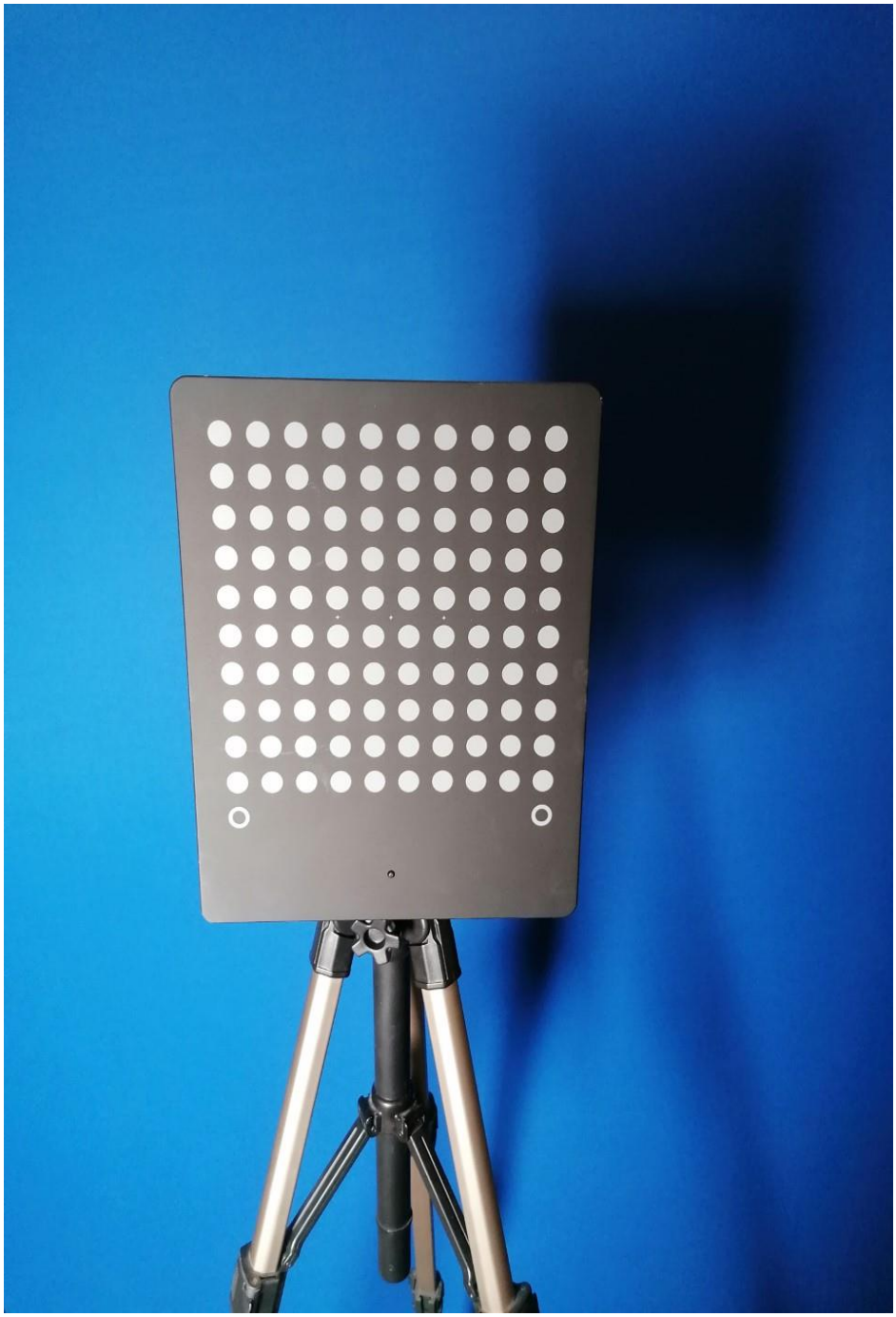

Figure 26: The calibration target used for the process of calibration

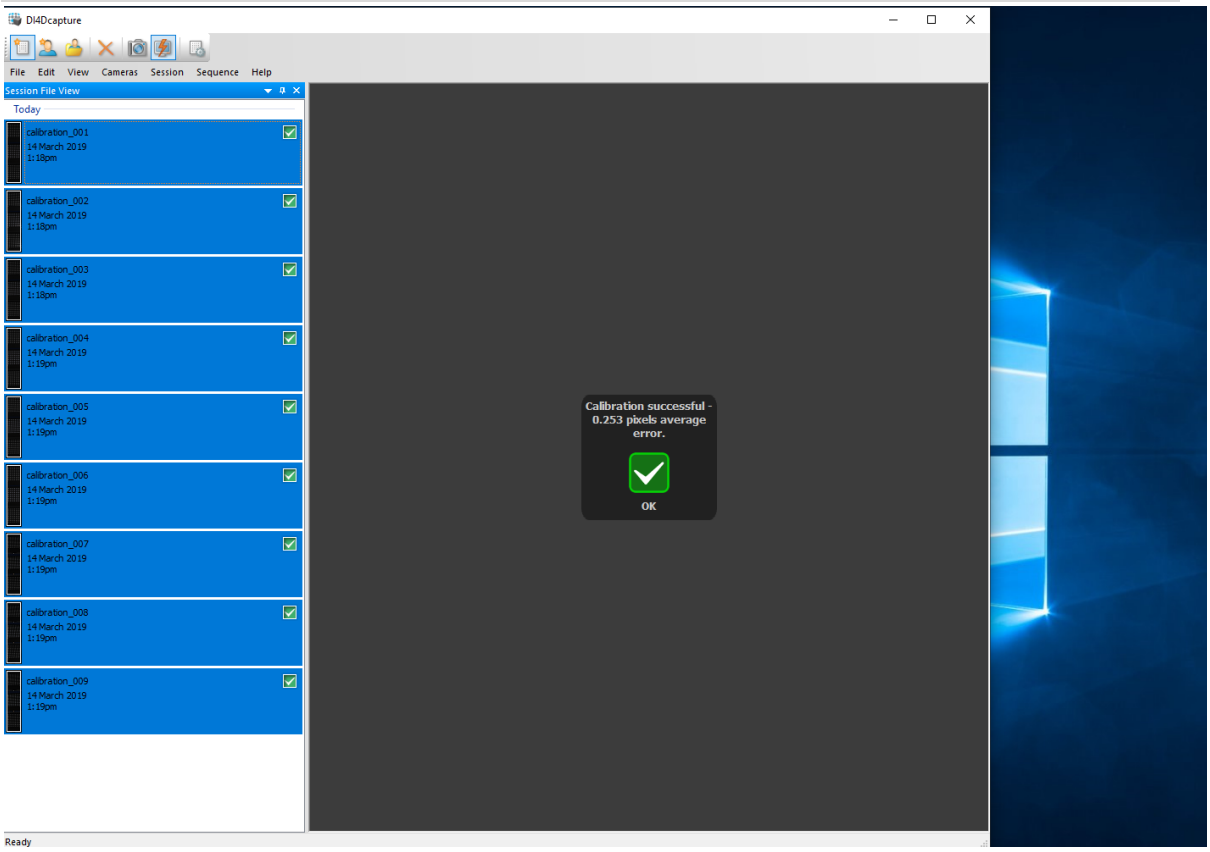

Figure 27: Automatic Calibration process prior to the imaging session

3.7.3. Imaging and Capture Protocol

Prior to each imaging session, participants were shown how to perform each expression by means of visual cue cards and observation-based training. Each participant was then asked to sit in a relaxed and upright position, 95 cm away from the camera in front of a blue screen before imaging was undertaken.

The 'live preview' function provided by the Di4D capture software enabled the operator to make sure the participant was positioned appropriately and in co-ordination with the three cameras on the 4D system. The lighting system was set to maximum intensity prior to the calibration and imaging session.

In order to ensure standardization of the capture, each participant was asked to:

- Remove spectacles, facial jewelry like nose rings, ear-rings etc. which may hinder

the imaging and analysis.

- Remain still during the capture session. Children, especially at the ages of 8 to 10 years have the tendency to move and swing their legs during the performance of facial expressions. Excessive bodily movement during the imaging session could lead to the data being noisy and interfere with corresponding analysis.

- Wear a head cap in order to keep all hair away from the forehead and the neck.

- Perform 4 facial expressions: -

    a. **Maximum Smile**- Participants were asked to bite their posterior teeth together and smile as wide as possible exposing their teeth and ensuring maximum stretching of the commissures (Figure 28).

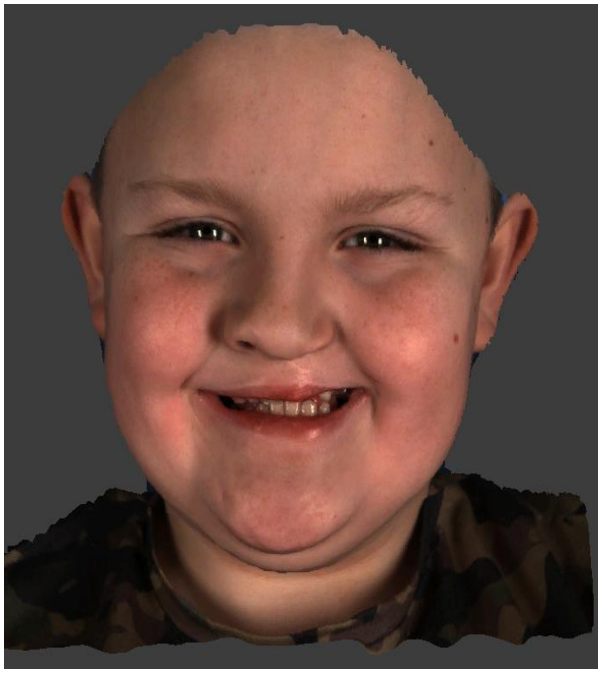

Figure 28: Maximum Smile at its peak phase

b. **Cheek Puff**- Participants were asked to bite their posterior teeth together and ensure their lips are in gentle contact while they blow out their cheeks maximally (Figure 29).

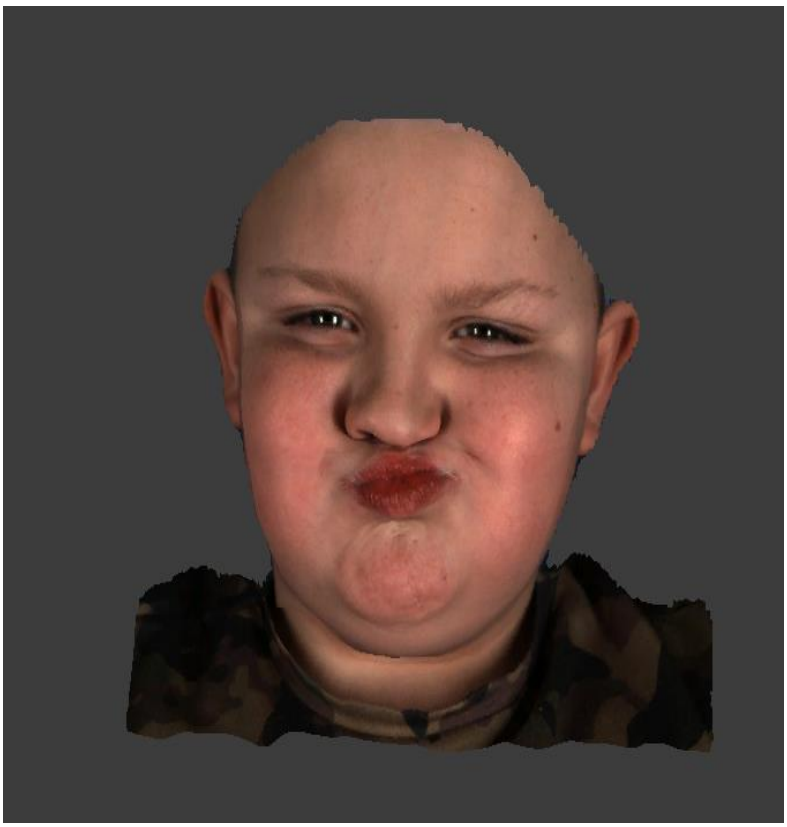

Figure 29: Cheek Puff at its peak phase

c. **Lip Purse**- Participants were instructed to press their lips in gentle contact and pout their lips or pretend to whistle (Figure 30).

Figure 30: Lip Purse at its peak phase

d. **Grimace**- Participants were asked to bite on their posterior teeth, begin with lips in gentle contact and perform a sad face by maximum eversion of the lower lip as possible (Figure 31).

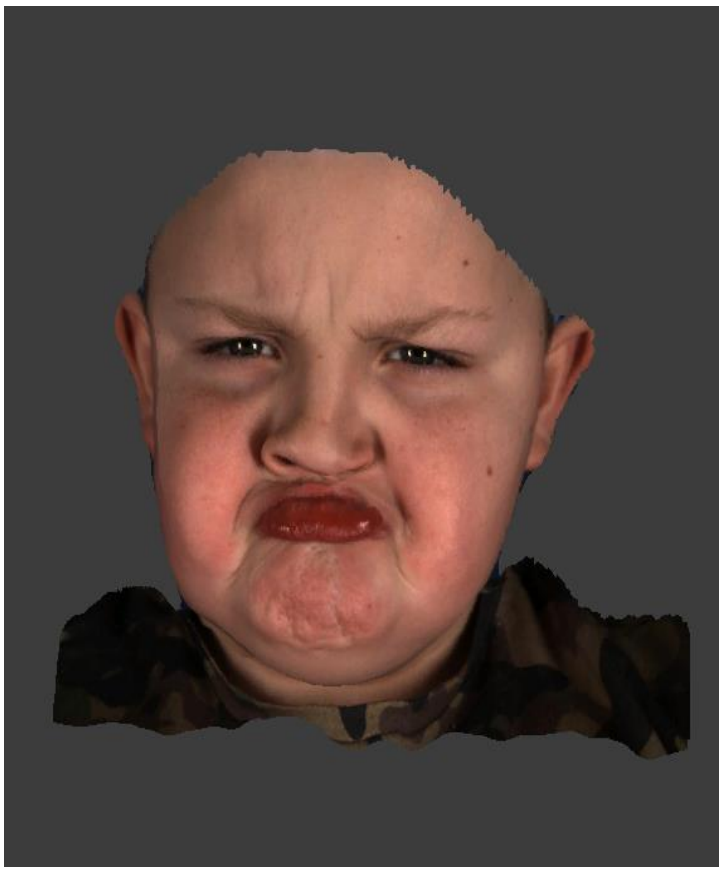

Figure 31: Grimace at its peak phase

The Di4D system captures these expressions at a frame rate of 60 frames per second. Each expression took roughly around 3 to 4 seconds to capture. Participants were asked to start each expression at a state of rest, and slowly progressing to a maximum or peak expression as much as possible before coming back to a state of rest. Each expression was captured three times to ensure selection of the image sequence with the best quality and standardized

movements with respect to time. Following the selection of the appropriate image sequence, the 4D image was built and saved on the PC.

If participants moved during the imaging session, the procedure was repeated.

In this study, we used deliberate facial expressions rather than spontaneous facial expressions stimulated by an external emotion. Facial expressions in this study were performed by maximum forced contraction of facial muscles. Spontaneous facial expressions (such as those generated in response to social or emotional stimuli) were found to possess a number of time related and movement related features in comparison to deliberate or forced maximum facial movement- it was seen in previous research work in facial movement analysis that spontaneous facial expressions tended to be shorter in time duration, slower in actual performance (Hess & Kleck, 1997) and less asymmetric in lip movements (Hager & Ekman, 1997).

In addition to the above features in spontaneous smiles, our study required that all facial expressions be standardized or as similar to each other as possible not only within participants but also between individual participants. For example, in order to ensure uniformity of facial expressions, participants were asked to perform the facial expressions in similar time frames whilst following a specific countdown pattern which enabled them to start the expressions at rest, build up towards a maximum stretch of muscle and terminate the facial expressions with a final resting stage. This uniformity of performance of facial expression could only be achieved by utilizing deliberate facial expressions. Spontaneous facial expressions in response to specific stimuli vary in speed of performance as well as duration as mentioned before and therefore it would not have been possible to maintain uniformity or standardization of facial expressions using spontaneous facial expressions.

Furthermore, different individuals show different emotional response to stimuli and therefore the concept of standardization was not achievable using

spontaneous facial expressions. This difference in forced and spontaneous facial expressions was presented in works by Cohn & Schmidt (2004) and Frank et al. (1993) wherein it was seen that deliberate facial expressions have faster onset and offsets than spontaneous expressions. Movement asymmetry was also seen to be higher in deliberate facial expressions.

Figure 32: 5 frames selected from the sequence of images during maximal smile

3.8. Image Processing

Each of the facial expressions captured were imported to Di4DView Software. Out of the roughly 180 or so frames generated for each expression, 5 frames were selected by the operator for the assessment of asymmetry (Figure 32). The 5 frames were as follows: -

Frame 1- Initial resting face

Frame 2- Frame between rest and peak expression (arithmetic mid-point between frame 1 and frame 3)

Frame 3- Peak/ maximum expression

Frame 4- Frame between peak/maximum expression and final resting position (arithmetic mid-point between frame 3 and frame 5)

Frame 5- Final resting face (End of the expression)

The processing of the video sequence requires the first step of manually identifying and digitizing 29 landmarks on the facial surface (Al-Hiyali et al., 2015).

The DiView software provides a dual display panel (Figure 33) with the generic mesh shown in one panel and the resting frame (Frame 1) of each expression shown in the other panel. The generic mesh is manually landmarked following the same sequence of placement of landmarks as the resting frame.

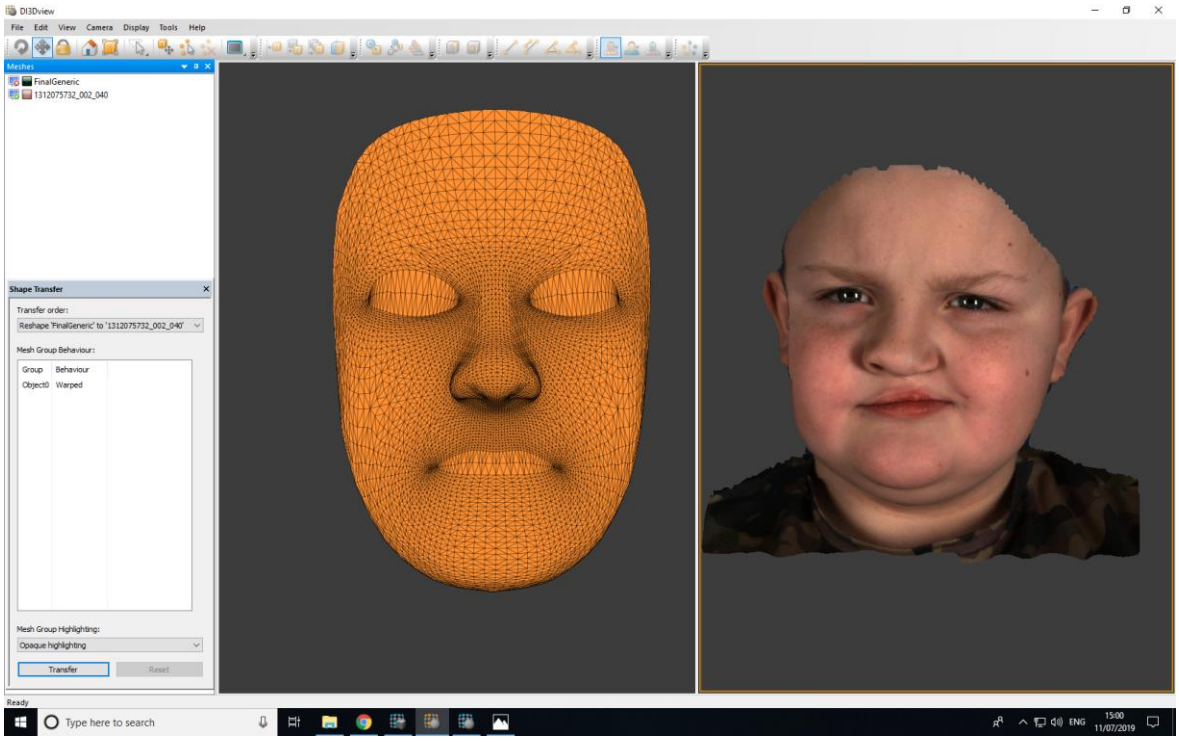

Figure 33: The dual display panel in Di3D View software

For the analysis of asymmetry of facial expressions, a generic face mesh was applied (Figure 34). A generic mesh is a universally applicable facial surface representing morphological information of an average face, which consists of common morphological characteristics within the population. The generic mesh consists of approximately 7000 triangulated vertex "points", whose 3D coordinates are fixed.

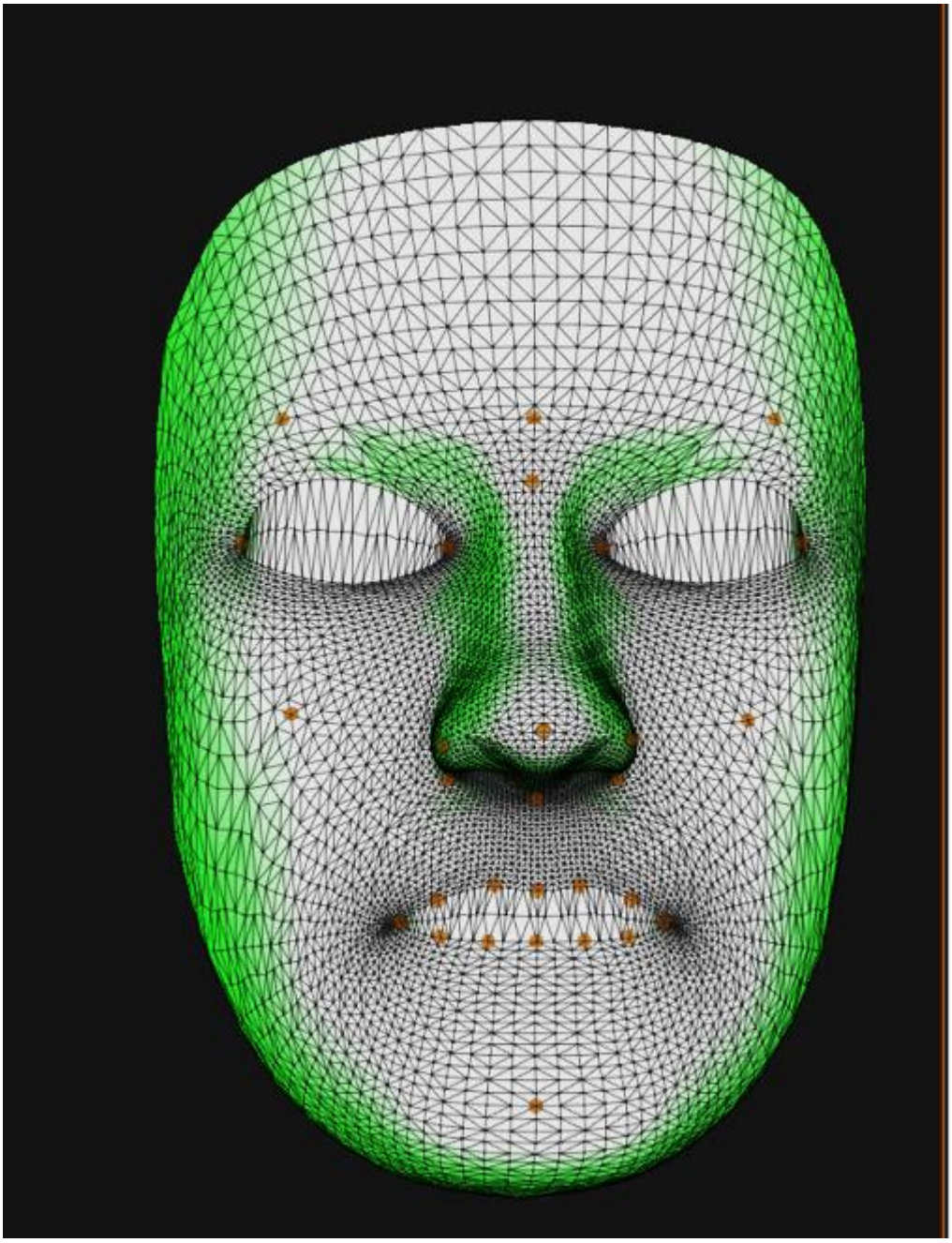

Figure 34: Generic mesh with landmarks

This generic mesh was elastically deformed in a process known as mesh conformation to represent the patient's/participant's underlying facial morphology, thus creating a conformed mesh specific to each patient. This process of conformation (Figure 38) was started by manually identifying and digitizing 29 facial landmarks (Table 2) Al-Hiyali *et al*. (2015) on the generic mesh as well as on the 3D facial model on the resting frame at the beginning of each expression (Figure 35). The landmarks were then automatically tracked throughout the entire sequence of 3D facial images. The 29 facial landmarks employed in the manual digitization process involving the first frame out of the five selected frames helped

purely in the conformation process of the generic mesh. The rationale for selecting these landmarks was based on prior studies in the field of facial asymmetry measurement and morphometrics by Al-Hiyali et al. (2015) and Farkas et al. (1994). For the purpose of morphometrics and application on the human face, a detailed definition of landmarks was provided by Farkas (1994) and this was the standard reference for selection of these landmarks. A facial landmark is a point on the face that plays a discriminative role or may serve as an anchor point on a graph of the face and occupies the same position in homologous species. The 27 landmarks used in the Al- Hiyali study were based on the set of landmarks defined by Farkas (1994). The number of landmarks used in facial analysis studies vary and range from a few primary landmarks (such as the nose tip and corner of the eyes and mouth) in facial recognition analysis to a much higher number and well distributed arrangement of 30 to 80 landmarks in facial expression analysis.

The human face is a three-dimensional structure and therefore analysing the shape or assessing facial asymmetry requires identification of landmarks which provides complete information of the facial topology including curvatures and edges on the face. In the case of our study, facial landmarks were used for the conformation of the generic mesh. The conformation process allows the generic mesh to replicate the 3D structure and morphology of the patients face and therefore a large coverage of landmarks was considered which included extra landmarks on the upper and lower lips (the upper middle lateral and lower middle lateral lip points- landmarks 25-28) to ensure that every important surface of the face was well represented during the conformation process.

Classification of facial landmarks

In most anthropometric studies, landmarks can be classified as anatomical landmarks (where two different surfaces or tissues meet), geometrically defined landmarks (where geometric principles are used to identify landmarks) and extremal landmarks (landmarks identified on curvatures and extremes of the surface). Bookstein (1991) stated that out of all the given landmark types, only the anatomical landmarks were actual biological loci. Digital anthropometry introduced other landmark classifications which could only be measured mathematically or geometrically, called pseudo-landmarks. Sliding or interpolated landmarks are pseudo-landmarks belonging to a curved surface and

placed between anatomical landmarks (Hennessy and Moss, 2001). Sliding landmarks were used to provide outline information on the facial morphology which other anatomic landmarks could not provide and thus provided coverage in areas where conventional landmarks could not do so. According to Bookstein (1991) no anatomical landmarks exist in the cheeks and forehead and in such cases, pseudo-landmarks play a key role in providing comprehensiveness to the assessment.

Landmarks of the face could also be classified as two main groups- fiducial and ancillary or primary and secondary landmarks. The primary or the fiducial landmarks are the more distinct landmarks such as the corner of the lips and the tips of the nose etc. Secondary landmarks are those such as nostrils, cheek, nasion and other points in between primary landmarks which play a more prominent role in increasing coverage and comprehensiveness in facial analysis.

Despite poor reliability scores certain landmarks like the zygion were included to provide more comprehensiveness to the analysis. This was done to ensure that the conformation process was accurate, reliable and comprehensive. The mean error of landmarking was seen to be 0.66mm.

Table 2: Names and definitions of landmarks manually digitized on the first 3D frame

Landmark number	Landmark Name	Description
1 and 2	Superciliary points	Points located above the most superior part of the eyebrows
3 and 6	Exocanthion	Points at outer corner of the eye fissure
4 and 5	Endocanthion	Points at the inner corner of the eye fissure
7 and 8	Zygion	Most prominent point on the cheek area beneath the outer canthus and slightly medial to the vertical line passing through it.
9	Nasion	The mid-point on the soft tissue contour of the base of the nasal root at the level of the frontonasal suture
10	Pronasale	The most anterior mid-point of the nasal tip
11	Pogonion	The most anterior midpoint of the chin
12	Subnasale	Midpoint of angle at the columella base where the lower border of the nasal septum and the surface of the upper lip meet
13 and 14	Subalare	Point on the margin of the base of the nose where the ala disappears into the upper lip skin

Table 2: Names and definitions of landmarks manually digitized on the first 3D frame

Landmark number	Landmark Name	Description
15 and 16	Alar Curvature	Most lateral point on the curved base line of each ala
17 and 18	Cheilion	Point located at the corner of each labial commissure
19	Labrale Superius	The mid-point of the vermilion line of the upper lip
20	Labrale Inferius	The mid-point on the vermilion line of the lower lip
21 and 22	Crista Philtri Left and Right	Peak of cupids bow left and right
23 and 24	Corresponding lower lip points to crista philtri left and right	Corresponding points on lower lip to crista philtri left and right
25 and 26	Upper middle lateral lip points	Midpoints located between cheilion and crista philtri left and right
27 and 28	Lower middle lateral lip points	Midpoint between cheilion and 23 and between cheilion and 24
29	Glabella	Midline point between eyebrows

TABLE 2: Names and definitions of landmarks manually digitized on the first 3D frame

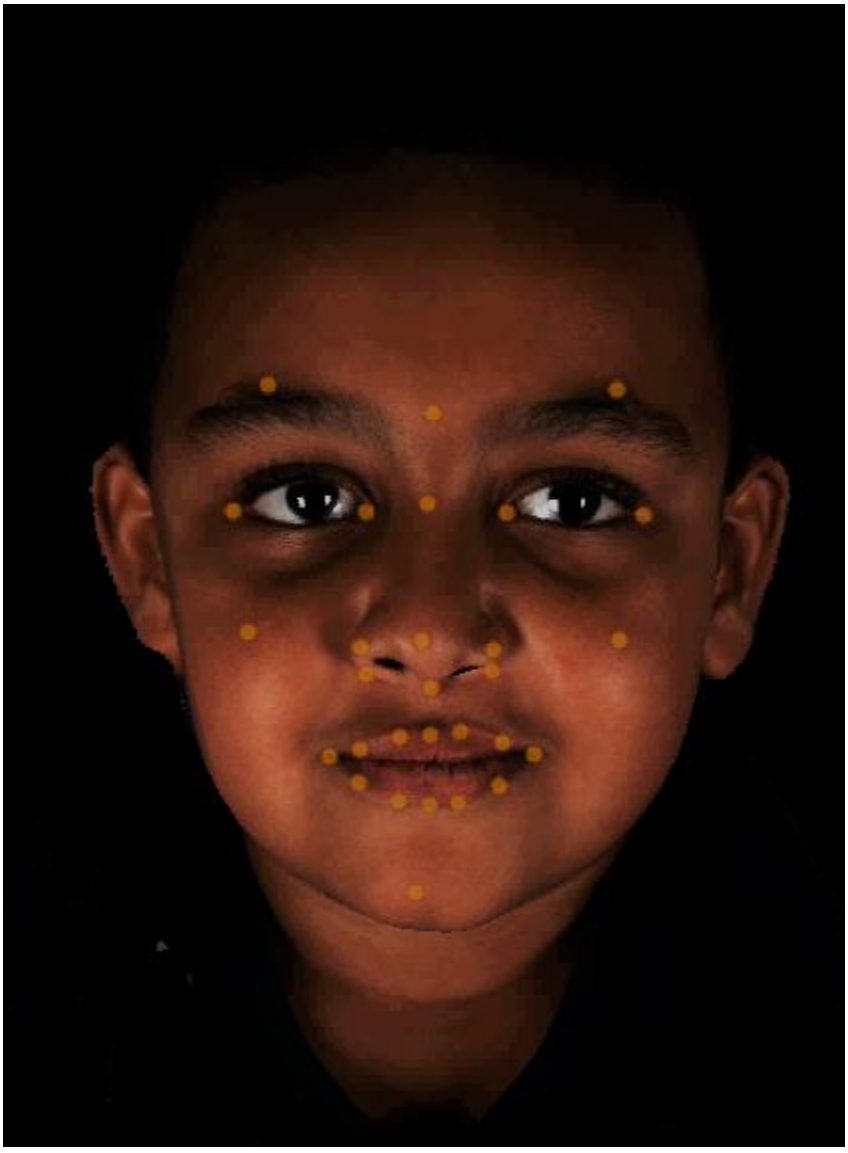

Figure 35: Landmarked points on the first 3D frame of a UCLP case

The landmarks initiated the 3D mapping of the mesh on the face which was followed by elastic deformations to deform the mesh to the face shape of the participant (Figure 36). The accuracy of this process has been validated (Al Mukhtar *et al*, 2017). The process of conformation to ensure that the generic mesh deforms on to the 3D facial image involves two steps- an initial semi-automatic non-linear warping followed by a completely automated elastic deformation. The conformed face mesh was tracked along the subsequent frames of each expression. The accuracy of the tracking has been validated (Al Anezie *et al.*, 2015). The process of automatic tracking of the vertices of the conformed mesh through the sequence of 3D images of each facial expression was a complex one and involves several thousand points on the surface of the conformed mesh

starting from the first frame to the last frame to be tracked and their displacement and movement recorded in real time. The tracked conformed mesh subsequently makes analysis easier and less time consuming alongside eliminating the need to manually landmark and conform each and every frame in the expression sequence which would result in volumes of data being generated and a tedious process of manual landmarking which would take a long period of time.

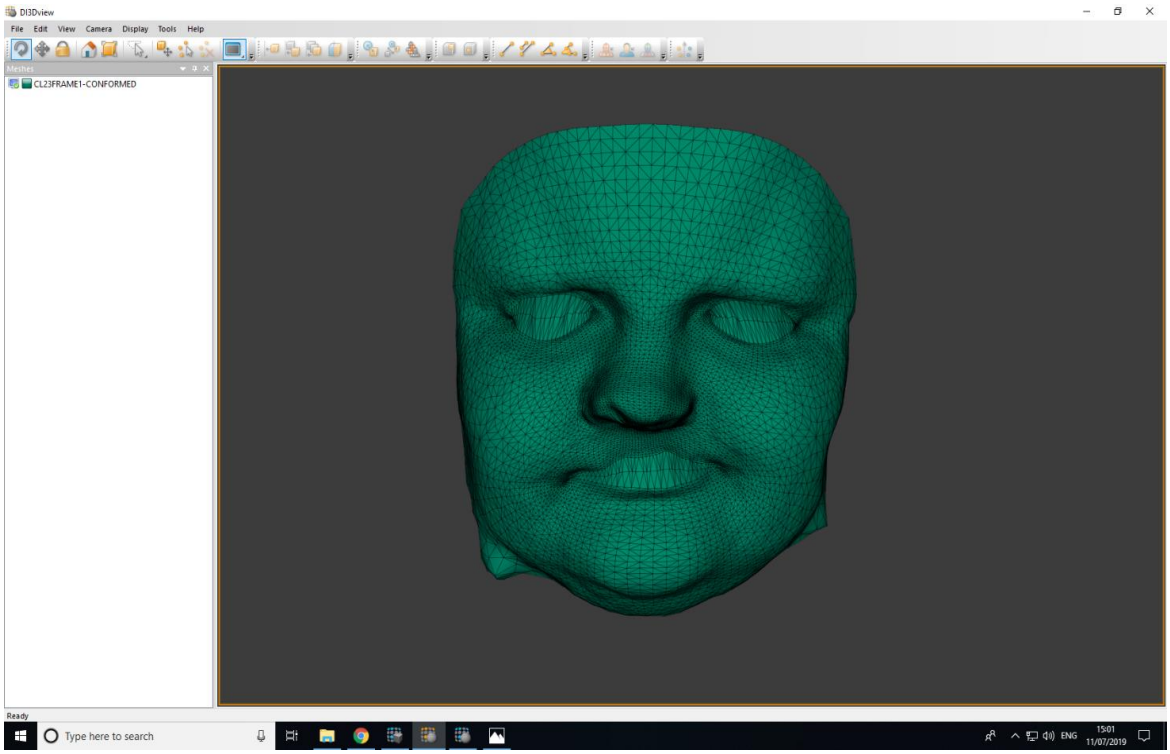

Figure 36: The Conformed mesh resembling the UCL patient 3D facial morphology

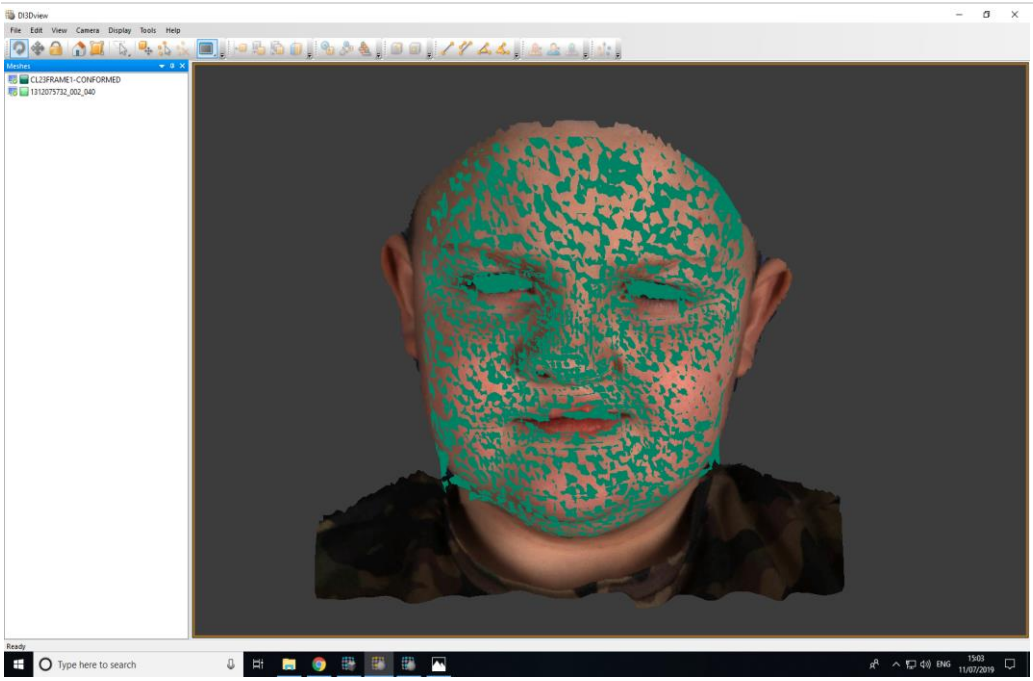

Figure 37: The conformed mesh being checked to fit over the patient's 3D facial image

Figure 38: Conformation process- A: Wireframe model of generic mesh B: 3D frame of initial resting face C: Conformation process D: Conformed mesh surface model

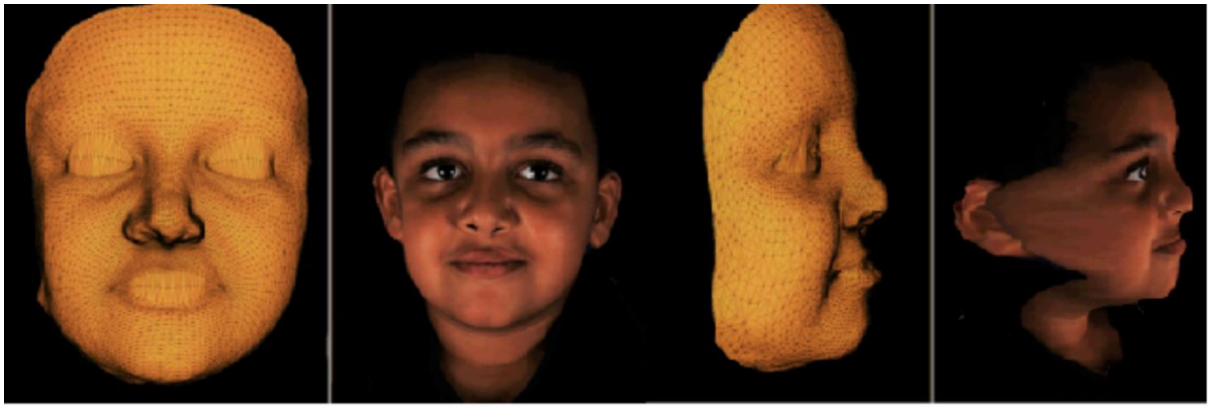

Figure 39: Conformed generic mesh in frontal and lateral view to show similarity with patient 3D image [A. the conformed mesh (wireframe model) and the corresponding 3D image in frontal view B. the conformed mesh (wireframe model) and the corresponding 3D image in lateral view]

Following manual landmarking on the model of the start of the expression (Frame 1), a corresponding conformed mesh was generated. The conformed mesh was stored and saved in .obj format. Mesh tracking (tracking and recording) of the movement of the several thousand vertices on the mesh during each expression was carried out for each UCL case and control using the Di4D view software. Mesh tracking data was stored and saved in a '.pc2' format.

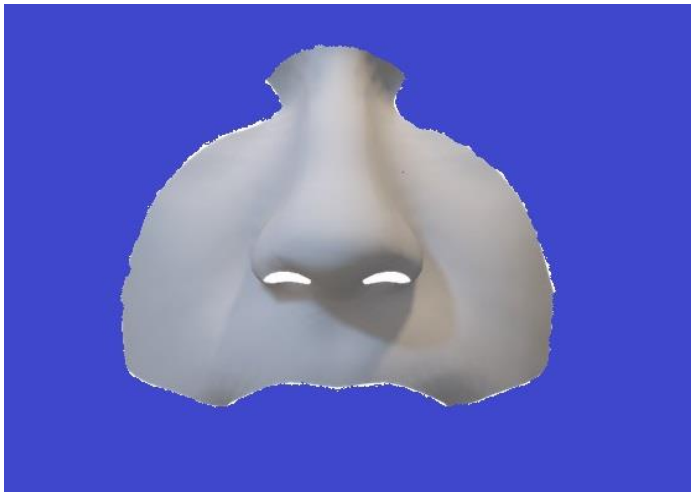

FIGURE 40: Extracted Nasolabial region

3.9. Assessment of facial asymmetry

For each of the five frames (3D images) obtained per patient/control, a mirror image was created by reflecting the 3D conformed mesh on a reference plane (an arbitrary mathematical plane acting as a mirror). In the mirror, images with right sided cleft become left sided and vice-versa. This procedure of mirroring was carried out for each the 5 selected frames of the captured 3D sequences of facial images during each expression in both the UCL group and the control group.

For obtaining asymmetry scores, each of the 5 selected conformed frames and their mirror images were superimposed using Partial Ordinary Procrustes Analysis. This algorithm aligns two shapes or images using components of translation and rotation to ensure optimum superimposition between images.

3.9.1. The Partial Ordinary Procrustes Analysis

The partial ordinary Procrustes analysis forms the principle of several methods of geometric morphometrics. It is a method of matching and comparing two shapes or configurations of points optimally by including transformation processes such as translation and rotation. Procrustes analysis usually works by considering one of the shapes a target and correspondingly matching the other to it. Translation involves bringing the 2 shapes closer to each other by ensuring the configurations meet at a common centroid. The centroid of an object is the mean of all its configuration points or the geometric center. In other words, the x, y and z coordinates of the centroid is the mean values of the x, y and z coordinates for all landmarks in the objects. The process in simpler terms ensures that the objects in question have the same centroid. In partial Procrustes analysis the step of scaling is not carried out, therefore preserving the size of the configurations. The differences in orientation between the shapes in question are further removed by

rotating one of the shapes (the target) around the common centroid until it shows minimal distance between its vertices and those of the reference shape. The disparity in vertices between the target and the reference shapes are measured as the sum of squared distances between vertices of the two shapes. This is the Procrustes distance. The two shapes are optimally aligned when the Procrustes distance is minimized.

3.9.2. Measurement of facial asymmetry in dynamic form

Following the superimposition, the asymmetry scores were ascertained by measuring the distances between corresponding vertices of the original and mirrored 3D surface meshes. In perfect symmetry, the distance between the original and mirrored image equaled zero. This resulted in five asymmetry scores (one for each of the five frames) per case/control. The asymmetry score was calculated as the average distance between corresponding vertices in the region of interest.

A major disadvantage of using whole face asymmetry scores, is that larger asymmetry scores of certain anatomical regions of the face may be diluted by smaller asymmetry scores in other regions of the face. In order to overcome this limitation, regional asymmetry scores specific to the nasolabial region were measured. (Figure 40).

3.9.3. Color Maps

The total asymmetry scores were illustrated in colors ranging from dark blue to red. The color-coded map (Figure 41) represented the size of the distances between the corresponding vertices of the superimposed meshes. As the distance between corresponding vertices has increased, the color changed from blue to sky blue to yellow to orange and finally red, the color red indicating higher areas of asymmetry. The intensity of the colors on the map represents the distance between the vertex of the mesh and that of its mirrored mesh.

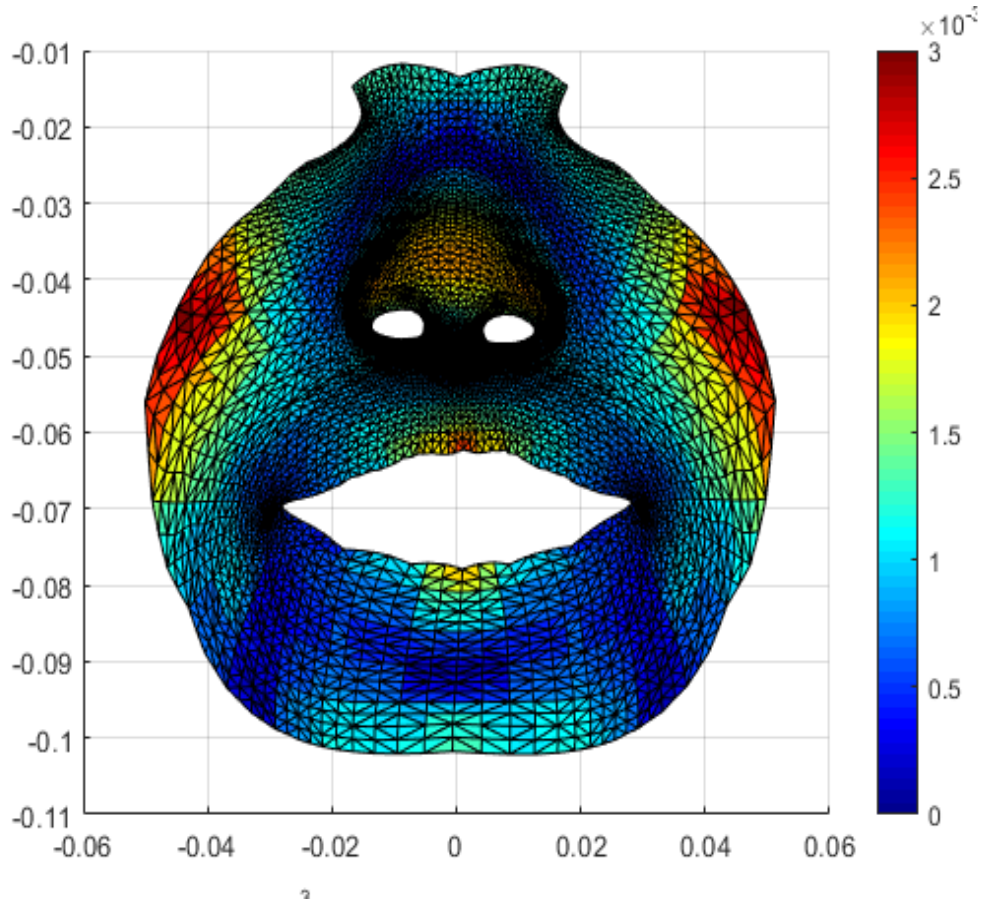

Figure 41: Asymmetry scores as seen in the color map

Directionality of asymmetry was also assessed in the x y and z directions or the horizontal, vertical and antero-posterior directions. The difference between the original and mirrored meshes in each spatial plane was also represented by a color-coded map. In the medio-lateral direction, displacement to the left was shown in red and displacement to the right was shown in blue (Figure 42). In the vertical direction, upward displacement was shown in red and downward displacement in blue. In the antero-posterior direction, displacement towards the observer was shown in red and displacement away from the observer was shown in blue.

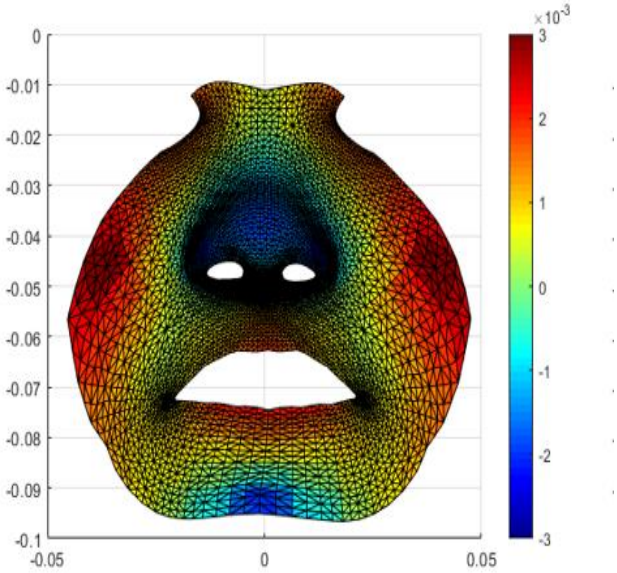

Figure 42: Asymmetry in mediolateral direction during a facial expression- areas in red showing displacement to the left and areas in blue to the right

3.10. Errors of Landmarking- the reliability of the study

Analysis of the errors of landmarking (intra-operator reliability) was carried out by repeating the digitization of the facial landmarks on 10 randomly selected cases, separated by a week's interval, by the same operator. The difference in landmarking and its impact on the conformation process were statistical analyzed using student t-test.

3.11. Statistical Tests

Repeated measures ANOVA was used to statistically analyse significant differences in asymmetry scores between and within the groups. A repeated measures model represents a model fitted to data with multiple measurements per subject. The model comprises data, fitted coefficients, covariance parameters, design matrix, error degrees of freedom, and between- and within-subjects factor names. Repeated measures ANOVA results in a table which includes a term representing all differences across the within-subject factors. P value <0.05 with Greenhouse- Geisser adjustment indicated significant differences across the within-subject factors. Estimated marginal means was used in order to obtain graphical representation of asymmetry scores for each of the five frames per facial expression.

4 Results

Contents

Errors of Landmarking

No statistically significant differences were detected between the repeated digitization of the anatomical landmarks ($p<0.05$)

Reproducibility	Mean (mm)	std	p-values
x	-0.07	0.68	0.0664 > 0.05
y	-0.01	0.45	0.7963 > 0.05
z	-0.03	0.47	0.3467 > 0.05

The mean distance error is 0.66mm with the STD of 0.67mm

4.1. Maximum Smile

The magnitude of facial asymmetry was measured during the maximum smile expression and evaluated in the total face, mediolateral plane, vertical plane and antero-posterior plane. Results were shown in the form of color maps which showed increasing asymmetry as the colors changed from blue to yellow to orange to red. Asymmetry in the spatial planes was also seen in the color maps and described individually under the respective sections.

Summary of results during maximal smile:

Significant differences were seen in asymmetry scores for all five frames between UCL patients and the control group. It was seen that asymmetry was prominent in the nasal regions- the nasal tip and alar regions as well as the upper lip vermillion border, the philtrum and columella. Lower lip showed involvement also. Asymmetry was seen to be accentuated with performance of the maximum smile with maximum asymmetry in the UCL group seen in frame 4 (midway between peak expression and final resting state). In the X direction, the nasal tip and ala and other parts of the nose deviated to the left side or the non-cleft side. The vermillion border of the upper lip and philtral areas deviated towards the right side or cleft side. Asymmetry in the X direction as seen to be highest in frame 3 or peak expression. The vertical asymmetry after surgical correction were seen to be minimal during maximal smile. Anteroposterior asymmetry was observed at the alar regions of the nose, the philtrum, upper lip and was seen to be highest in frame 4 (mid-way between peak expression and final rest).

4.1.1. Total face asymmetry during Maximum Smile

Maximum smile expression was recorded, and 5 frames were chosen for evaluation of the magnitude of facial asymmetry and to study the dynamics of facial movement.

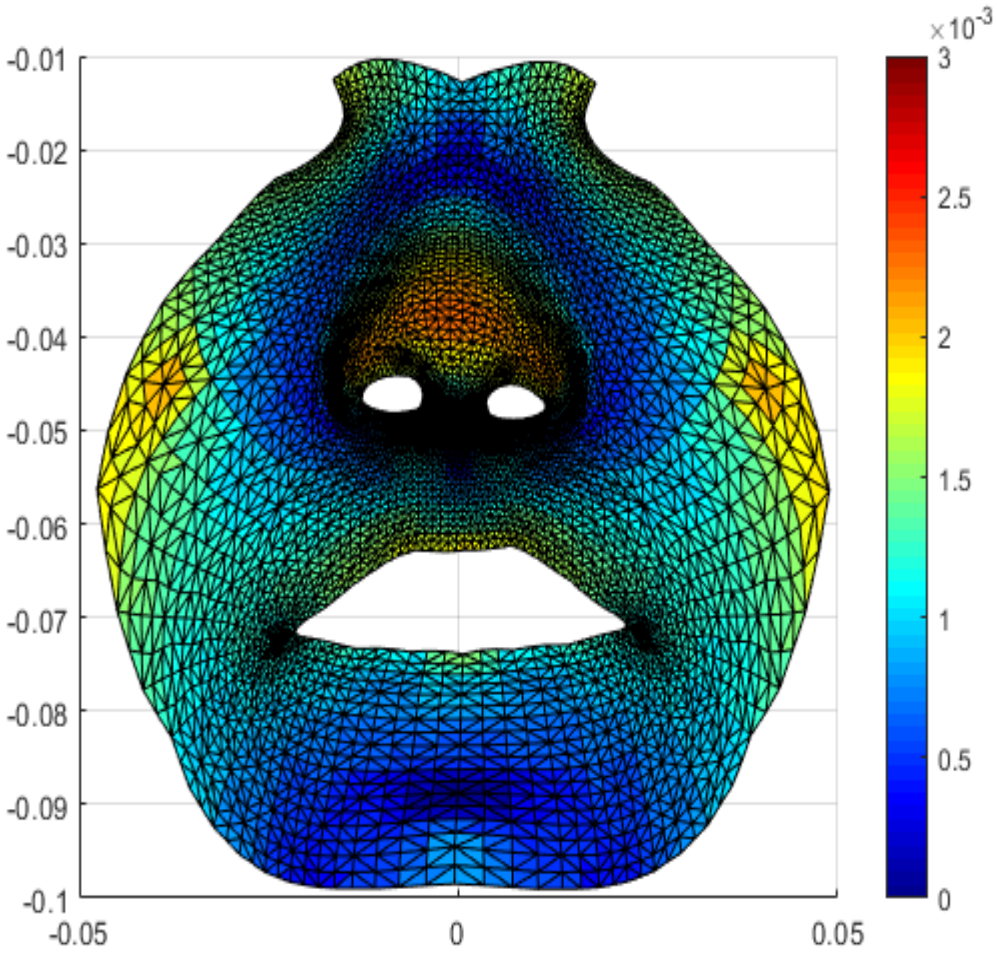

Figure 43: *FRAME 1*- Color map of the total face asymmetry in frame 1 in the UCL patients during maximal smile. The red color represents increased asymmetry. The blue color represents decreased asymmetry. Areas in green represent zero distance between the original and mirrored meshes (no asymmetry).

Frame 1 in figure 43 shows higher residual asymmetry in areas around the nasal tip and alar regions (patches of red interspersed with yellow patches). Mild yellow patches were seen in the upper lip vermillion border as well as a small part of the lower lip. This is indicative of increased residual asymmetry present in the upper lip vermillion border. Most of the residual asymmetry in frame 1 was seen in the nasal regions and the upper lip. Frame 1 is the resting frame wherein the face is resting with no facial movement. This residual asymmetry therefore corresponds to facial asymmetry present even before the performance of facial expression.

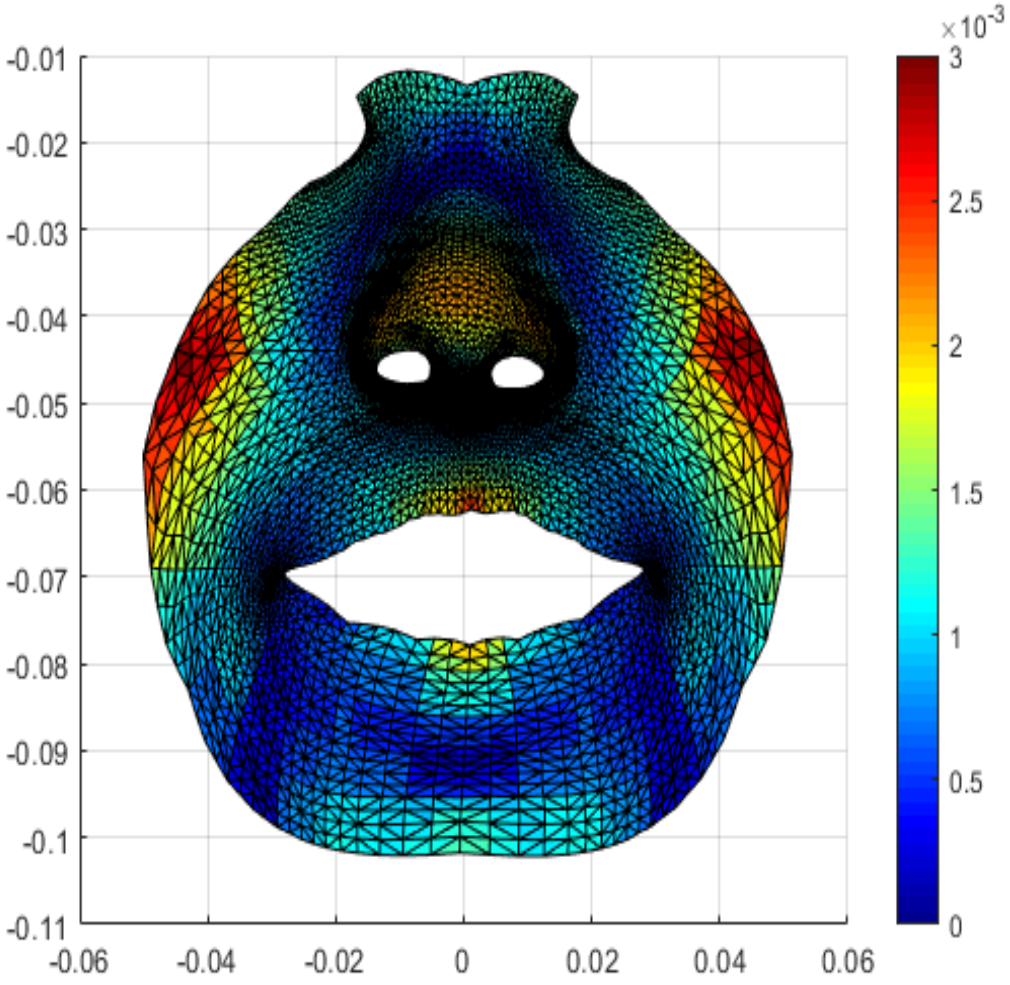

Figure 44: *FRAME 2* Color map of the <u>total face asymmetry</u> in frame 2 in the UCL patients during <u>maximal smile</u>. The red color represents increased asymmetry. The blue color represents decreased asymmetry. Areas in green represent zero distance between the original and mirrored meshes (no asymmetry).

Frame 2 in figure 44 shows higher residual asymmetry in areas around the nasal tip and alar regions (patches of mild red interspersed with yellow patches). A deep red patch and a yellow patch was seen in the upper lip vermillion border. Yellow patches were seen in the vermillion border of the lower lip as well. This is indicative of increased residual asymmetry present in the upper lip vermillion border and a small part of the lower lip. Similar to frame 1, most of the residual asymmetry in frame 2 was seen in the nasal regions and the upper lip. Frame 2 is the quarterly frame wherein the muscles are beginning to contract to bring the face to peak expression.

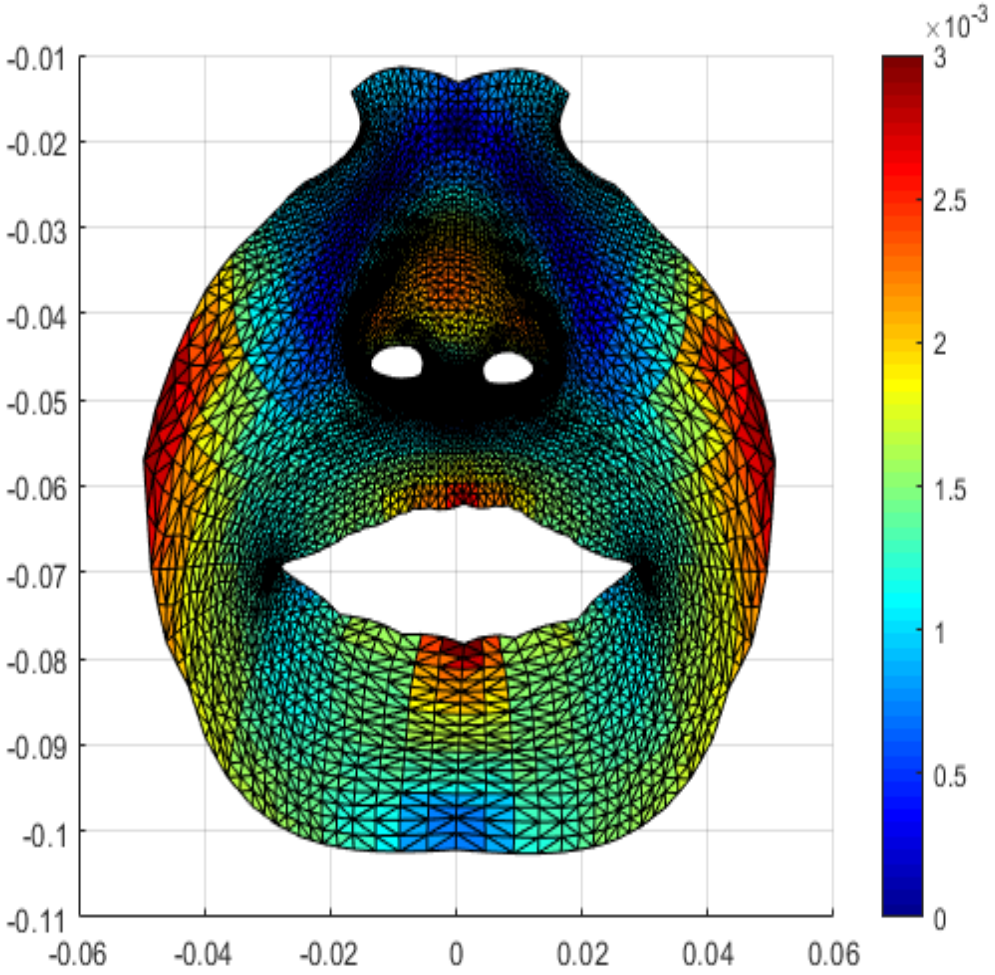

Figure 45: *FRAME 3* Color map of the <u>total face asymmetry</u> in frame 3 in the UCL patients during <u>maximal smile</u>. The red color represents increased asymmetry. The blue color represents decreased asymmetry. Areas in green represent zero distance between the original and mirrored meshes (no asymmetry).

Frame 3 in figure 45 shows higher residual asymmetry in areas around the nasal regions and ala of the nose. This is seen as red patches in these areas alongside yellow areas in the nasal tip. The yellow color near the upper vermillion in frame 2 became a distinct red patch in frame 3 indicating higher asymmetry levels in frame 3 as compared to frame 2 in areas including the upper lip vermillion and surrounding areas. Frame 3 is the peak frame wherein the muscles are contracting the maximum in order to enable peak facial expression of maximum smile. This goes to show that facial expressions accentuate facial asymmetry from a state of rest to a state of maximum movement.

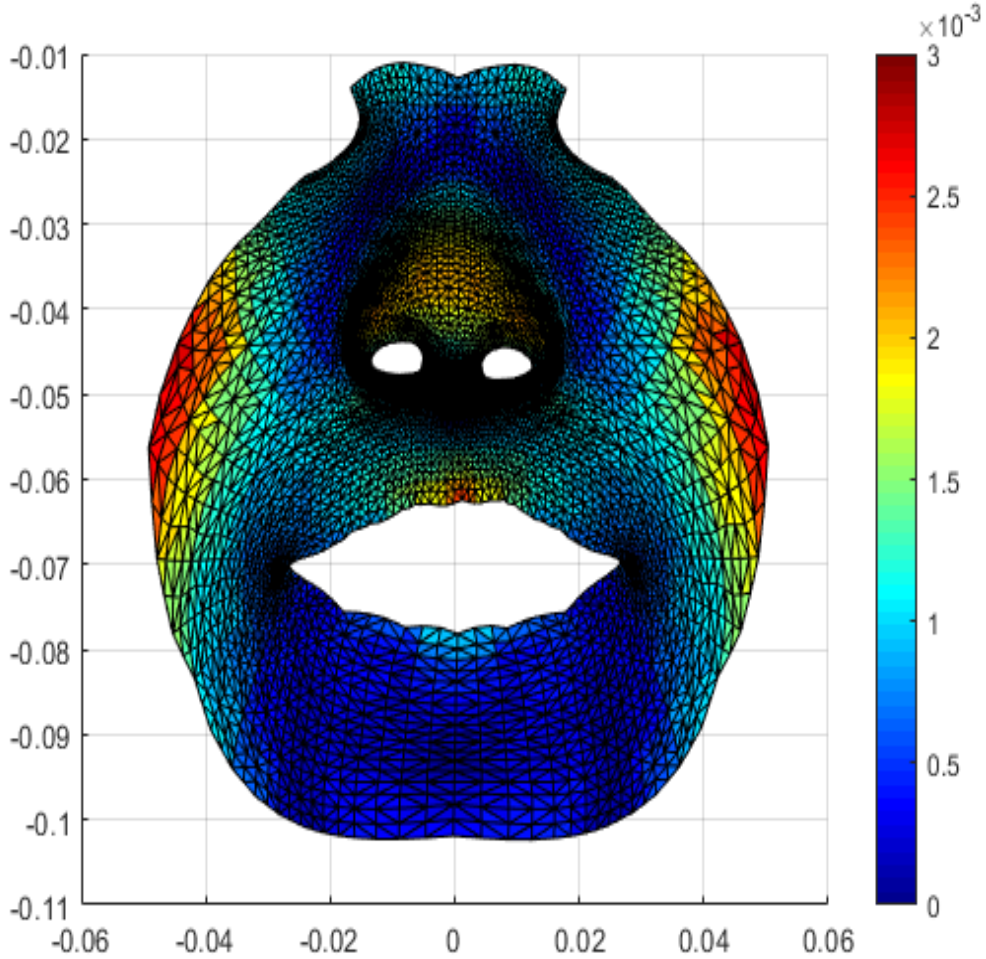

Figure 46: ***FRAME 4*** **Color map of <u>the total face asymmetry</u> in frame 4 in the UCL patients during <u>maximal smile.</u> The red color represents increased asymmetry. The blue color represents decreased asymmetry. Areas in green represent zero distance between the original and mirrored meshes (no asymmetry).**

Frame 4 in figure 46 shows higher residual asymmetry in areas around the nasal regions and ala of the nose as well as a small patch near the vermillion of the upper lip. The red patch which was a deeper shade of red in frame 2 and 3 around the nasal regions is seen to have become a lighter shade of red and yellow in frame 4 as the muscles are trying to return back to their state of rest following peak expression. The yellow and red shades seen around the lower lip areas in frame 3 is seen to turn into a shade of blue in frame 4 indicating that asymmetry is decreased in this region as compared to the previous frames.

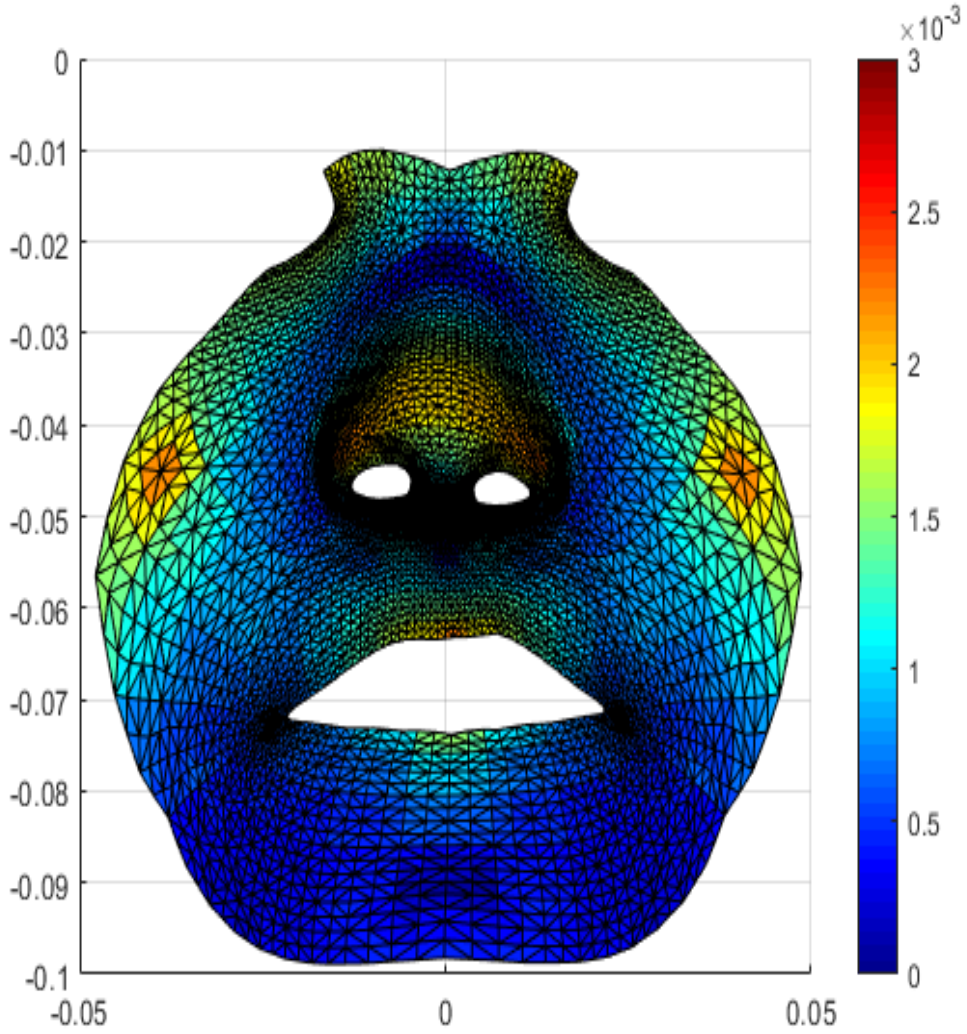

Figure 47: *FRAME 5* Color map of the total face asymmetry in frame 5 in the UCL patients during maximal smile. The red color represents increased asymmetry. The blue color represents decreased asymmetry. Areas in green represent zero distance between the original and mirrored meshes (no asymmetry).

Frame 5 in figure 47 shows high residual asymmetry in areas around the nasal regions and ala of the nose as well as a small patch near the vermillion of the upper lip. Following the pattern similar to frame 1, frame 5 is the final resting state of the muscles and the face is at a state of relaxation as there is no facial movement in this frame. Mild asymmetry returns in the vermillion border of the lower lip indicated by a light-yellow color.

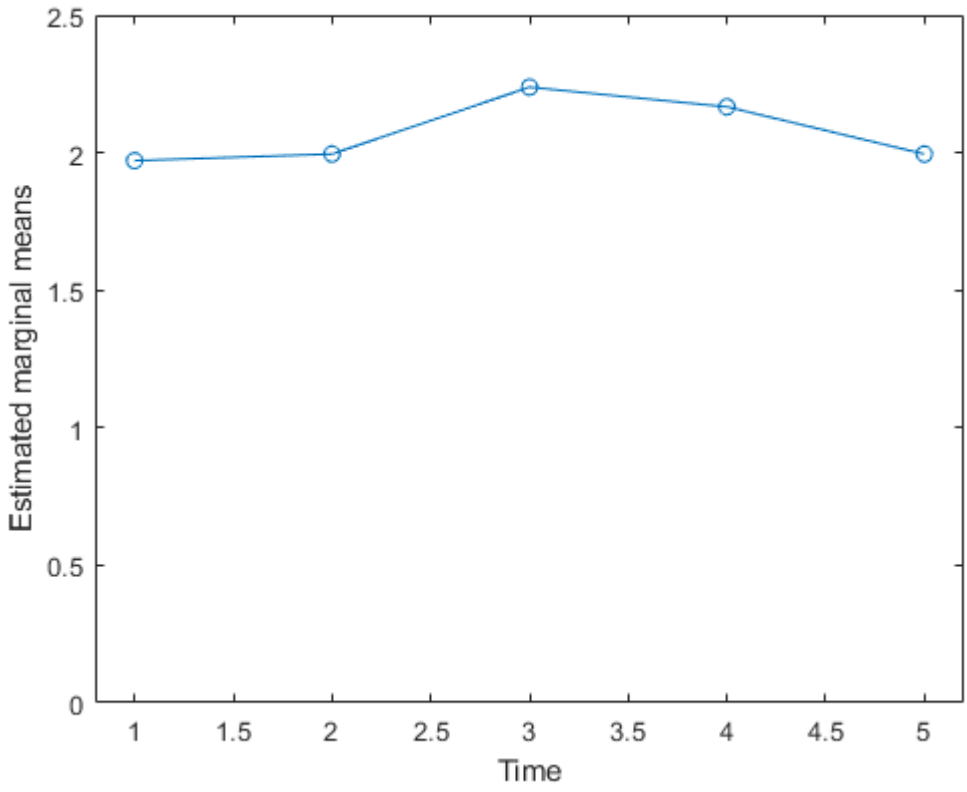

Figure 48: Asymmetry scores in the total face between 5 frames during maximum smile

Asymmetry scores during maximal smile in the total face in the UCL group showed frame 3 and frame 4 to be highest as compared to the other frames which signifies that the maximum smile expression accentuates facial asymmetry (Figure 48).

4.1.2. Asymmetry in mediolateral plane (X plane) during Maximal Smile

Facial asymmetry was also seen directionally in the x, y and z spatial planes and the color spectrum and readings assigned for this was slightly different as compared to total face asymmetry. Asymmetry to the right side (cleft side) was shown in red and asymmetry to the left side (non-cleft side) was shown in blue. All 3D images were standardized such that the patient's left side was the cleft side and the patient's right side was the non-cleft side.

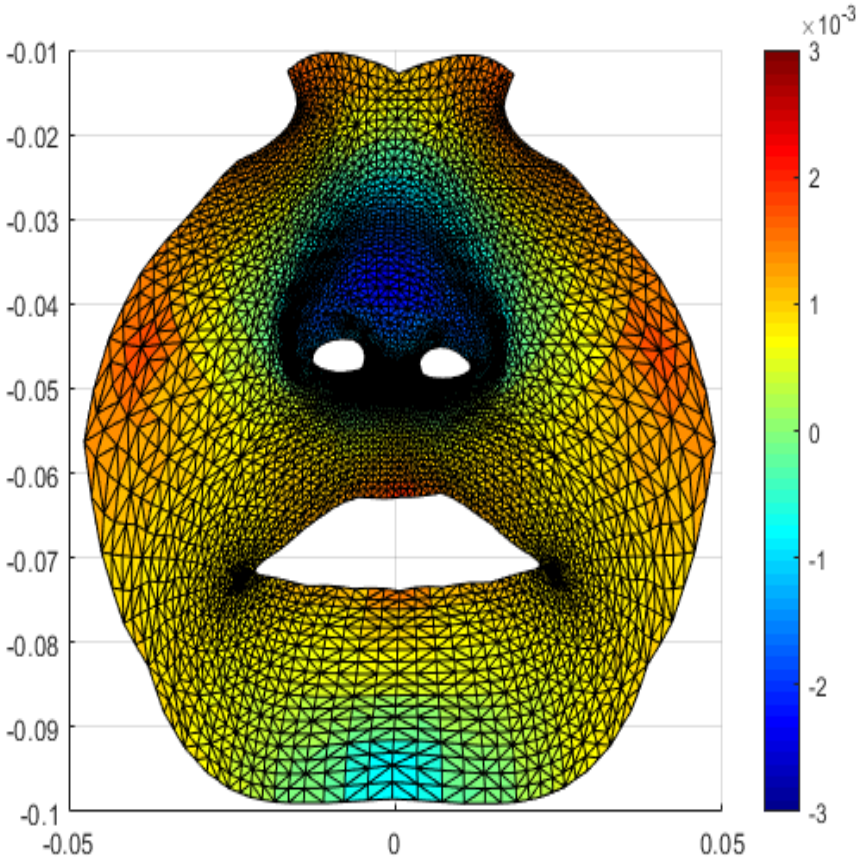

Figure 49: *FRAME 1* Color map of the average asymmetry in the mediolateral (X direction) direction in frame 1 in UCL patients during maximal smile. The red color represents asymmetry towards the right. The blue color represents asymmetry to the left side.

The color map in figure 49 shows asymmetry distribution in frame 1 in the mediolateral direction during maximal smile. The nasal tip, ala and other parts of the nose are standing out with darkest shades of blue, indicative of nasal tip deviation to the left side or the non-cleft side. The vermillion border of the upper lip and philtral areas show patches of yellow and red indicative of increased deviation and asymmetry towards the right side or the cleft-side. The base of the columella also shows mild deviation to the right side seen as patches of yellow. The lower lip also shows patches of yellow and red indicative of deviation to the right side.

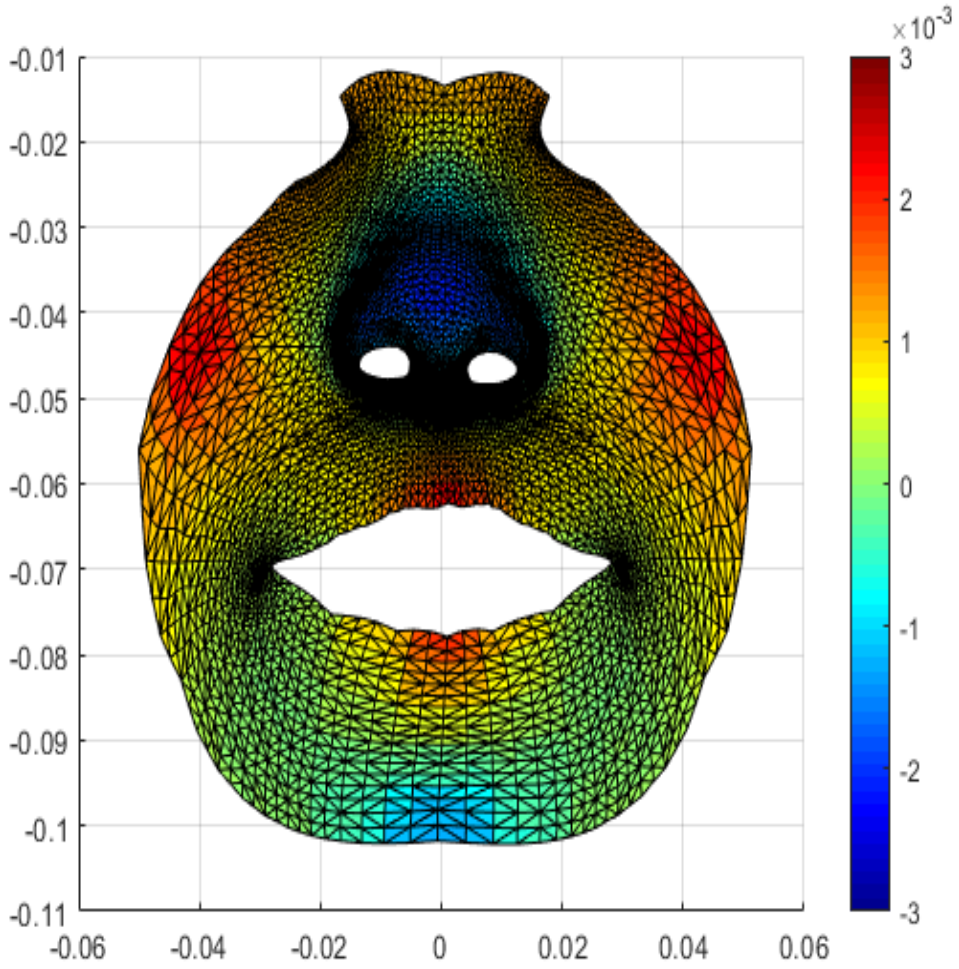

Figure 50: ***FRAME 2*** **Color map of the average asymmetry in the X direction in frame 2 in UCL patients during maximal smile. The red color represents asymmetry towards the right. The blue color represents asymmetry to the left side.**

The color map in figure 50 shows asymmetry distribution in frame 2 in the mediolateral direction during maximal smile. The nasal tip and ala and other parts of the nose were once again standing out with darkest shades of blue, indicative of nasal tip deviation to the left side or the non-cleft side. The vermillion border of the upper lip and philtral areas show patches of darker yellow and darker red indicative of increased deviation and asymmetry (compared to frame 1) towards the right side or the cleft side. The base of the columella shows deviation to the left side or the non-cleft side. Lower lip areas showed a deeper shade of red indicating increased deviation to the right side or cleft side. Frame 2 is the frame where the beginning of movement in the facial muscles results in accentuation of asymmetry.

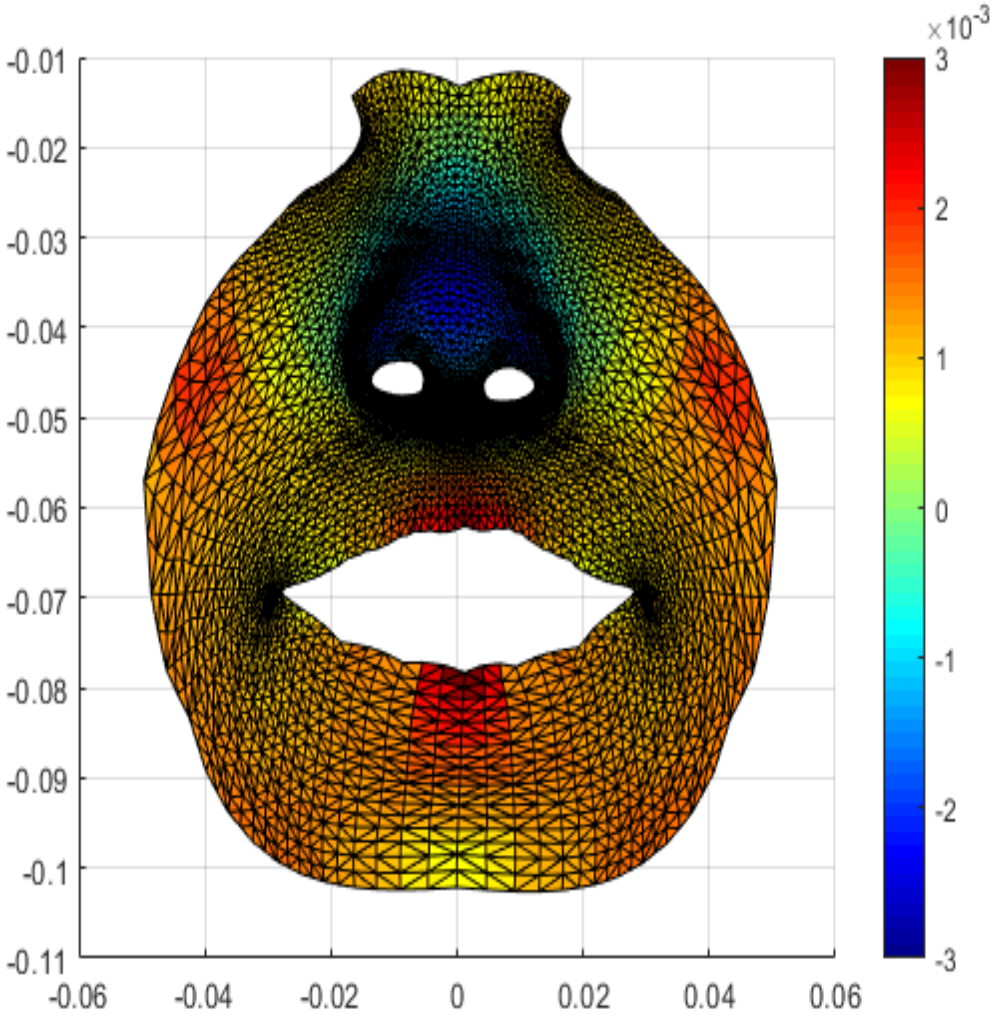

Figure 51: *FRAME 3* Color map of the average asymmetry in the X direction in frame 3 in UCL patients during maximal smile. The red color represents asymmetry towards the right. The blue color represents asymmetry to the left side

The color map in figure 51 shows asymmetry distribution in frame 3 in the mediolateral direction. The nasal tip, ala and other parts of the nose were seen with darkest shades of blue, indicative of nasal tip and alar deviation to the left side or the non-cleft side. The vermillion border of the upper lip and philtral areas showed darker areas of red indicative of increased deviation and asymmetry (compared to frame 2) towards the right side or cleft side. The base of the columella also shows deviation to the left or non-cleft side. Lower lip areas showed a deeper shade of red indicating increased deviation to the right side. Frame 3 is the peak expression frame where the muscles are in their maximum state of contraction to achieve peak facial expression.

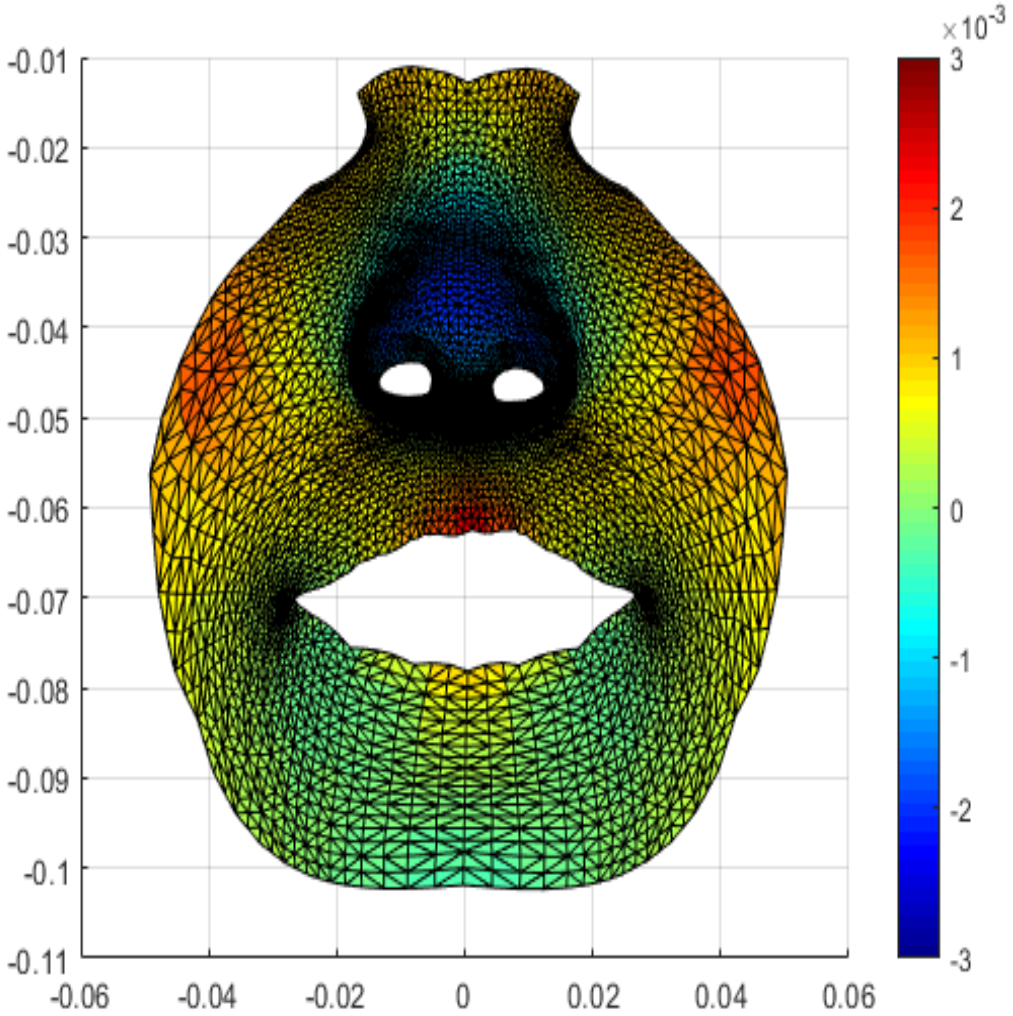

Figure 52: *FRAME 4* Color map of the average asymmetry in the <u>X direction</u> in frame 4 in UCL patients during <u>maximal smile</u>. The red color represents asymmetry towards the right. The blue color represents asymmetry to the left side.

The color map in figure 52 shows asymmetry distribution in frame 4 in the mediolateral direction during maximal smile. The nasal tip and ala and other parts of the nose were seen with darkest shades of blue, indicative of nasal tip and alar deviation to the left side or non-cleft side. The vermillion border of the upper lip and philtral areas showed less intense areas of red and yellow indicative of asymmetry lesser than frame 3. The intense red patch seen on the lower lip in frame 3 showed yellow patches in frame 4 indicative of lesser deviation to the right side as compared to frame 3 as the face is returning to a state of rest. Commissures were seen as green patches indicative of no differences in symmetry.

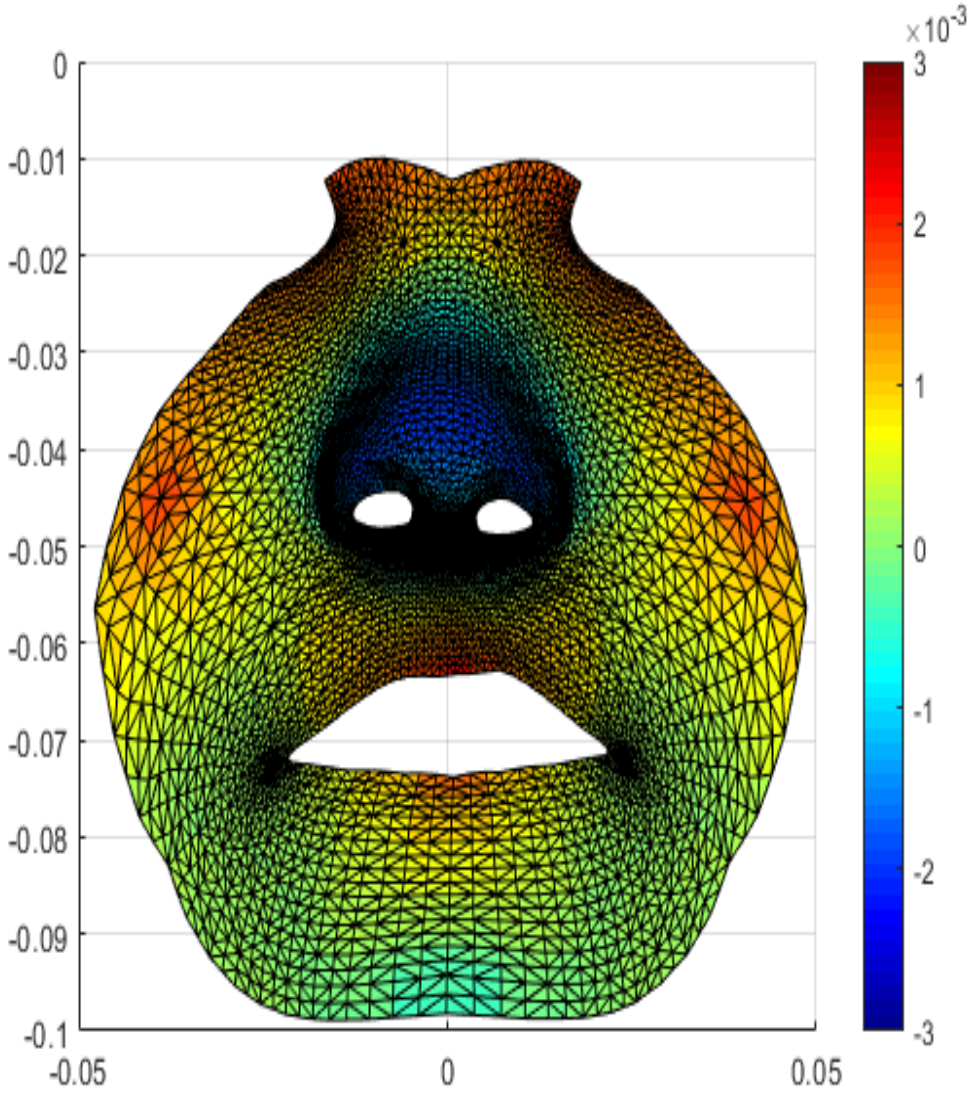

Figure 53: *FRAME 5* Color map of the average asymmetry in <u>the X direction</u> in frame 5 in UCL patients during <u>maximal smile</u>. The red color represents asymmetry towards the right. The blue color represents asymmetry to the left side.

The color map in figure 53 shows asymmetry distribution in frame 5 in the mediolateral direction. The nasal tip and ala and other parts of the nose were seen with darkest shades of blue, indicative of nasal tip and alar deviation to the left side or non-cleft side. The vermillion border of the upper lip and philtral areas showed areas of red and yellow indicating deviation to the right side slightly more than frame 4. Commissures were seen as green patches indicative of no differences in symmetry. The vermillion border of the lower lip converted from a yellow color to a deep red color patch in frame 5 indicating increased asymmetry to the right side as compared to frame 4. This residual asymmetry is seen in the final resting state of the face wherein all the muscles are in a state of rest.

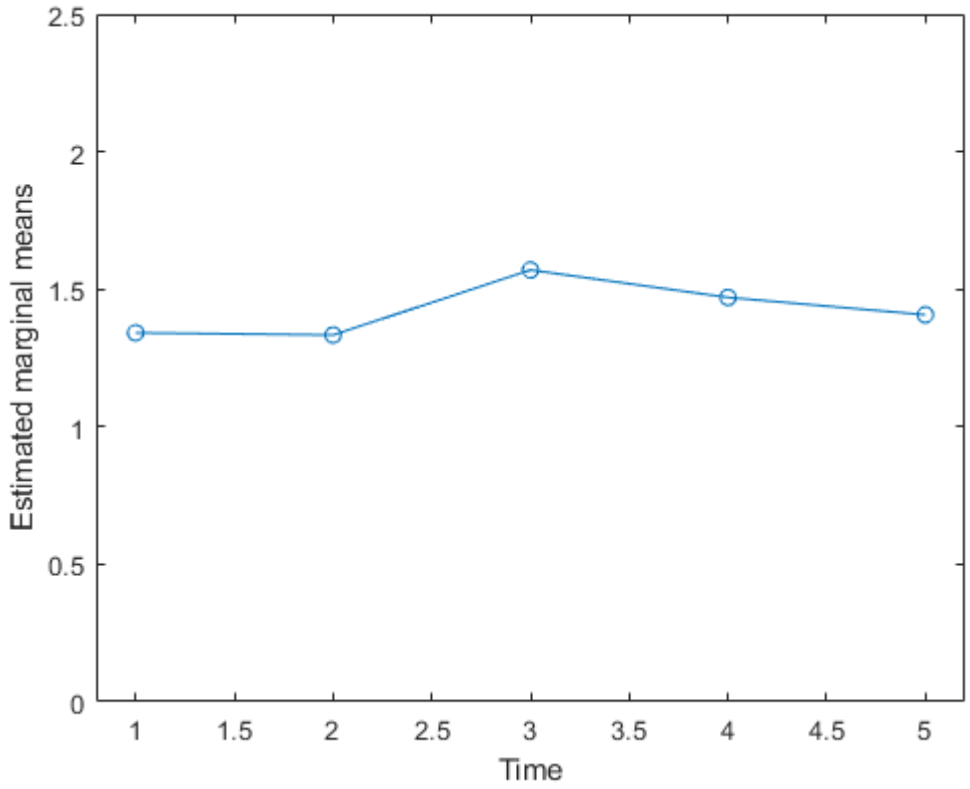

Figure 54: Asymmetry scores in the X direction between 5 frames during maximum smile

Asymmetry was accentuated during performance of the facial expression and frame 3 and 4 demonstrated higher asymmetry. The magnitude of asymmetry at these frames (3 and 4) were significantly different in comparison to the first frame recorded at rest ($p<0.05$). This confirms maximum smile exaggerates the asymmetry which is noted at the rest pose (Figure 54).

4.1.3. Asymmetry in Vertical (Y plane) during Maximal Smile

Asymmetry in the upward direction was seen as areas of yellow and red and asymmetry in downward direction was seen as areas of blue.

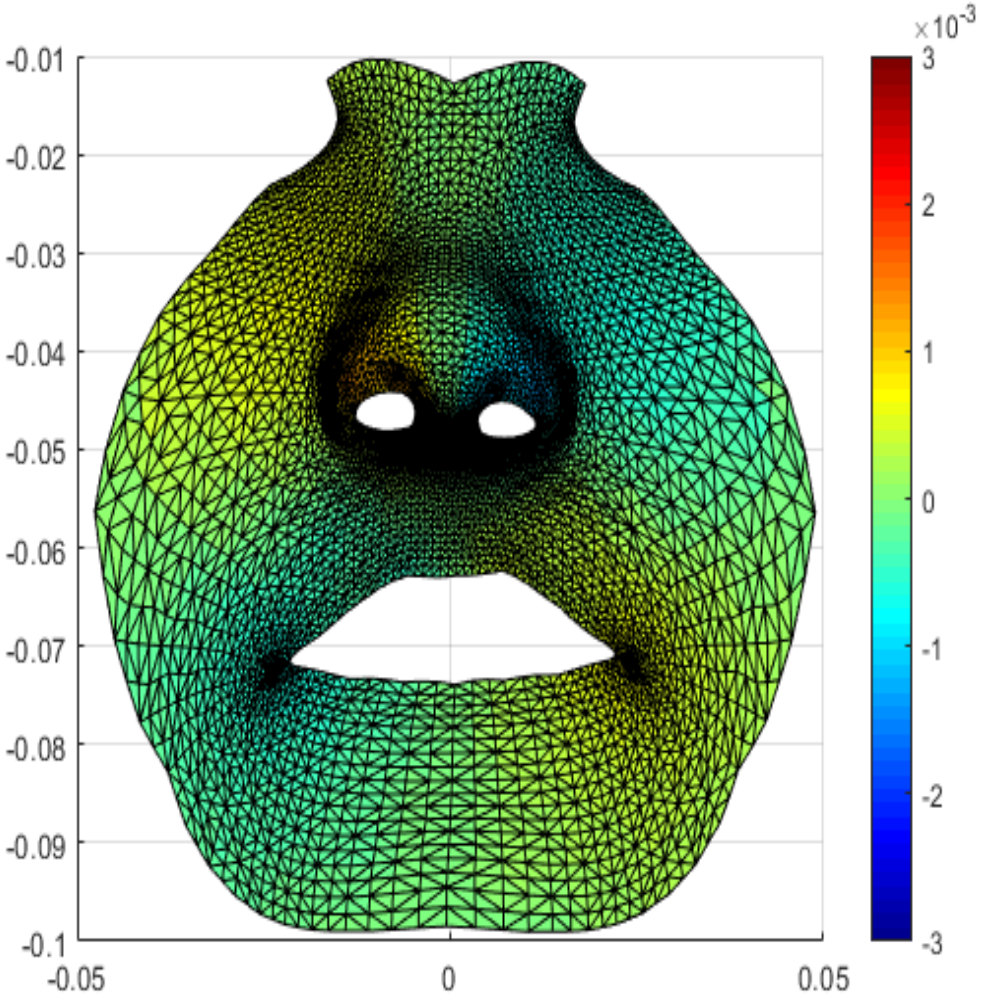

Figure 55: *FRAME 1* Color map of the asymmetry in the Y direction in frame 1 in UCL patients during maximal smile. The red color represents asymmetry in upward direction. The blue color represents asymmetry in a downward direction.

Figure 55 represents color map of asymmetry distribution in frame 1 in the vertical direction in UCL patients. Mostly areas of green and light green are seen in the nasolabial region indicative of minimal vertical changes occurring in frame 1 of the maximal smile. Frame 1 is the resting state of the face. The left ala of the nose shows a slight blue patch indicating deviation in downward direction and the right ala shows mild yellowish red color indicating deviation in upwards direction. Mild blue color on the right side of the upper lip indicates downward deviation and left side of the lip shows upward deviation indicated by its mild yellow color.

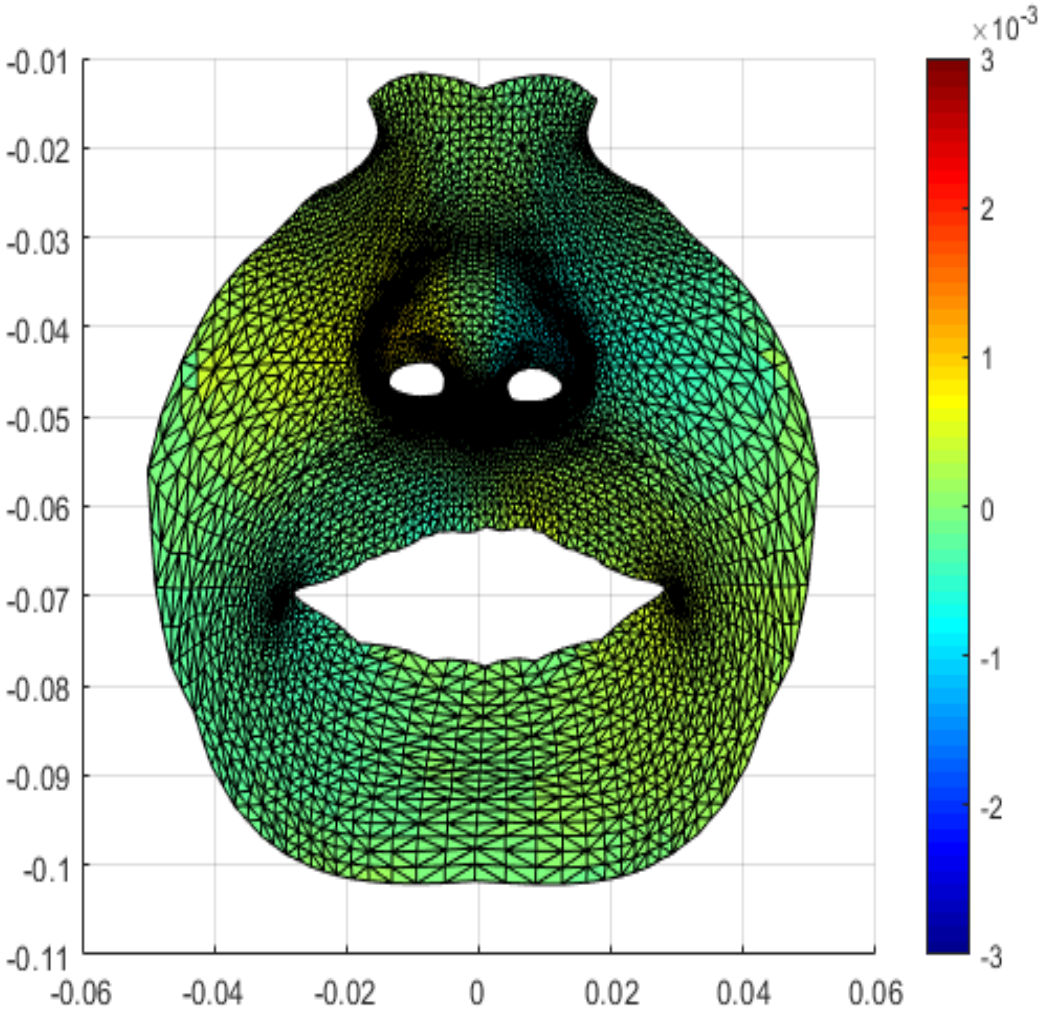

Figure 56: *FRAME 2* Color map of the asymmetry in the Y direction in frame 2 in UCL patients during maximal smile. The red color represents asymmetry in upward direction. The blue color represents asymmetry in a downward direction.

Figure 56 represents color map of asymmetry distribution in frame 2 in the vertical direction in UCL patients. Mostly areas of green and light green are seen in the nasolabial region indicative of minimal vertical changes occurring in frame 2 of the maximal smile. The left ala of the nose shows slight blue patch indicating deviation in downward direction and the right ala shows mild yellowish red color indicating deviation in upwards direction. This frame was more or less similar to frame 1 indicating minimum changes in vertical direction with increasing movement.

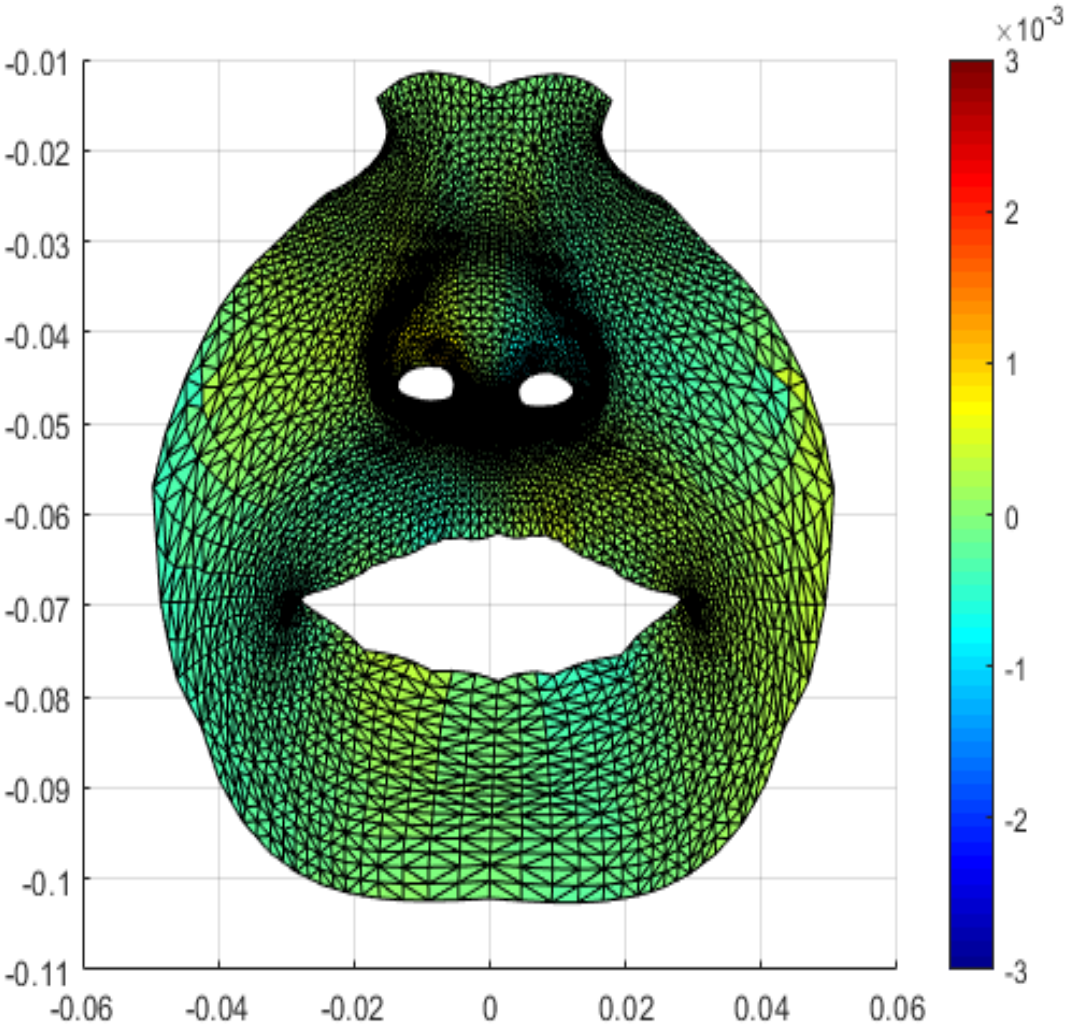

Figure 57: *FRAME 3* Color map of the asymmetry in the <u>Y direction</u> in frame 3 in UCL patients during <u>maximal smile</u>. The red color represents asymmetry in upward direction. The blue color represents asymmetry in a downward direction.

Frame 3 (Figure 57) of the maximal smile in the Y direction was similar to that of frame 2 and 1 indicating no changes in vertical direction during the maximum smile.

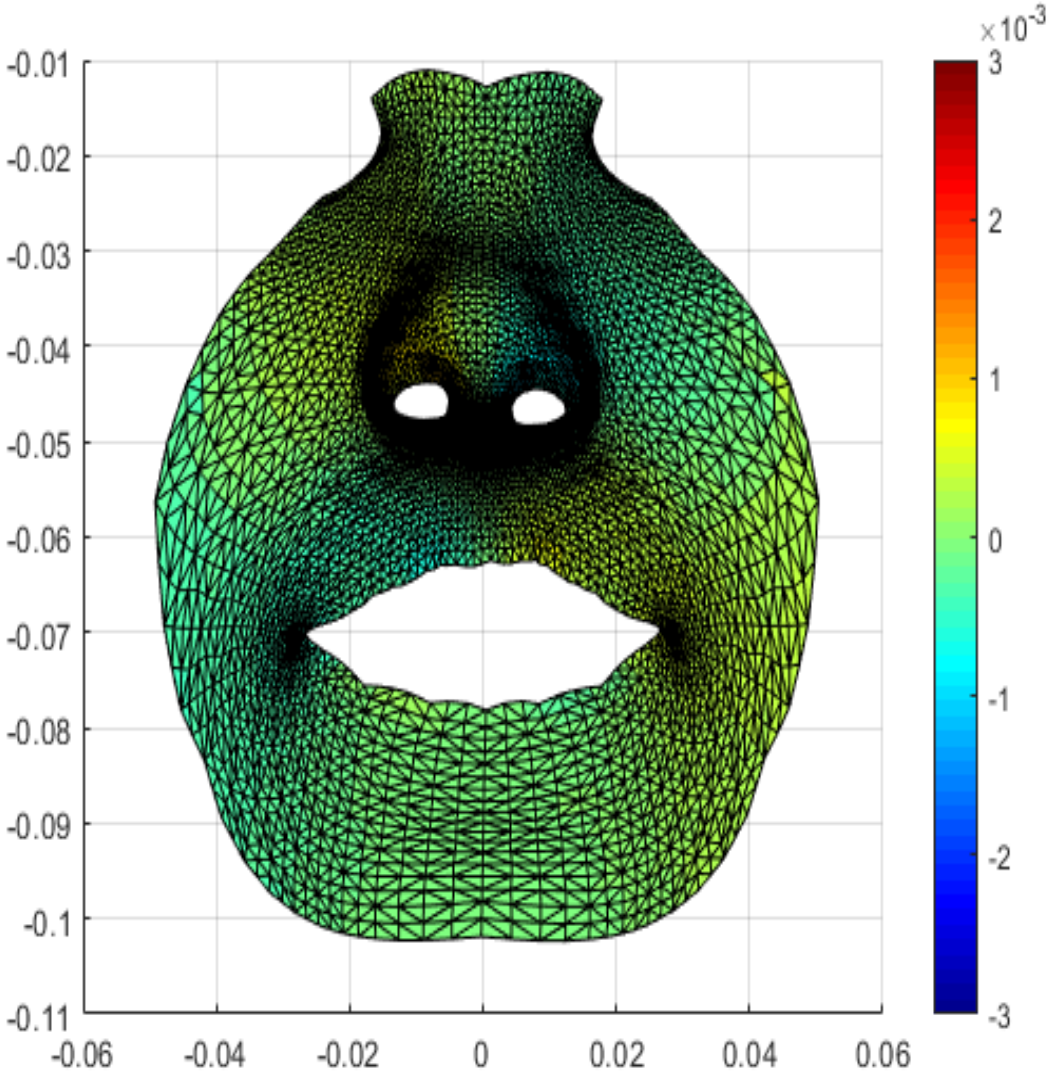

Figure 58: *FRAME 4* Color map of the asymmetry in the Y direction in frame 4 in UCL patients during maximal smile. The red color represents asymmetry in upward direction. The blue color represents asymmetry in a downward direction.

Frame 4 (Figure 58) in the vertical direction was no different from the prior frames indicating no change in the vertical direction.

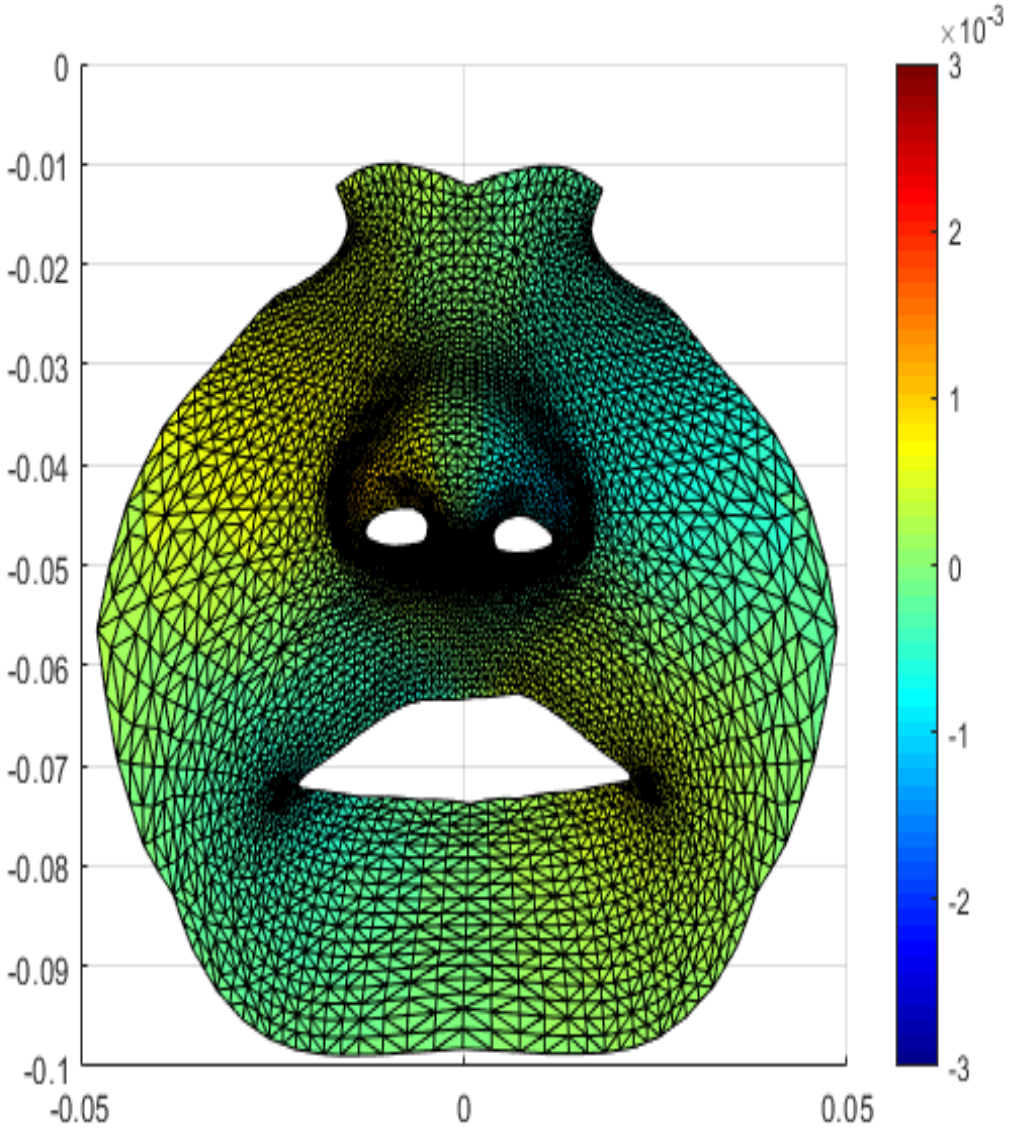

Figure 59: *FRAME 5* Color map of the asymmetry in the Y direction in frame 5 in UCL patients during maximal smile. The red color represents asymmetry in upward direction. The blue color represents asymmetry in a downward direction.

Frame 5 (Figure 59) in the vertical direction in UCL patients showed no changes in asymmetry in comparison to the prior frames. This indicates that minimum

vertical changes were seen in the maximum smile facial expression and that facial movement did not affect asymmetry in the vertical dimension.

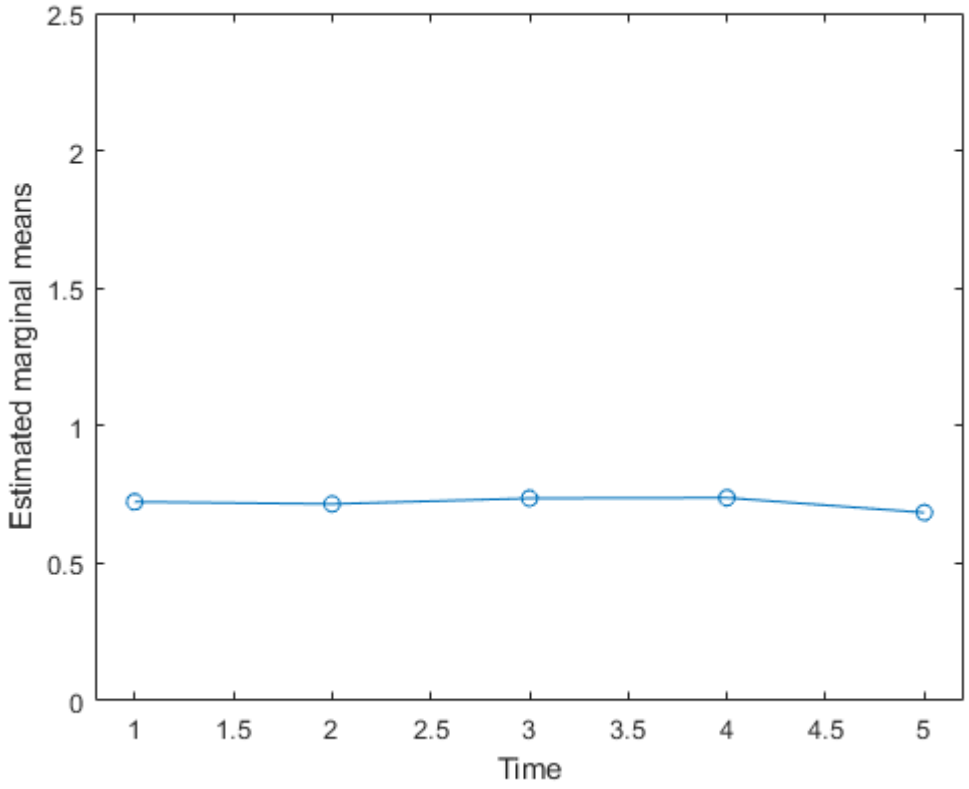

Figure 60: Asymmetry scores in the Y direction between 5 frames during maximum smile

In the Y direction, minimum changes were seen during maximal smile as seen in the estimated marginal means graph, indicating that vertical changes were minimal during maximum smile.

4.1.4. Asymmetry in Antero-posterior (Z plane) during Maximal Smile

Asymmetry in the Z direction or antero-posteriorly was represented on the color map using a different color scale. Areas in red indicated deviation and

asymmetry towards the observer (anteriorly or in a forward direction). Areas in blue indicated deviation away from the observer (posteriorly or in backward direction).

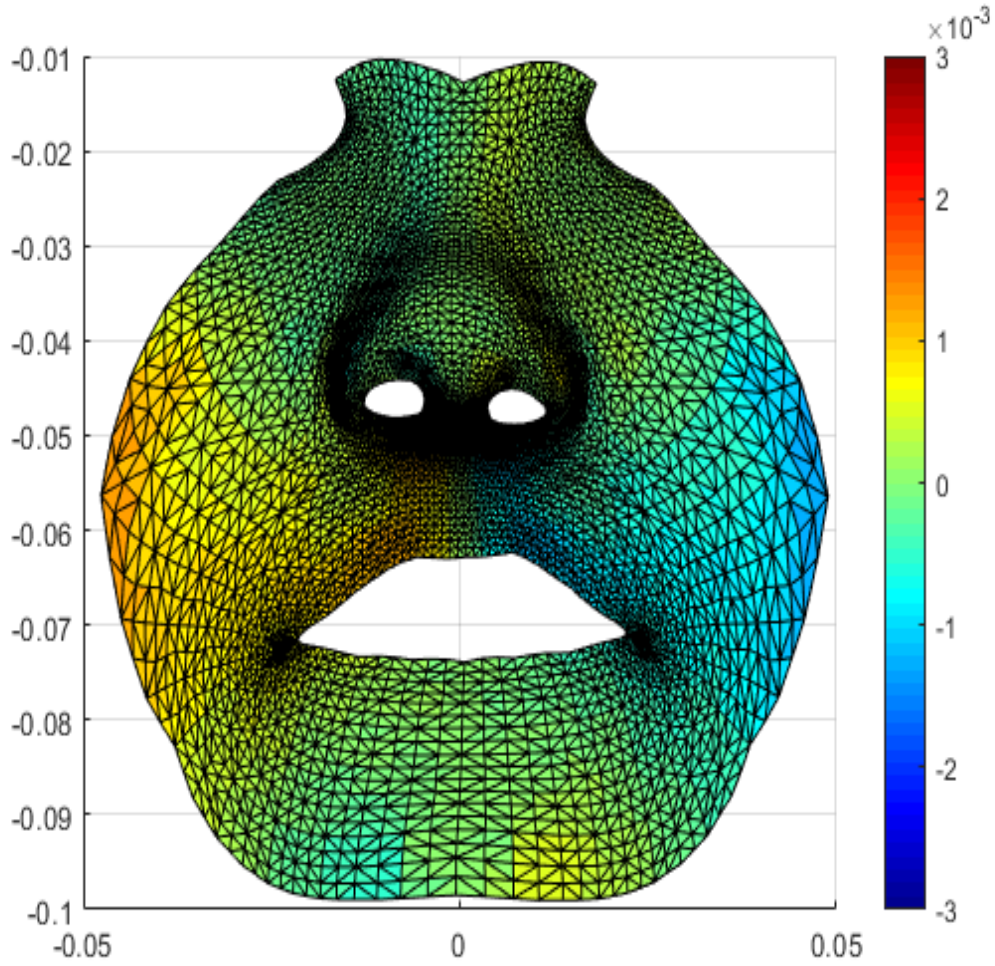

Figure 61: *FRAME 1* Color map of the average asymmetry in the <u>Z direction</u> in frame 1 in UCL patients during <u>maximal smile</u>. The red color represents asymmetry in a forward (towards observer) direction. The blue color represents asymmetry in a backward direction (away from observer).

Frame 1 (Figure 61) of the maximum smile in the antero-posterior direction shows areas of green in the nasal tip and alar regions of the nose indicating minimal to no change in asymmetry. The left side vermillion border of the upper lip shows a patch of blue indicating posterior or backward deviation. The right

side of the vermillion border of the upper lip had a shade of yellow and light red which indicated anterior deviation towards the observer. The remaining areas showed minimal changes.

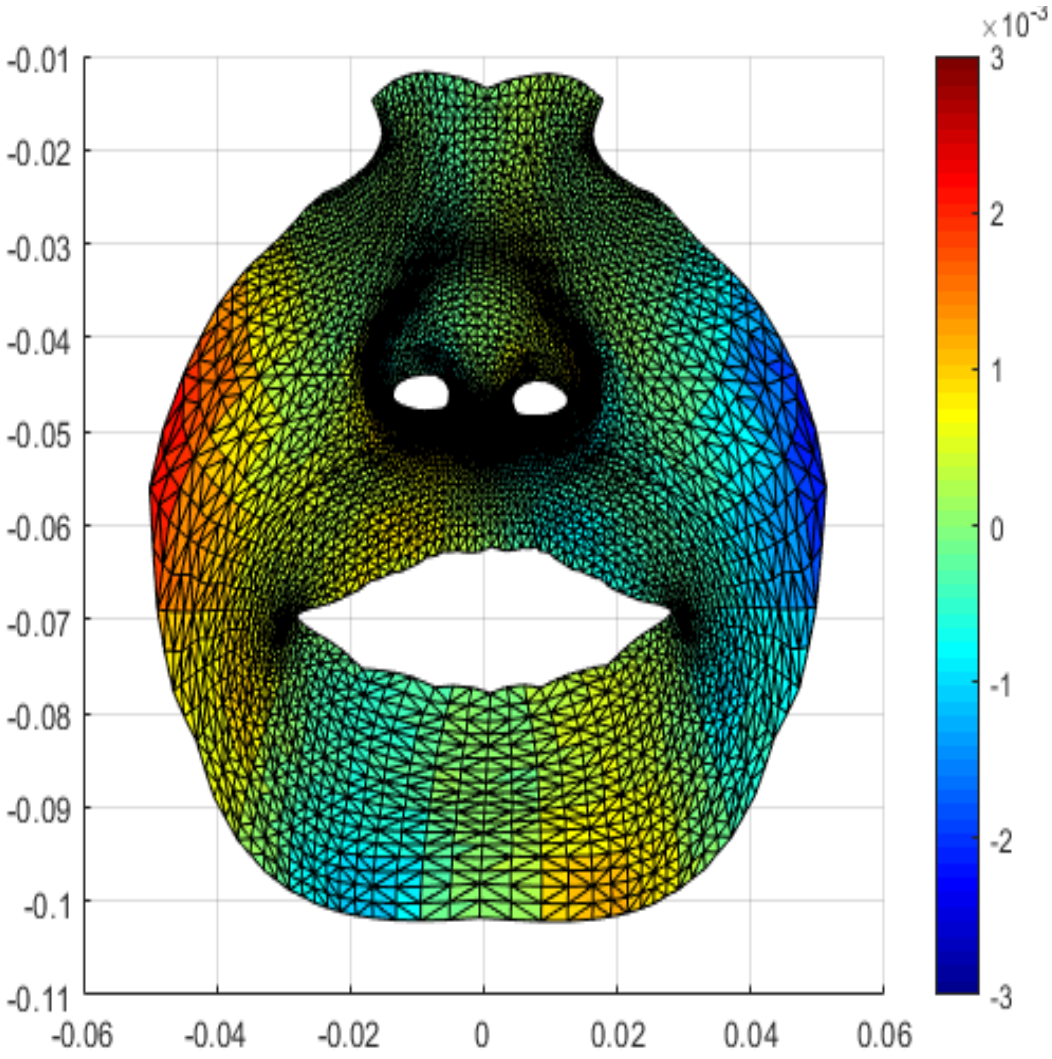

Figure 62: *FRAME 2* Color map of the average asymmetry in the Z direction in frame 2 in UCL patients during maximal smile. The red color represents asymmetry in a forward (towards observer) direction. The blue color represents asymmetry in a backward direction (away from observer).

The left side vermillion border of the upper lip shows a patch of blue indicating posterior or backward deviation. The right side of the vermillion border of the upper lip had a shade of yellow and light red which indicated anterior deviation towards the observer. The lower lip shows color trend in the opposite with the right side of the lower lip showing areas of blue indicating deviation posteriorly and the left side of the lower lip showing patches of yellow indicating anterior

deviation. The left nostril and surrounding alar regions showed slight yellowish coloration indicating mild anterior deviation as compared to the right sided nostril.

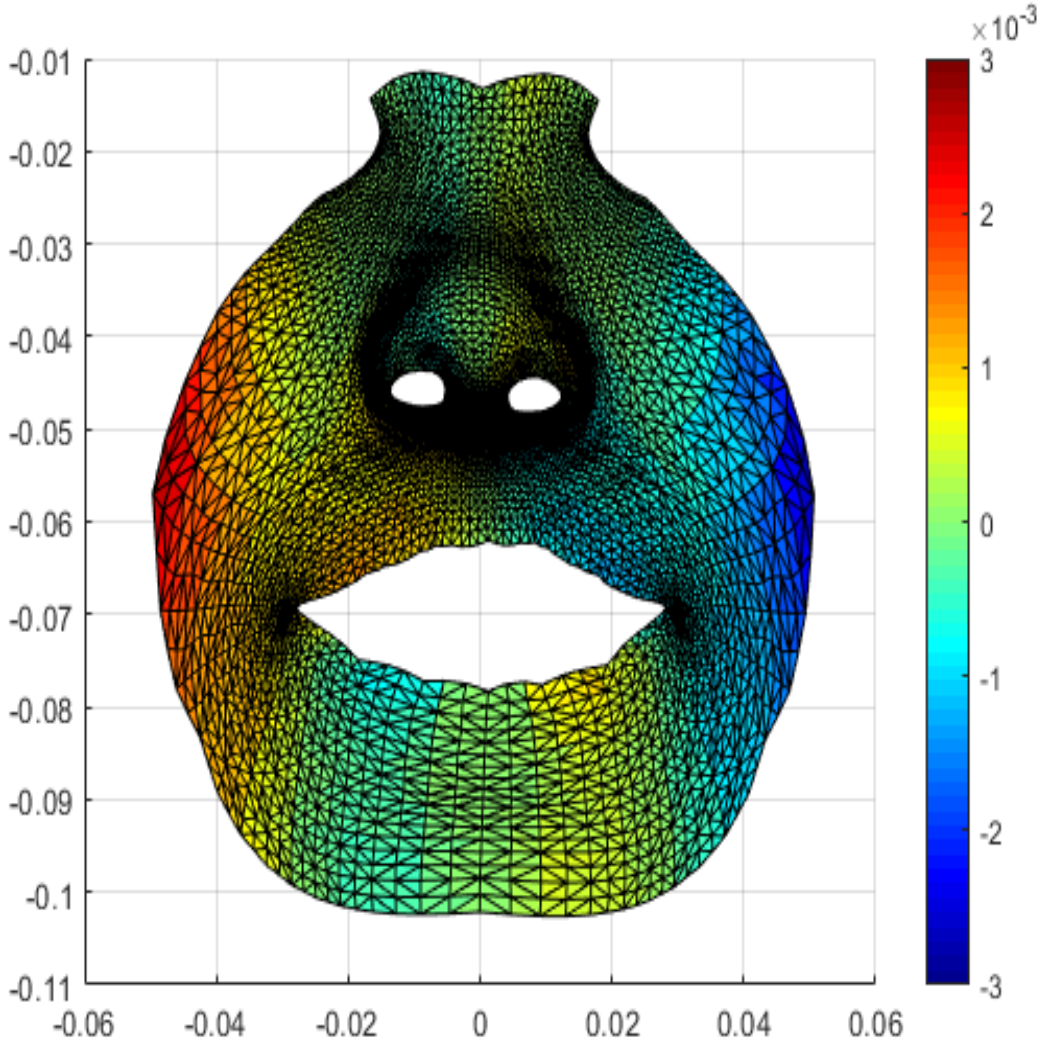

Figure 63: *FRAME 3* Color map of the average asymmetry in the Z direction in frame 3 in UCL patients during maximal smile. The red color represents asymmetry in a forward (towards observer) direction. The blue color represents asymmetry in a backward direction (away from observer).

In figure 63, the left side vermillion border and philtrum of the upper lip shows a patch of blue indicating posterior or backward deviation. The right side of the vermillion border and philtrum of the upper lip had a shade of yellow and light red which indicated anterior deviation towards the observer. The lower lip shows color trend in the opposite with the right side of the lower lip showing areas of blue indicating deviation posteriorly and the left side of the lower lip showing

patches of yellow indicating anterior deviation. The left nostril and surrounding alar regions showed slight yellowish coloration indicating mild anterior deviation as compared to the right sided nostril which showed a blue patch indicating posterior deviation. Frame 3 is the peak movement which showed accentuated movement and greater deviation.

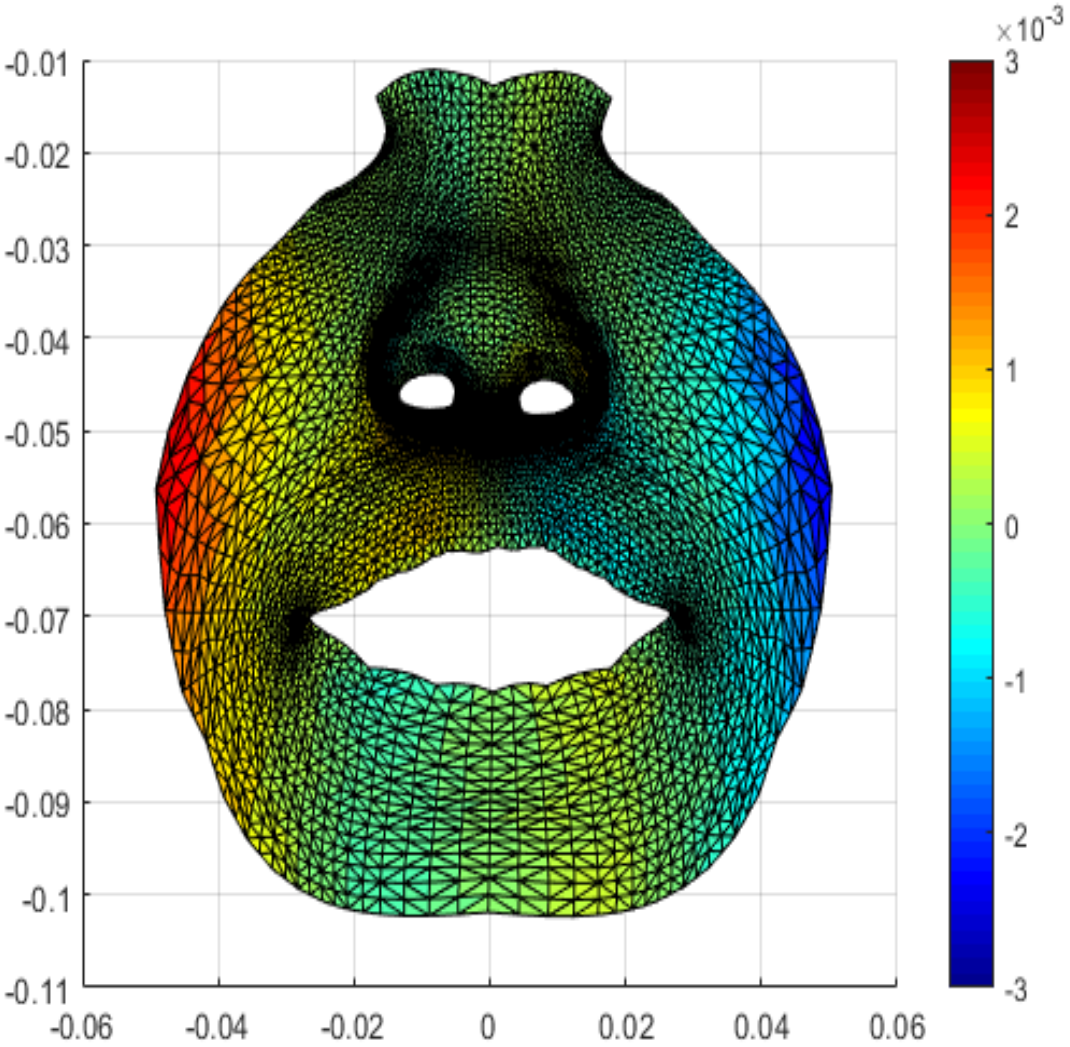

Figure 64: *FRAME 4* Color map of the average asymmetry in the Z direction in frame 4 in UCL patients during maximal smile. The red color represents asymmetry in a forward (towards observer) direction. The blue color represents asymmetry in a backward direction (away from observer).

Frame 4 (Figure 64) which is midway between peak expression and final resting state shows similar color pattern to frame 3 except that the colors were milder

in intensity indicating decreased asymmetry as compared to frame 3. Nasal regions were seen to return to a green color indicating minimal changes in frame 4.

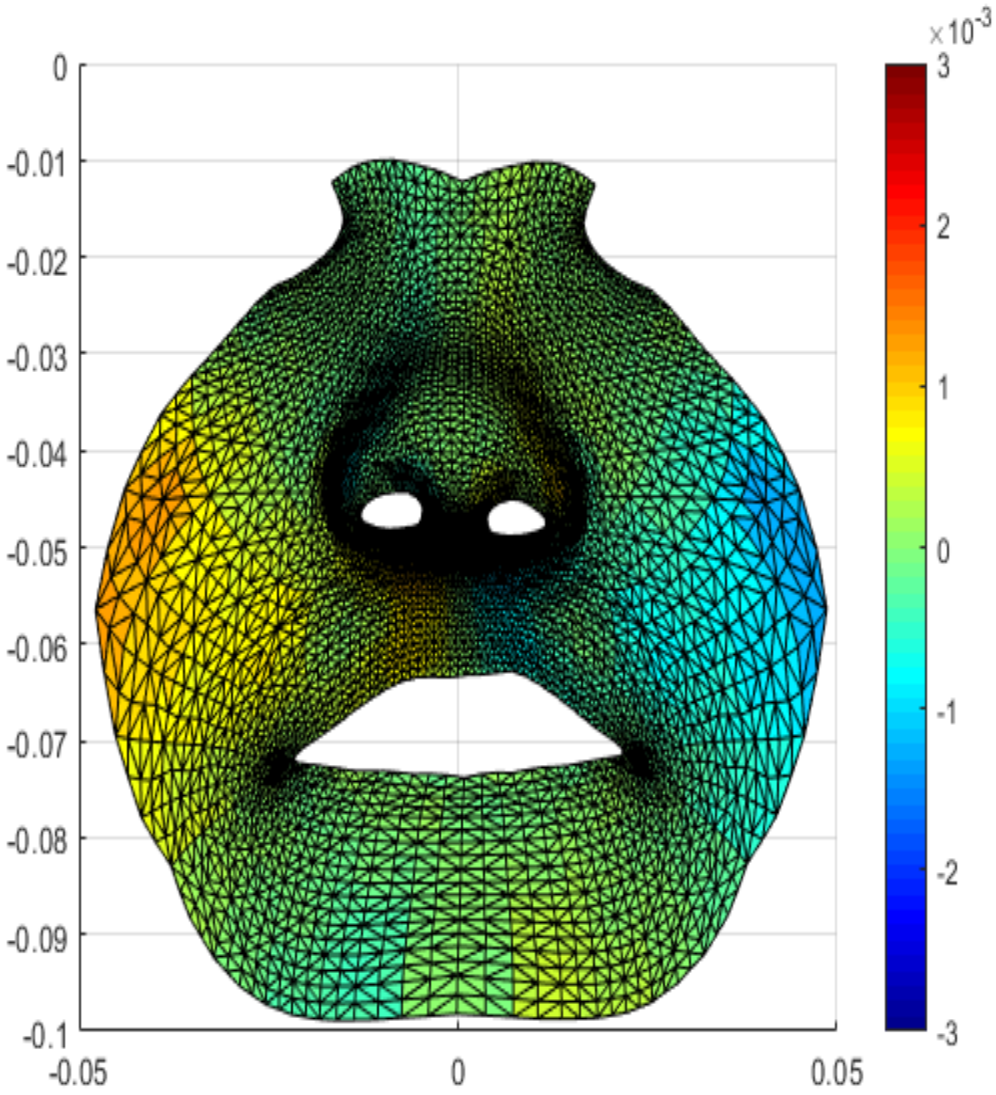

Figure 65: *FRAME 5* Color map of the average asymmetry in the Z direction in frame 5 in UCL patients during maximal smile. The red color represents asymmetry in a forward (towards observer) direction. The blue color represents asymmetry in a backward direction (away from observer).

Frame 5 (Figure 65) showed minimum changes in asymmetry represented by areas of green in most regions including the nasal tip and ala of the nose. The left upper philtrum and upper lip showed posterior deviation as compared to the

right upper philtrum and lip which showed anterior deviation but with lesser intensity as compared to frame 4.

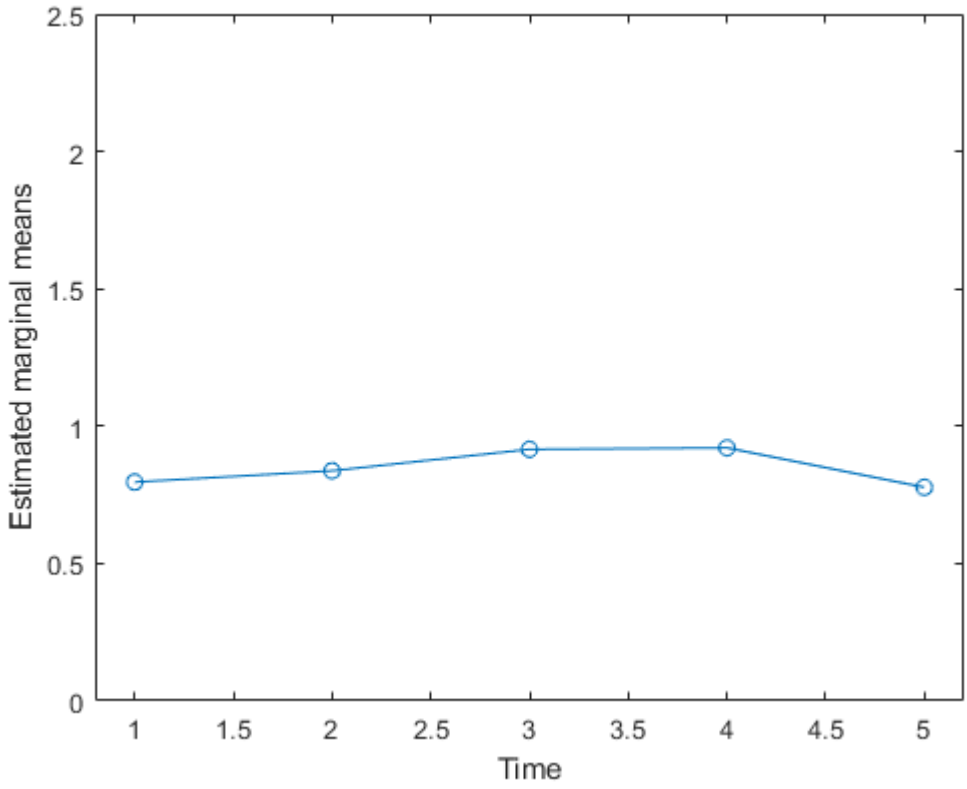

Figure 66: Asymmetry scores in the Z direction between 5 frames during maximum smile

Asymmetry scores in the Z direction in the UCL group showed increased asymmetry in frame 3 and 4 with highest asymmetry noted in frame 4. The differences in asymmetry scores were not visible due to the differences being small.

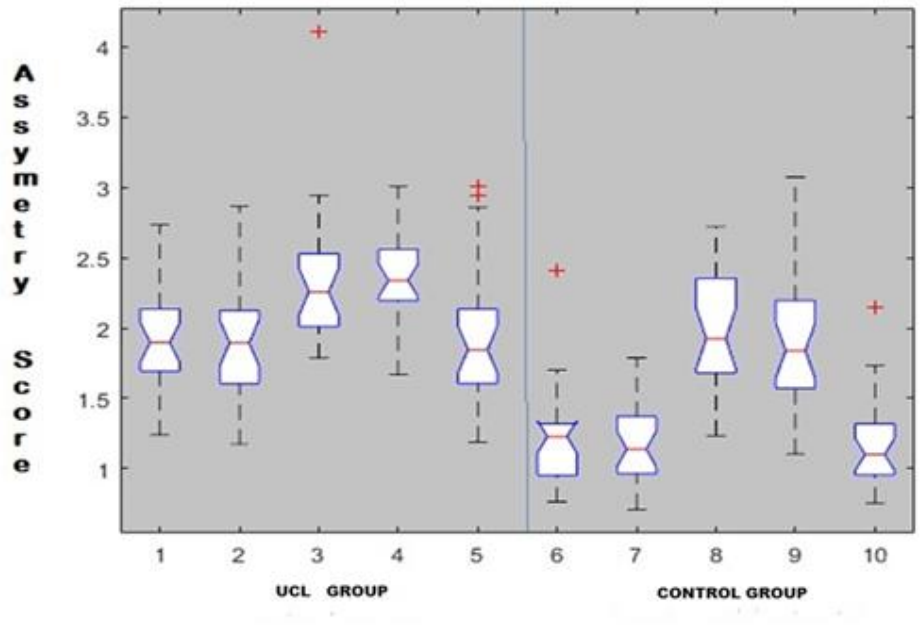

Figure 67: Box plot of asymmetry scores between UCL and controls during maximum smile

Asymmetry in the UCL group was seen to be higher in the mid-way frame (frame 4-mid-way between maximum smile and final resting stage) followed by the frame at peak expression. Significant difference was seen in asymmetry scores between frame 2, 3, 4 and the remaining frames within the UCL group. Likewise, frame 5 of the UCL cases showed clear residual asymmetry that was significantly different from the first frame or the frame with face in resting position. Significant differences were seen between the UCL group and control group for all frames.

4.2. Cheek Puff

Summary of results during cheek puff

Significant differences were seen in all frames between the UCL group and the control group during the cheek puff. No significant differences were seen in asymmetry scores between all frames within the UCL group in the whole face, x and y direction. The differences in asymmetry scores in all frames of the UCL group were significantly different ($p<0.001$) only in the z direction (anteroposterior direction).Asymmetry in the UCL group was seen to be higher in the mid-way frame (frame 2-mid-way between initial resting frame and peak expression of cheek puff) followed by frame 4 for whole face, x and z directions. Asymmetry in the total face was seen most pronounced in frame 2 as the face was moving into the phase of peak facial expression. In the X direction, asymmetry was most noted in the alar regions and philtrum and upper lip regions. Vertical asymmetries were minimal. Anteroposterior asymmetry was most noted in frame 2 in areas around the ala of the nose and upper lip vermillion and philtrum.

4.2.1. Total face asymmetry during Cheek Puff

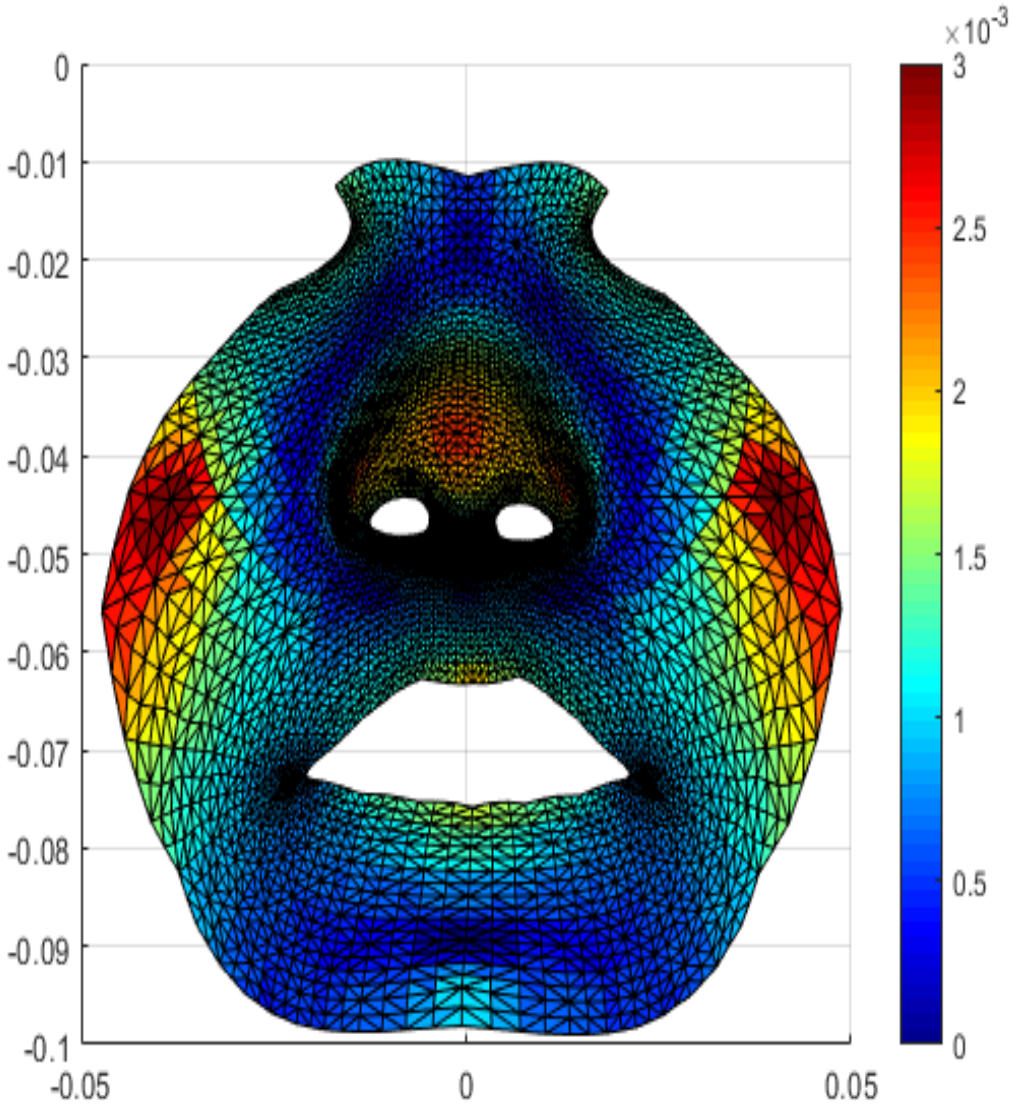

Figure 68: *FRAME 1* Total face asymmetry in frame 1 during Cheek Puff. The green color represents no asymmetry, the dark blue color indicates minimum asymmetry, and the dark red indicates increased asymmetry

Frame 1 in figure 68 shows higher residual asymmetry in areas around the nasal tip and alar regions (patches of red interspersed with yellow patches). Mild

yellow patches were seen in a portion of the upper lip vermillion border as well as a small part of the lower lip, indicating higher asymmetry in a small portion of both the upper and lower lip. Most of the residual asymmetry in frame 1 was seen in the nasal regions and the upper lip. Frame 1 is the resting frame wherein the face is resting with no facial movement.

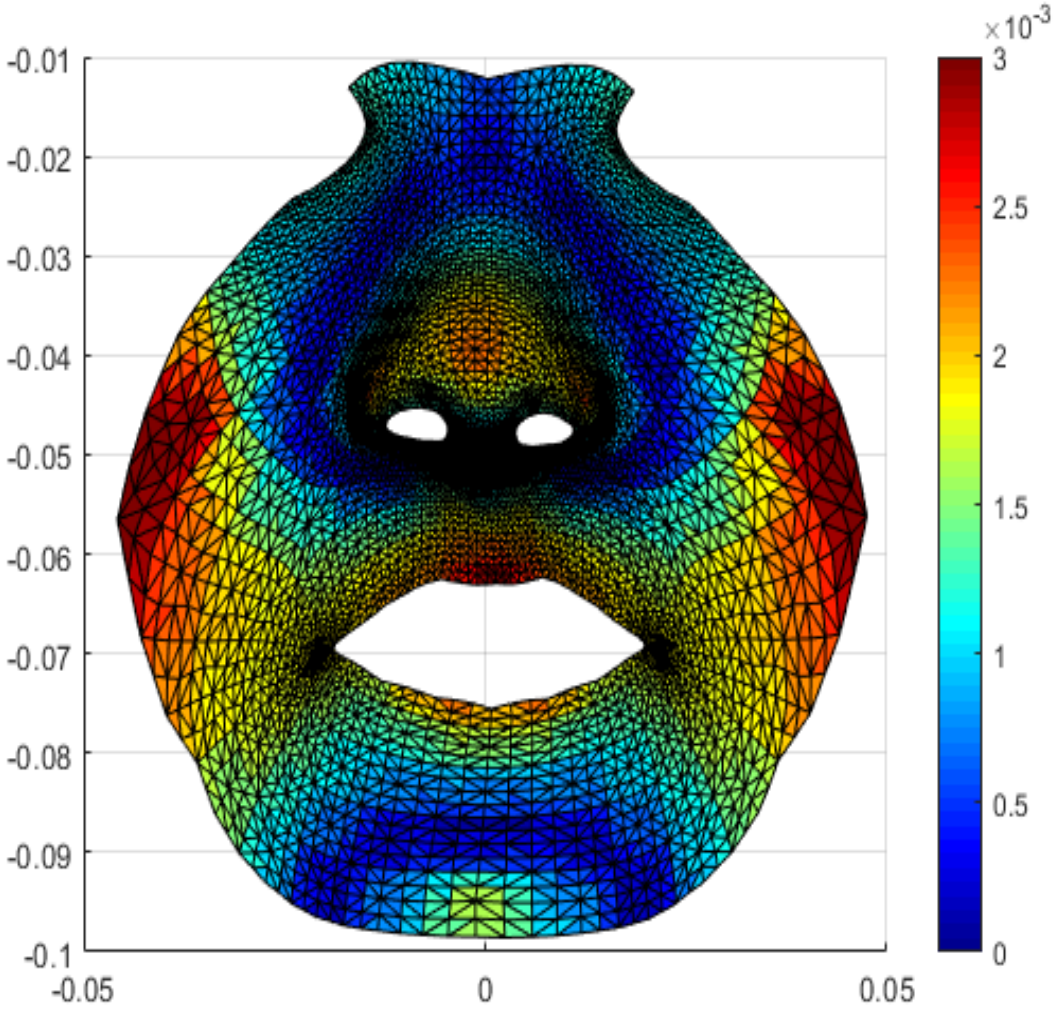

Figure 69: ***FRAME 2*** **Total face asymmetry in frame 2 during Cheek Puff. The green color represents no asymmetry, the dark blue color indicates minimum asymmetry, and the dark red indicates increased asymmetry.**

Frame 2 (Figure 69) shows increased asymmetry in the nasal tip and alar regions of the nose indicated by yellow and red areas. This was seen to be more intense as compared to frame 1 which was the resting frame. Areas around vermillion border of the upper lip, the philtrum, vermillion border of lower lip and the commissures showed yellow patches which was indicative of higher asymmetry in these regions as the muscles associated with cheek puff were contracting to bring the nasolabial region to peak expression state.

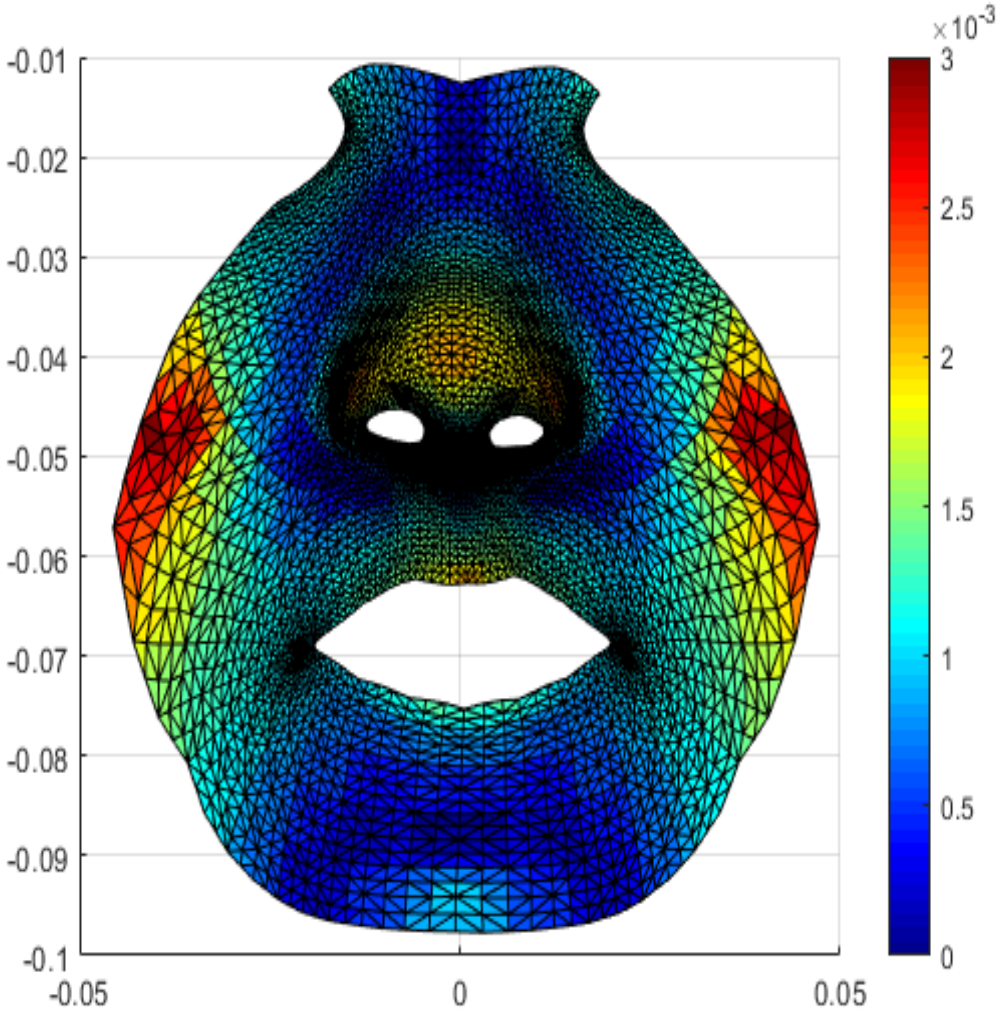

Figure 70: *FRAME 3* Total face asymmetry in frame 3 during Cheek Puff. The green color represents no asymmetry, the dark blue color indicates minimum asymmetry, and the dark red indicates increased asymmetry.

Frame 3 (Figure 70) showed increased asymmetry in the nasal tip and alar regions but less as compared to frame 2. Likewise, in the upper lip vermillion border, asymmetry was lesser than in frame 2. The lower lip showed areas of blue which indicated lesser asymmetry. Commissures of the mouth also showed decreased asymmetry as compared to frame 2.

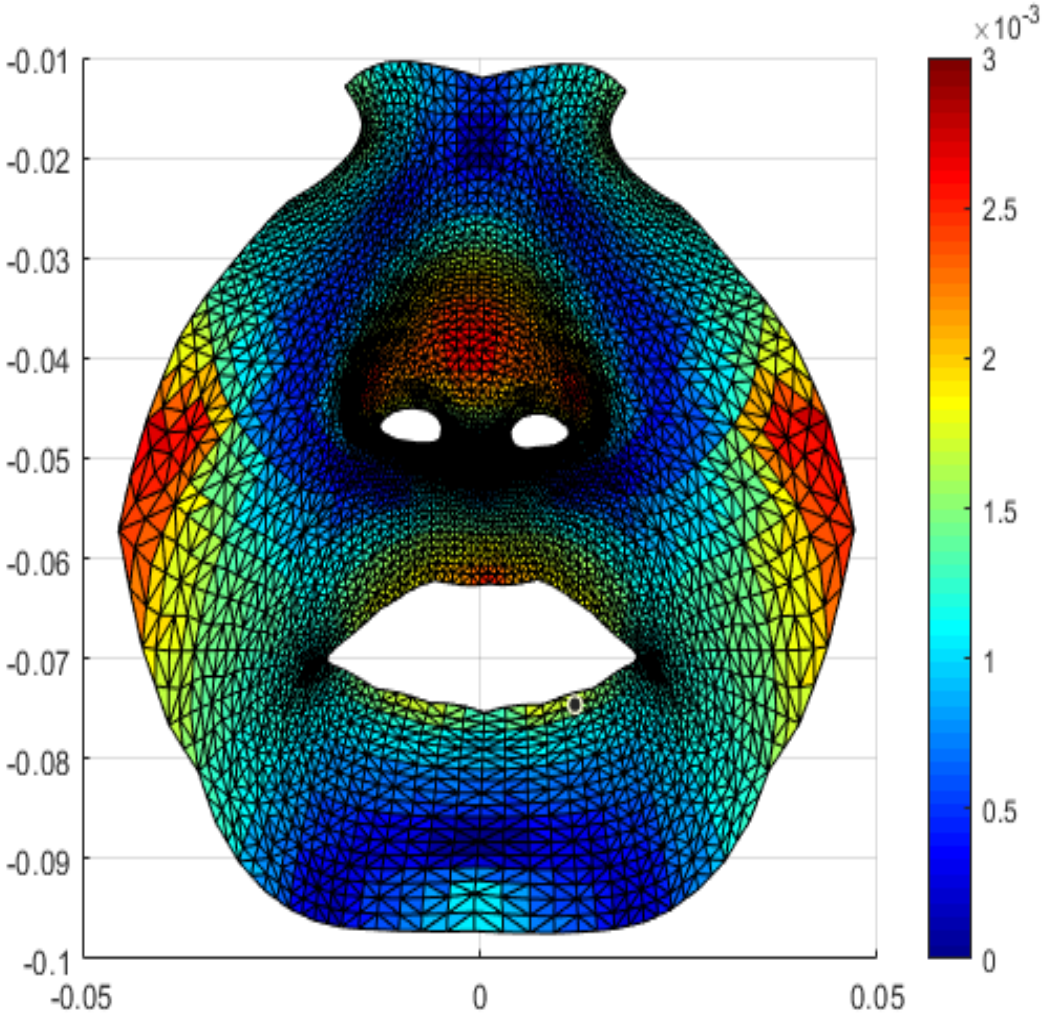

Figure 71: *FRAME 4* Total face asymmetry in frame 4 during Cheek Puff. The green color represents no asymmetry, the dark blue color indicates minimum asymmetry, and the dark red indicates increased asymmetry.

Asymmetry in frame 4 (Figure 71) was seen to be increased around nasal tip and alar regions as compared to frame 3 indicated by the red color. Upper lip vermillion border also showed higher asymmetry indicated by the yellow patches and parts of the lower lip showed a slight increase in asymmetry. Commissures of the mouth remained the same as frame 3.

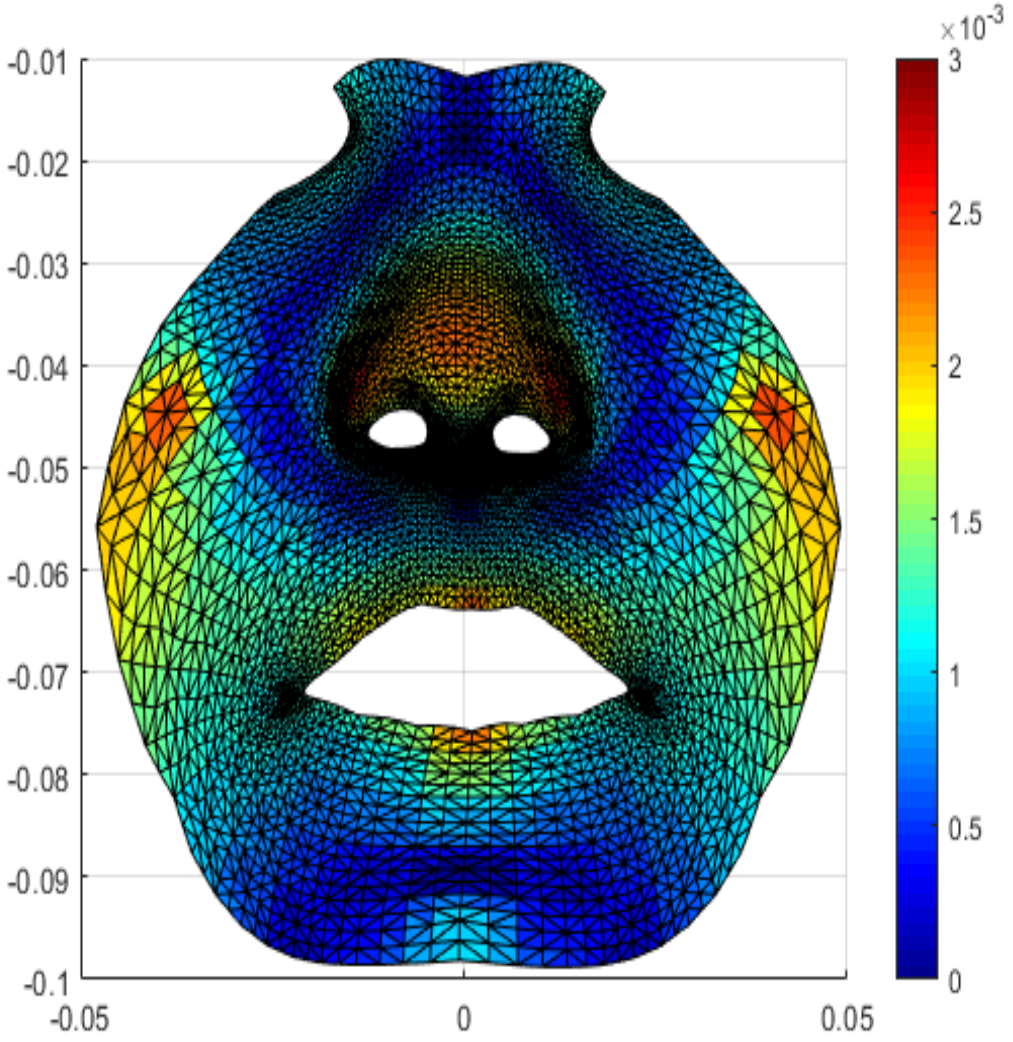

Figure 72: *FRAME 5* Total face asymmetry in frame 5 during Cheek Puff. The green color represents no asymmetry, the dark blue color indicates minimum asymmetry, and the dark red indicates increased asymmetry.

The resting frame or frame 5 (Figure 72) showed high residual asymmetry in the nasal regions but was lesser as compared to frame 4. Areas of the upper and lower lip showed patches of residual asymmetry even at rest which indicated residual asymmetry persists even after completion of facial movement and the face coming to rest.

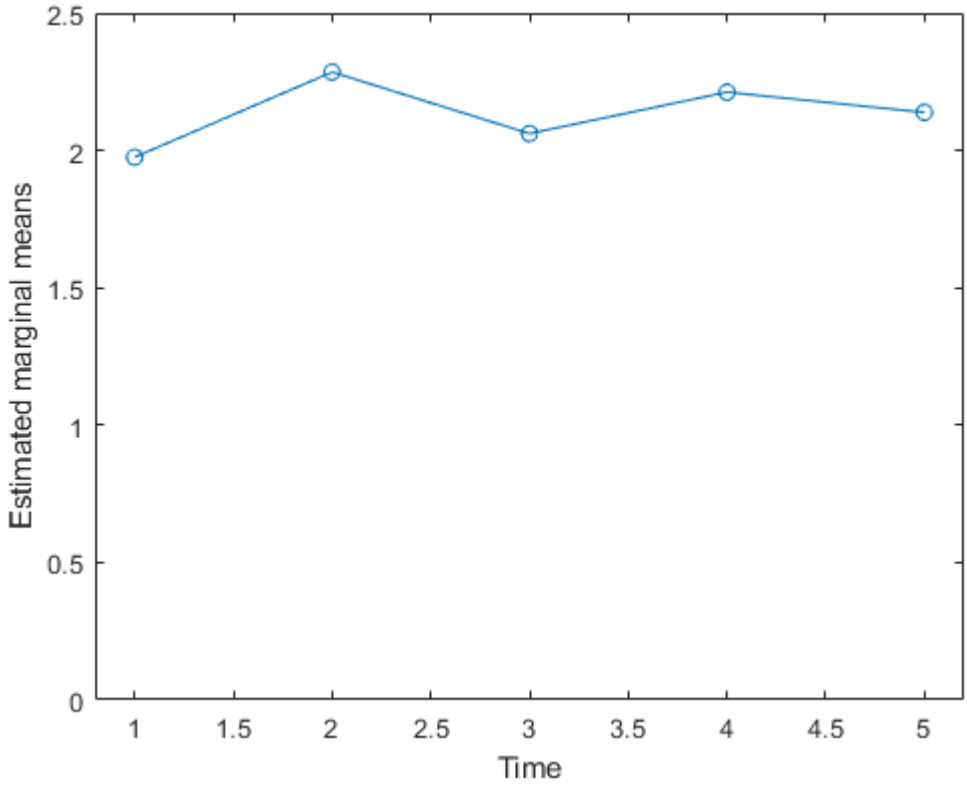

Figure 73: Asymmetry scores between 5 frames in total face during Cheek Puff in the UCL group

It was seen in the graph (Figure 73) that frame 2 and 4 were highest in asymmetry in the total face during cheek puff as compared to peak expression frame (frame 3). Differences between frames were not significant in the total face asymmetry scores.

4.2.2. Asymmetry in Medio-lateral (X plane) during Cheek Puff

Facial asymmetry was also seen directionally in the x, y and z spatial planes and the color spectrum and readings assigned for this was slightly different as compared to total face asymmetry. Asymmetry to the right side (cleft side) was shown in red and asymmetry to the left side (non-cleft side) was shown in blue.

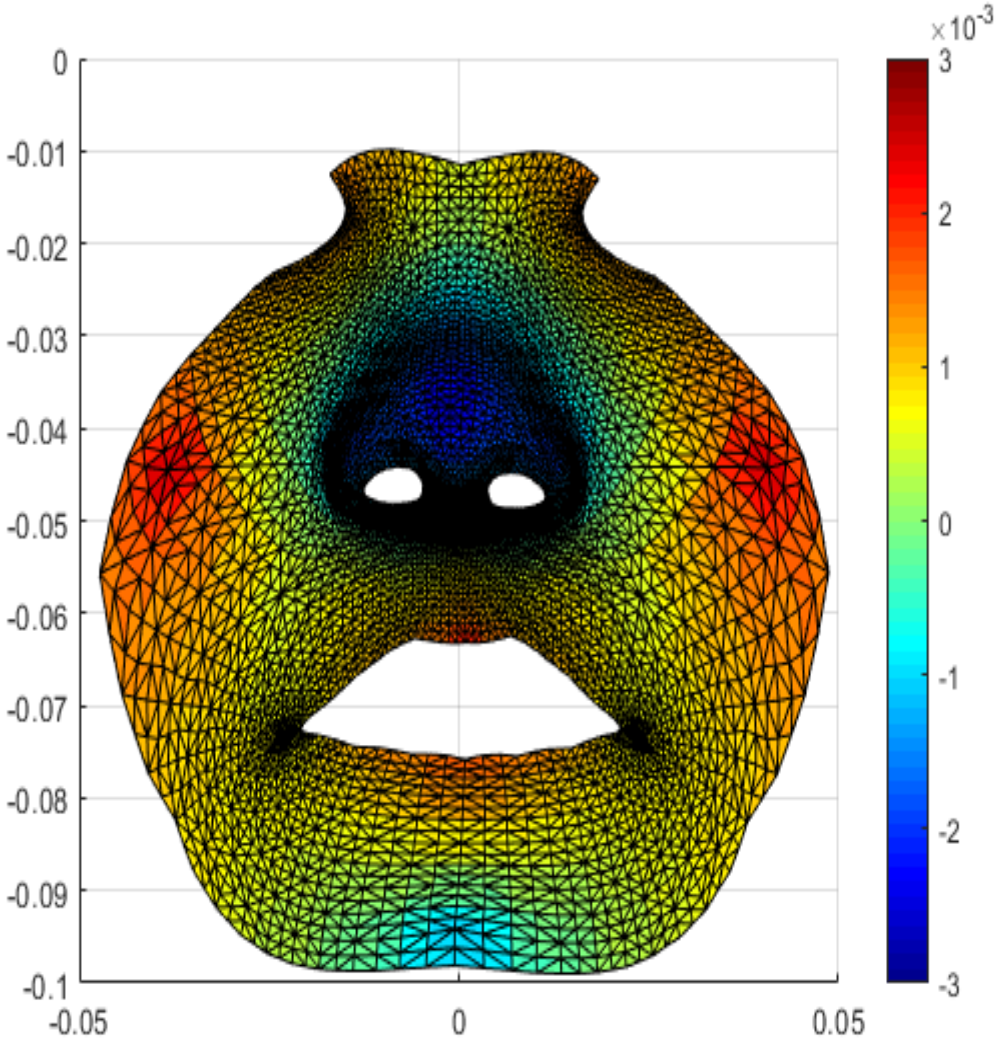

Figure 74: *FRAME 1* Color map of the average asymmetry in the X direction in frame 1 in UCL patients during cheek puff. The red color represents asymmetry towards the right. The blue color represents asymmetry to the left side.

The areas around the nose, nasal tip and alar regions showed deviation to the left side (non-cleft side) (Figure 74). The philtrum, upper lip, lower lip and commissures of the mouth showed deviation and increased asymmetry to the right side (cleft side) indicated by yellow and red patches.

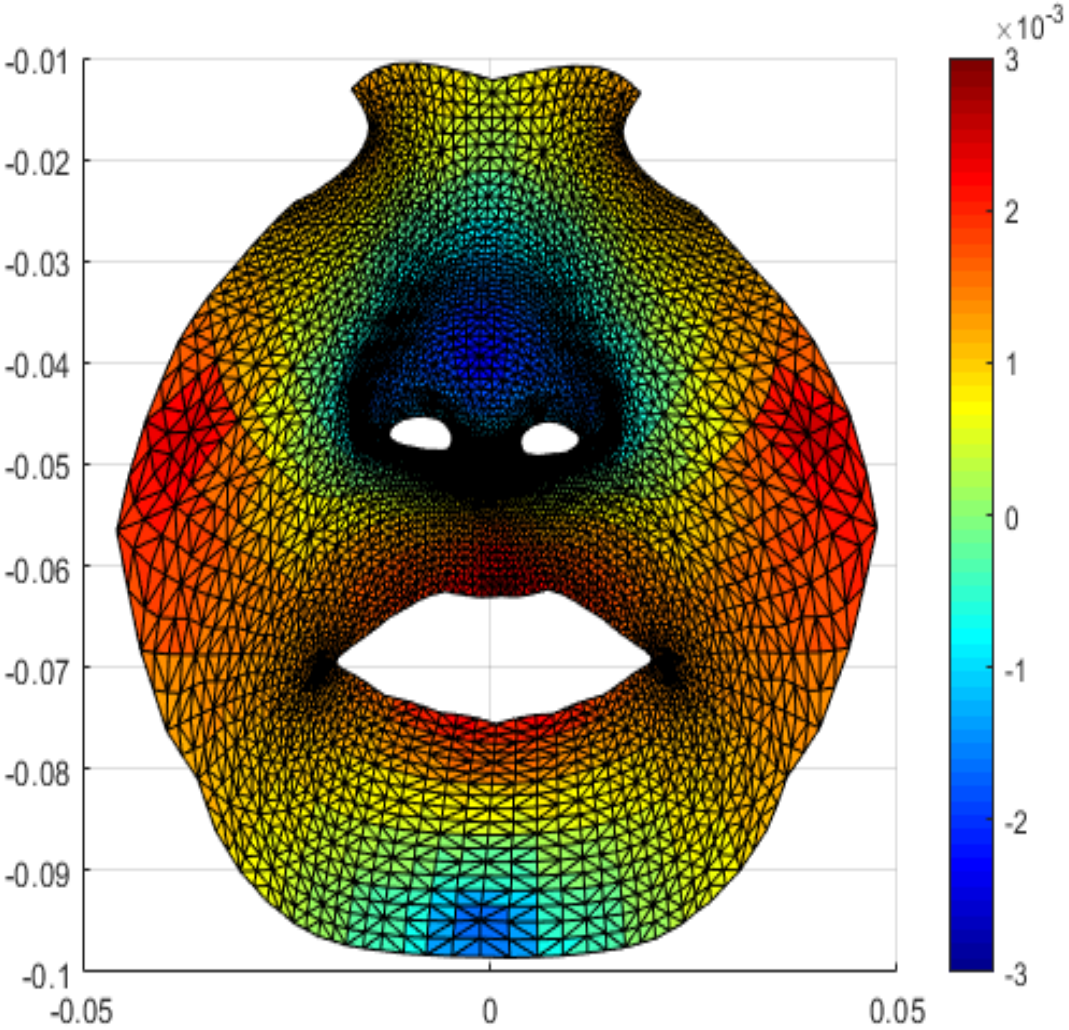

Figure 75: *FRAME 2* Color map of the average asymmetry in the X direction in frame 2 in UCL patients during cheek puff. The red color represents asymmetry towards the right. The blue color represents asymmetry to the left side.

In figure 75, the areas around the nose, nasal tip and alar regions showed deviation to the left side or the non-cleft side. The philtrum, upper lip, lower lip and commissures of the mouth showed deviation to the right side indicated by yellow and red patches with higher intensity of color indicative of increased asymmetry as compared to frame 1.

Both upper and lower lip showed darker red patches as compared to frame 1.

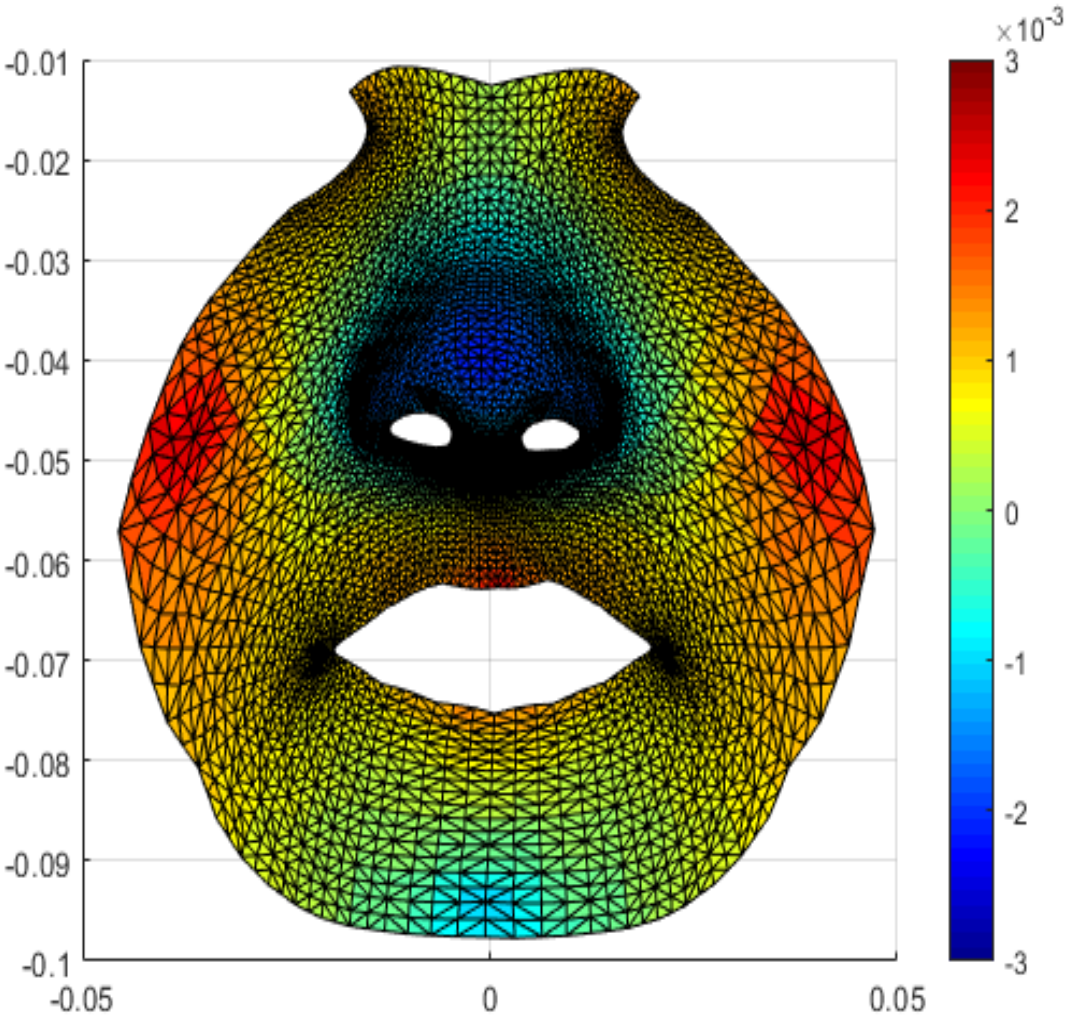

Figure 76: *FRAME 3* Color map of the average asymmetry in the X direction in frame 3 in UCL patients during cheek puff. The red color represents asymmetry towards the right. The blue color represents asymmetry to the left side.

In figure 76, asymmetry in the nasal tip and alar regions remained the same as frame 1 and 2 (deviated to the left or non-cleft side). The upper and lower lip remained deviated to the right, but the asymmetry was lower as compared to frame 2 where the patches of red were now replaced by yellow patches.

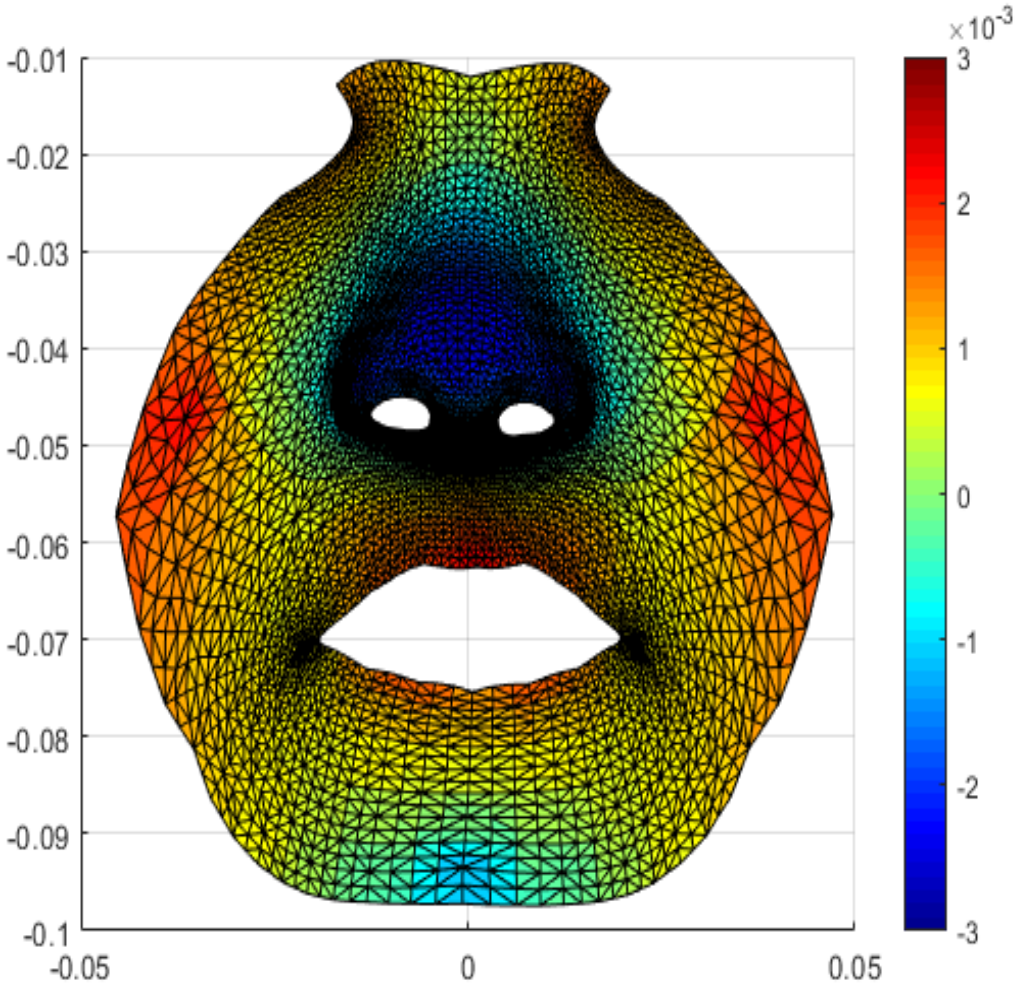

Figure 77: *FRAME 4* Color map of the average asymmetry in the <u>X direction</u> in frame 4 in UCL patients during <u>cheek puff</u>. The red color represents asymmetry towards the right. The blue color represents asymmetry to the left side.

In figure 77, asymmetry in the nasal tip and alar regions remained the same as frame 1 and 2 (deviated to the left). The upper and lower lip remained deviated to the right with higher asymmetry as compared to frame 3 indicated by red areas on both.

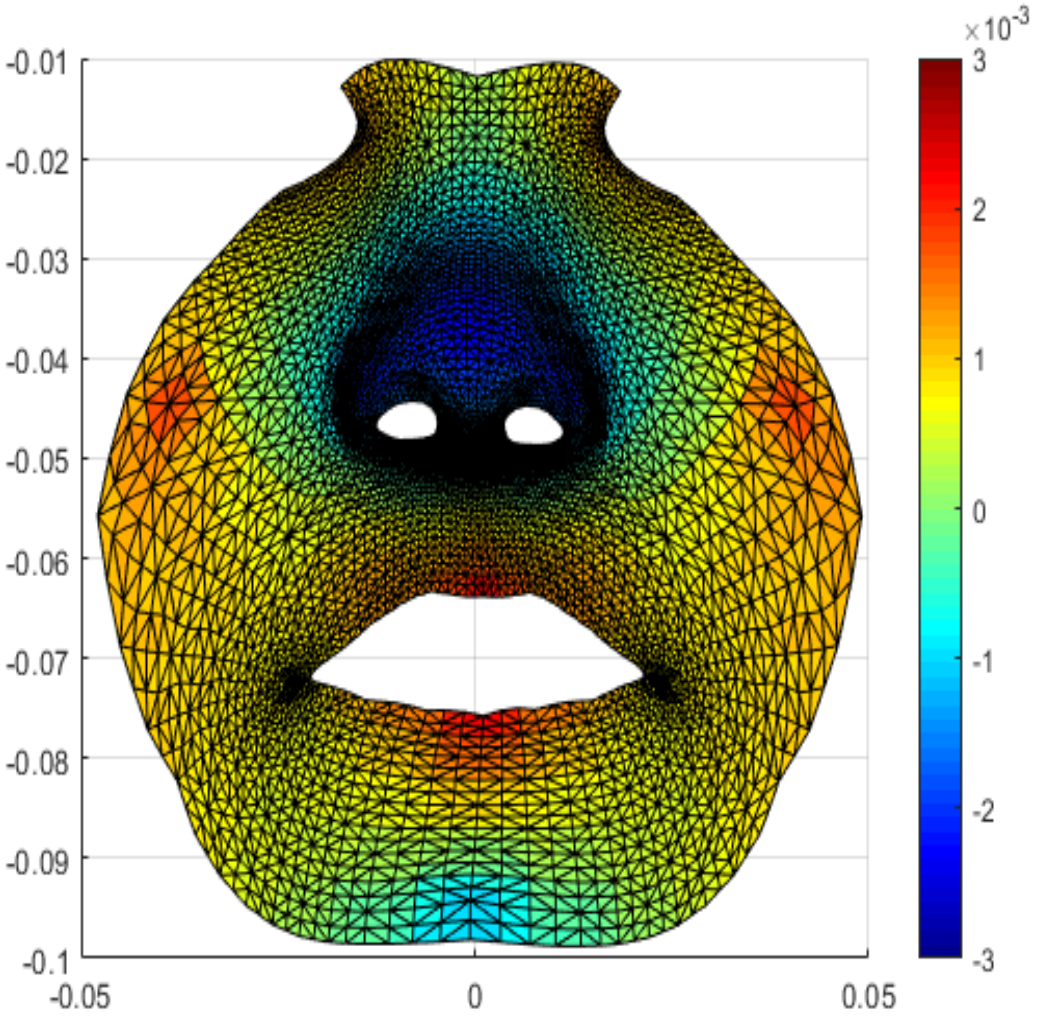

Figure 78: *FRAME 5* Color map of the average asymmetry in the X direction in frame 5 in UCL patients during cheek puff. The red color represents asymmetry towards the right. The blue color represents asymmetry to the left side.

In figure 78, residual asymmetry, in frame 5 persisted in the upper and lower lip with deviation to the right side. The philtrum showed left sided deviation as well. The nasal tip and alar regions remained the same as previous frames.

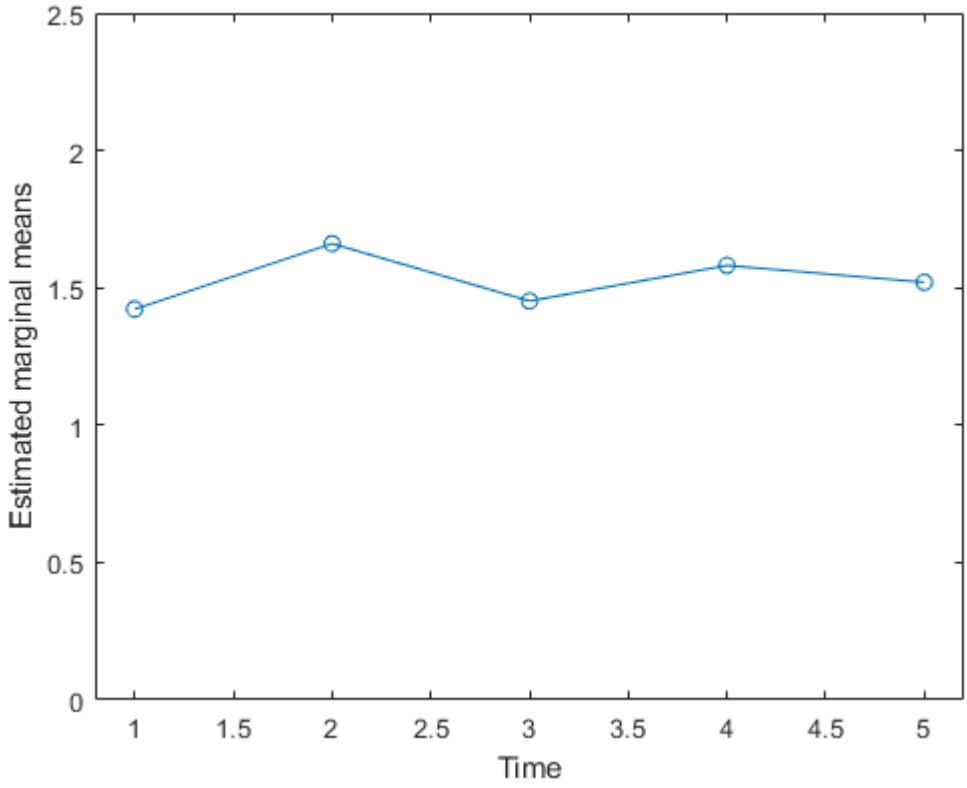

Figure 79: Asymmetry scores in the X direction between 5 frames during cheek puff

Asymmetry in the X direction as seen in the marginal means graph in figure 79, showed highest scores in frame 2, followed by frame 4 (the two quarterly frames) followed by frame 5 or the resting frame. Similar to the total face, differences in asymmetry scores between frames were minimum and not significant.

4.2.3. Asymmetry in Vertical (Y plane) during Cheek Puff

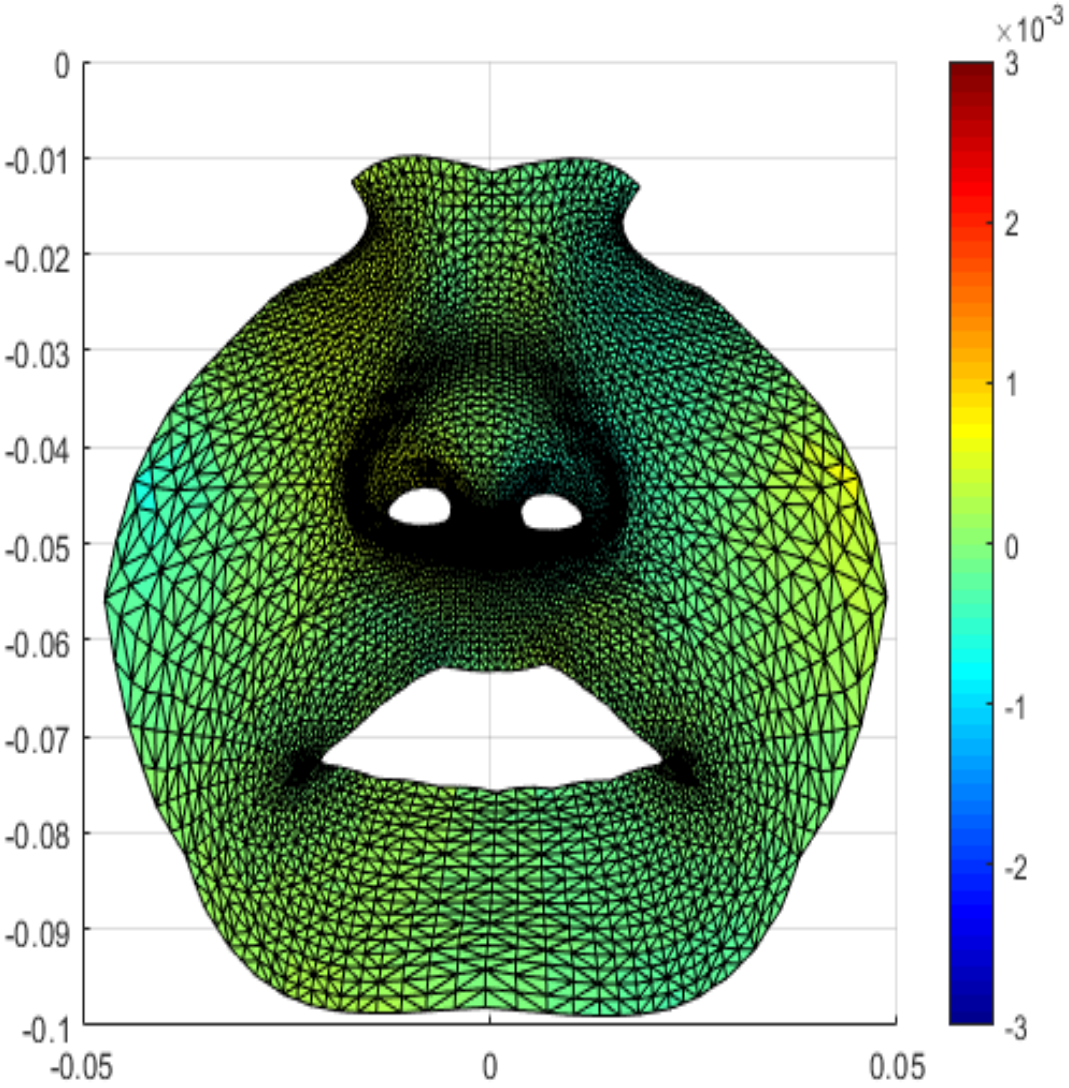

Figure 80: ***FRAME 1*** **Color map of the asymmetry in the Y direction in frame 1 in UCL patients during cheek puff. The red color represents asymmetry in upward direction. The blue color represents asymmetry in a downward direction.**

Frame 1 (Figure 80) shows minimum change in asymmetry as indicated by a general area of green around the nasolabial region. Slight bluish color seen on the left alar region indicative of mild deviation in the downward direction.

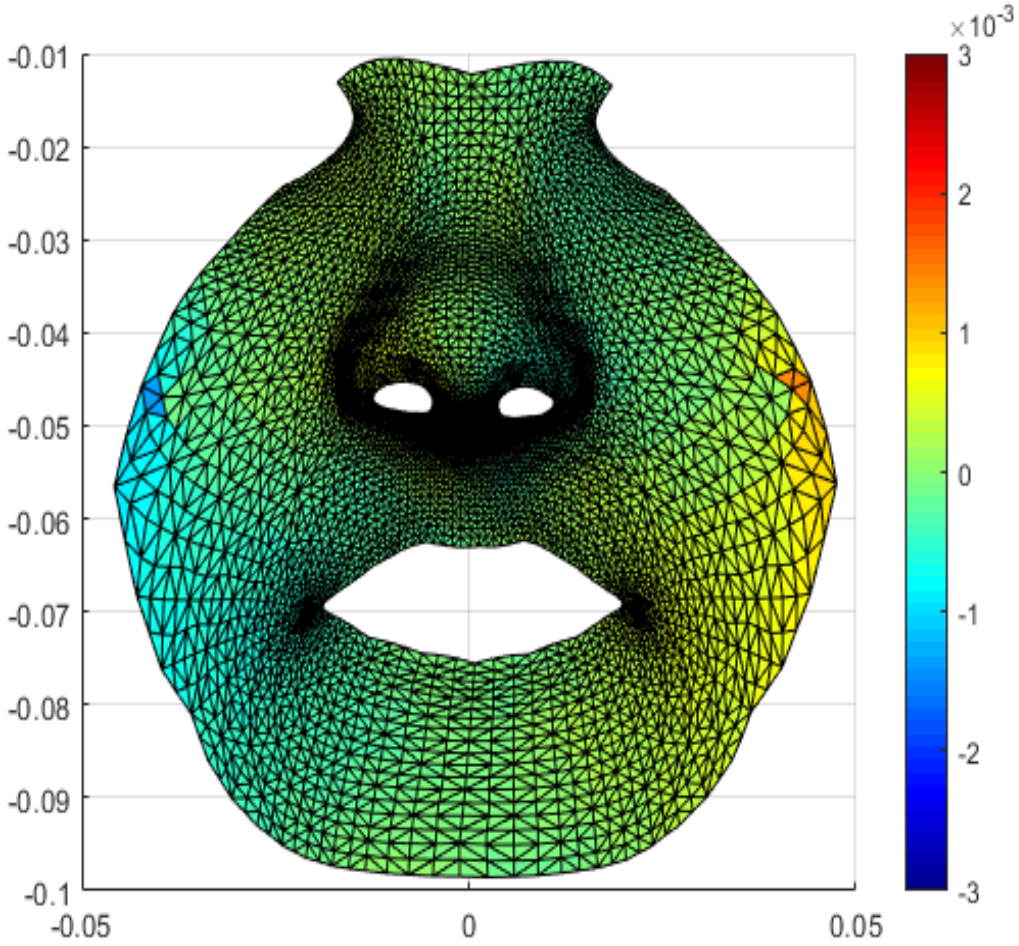

Figure 81: *FRAME 2* Color map of the asymmetry in the Y direction in frame 2 in UCL patients during cheek puff. The red color represents asymmetry in upward direction. The blue color represents asymmetry in a downward direction.

Asymmetry in frame 2 (Figure 81) showed minimum changes as compared to frame 1 as represented by areas of green. The right commissure and part of the vermillion of upper lip showed deviation in downward direction whereas the left

vermillion and left commissure of the mouth showed deviation in upward direction as seen by mild yellow coloration. Left alar showed deviation in downward direction and right ala showed upward deviation similar to frame 1.

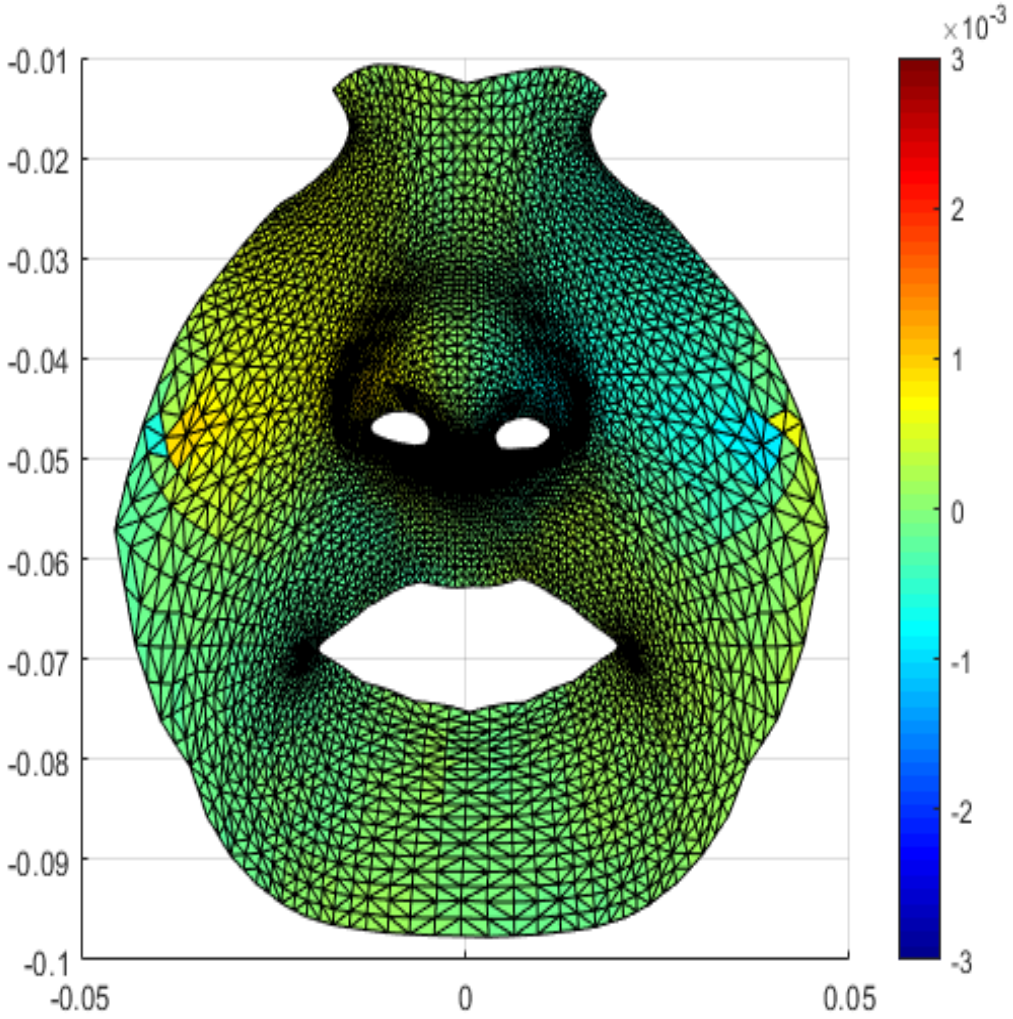

Figure 82: *FRAME 3* Color map of the asymmetry in the Y direction in frame 3 in UCL patients during cheek puff. The red color represents asymmetry in upward direction. The blue color represents asymmetry in a downward direction.

In figure 82, in frame 3, the right commissure, philtrum and part of the vermillion of upper lip showed deviation in downward direction whereas the left vermillion, philtral column and left commissure of the mouth showed deviation in upward direction as seen by mild yellow coloration. Left ala showed deviation in downward direction and right ala showed upward deviation similar to frame 2.

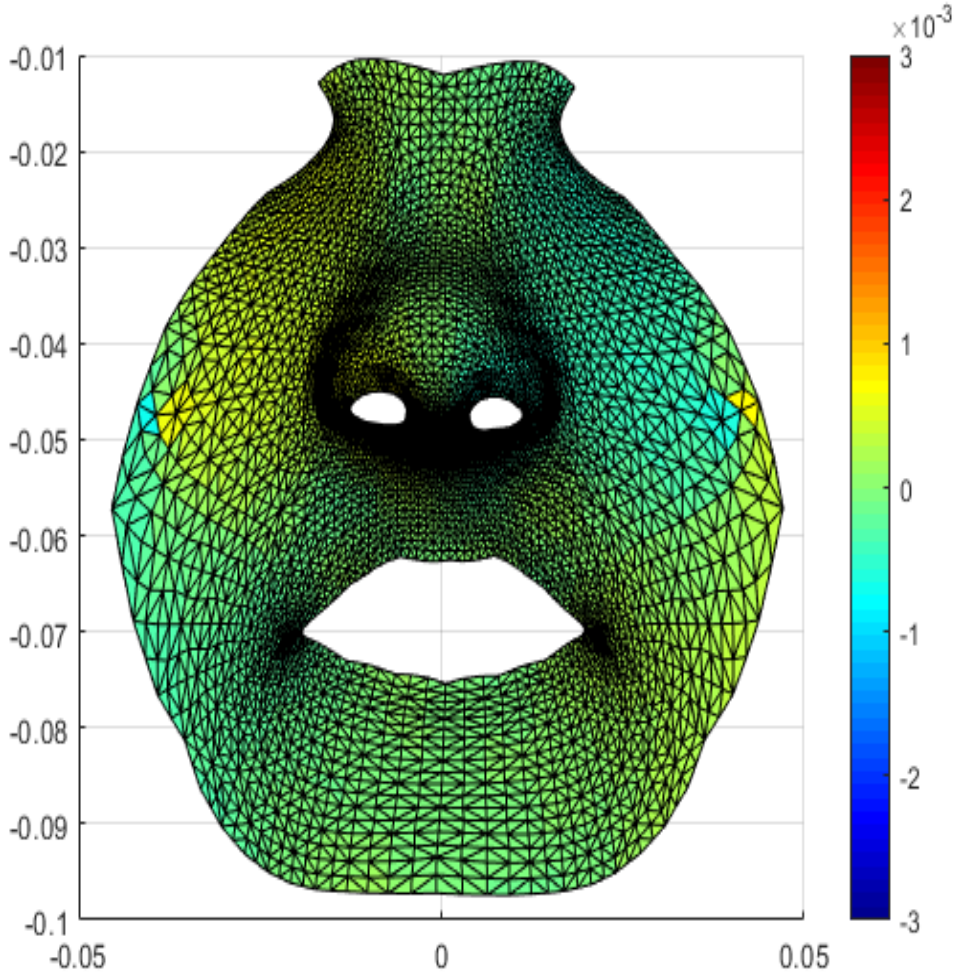

Figure 83: ***FRAME 4*** **Color map of the asymmetry in the Y direction in frame 4 in UCL patients during cheek puff. The red color represents asymmetry in upward direction. The blue color represents asymmetry in a downward direction.**

Asymmetry in frame 4 (Figure 83) showed minimum changes- the philtrum and vermillion border of upper lip showed decreased asymmetry as compared to frame 3. Left alar showed deviation in downward direction and right ala showed upward deviation similar to frame 1.

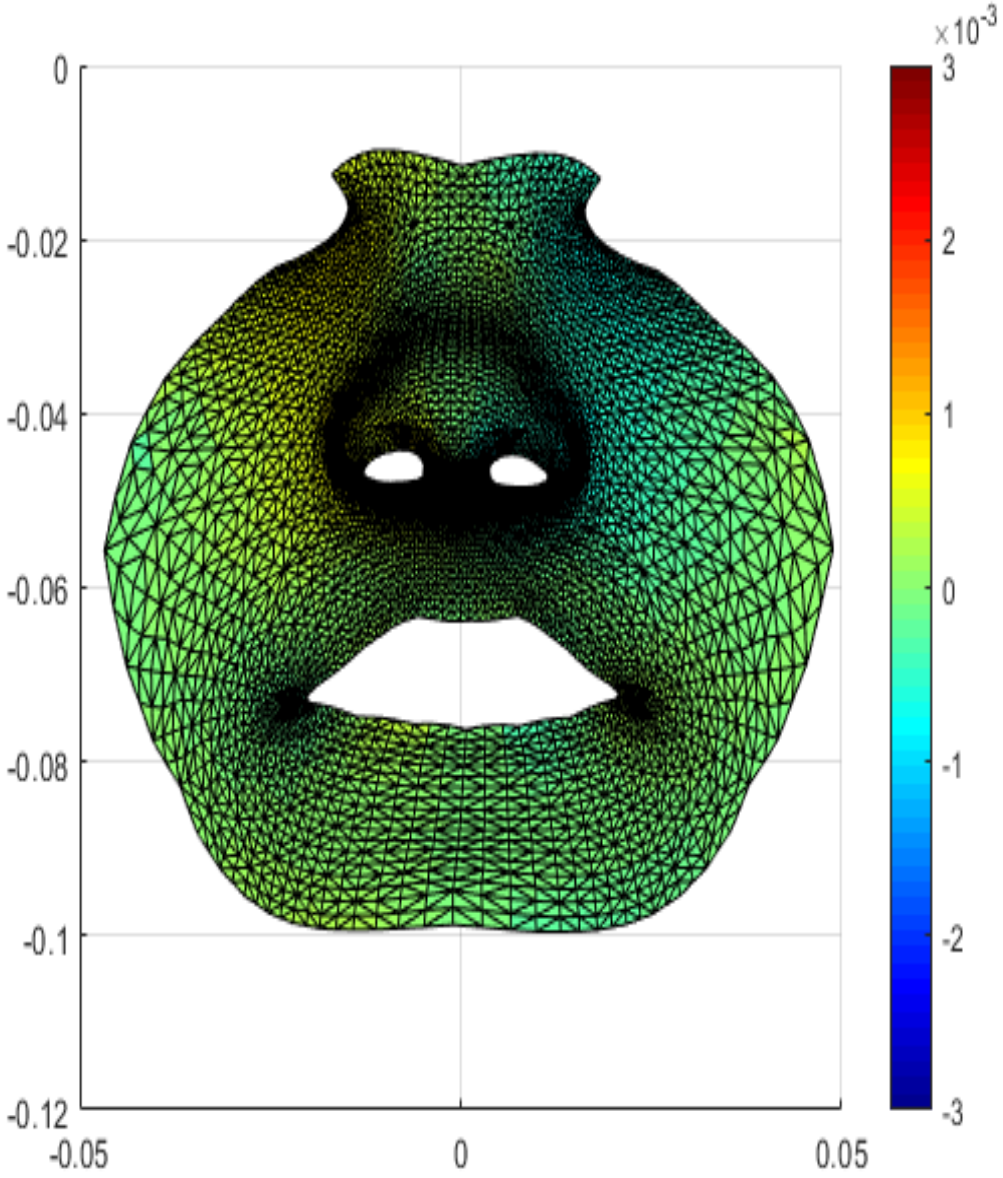

Figure 84: *FRAME 5* Color map of the asymmetry in the Y direction in frame 5 in UCL patients during cheek puff. The red color represents asymmetry in upward direction. The blue color represents asymmetry in a downward direction.

Frame 5 or the resting frame (Figure 84) showed minimum changes similar to frame 1. Left alar showed deviation in downward direction and right ala showed upward deviation similar to frame 1.

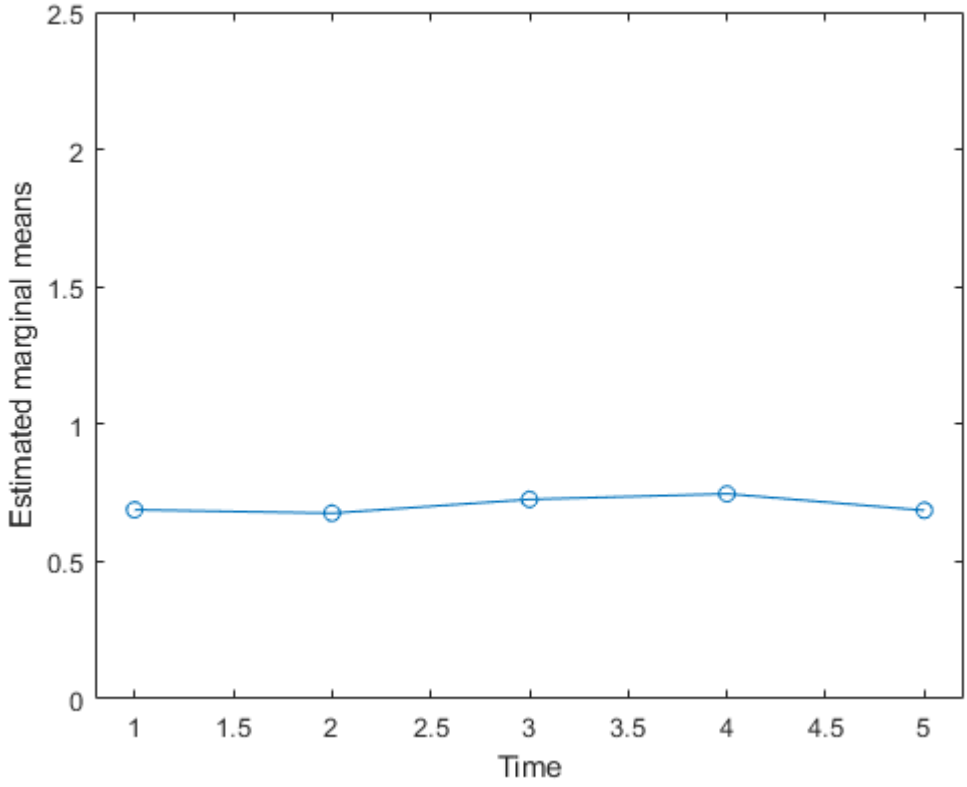

Figure 85: Asymmetry scores between 5 frames in Y direction during cheek puff

Differences in asymmetry scores in Y direction during cheek puff were minimum thus showing that vertical changes in asymmetry during performance of the cheek puff were minimum (Figure 85).

No significant differences were seen in the asymmetry scores between all frames in the Y direction.

4.2.3. Asymmetry in Antero-Posterior (Z plane) during Cheek Puff

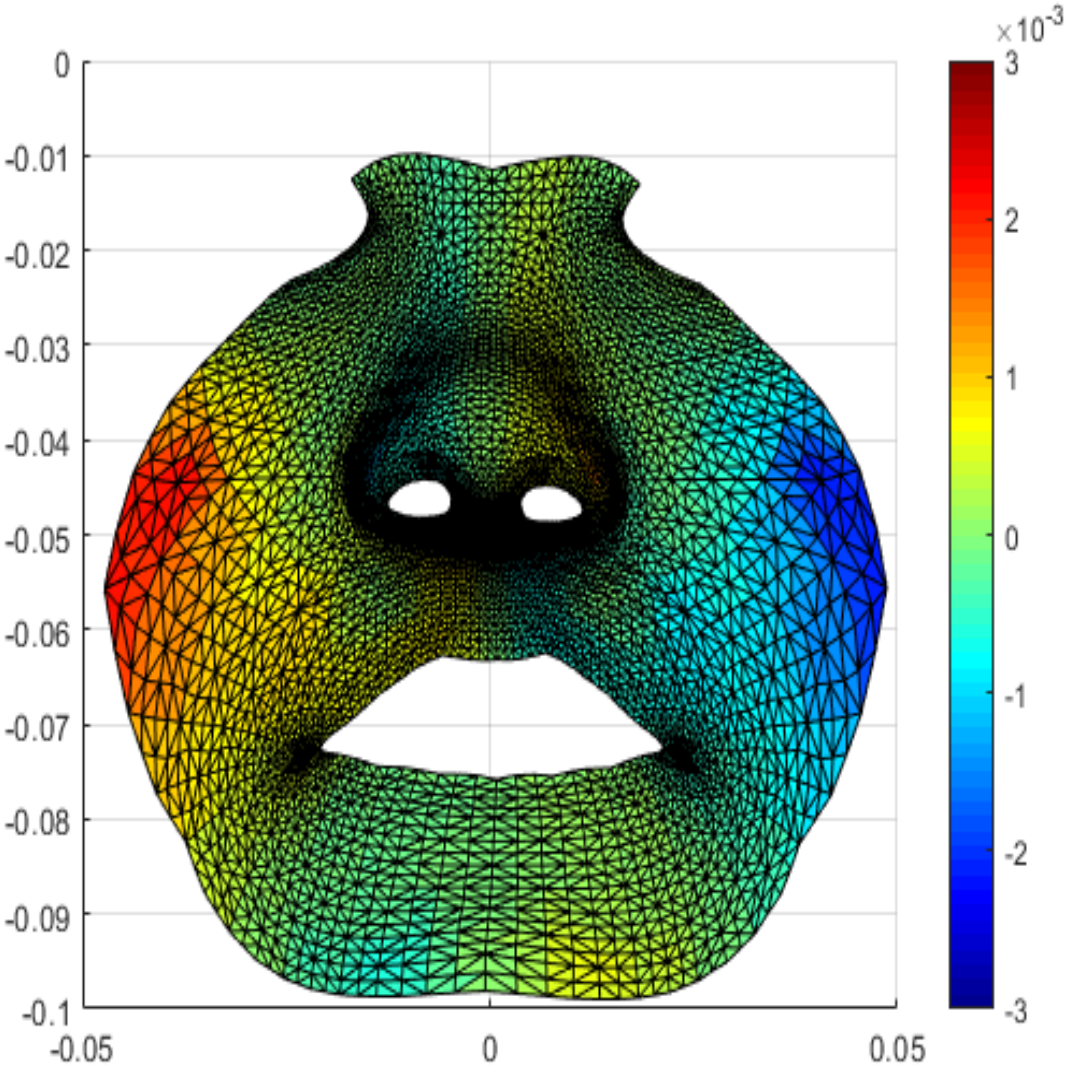

Figure 86: *Frame 1* Color map of the average asymmetry in the Z direction in frame 1 in UCL patients during cheek puff. The red color represents asymmetry in a forward (towards observer) direction. The blue color represents asymmetry in a backward direction (away from observer).

Frame 1 (Figure 86) or the resting frame in cheek puff in the Z direction showed the left ala of the nose deviated anteriorly and the right ala deviated posteriorly. The left sided philtrum and left vermillion border of the upper lip was deviated posteriorly whereas the right sided philtrum and vermillion border of the upper lip was seen to be deviated anteriorly.

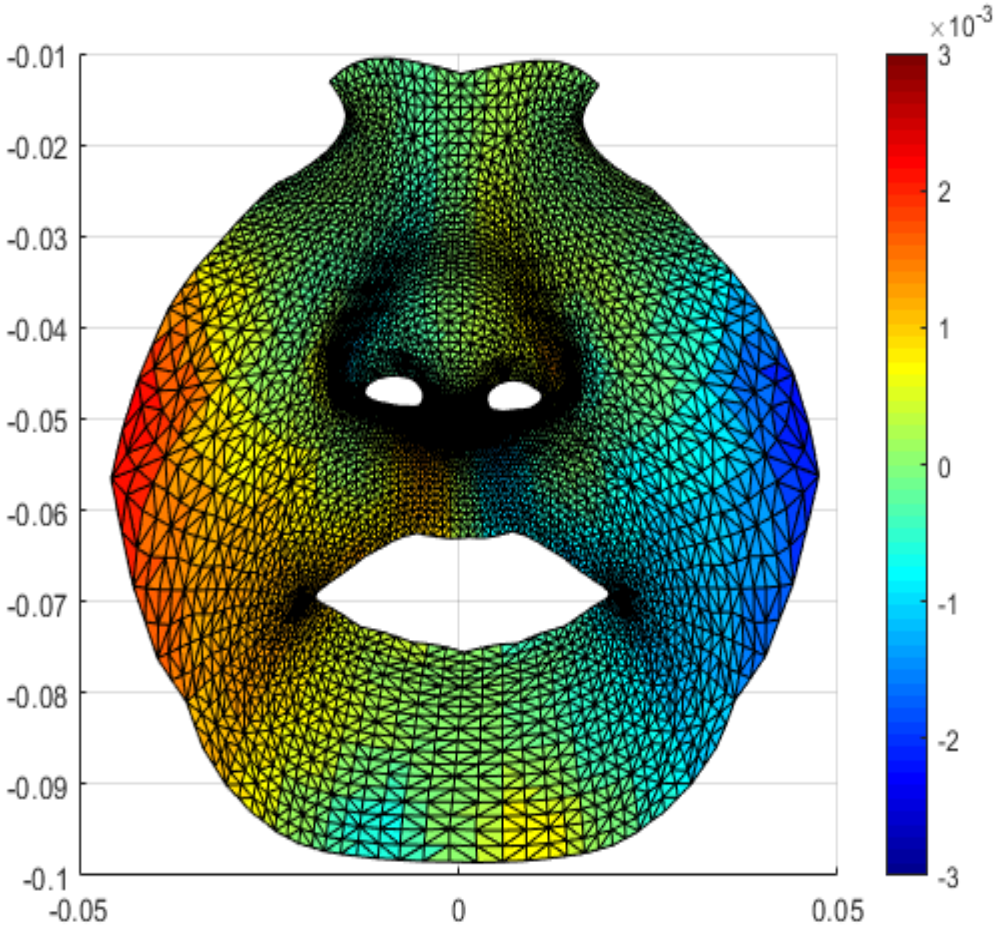

Figure 87: *Frame 2* Color map of the average asymmetry in the Z direction in frame 2 in UCL patients during cheek puff. The red color represents asymmetry in a forward (towards observer) direction. The blue color represents asymmetry in a backward direction (away from observer).

Frame 2 (Figure 87) of the cheek puff in the Z direction showed the levels of asymmetry increase as the left ala of the nose deviated anteriorly and the right ala deviated posteriorly. The left sided philtrum and left vermillion border of the upper lip was deviated posteriorly, greater than in frame 1 whereas the right sided philtrum and vermillion border of the upper lip was seen to be deviated anteriorly, greater than in frame 1.

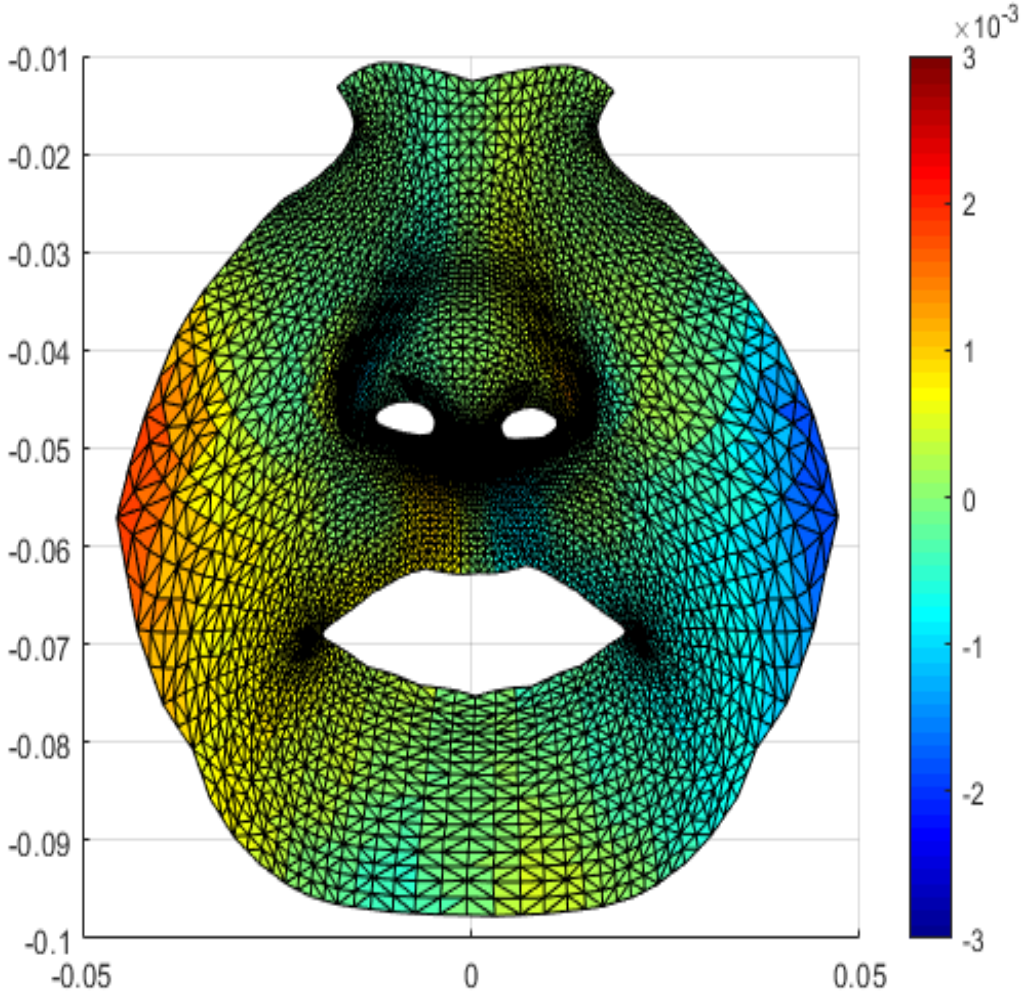

Figure 88: *FRAME 3* Color map of the average asymmetry in the Z direction in frame 3 in UCL patients during cheek puff. The red color represents asymmetry in a forward (towards observer) direction. The blue color represents asymmetry in a backward direction (away from observer).

The midway frame (peak expression) was similar to frame 2 in terms of deviation and asymmetry (Figure 88) with the left philtrum and vermillion of the upper lip deviated posteriorly and the right philtrum and vermillion of upper lip deviated anteriorly.

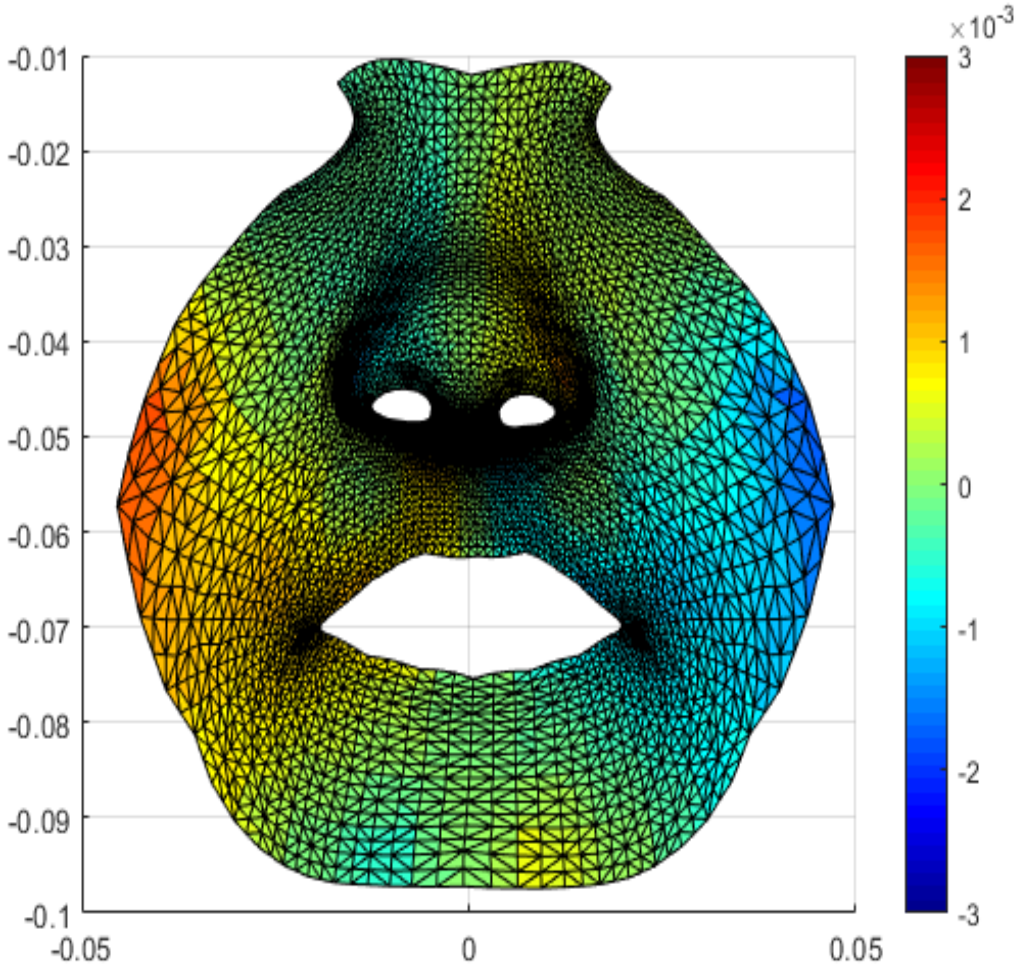

Figure 89: *FRAME 4* Color map of the average asymmetry in the Z direction in frame 4 in UCL patients during cheek puff. The red color represents asymmetry in a forward (towards observer) direction. The blue color represents asymmetry in a backward direction (away from observer).

Asymmetry in frame 4 was once again similar to frame 3 and 2 (Figure 89) with the alar regions and philtrum and vermillion border of the upper and lower lip showing deviation.

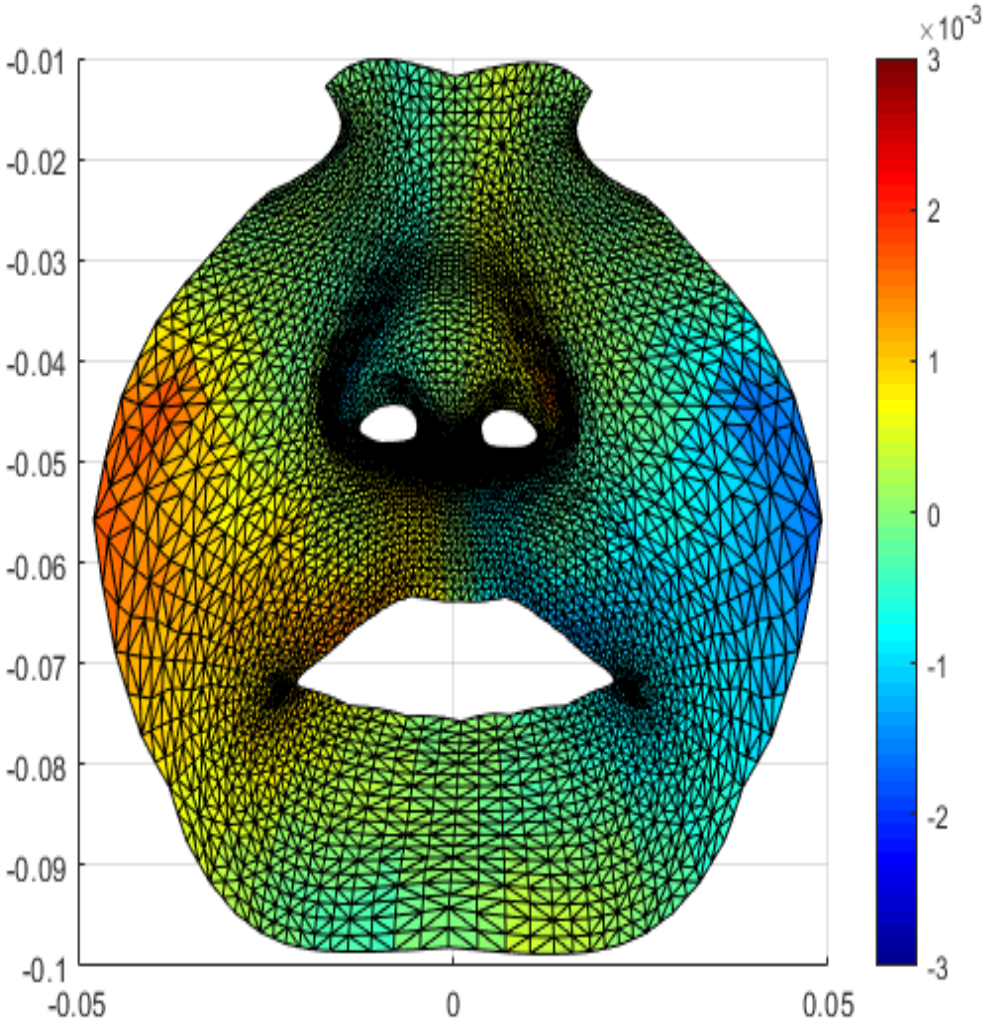

Figure 90: *FRAME 5* Color map of the average asymmetry in the Z direction in frame 5 in UCL patients during cheek puff. The red color represents asymmetry in a forward (towards observer) direction. The blue color represents asymmetry in a backward direction (away from observer).

It was seen in frame 5 (Figure 90) that residual asymmetry persisted even when the face was in a resting position. The asymmetry was similar to frame 4 with involvement in the upper lip, philtrum, and the alar regions of the nose.

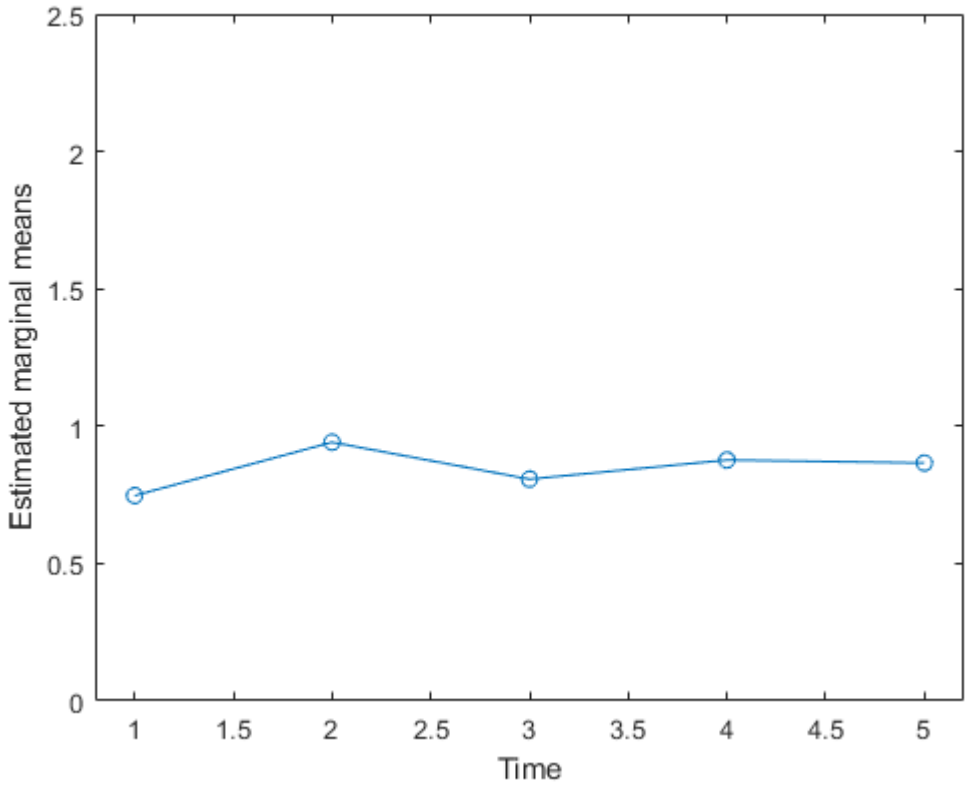

Figure 91: Asymmetry scores between 5 frames in the Z direction during Cheek puff

It was clear that asymmetry was highest in frame 2 followed by frame 4 in the antero-posterior direction (Figure 91). Significant differences were present between all the frames during cheek puff in the z direction.

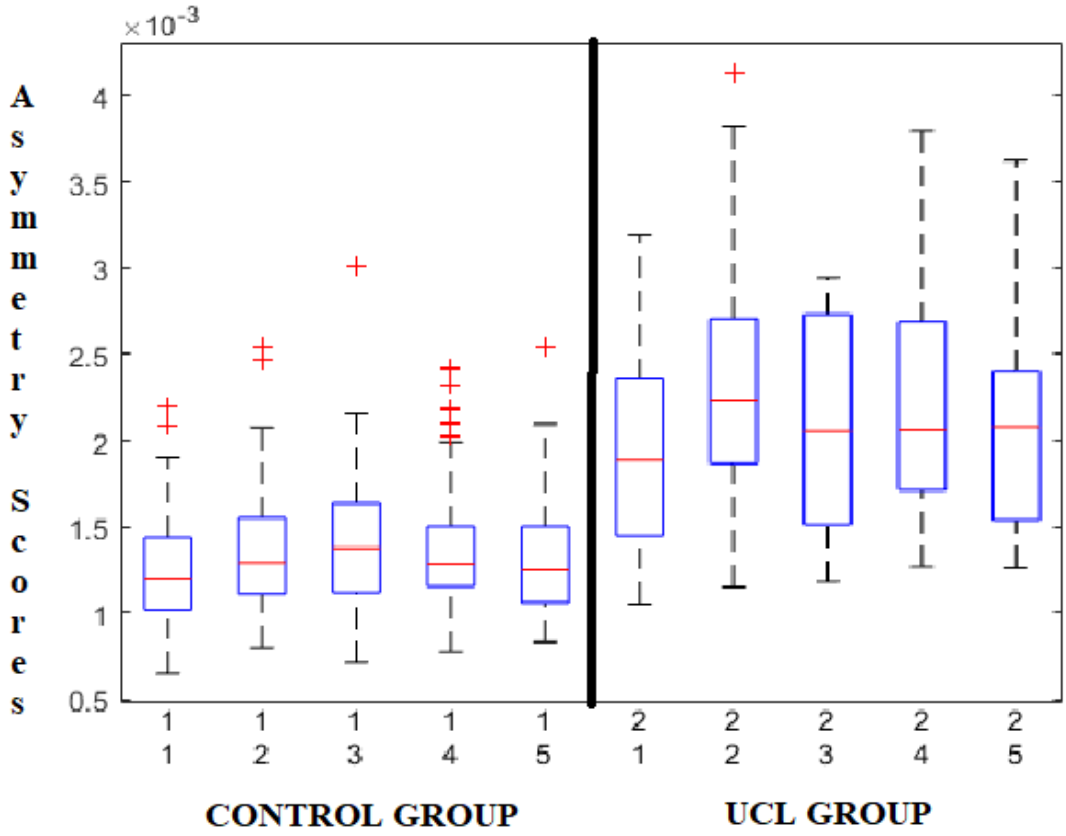

Figure 92: Boxplot of asymmetry scores between the UCL group and the controls during cheek puff

Average asymmetry scores were seen to be higher in the surgically managed UCL group than the controls. The differences in asymmetry scores in all frames of the two groups were significantly different ($p<0.001$). The trend in asymmetry scores within the control group differed from that of the surgically managed UCL group. Frame 3 (frame at peak expression) showed maximum asymmetry in the controls whereas frame 2 showed maximum asymmetry in the UCL group.

4.3. Lip Purse

Summary of results during lip purse:

Significant differences in asymmetry scores between the UCL group and the control group in all frames. Significant differences in asymmetry scores between the frames within the UCL group were seen in the whole face, x y and z directions. Asymmetry in the UCL group was seen to be higher in the peak frame (frame 3) followed by frame 4 and 2 for the whole face, x and the z direction. Asymmetry in the total face was most pronounced in the alar regions of the nose, the philtrum and upper lip vermillion border. In the X direction, the nose showed deviation to the left or non-cleft side whereas the upper lip and philtrum showed deviation to the right or cleft side, most pronounced in frame 3. Vertical asymmetries were seen to be minimal. Anteroposterior asymmetry was noted in areas around the philtrum and the alar regions and nasal tip and was highest in frame 3 or peak expression.

4.3.1. Asymmetry in the total face during Lip purse

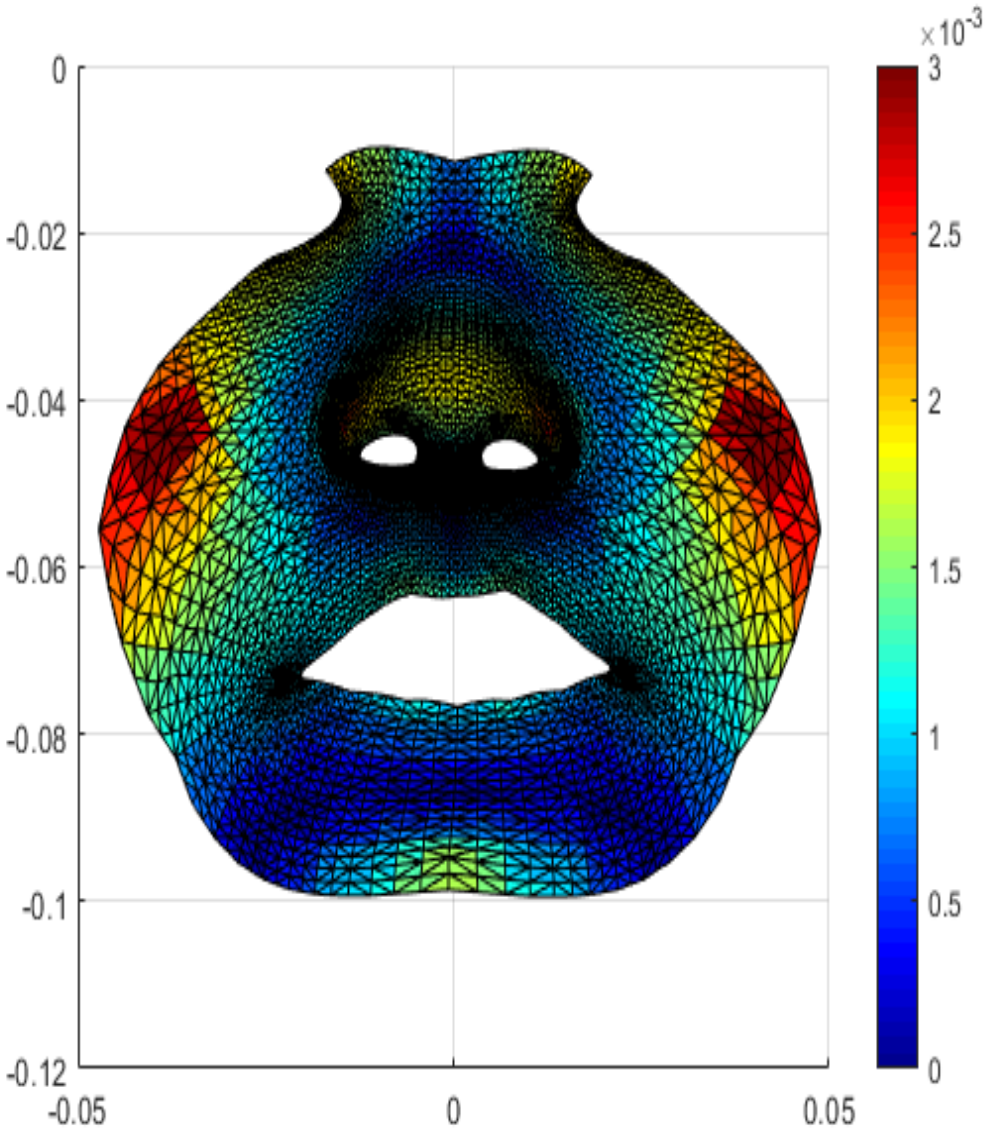

Figure 93: *Frame 1* Color map of the total face asymmetry in frame 1 in the UCL patients during Lip purse. The red color represents increased asymmetry. The blue color represents decreased asymmetry. Areas in green represent zero distance between the original and mirrored meshes (no asymmetry).

Residual asymmetry in frame 1 (Figure 93) was seen to be present in the nasal tip and alar regions of the nose indicated by a yellow and red color. Vermillion of upper and lower lip showed decreased levels of asymmetry as the face was at rest.

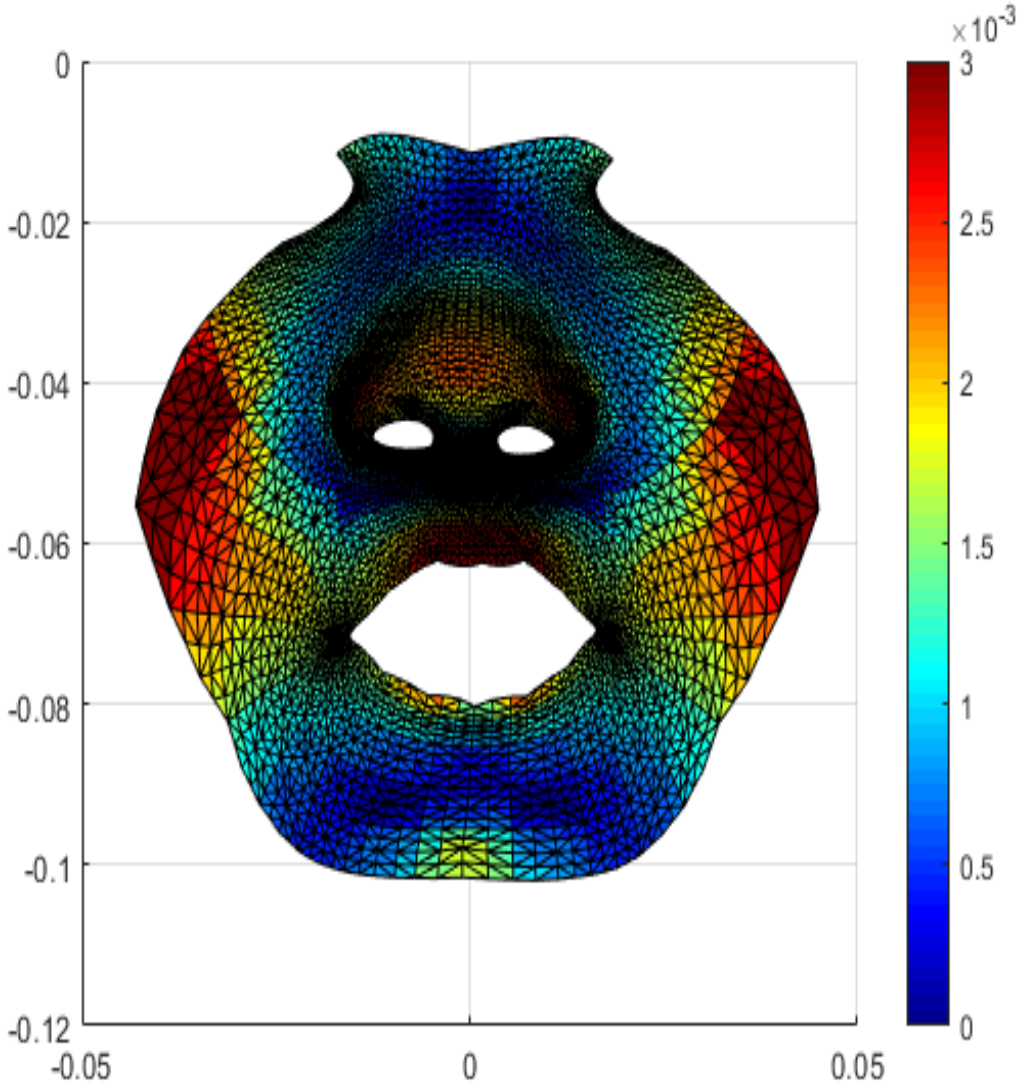

Figure 94: *FRAME 2* Color map of the <u>total face asymmetry</u> in frame 2 in the UCL patients during <u>Lip purse</u>. The red color represents increased asymmetry. The blue color represents decreased asymmetry. Areas in green represent zero distance between the original and mirrored meshes (no asymmetry).

Frame 2 (Figure 94) of the lip purse in the UCL group in the total face showed increased asymmetry in the nasal tip and alar regions. The vermillion border of upper lip, philtrum and commissures showed increased asymmetry as indicated by dark red shades. The lower lip also showed increased asymmetry as compared to frame 1.

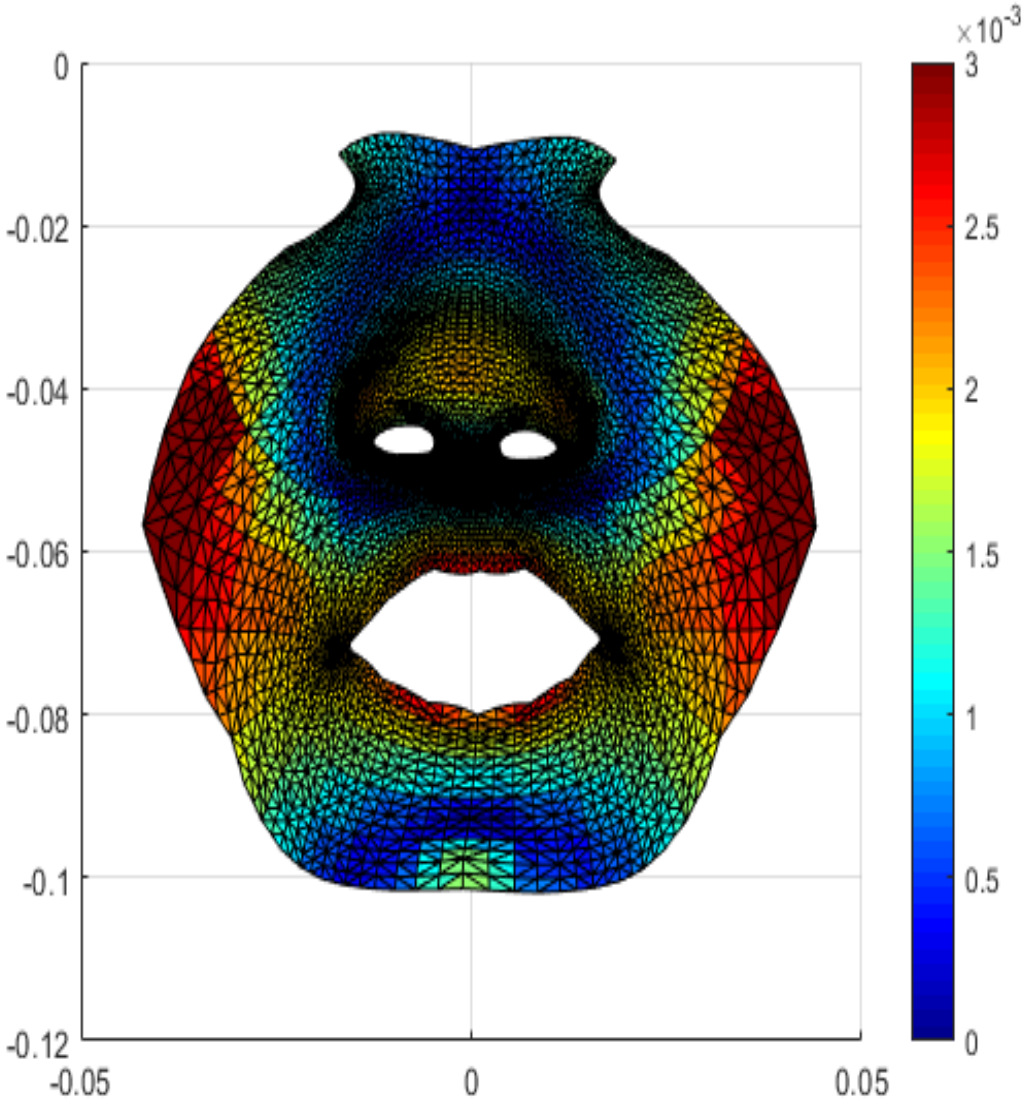

Figure 95: *FRAME 3* Color map of the <u>total face asymmetry</u> in frame 3 in the UCL patients during <u>Lip purse.</u> The red color represents increased asymmetry. The blue color represents decreased asymmetry. Areas in green represent zero distance between the original and mirrored meshes (no asymmetry).

Frame 3 (Figure 95) of the lip purse in the UCL group in the total face showed increased asymmetry in the nasal tip and alar regions. The vermillion border of upper lip, philtrum and commissures showed increased asymmetry as indicated by dark red shades. The lower lip also showed increased asymmetry as compared to frame 2 indicated by red color patches.

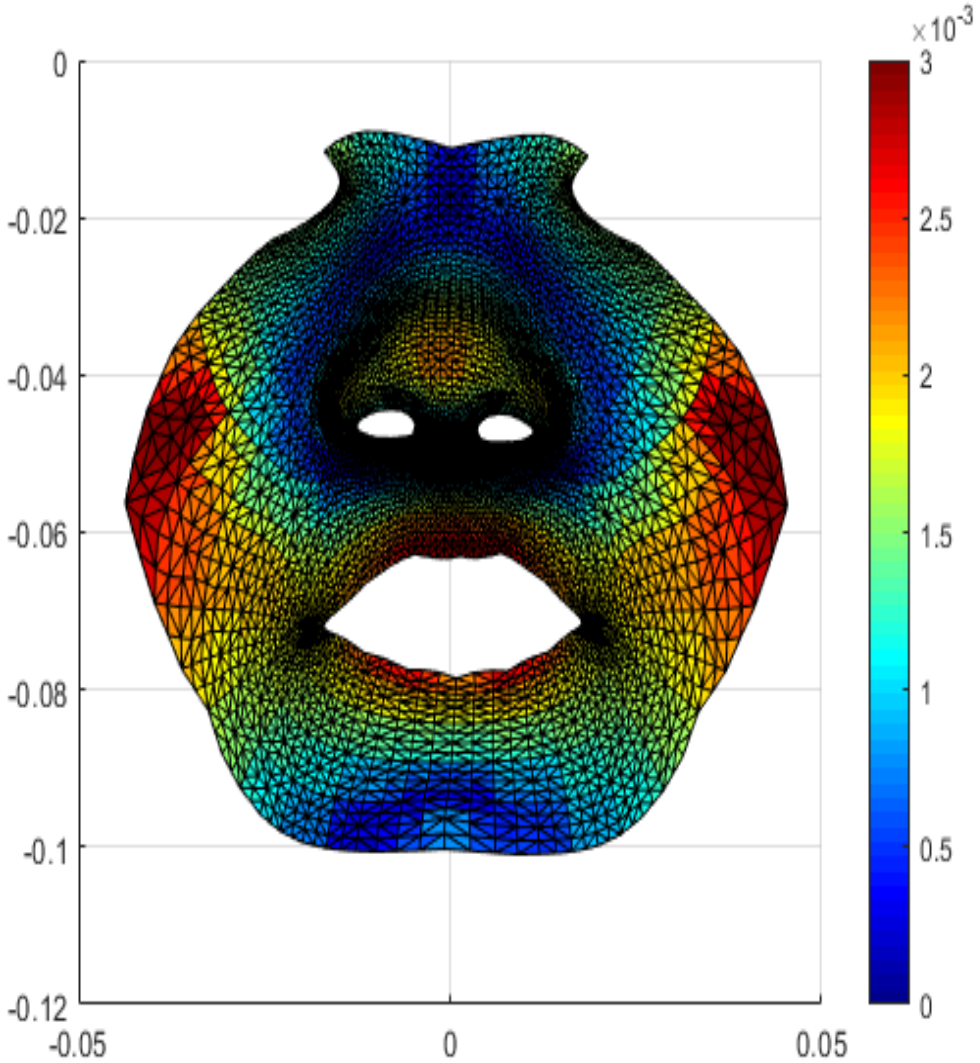

Figure 96: *FRAME 4* Color map of the <u>total face asymmetry</u> in frame 4 in the UCL patients during <u>Lip purse</u>. The red color represents increased asymmetry. The blue color represents decreased asymmetry. Areas in green represent zero distance between the original and mirrored meshes (no asymmetry).

Frame 4 (Figure 96) of the lip purse in the UCL group in the total face showed increased asymmetry in the nasal tip and alar regions. The vermillion border of upper lip, philtrum and commissures showed increased asymmetry as indicated by dark red shades. The lower lip also showed increased asymmetry as compared to frame 2 indicated by red color patches.

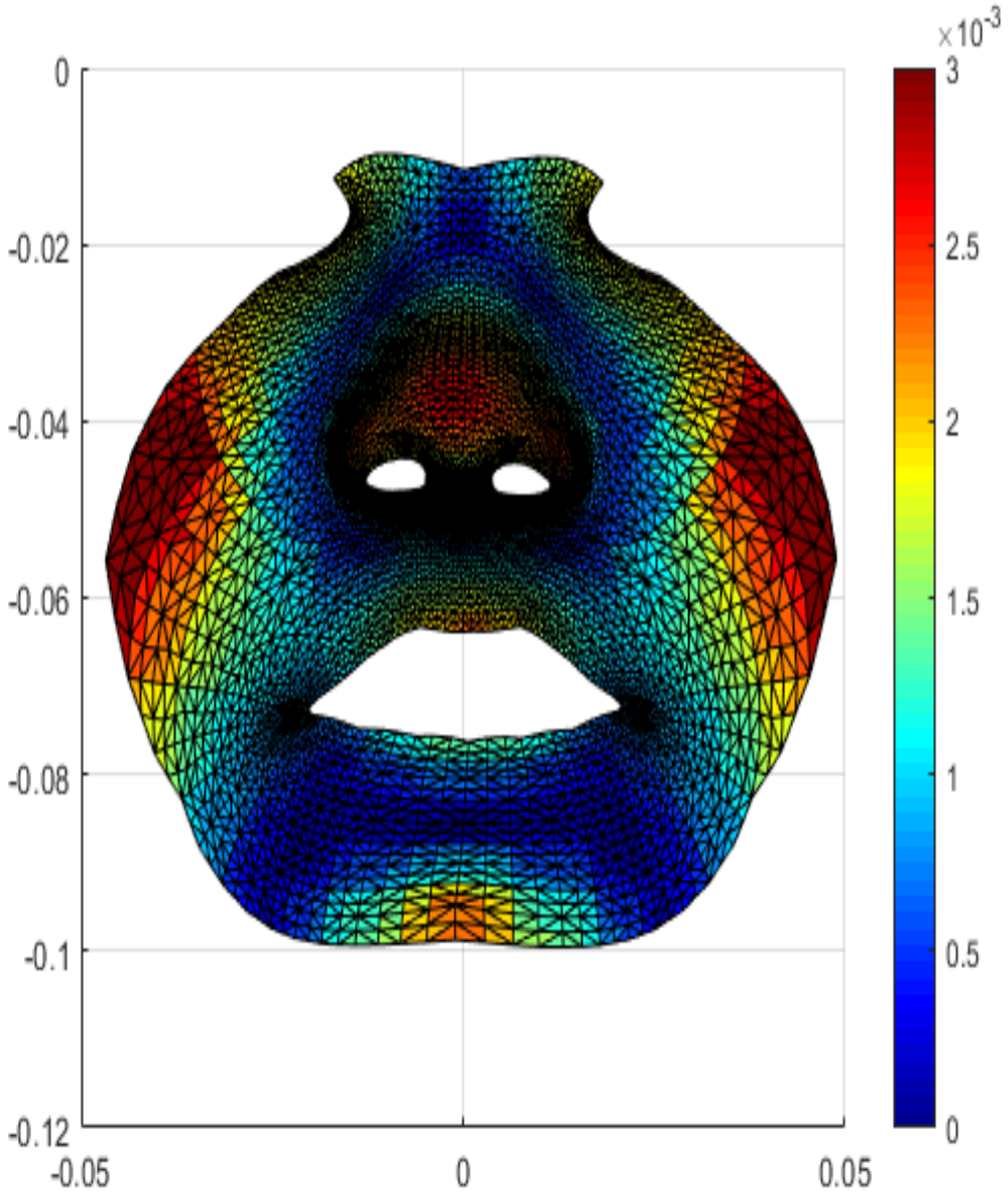

Figure 97: *FRAME 5* Color map of the <u>total face asymmetry</u> in frame 5 in the UCL patients during <u>Lip purse</u>. The red color represents increased asymmetry. The blue color represents decreased asymmetry. Areas in green represent zero distance between the original and mirrored meshes (no asymmetry).

Frame 5 (figure 97) of the total face showed increased asymmetry in the nasal tip and the ala regions indicated by a bright red patch. The asymmetry in the upper lip and lower lip decreased considerably as compared to the previous frames, as the face comes to a state of rest. A small yellow patch on upper lip suggested increased asymmetry persisted in that portion of the upper lip even after completion of the expression of lip purse.

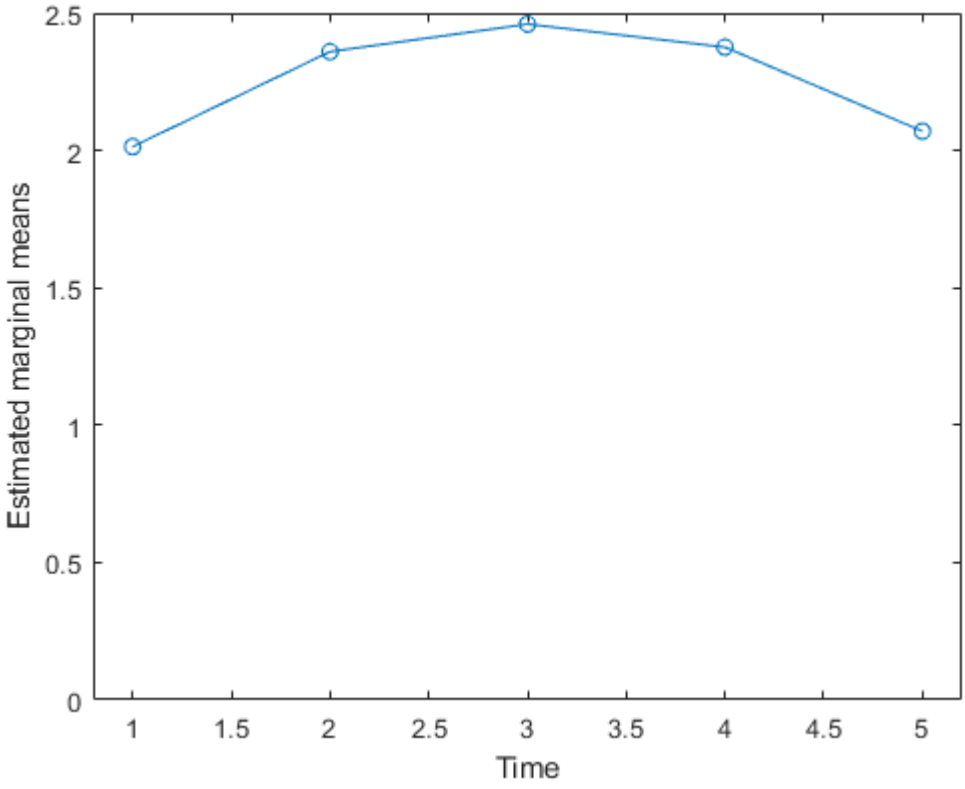

Figure 98: Asymmetry scores between 5 frames in the UCL group in total face during lip purse

The marginal means graph in figure 98 showed that frame 3 or the peak expression showed highest levels of asymmetry as compared to other frames. Significant differences were seen between all the frames in the total face during lip purse.

4.3.2. Asymmetry in the medio-lateral (X direction) during Lip Purse

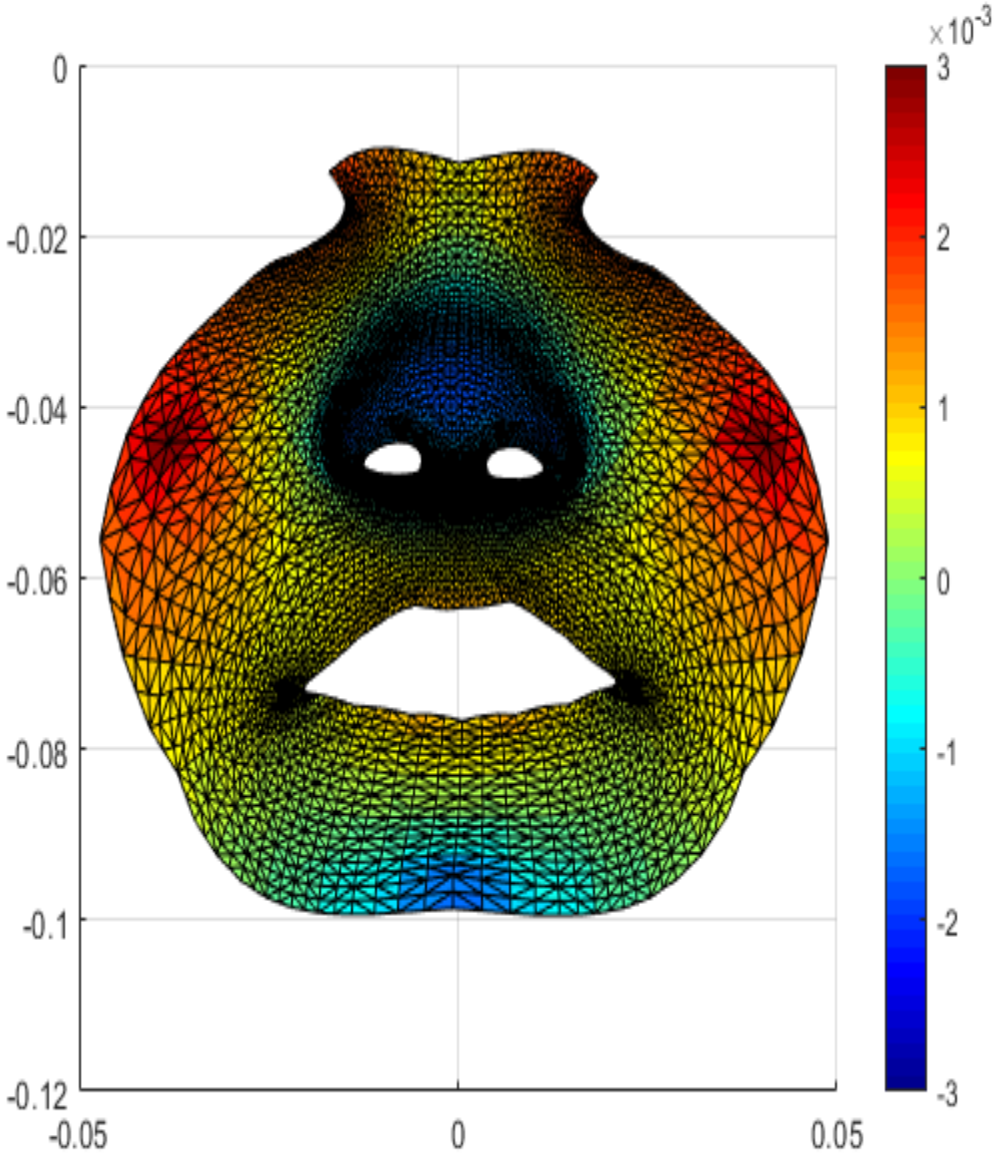

Figure 99: *FRAME 1* Color map of the average asymmetry in the X direction in frame 1 in UCL patients during lip purse. The red color represents asymmetry towards the right. The blue color represents asymmetry to the left side.

The color map in figure 99 shows asymmetry distribution in frame 1 in the mediolateral direction. The nasal tip and ala and other parts of the nose were seen with shades of blue, indicative of nasal tip deviation to the left side or the non-cleft side. The vermillion border of the upper lip and philtral areas show patches of yellow indicative of increased deviation and asymmetry towards the right side or cleft side. The base of the columella also shows mild deviation to the left or non-cleft side. The lower lip also shows patches of yellow and orange indicative of deviation to the cleft or right side

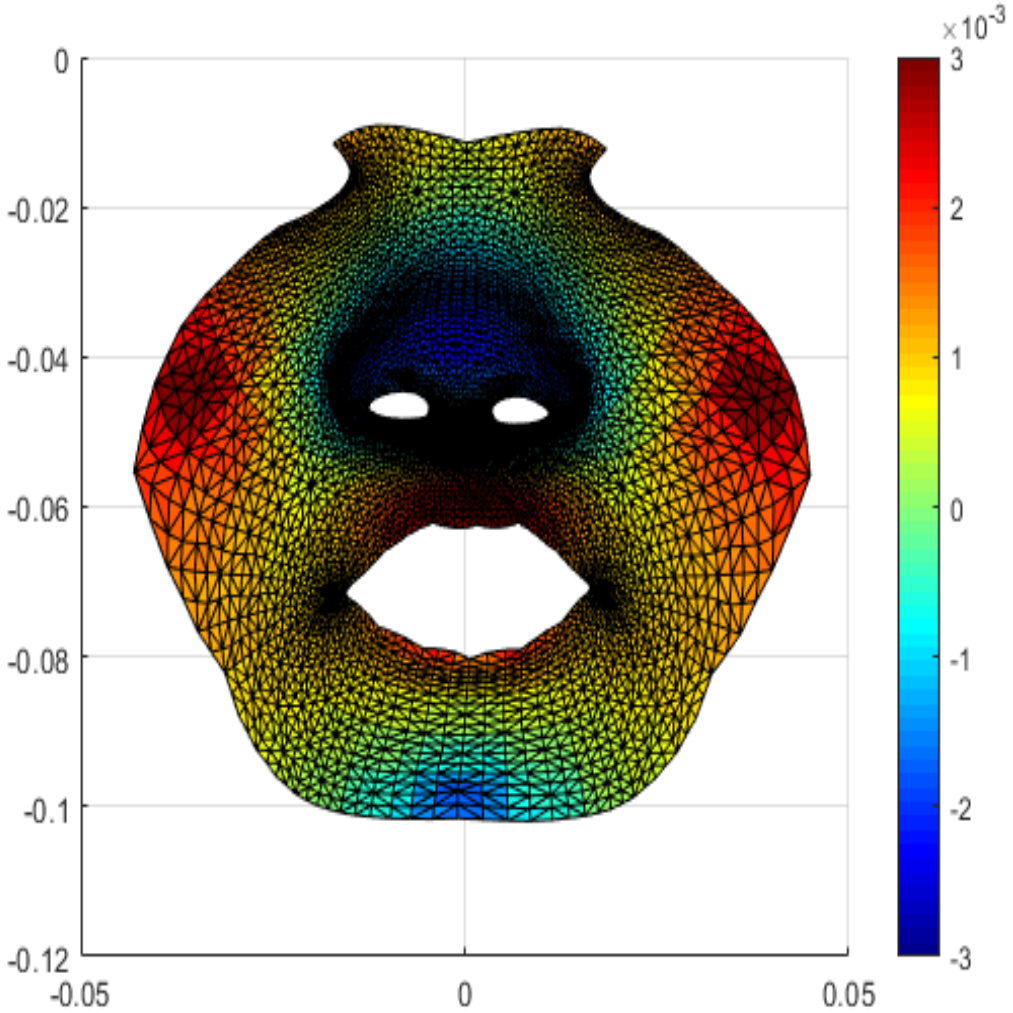

Figure 100: ***FRAME 2*** **Color map of the average asymmetry in the X direction in frame 2 in UCL patients during lip purse. The red color represents asymmetry towards the right. The blue color represents asymmetry to the left side.**

Frame 2 (Figure 100) of the lip purse in the X direction shows the nasal regions remaining unchanged, deviated to the left side or non-cleft side. The vermillion of upper lip and philtrum and columella were covered by dark red patches indicative of deviation towards the right side or cleft side. The vermillion of the lower lip also shows red color and signifies greater deviation to the right side as compared to frame 1.

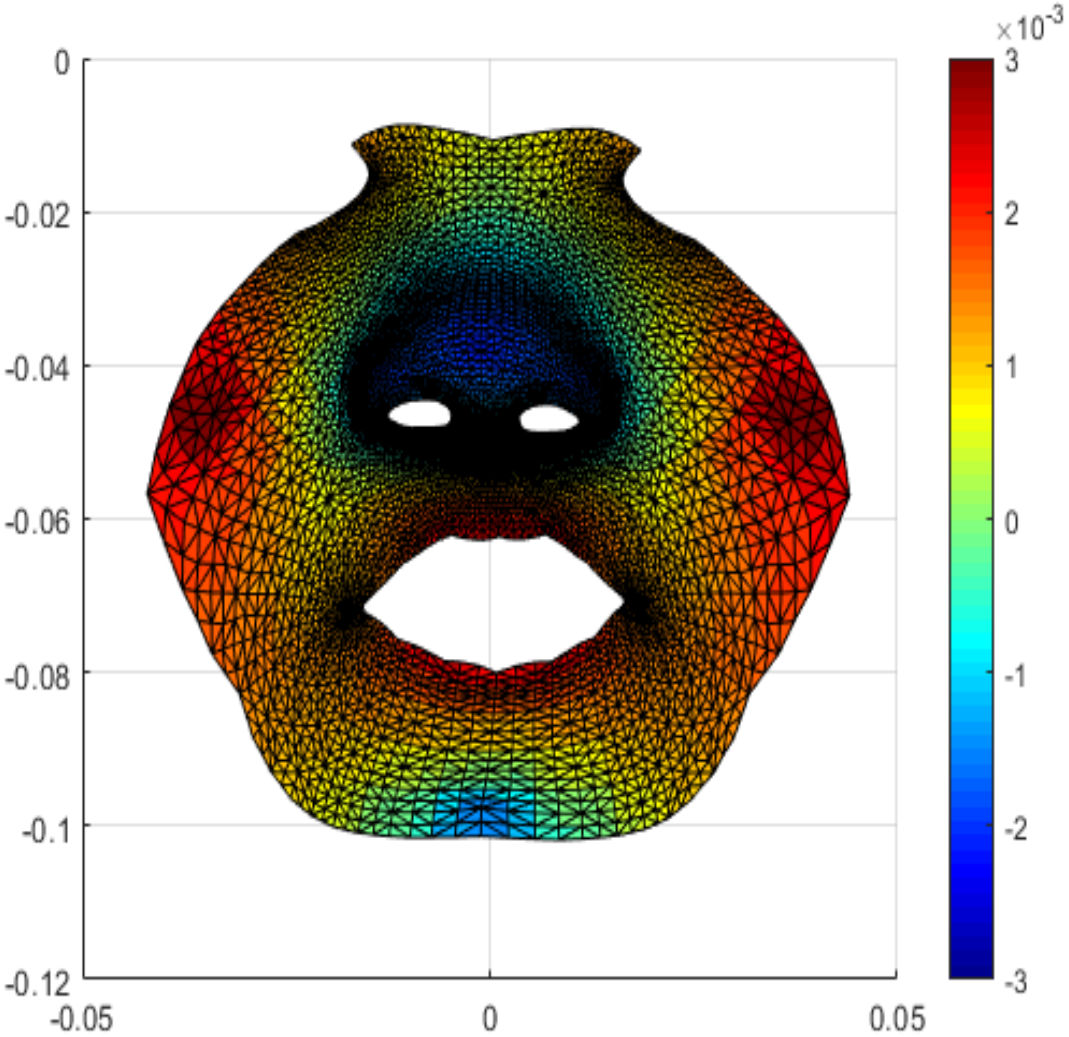

Figure 101: *FRAME 3* Color map of the average asymmetry in the X direction in frame 3 in UCL patients during lip purse. The red color represents asymmetry towards the right. The blue color represents asymmetry to the left side.

Frame 3 (figure 101) was seen to be similar to frame 2 with the nasal region remaining unchanged as compared to frame 2, the upper and lower lips showed greater deviation to the right side, as did the philtrum.

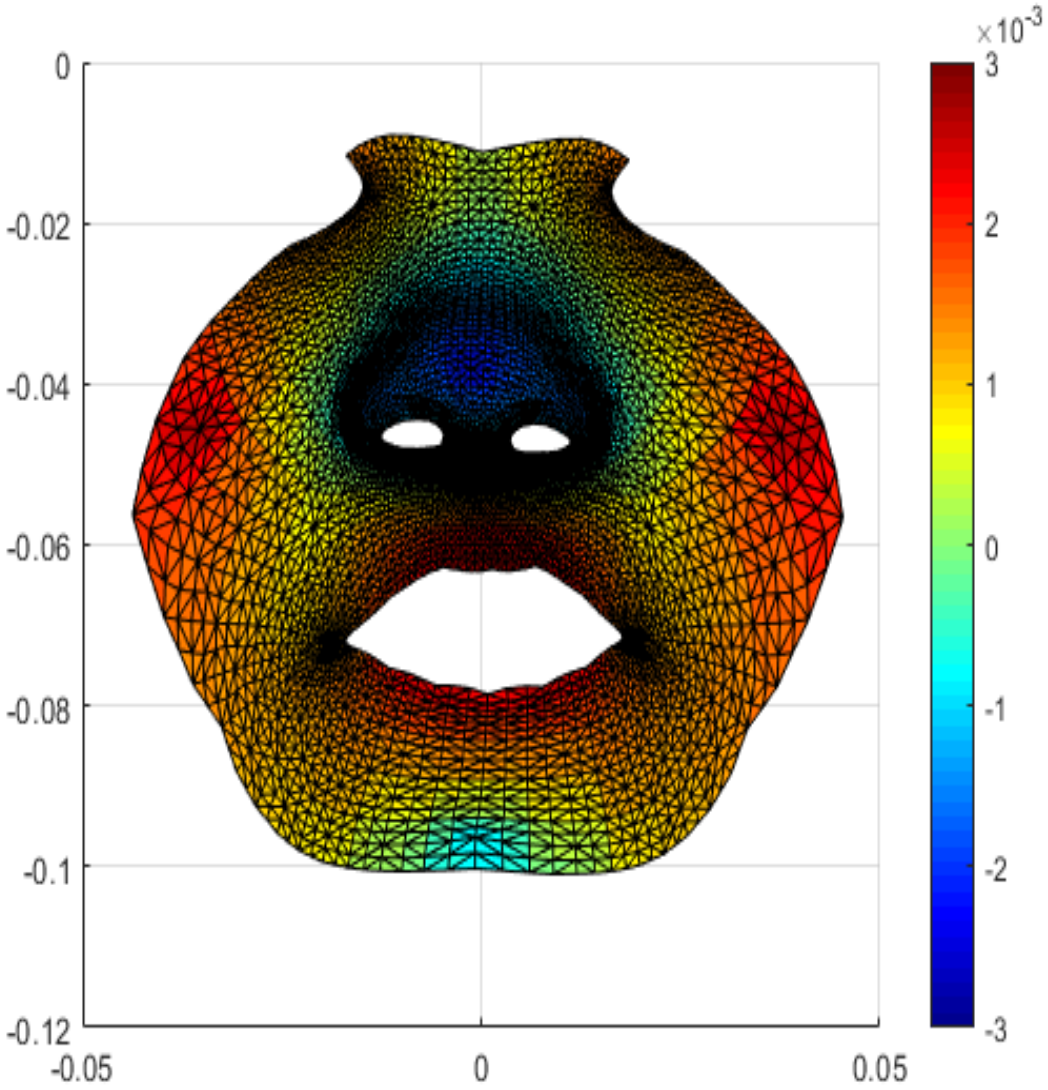

Figure 102: *FRAME 4* Color map of the average asymmetry in the X direction in frame 4 in UCL patients during lip purse. The red color represents asymmetry towards the right. The blue color represents asymmetry to the left side.

Frame 4 (Figure 102) was seen to be similar to frame 3 with the nasal region and columella remaining unchanged as compared to frame 2 and 3, the upper and lower lips showed greater deviation to the right side, as did the philtrum.

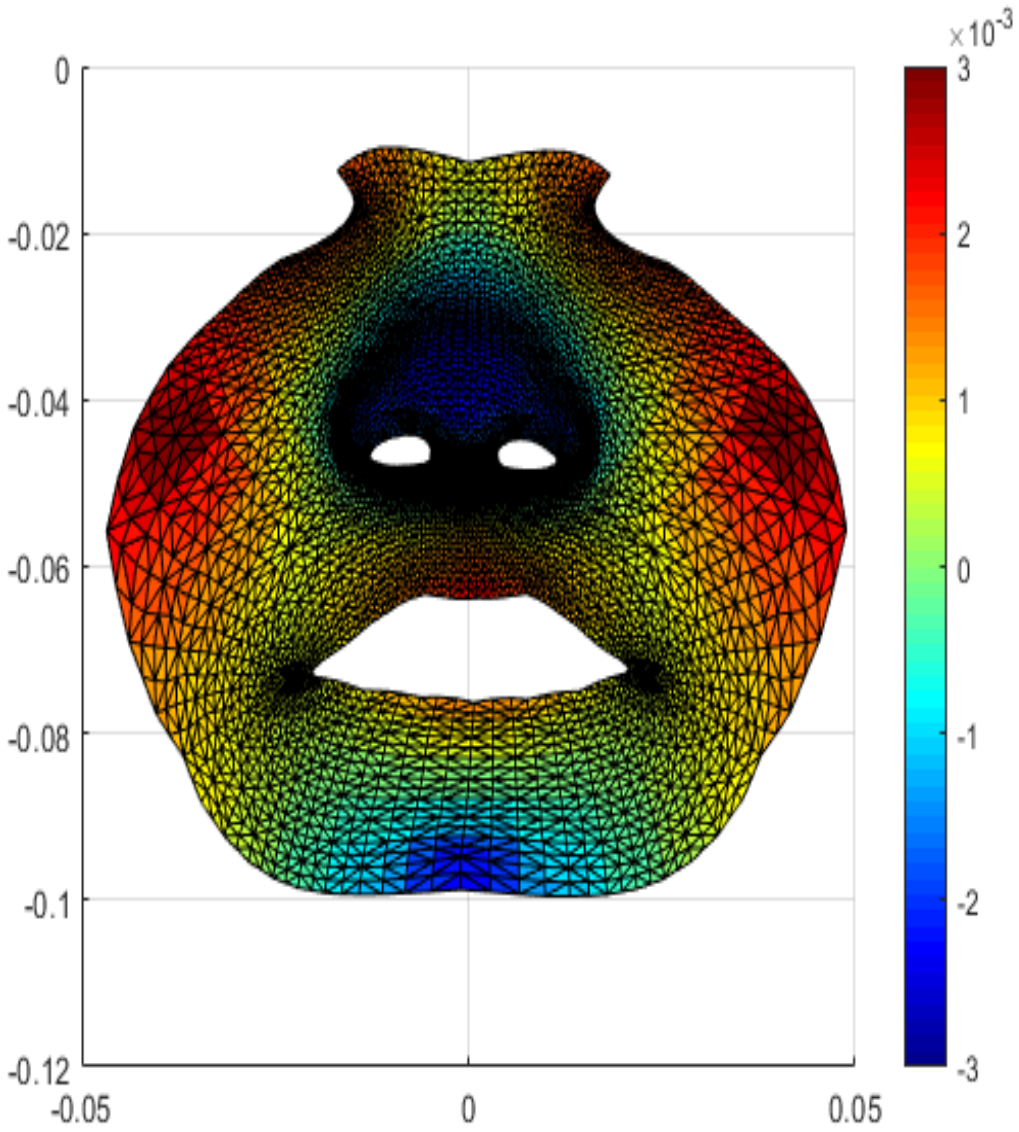

Figure 103: ***FRAME 5*** **Color map of the average asymmetry in the X direction in frame 5 in UCL patients during lip purse. The red color represents asymmetry towards the right. The blue color represents asymmetry to the left side.**

In frame 5, the nasal region remaining unchanged, the upper and lower lips showed lesser deviation to the right as compared the prior frames as was seen by the lighter shades of yellow and red in these areas.

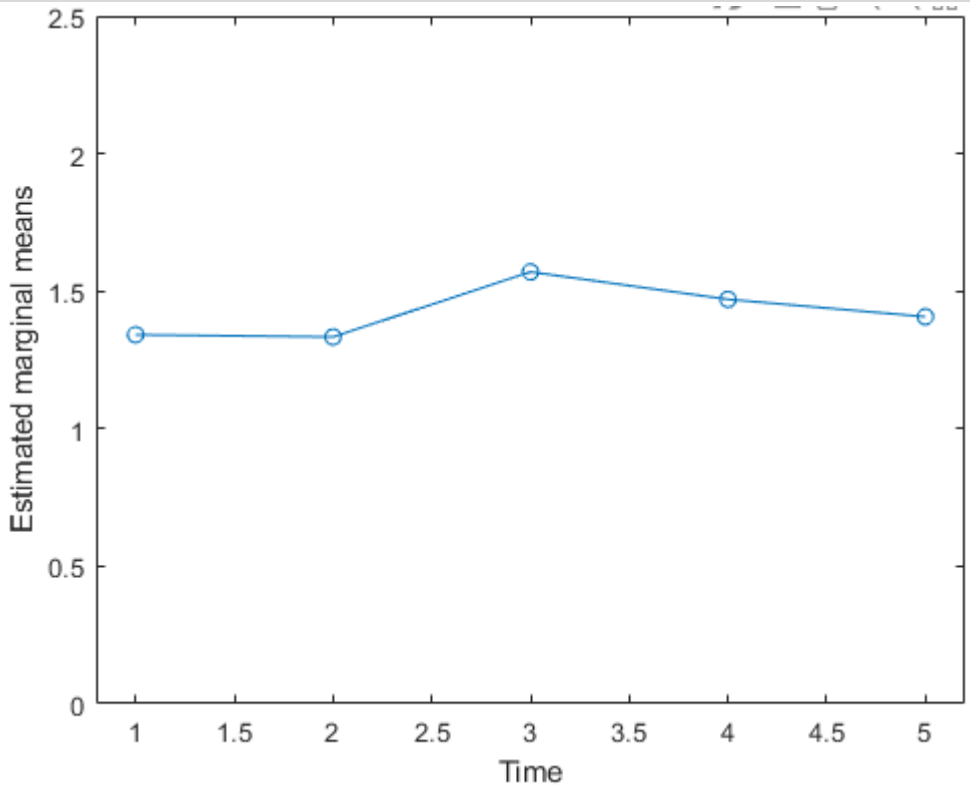

Figure 104: Asymmetry scores between 5 frames in lip purse in the X direction.

Asymmetry scores during lip purse in the X direction (figure 104) showed highest trend in frame 3 or peak expression followed by frame 4. Differences in asymmetry scores between frames were significant in the medio-lateral direction.

4.3.3. Asymmetry in the Vertical (Y direction) during Lip Purse

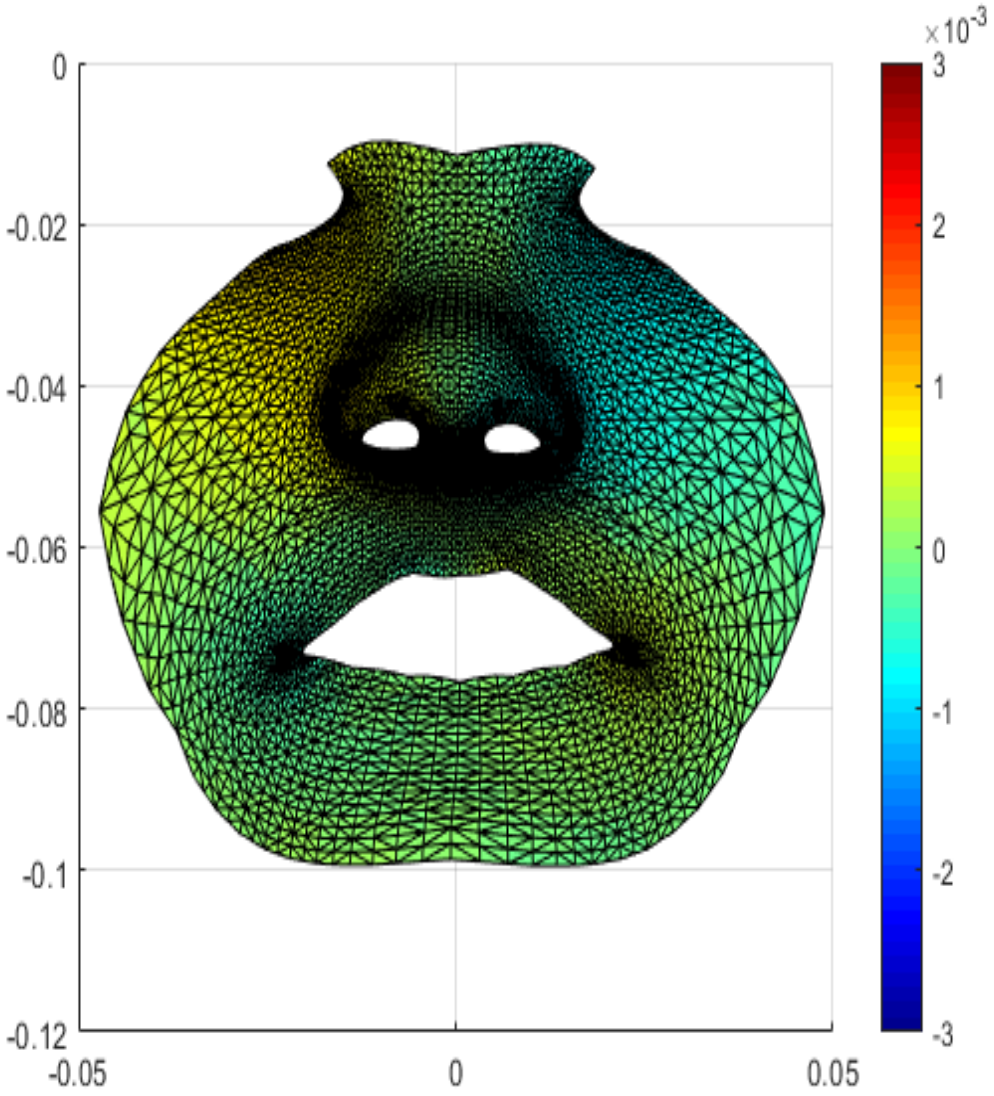

Figure 105: *FRAME 1* Color map of the asymmetry in the Y direction in frame 1 in UCL patients during lip purse. The red color represents asymmetry in upward direction. The blue color represents asymmetry in a downward direction.

Frame 1 of the lip purse in the Y direction was seen to be indicative of minimal changes in asymmetry with the green patches distributed evenly. The left ala showed a patch of blue indicative of a mild deviation in downward direction and

the right ala showed a yellow patch indicative of a mild deviation in upward direction.

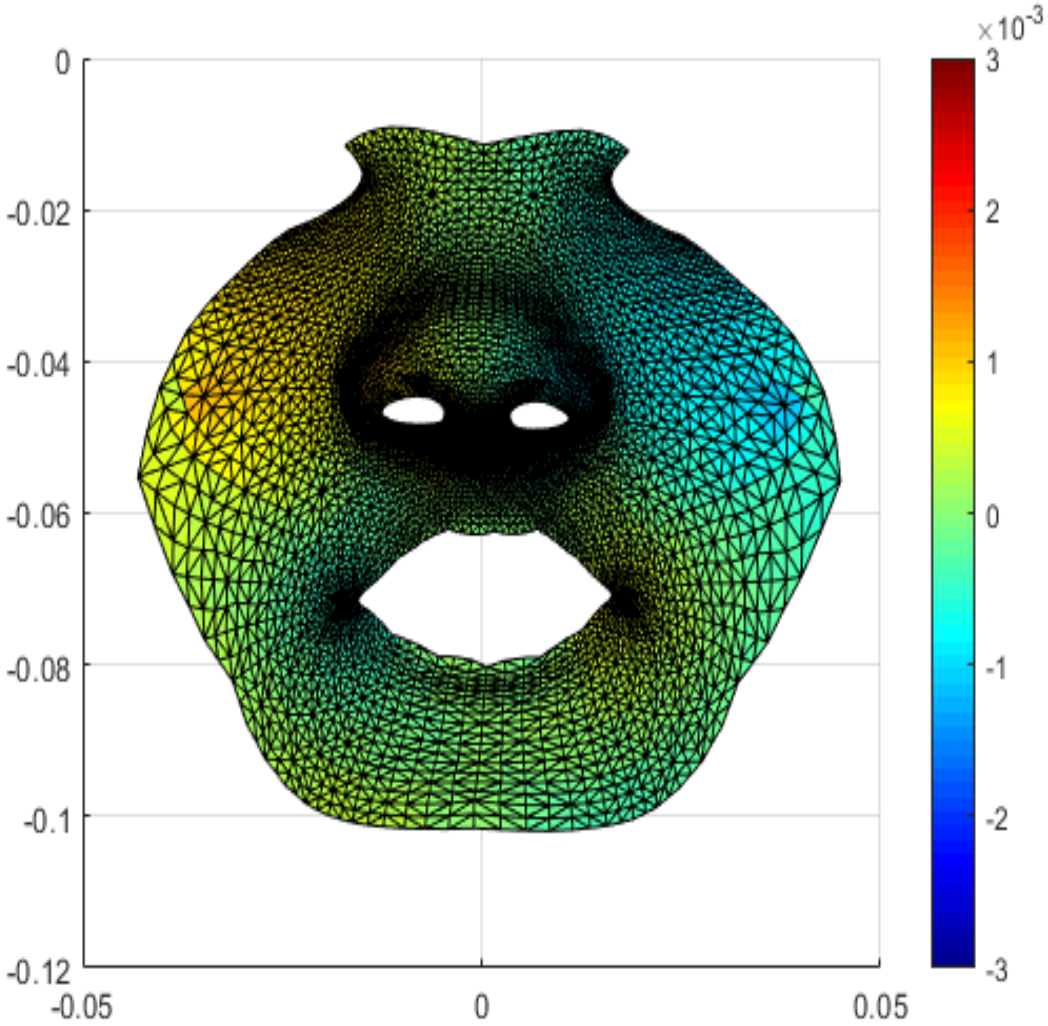

Figure 106: *FRAME 2* Color map of the asymmetry in the Y direction in frame 2 in UCL patients during lip purse. The red color represents asymmetry in upward direction. The blue color represents asymmetry in a downward direction.

Figure 106 represents color map of asymmetry distribution in frame 2 in the vertical direction in UCL patients during lip purse. Mostly areas of green and light green are seen in the nasolabial region indicative of minimal vertical

changes occurring in frame 2 of the lip purse. The left ala of the nose shows slight blue patch indicating deviation in downward direction and the right ala shows mild yellowish red color indicating deviation in upwards direction. This frame was more or less similar to frame 1 indicating minimum changes in vertical direction with increasing movement.

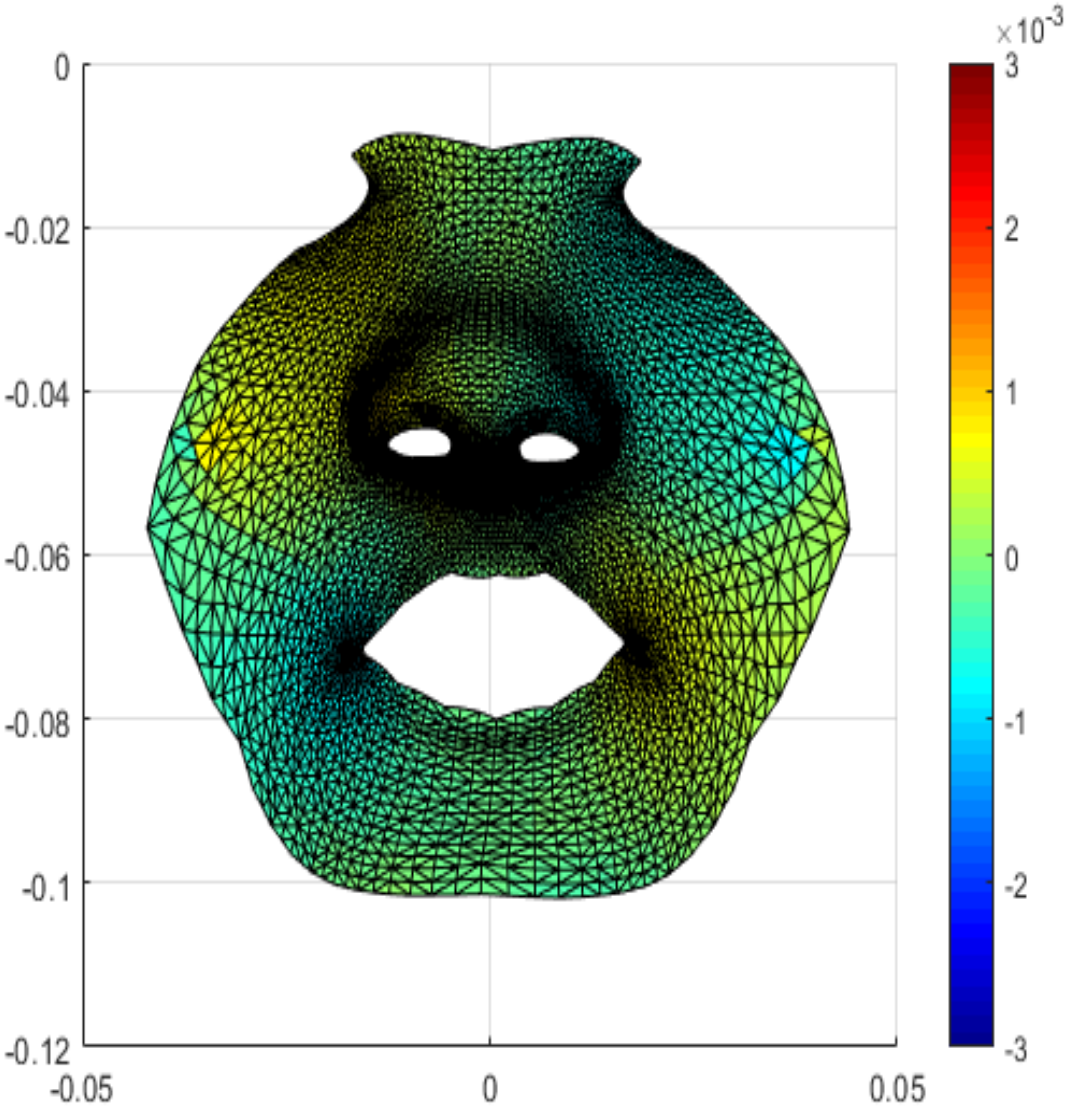

Figure 107: *FRAME 3* Color map of the asymmetry in the Y direction in frame 3 in UCL patients during lip purse. The red color represents asymmetry in upward direction. The blue color represents asymmetry in a downward direction.

Frame 3 (figure 107) of the maximal smile in the Y direction was similar to that of frame 2 and 1 indicating no changes in vertical direction during lip purse.

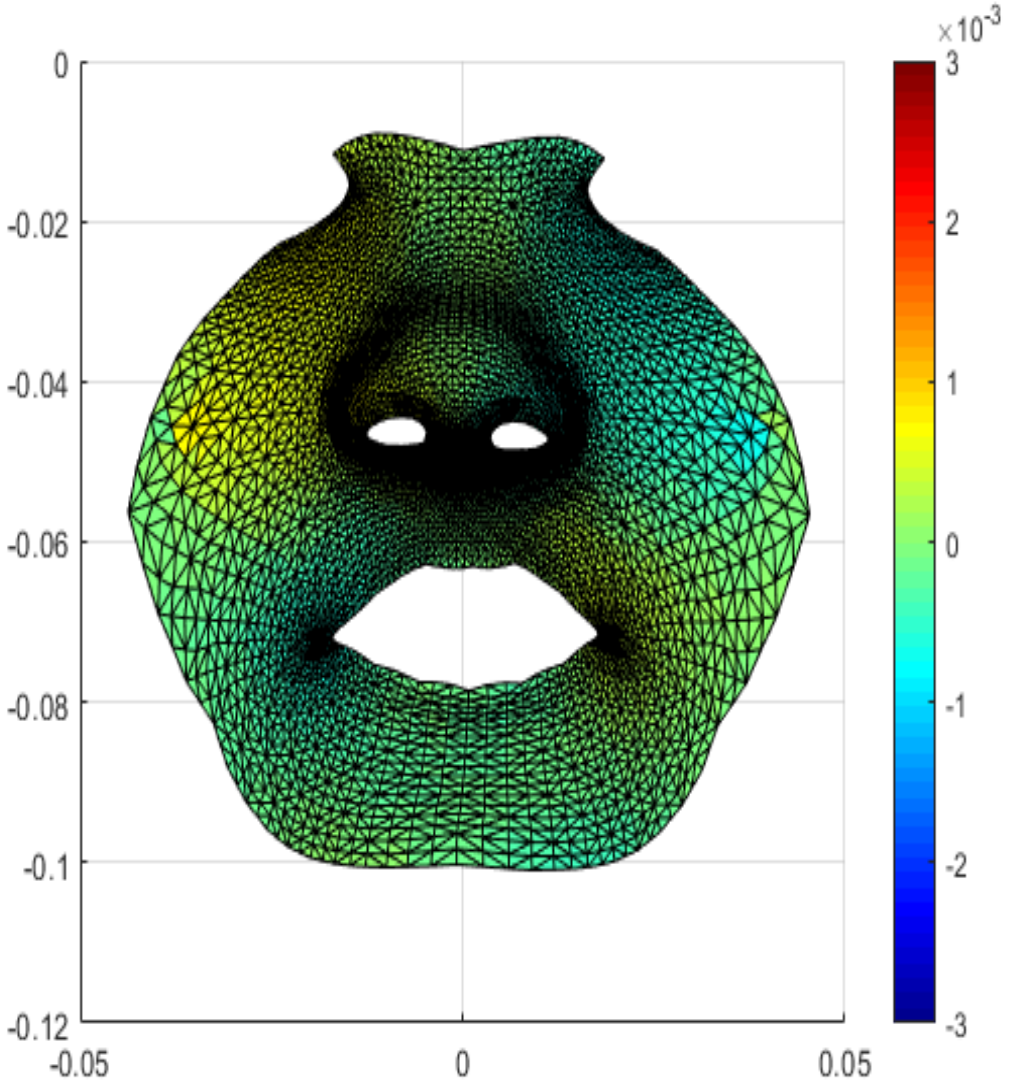

Figure 108: ***FRAME 4*** **Color map of the asymmetry in the Y direction in frame 4 in UCL patients. The red color represents asymmetry in upward direction. The blue color represents asymmetry in a downward direction.**

Frame 4 (Figure 108) in the vertical direction was no different from the prior frames indicating no change in the vertical direction.

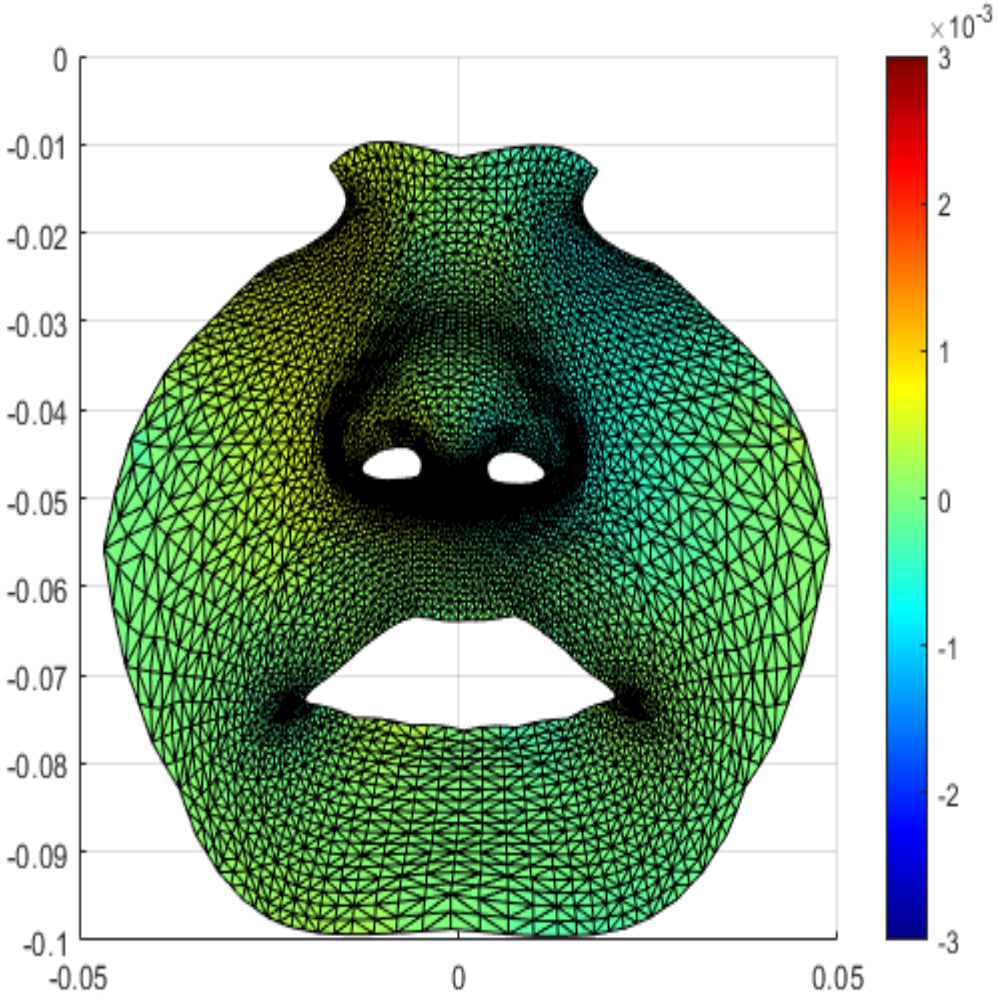

Figure 109: *FRAME 5* Color map of the asymmetry in the Y direction in frame 5 in UCL patients. The red color represents asymmetry in upward direction. The blue color represents asymmetry in a downward direction.

Frame 5 (Figure 109) of the lip purse in the Y direction showed increased residual asymmetry as compared to the other frames especially in areas around

the nose- the nasal alar regions. The right ala showed deviation in upward direction whereas the left ala showed deviation in downward direction. Parts of the right philtrum and vermillion border were also deviated in upward direction and showed higher asymmetry as compared to previous frames indicating that muscle tension persisted even after final resting state resulting in increased asymmetry in frame 5.

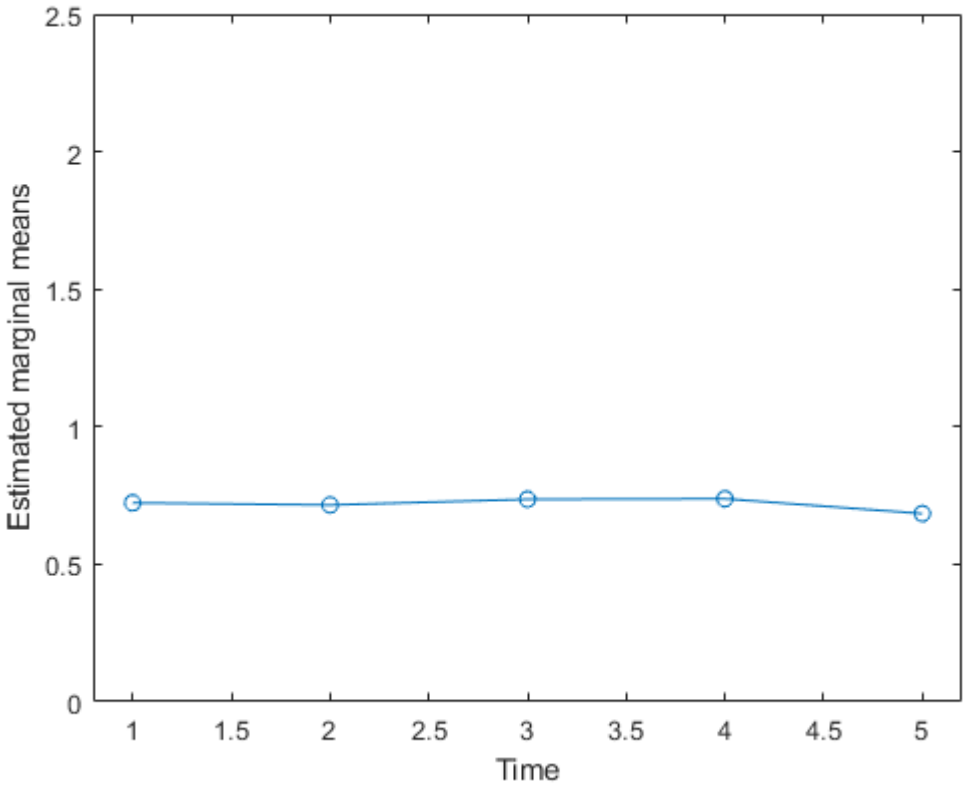

Figure 110: Asymmetry scores between 5 frames in lip purse in the Y direction.

It was seen in the graph that asymmetry differences between frames in the vertical direction were minimum indicating minimal changes in asymmetry in the vertical direction. Significant differences in asymmetry scores were seen between all frames in the Y direction.

4.3.4. Asymmetry in the antero-posterior (Z direction) during lip purse

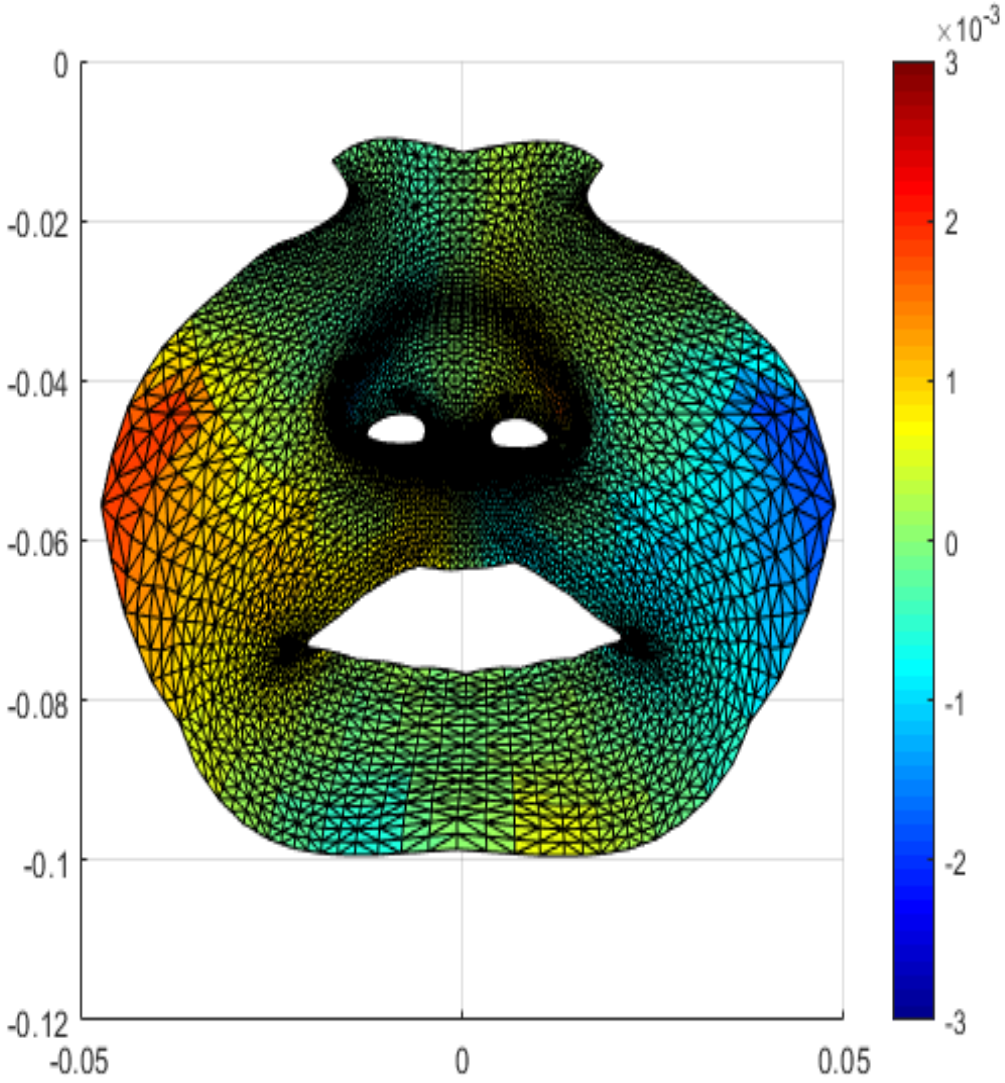

Figure 111: *FRAME 1* Color map of the average asymmetry in the Z direction in frame 1 in UCL patients during lip purse. The red color represents asymmetry in a forward (towards observer) direction. The blue color represents asymmetry in a backward direction (away from observer).

Frame 1 (Figure 111) of the lip purse in the antero-posterior direction showed the left side vermillion border of the upper lip shows a patch of blue indicating posterior or backward deviation. The right side of the vermillion border of the upper lip had a shade of yellow and light red which indicated anterior deviation towards the observer. The right ala region showed backward deviation whereas the left ala showed forward deviation.

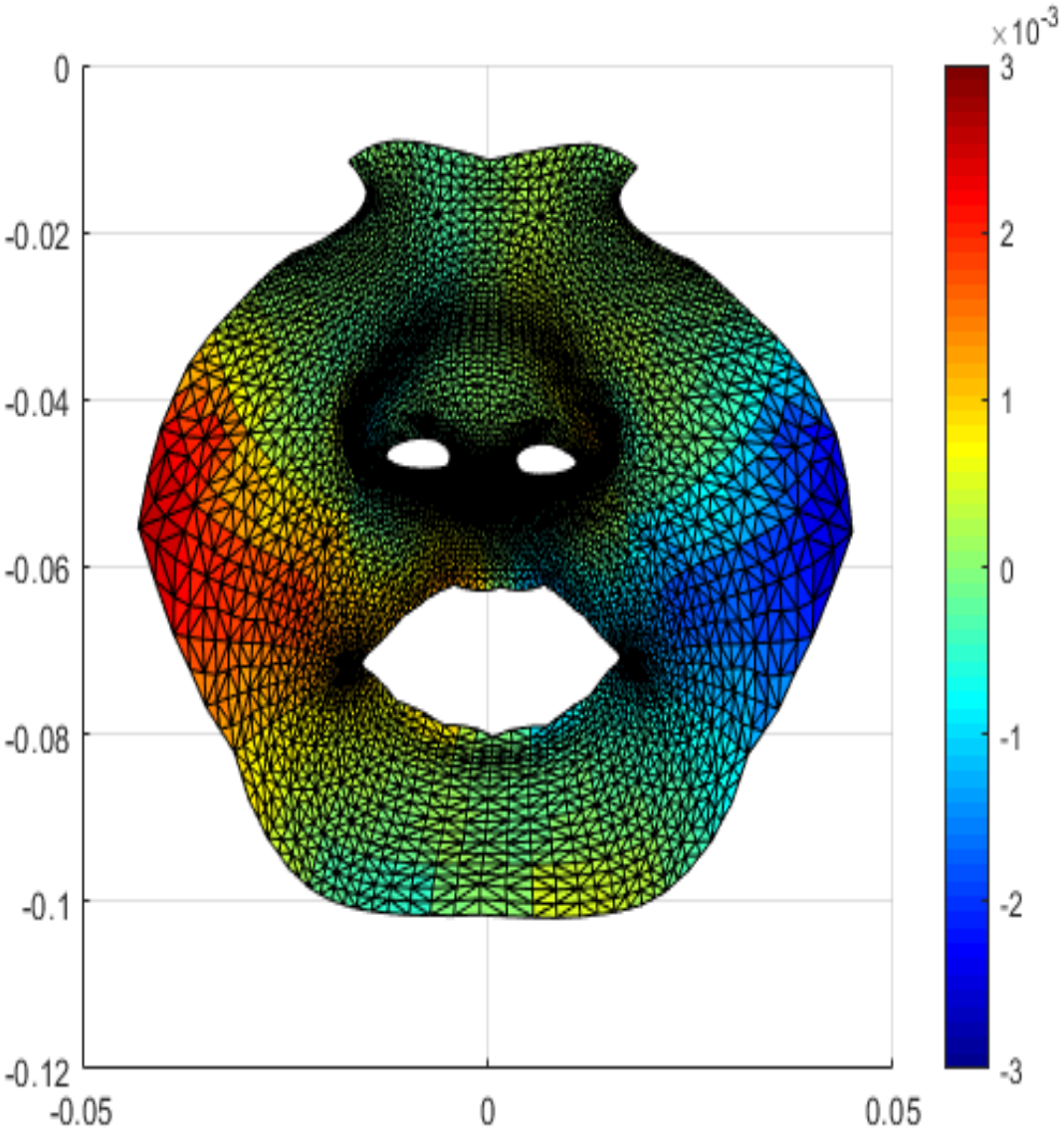

Figure 112: *FRAME 2* Color map of the average asymmetry in the Z direction in frame 2 in UCL patients during lip purse. The red color represents asymmetry in a forward (towards observer) direction. The blue color represents asymmetry in a backward direction (away from observer).

In frame 2 (Figure 112), the left side vermillion border of the upper lip shows a patch of blue indicating posterior or backward deviation. The right side of the vermillion border of the upper lip had a shade of yellow and red which indicated anterior deviation towards the observer. The lower lip showed similar color trend, with the right side of the lower lip showing areas of yellow indicating deviation anteriorly and the left side of the lower lip showing patches of blue indicating posterior deviation. The left nostril and surrounding alar regions showed slight yellowish coloration indicating mild anterior deviation as compared to the right sided nostril.

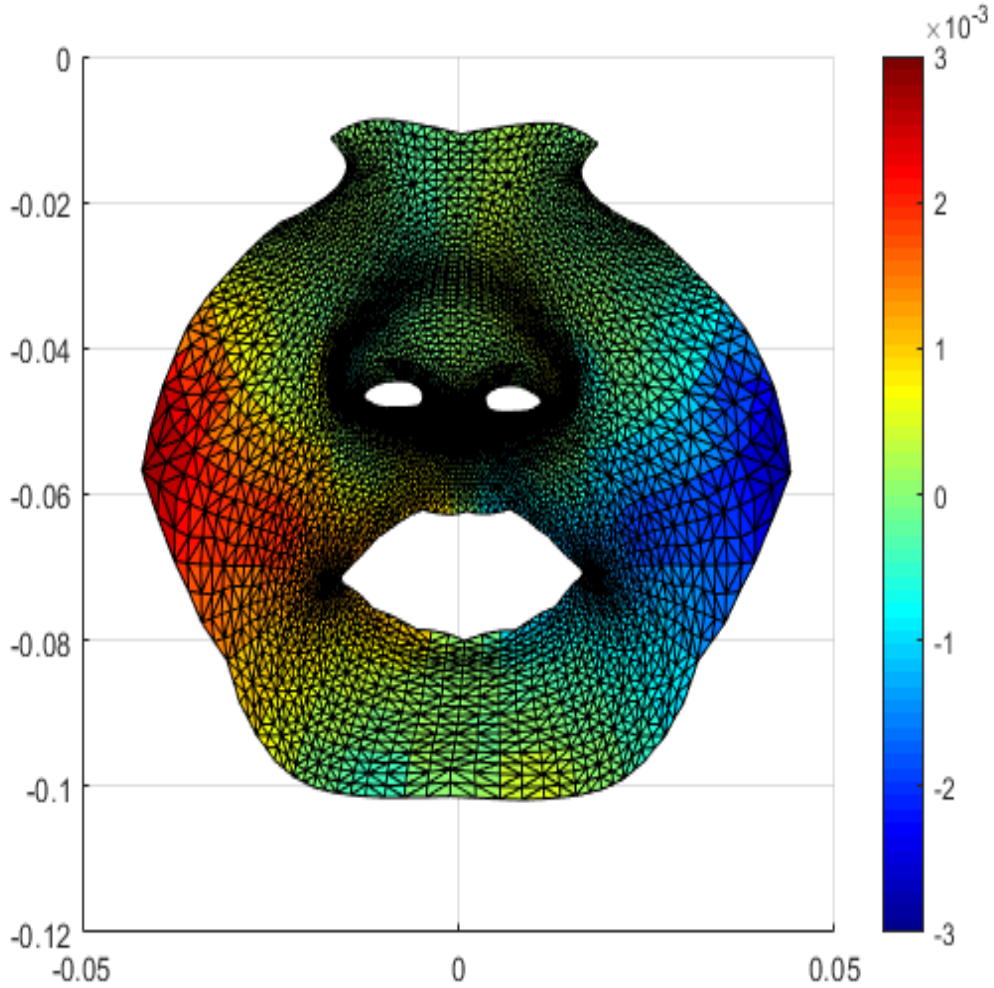

Figure 113: *FRAME 3* Color map of the average asymmetry in the Z direction in frame 3 in UCL patients during lip purse. The red color represents asymmetry in a forward (towards observer) direction. The blue color represents asymmetry in a backward direction (away from observer).

Frame 3 (figure 113) of the lip purse in the Z direction was similar to frame 2 in terms of deviation and asymmetry. The left side vermillion border of the upper lip showed a patch of blue indicating posterior or backward deviation. The right side of the vermillion border of the upper lip had a shade of yellow and red which indicated anterior deviation towards the observer.

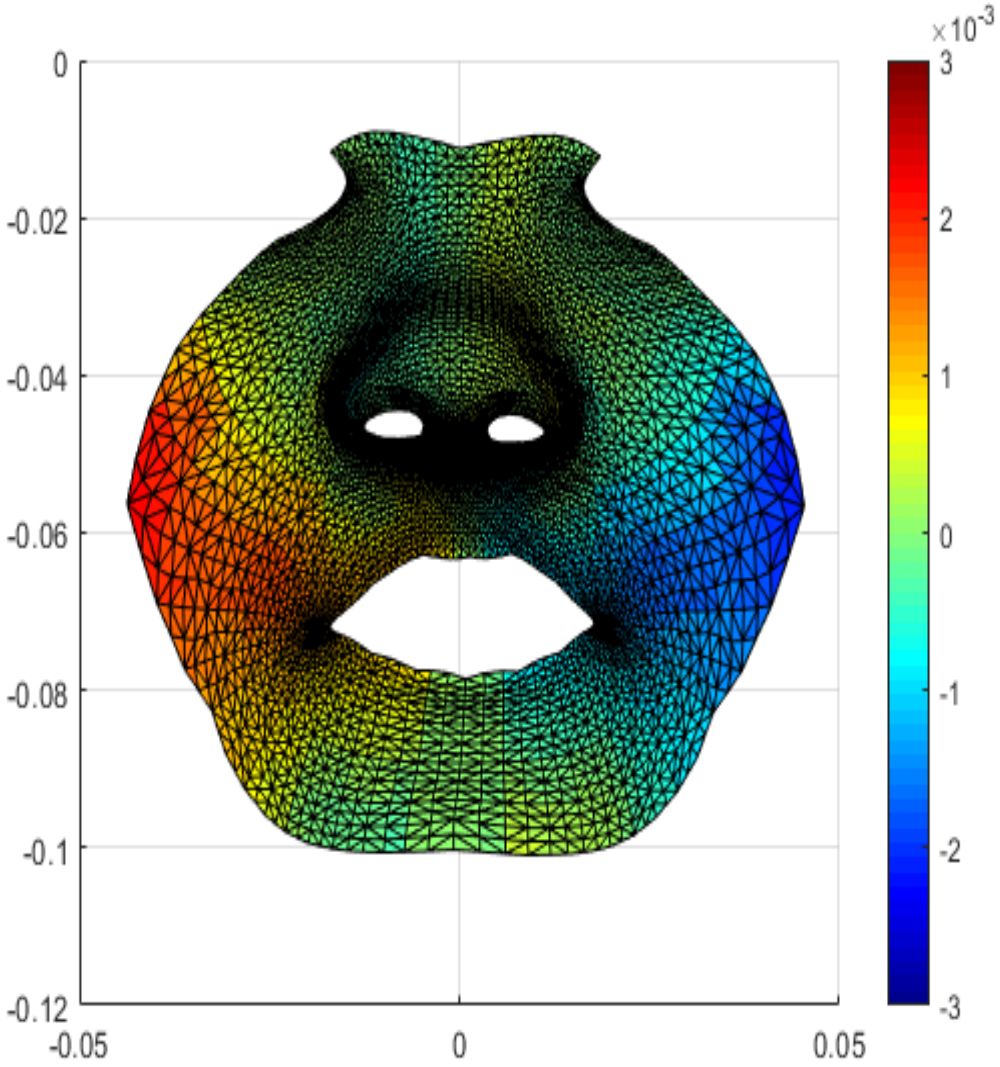

Figure 114: ***Frame 4*** **Color map of the average asymmetry in the Z direction in frame 4 in UCL patients during lip purse. The red color represents asymmetry in a forward (towards observer) direction. The blue color represents asymmetry in a backward direction (away from observer).**

Frame 4 (Figure 114) of the lip purse in the Z direction was similar to frame 3 but with higher intensity of color indicative of higher asymmetry especially in the vermillion borders of upper and lower lips.

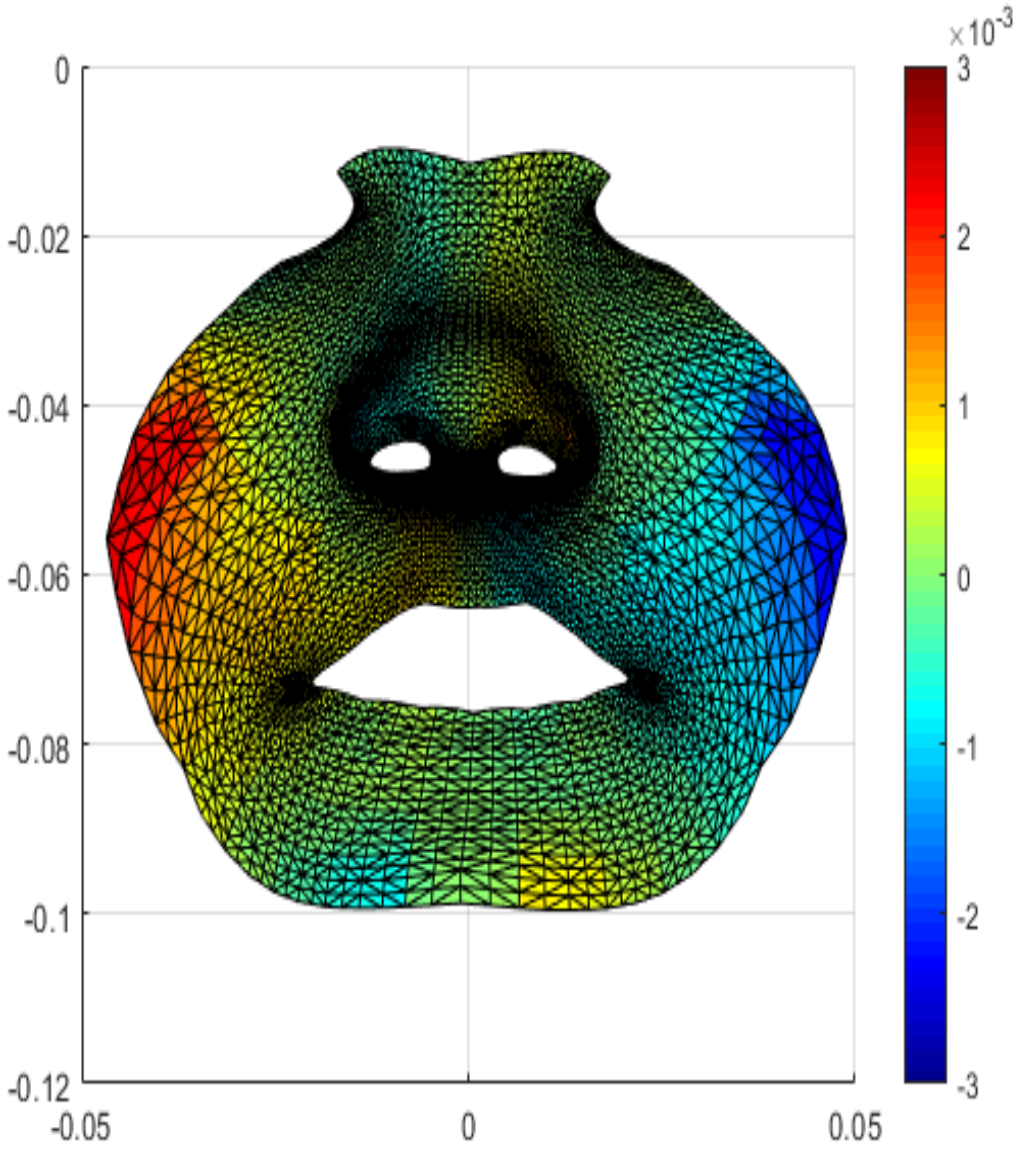

Figure 115: ***Frame 5*** **Color map of the average asymmetry in the Z direction in frame 5 in UCL patients during lip purse. The red color represents asymmetry in a forward (towards observer) direction. The blue color represents asymmetry in a backward direction (away from observer).**

Frame 5 (Figure 115) was similar to frame 1 in terms of distribution of asymmetry. Asymmetry was seen to be lesser as compared to frames 2,3 and 4 as the face came to rest.

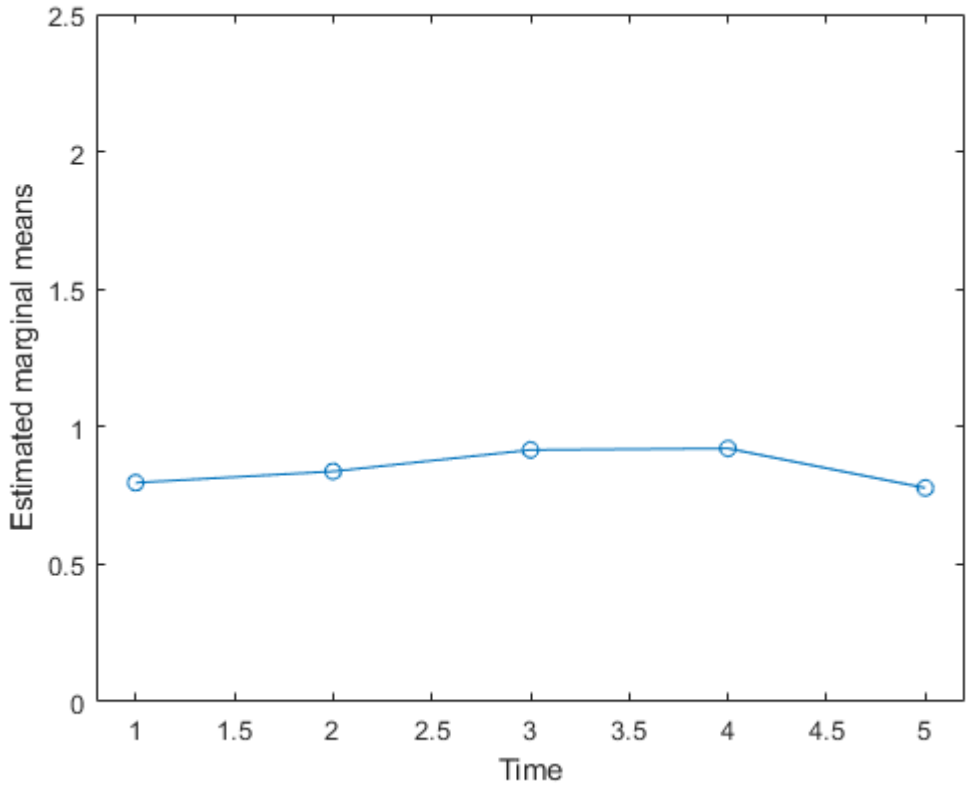

Figure 116: Asymmetry scores between 5 frames during lip purse in the Z direction.

The graph for marginal means asymmetry scores (Figure 116) showed highest asymmetry in frame 3 and 4. Significant differences existed between all frames during lip purse in the Z direction. Differences between frames were minimum in the graph due to changes being very small.

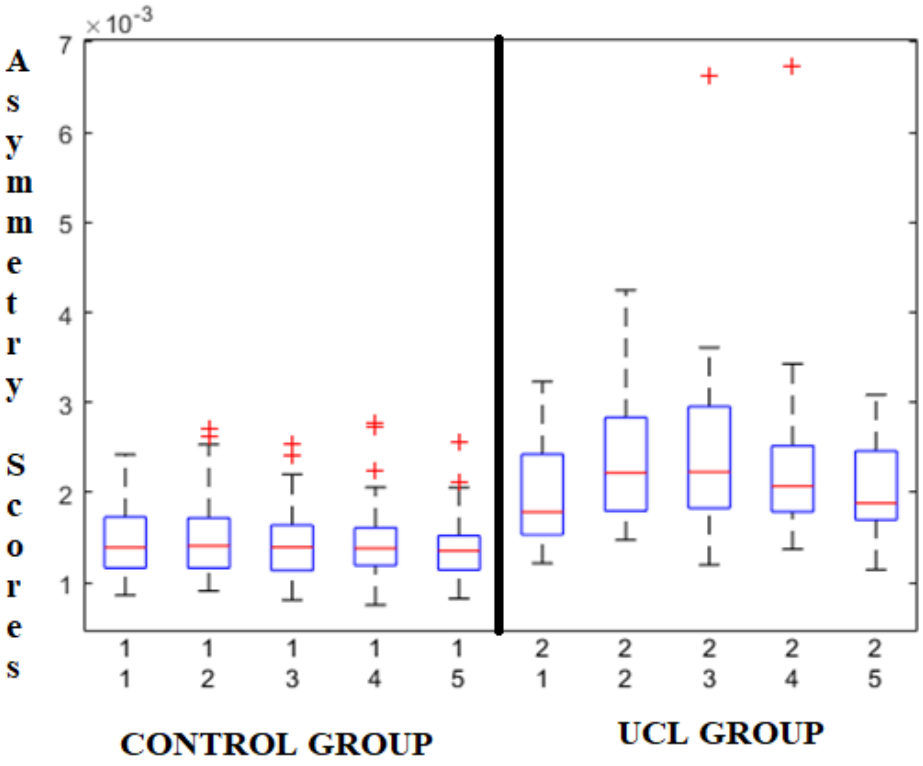

Figure 117: Asymmetry scores for lip purse in box plot between UCL group (1-5 on right) and the control group (1-5 on the left)

Asymmetry scores of the whole face (Figure 117) compared between the UCL cases and the controls between the 5 frames showed significant differences in all five frames between the two groups. Frame 3 in the controls showed highest asymmetry in the whole face similar to the trend in the UCL group suggesting that asymmetry is accentuated during peak facial movement.

4.4. Grimace

Summary:

Significant differences were seen in all frames between the UCL group and the control group during performance of grimace. No significant differences were seen in asymmetry scores between all frames within the UCL group in the whole face and x direction. The differences in asymmetry scores in all frames within the UCL group were significantly different ($p<0.001$) in the y (vertical) and z direction (anteroposterior direction). The X direction showed higher asymmetry in frame 3 followed by frame 2, with asymmetry most pronounced in the alar regions and nasal tip (left sided/non-cleft deviation) and the upper lip vermillion, the lower lip vermillion and philtrum (right sided deviation). Vertical asymmetries were minimal. The anteroposterior direction tended to show highest asymmetry in frame 4 followed by frame 2 with asymmetry highest in the regions of the ala and nasal tip along with the philtrum and upper lip.

4.4.1. Asymmetry in the total face during Grimace

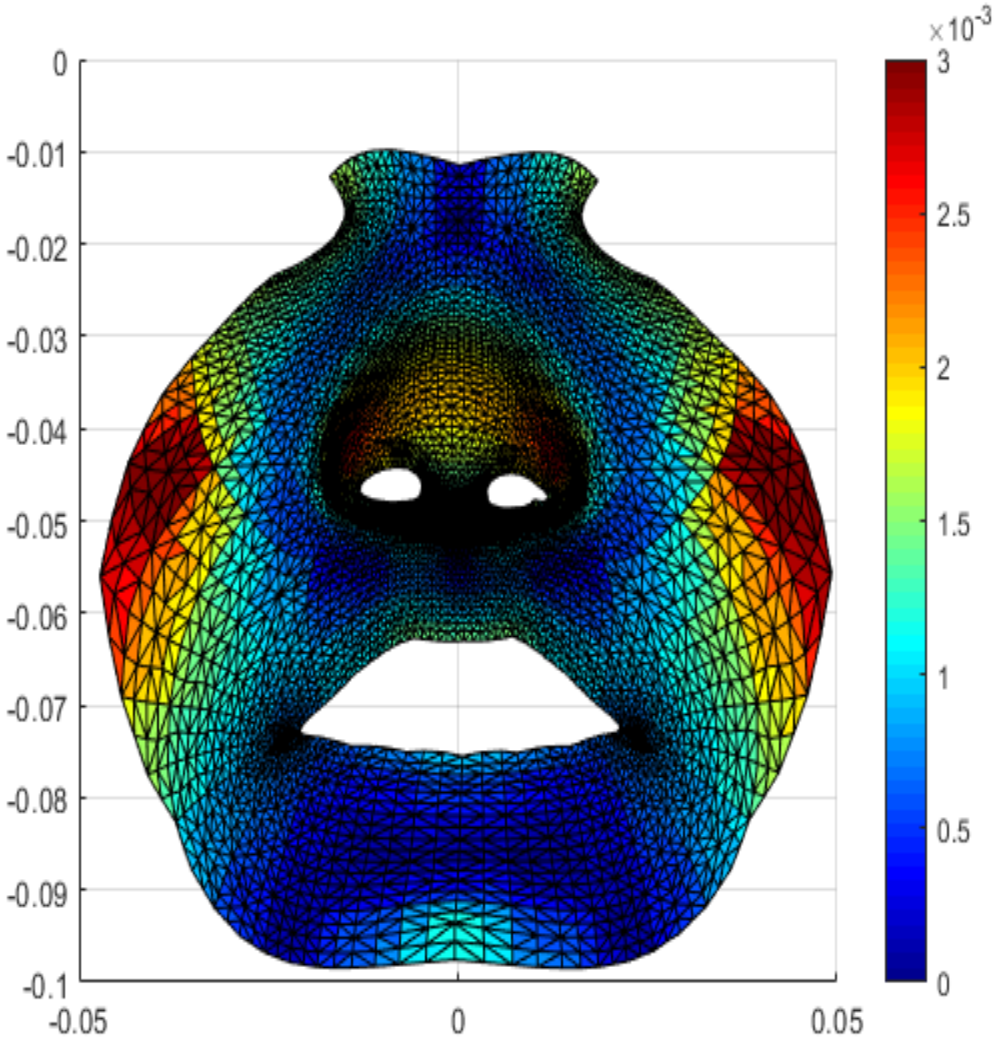

Figure 118: ***FRAME 1* Color *map of the total face asymmetry in frame 1 in the UCL patients during grimace. The red color represents increased asymmetry. The blue color represents decreased asymmetry. Areas in green represent zero distance between the original and mirrored meshes (no asymmetry).***

Frame 1 in figure 118 shows higher residual asymmetry in areas around the nasal tip and alar regions (patches of red interspersed with yellow patches). Mild

yellow patches were seen in the upper lip vermillion border. This is indicative of increased residual asymmetry present in the upper lip vermillion border.

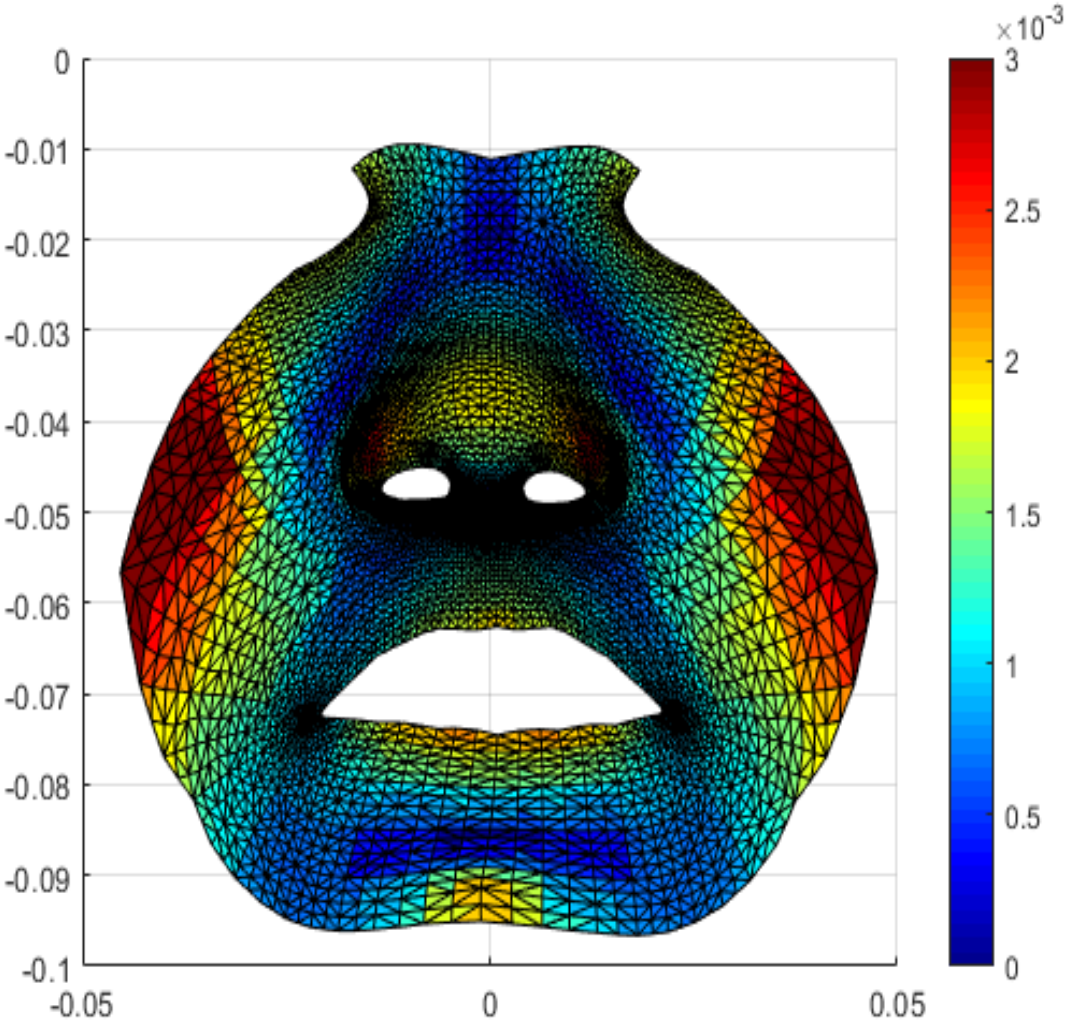

Figure 119: *FRAME 2* Color map of the <u>total face asymmetry</u> in frame 2 in the UCL patients during <u>grimace</u>. The red color represents increased asymmetry. The blue color represents decreased asymmetry. Areas in green represent zero distance between the original and mirrored meshes (no asymmetry).

Frame 2 (Figure 119) shows higher residual asymmetry in areas around the nasal tip and alar regions (patches of mild red interspersed with yellow patches). A yellow patch was seen in the upper lip vermillion border. Yellow patches were seen in the vermillion border of the lower lip as well. This is indicative of increased residual asymmetry present in the upper and lower lip vermillion.

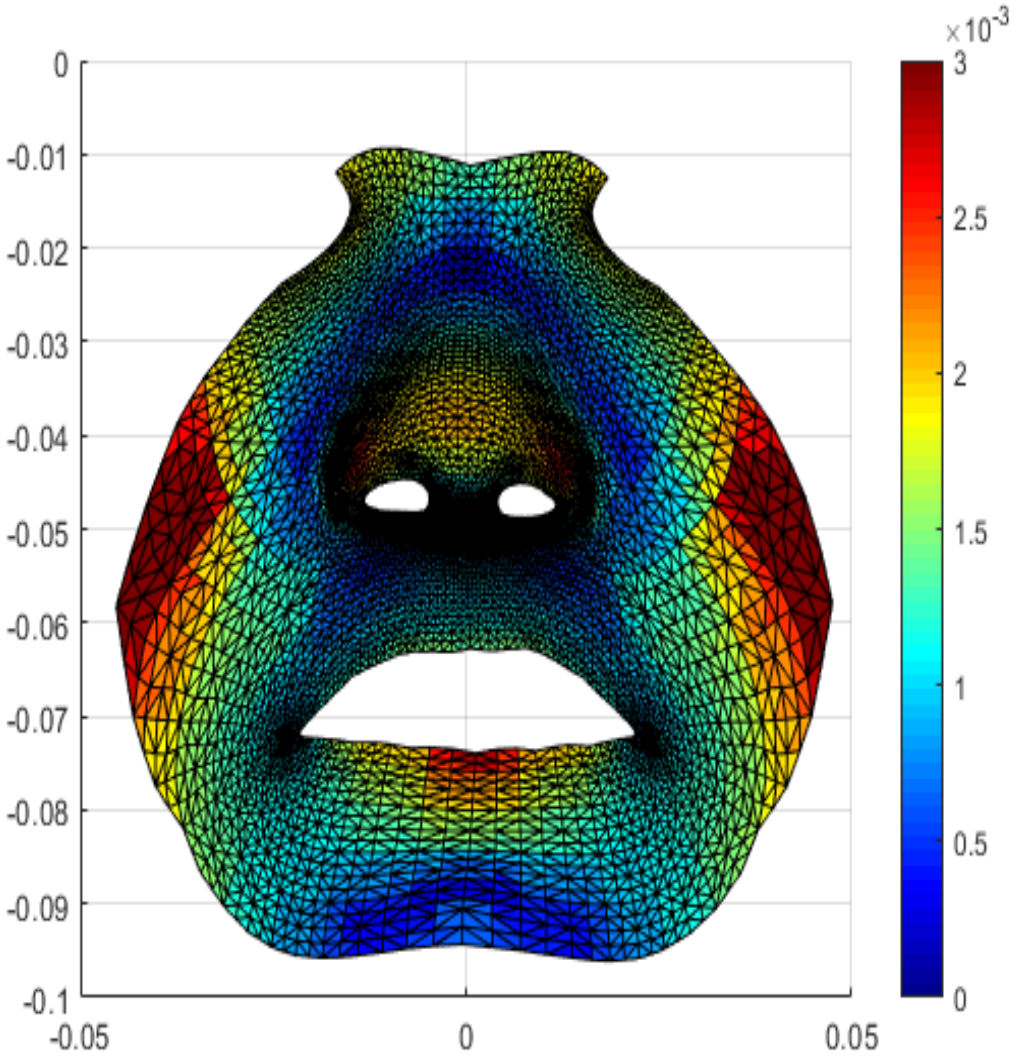

Figure 120: *FRAME 3* Color map of the <u>total face asymmetry</u> in frame 3 in the UCL patients during <u>grimace</u>. The red color represents increased asymmetry. The blue color represents decreased asymmetry. Areas in green represent zero distance between the original and mirrored meshes (no asymmetry).

Frame 3 (Figure 120) shows higher residual asymmetry in areas around the nasal tip and alar regions (patches of mild red interspersed with yellow patches). Yellow and dark red patches were seen in the vermillion border of the lower lip as well. This is indicative of increased residual asymmetry present in the lower lip vermillion. Asymmetry in the upper lip decreased as the color went from yellow to bluish.

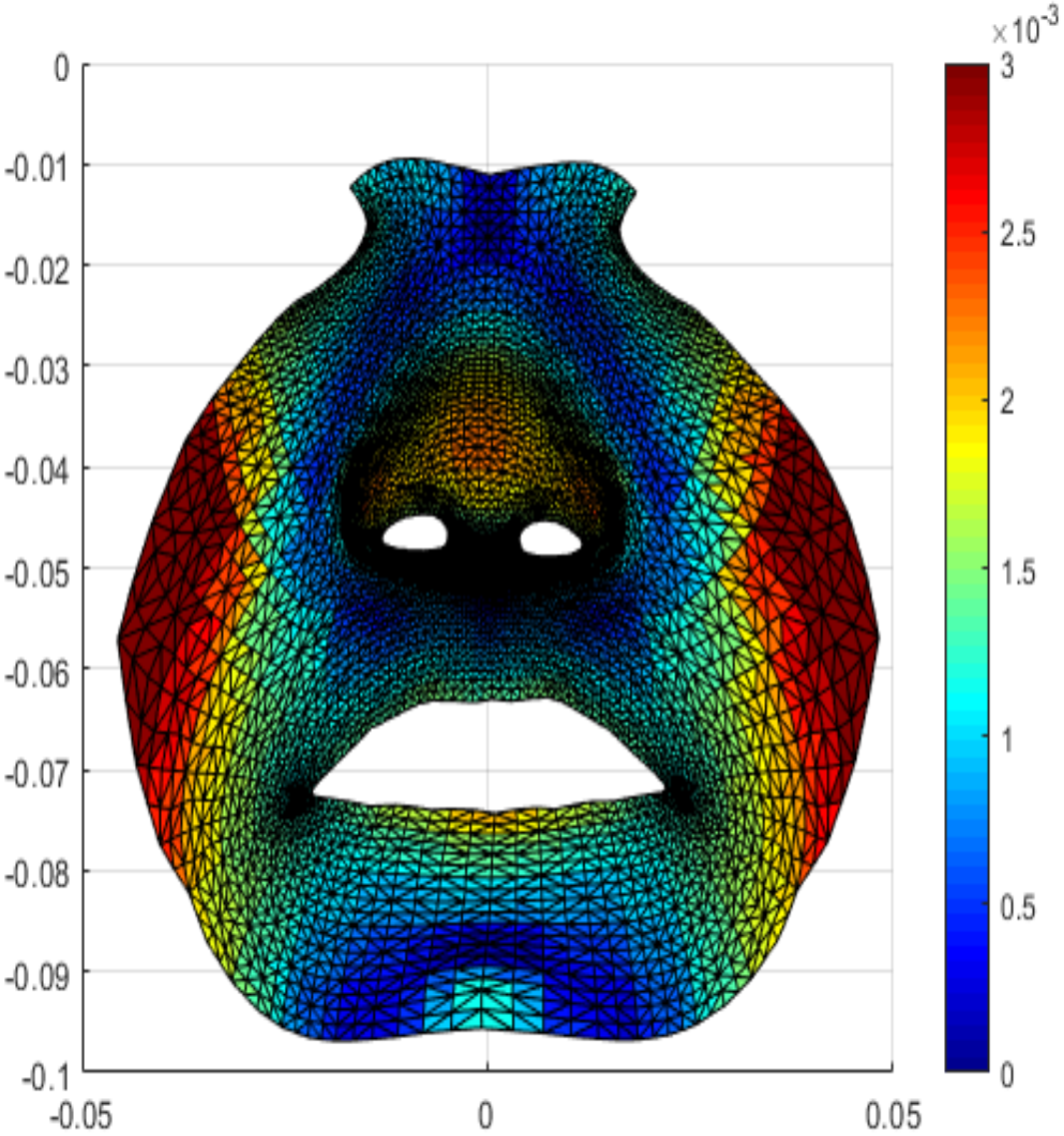

Figure 121: *FRAME 4* Color map of the <u>total face asymmetry</u> in frame 4 in the UCL patients during <u>grimace</u>. The red color represents increased asymmetry. The blue color represents decreased asymmetry. Areas in green represent zero distance between the original and mirrored meshes (no asymmetry).

Frame 4 (Figure 121) shows increased residual asymmetry in areas around the nasal tip and alar regions (patches of mild red interspersed with yellow patches). Yellow patches were seen in the vermillion border of the lower lip which was less than in frame 3, indicative of decreased residual asymmetry in the lower lip vermillion.

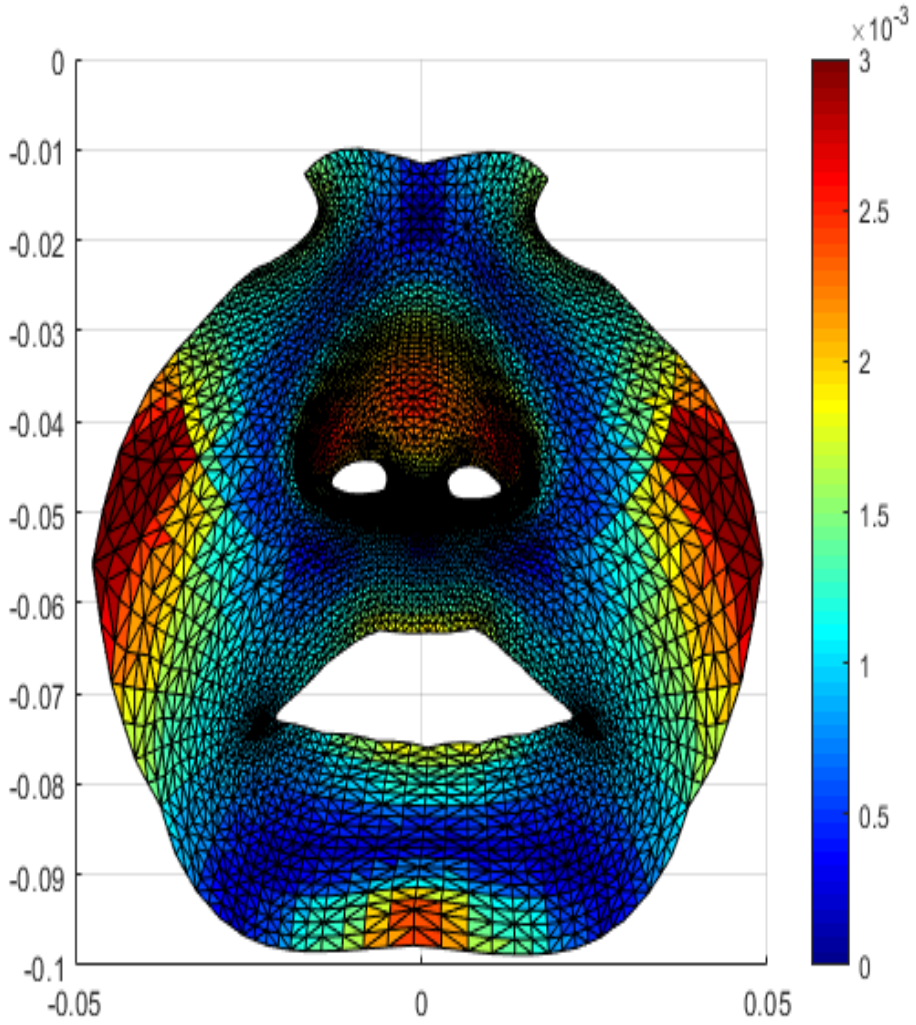

Figure 122: *FRAME 5* Color map of the <u>total face asymmetry</u> in frame 5 in the UCL patients during <u>grimace</u>. The red color represents increased asymmetry. The blue color represents decreased asymmetry. Areas in green represent zero distance between the original and mirrored meshes (no asymmetry).

Frame 5 (figure 122) showed increased asymmetry in the nasal tip and alar regions along with an increase in asymmetry in the upper and lower lip vermillion borders, indicating that even during rest the facial muscles hold a fair bit of tension which contributes to facial asymmetry.

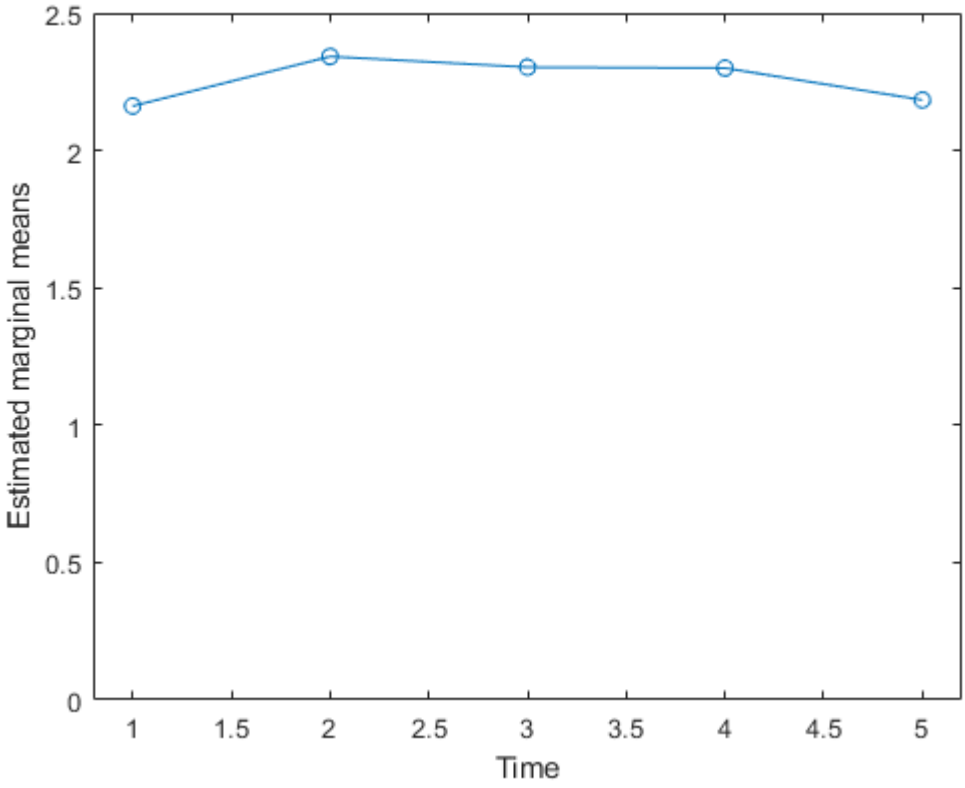

Figure 123: Asymmetry scores for 5 frames in total face during grimace

It was seen in the marginal means scores for asymmetry (Figure 123) that frame 2 showed highest asymmetry score followed by frames 3 and 4. No significant differences were seen between frames during grimace.

4.4.2. Asymmetry in the mediolateral (X direction) during Grimace

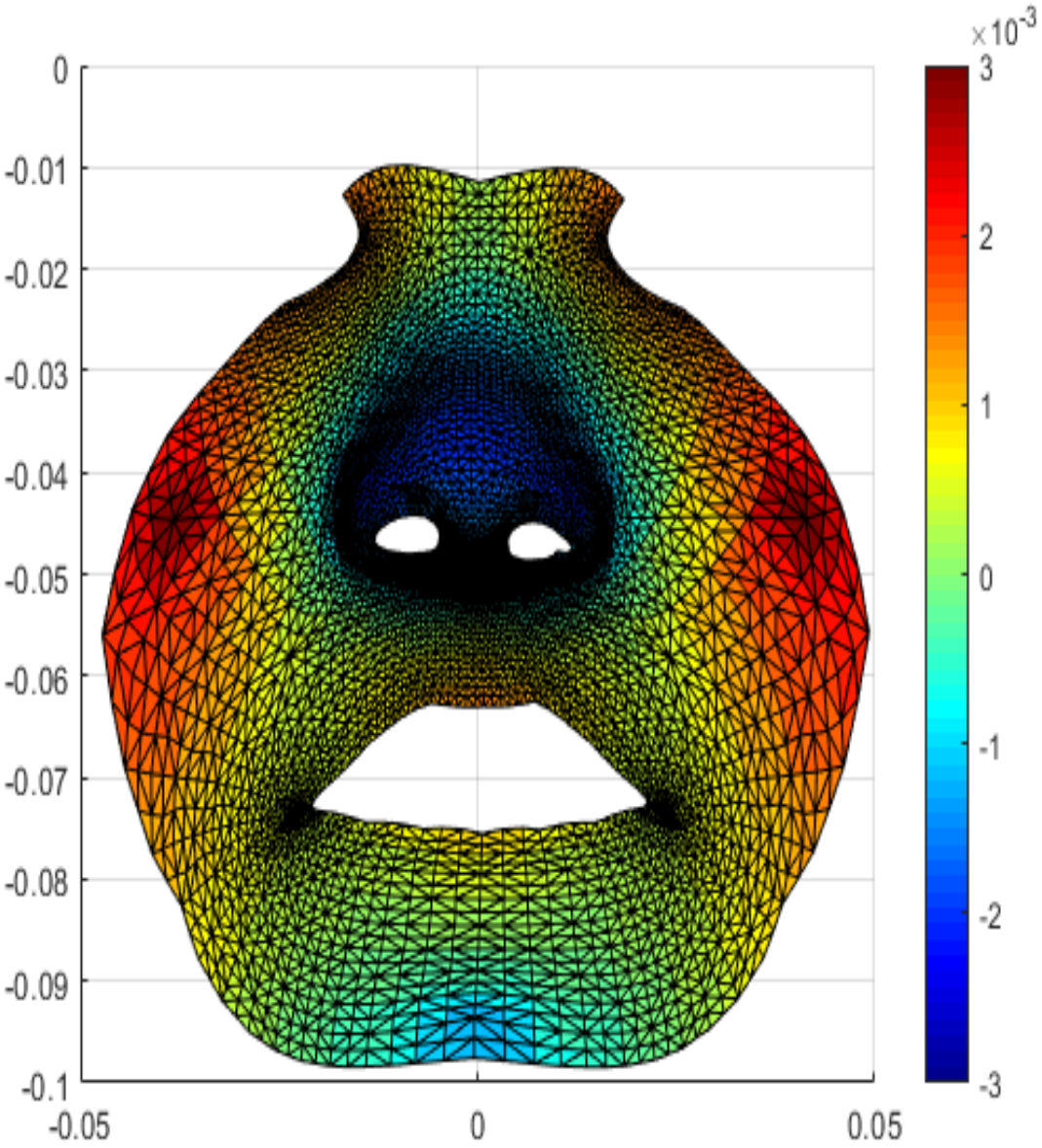

Figure 124: ***FRAME 1*** **Color map of the average asymmetry in the X direction in frame 1 in UCL patients during grimace. The red color represents asymmetry towards the right. The blue color represents asymmetry to the left side.**

The color map in figure 124 shows asymmetry distribution in frame 1 in the mediolateral direction. The nasal tip and ala and other parts of the nose are standing out with darkest shades of blue, indicative of nasal tip deviation to the left side or the non-cleft side. The vermillion border of the upper lip and philtral areas show patches of yellow and red indicative of increased deviation and asymmetry towards the right side or cleft side. The base of the columella also shows mild deviation to the left or non-cleft side seen as patches of yellow. The lower lip also shows patches of yellow and red indicative of deviation to the cleft right side.

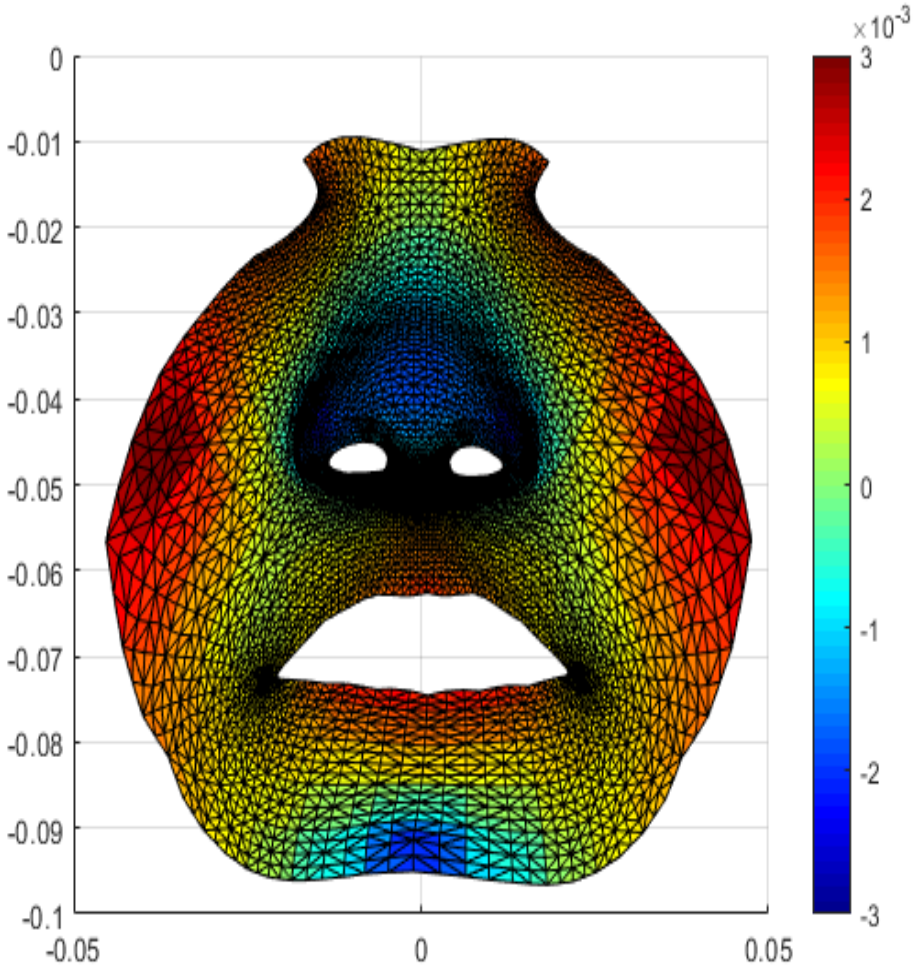

Figure 125: *FRAME 2* Color map of the average asymmetry in the X direction in frame 2 in UCL patients during grimace. The red color represents asymmetry towards the right. The blue color represents asymmetry to the left side.

The color map in figure 125 shows asymmetry distribution in frame 2 in the mediolateral direction. The nasal tip and ala and other parts of the nose were seen with darkest shades of blue, indicative of nasal tip deviation to the left side or the non-cleft side. The vermillion border of the upper lip and philtral areas show patches of darker yellow and darker red indicative of increased deviation and asymmetry (compared to frame 1) towards the right side or cleft side. Lower lip areas showed a deeper shade of red indicating increased deviation to the right side. Frame 2 is the frame where the beginning of movement in the facial muscles results in accentuation of asymmetry.

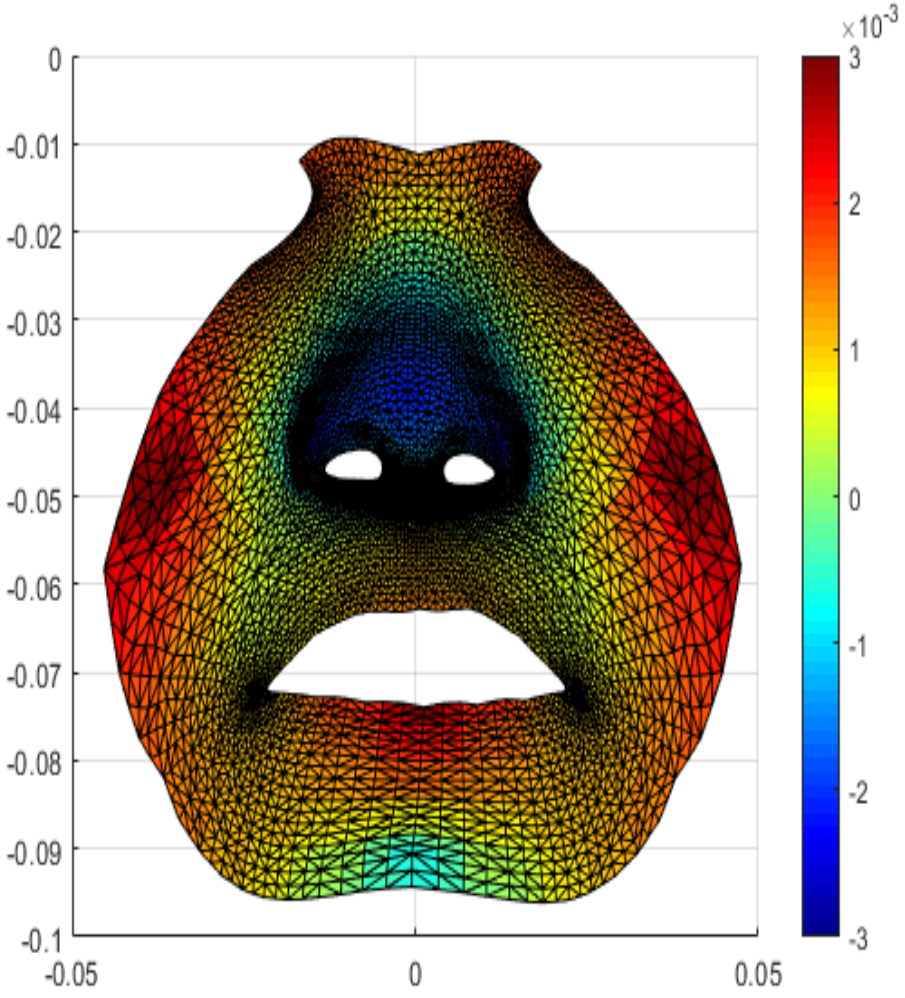

Figure 126: *FRAME 3* Color map of the average asymmetry in the X direction in frame 3 in UCL patients during grimace. The red color represents asymmetry towards the right. The blue color represents asymmetry to the left side.

Frame 3 (figure 126) showed increased asymmetry indicated by darker shades of red in the lower lip vermillion border. The upper lip showed slightly decreased asymmetry as compared to frame 2. Both upper and lower lip showed deviation to the right or cleft side. The nasal alar regions and nasal tip showed deviation to left non-cleft side and remained unchanged.

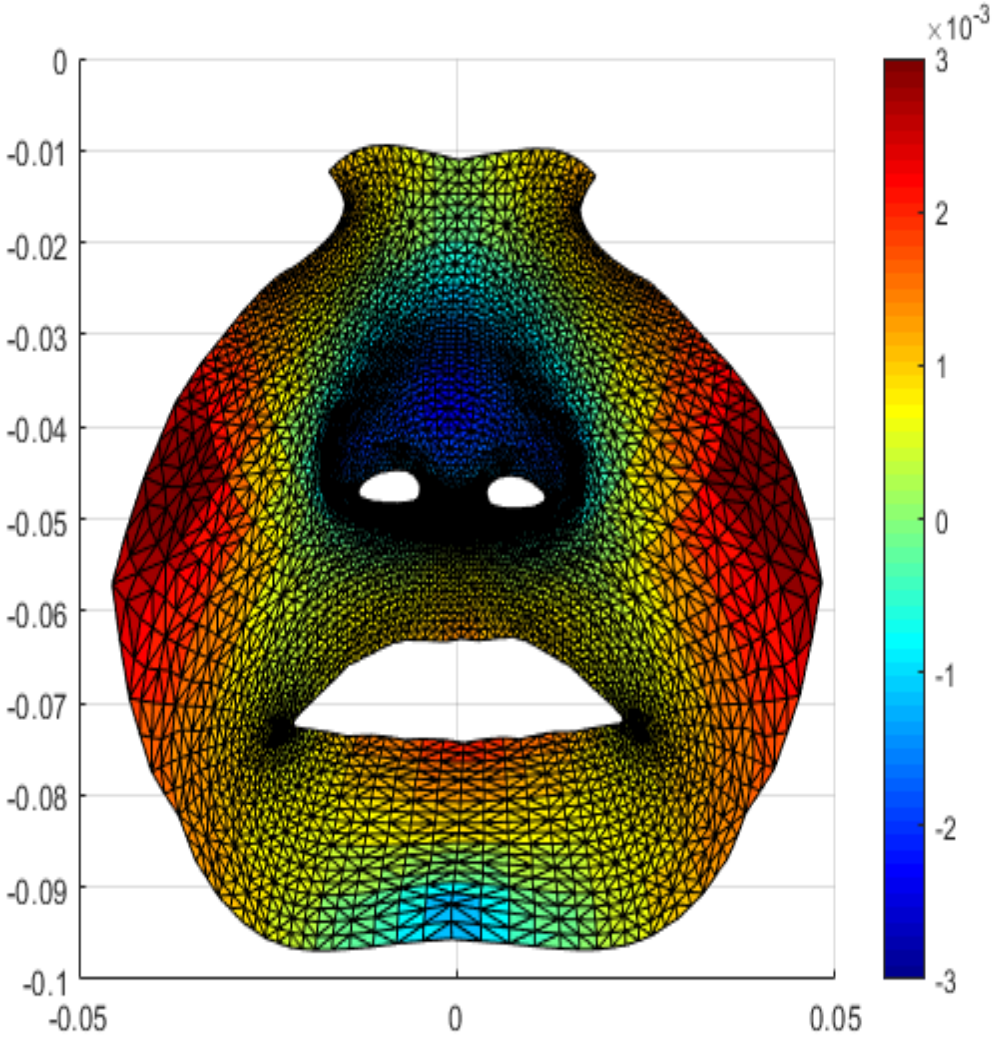

Figure 127: ***FRAME 4*** **Color map of the average asymmetry in the X direction in frame 4 in UCL patients during grimace. The red color represents asymmetry towards the right. The blue color represents asymmetry to the left side.**

Frame 4 (figure 127) was similar to frame 3 with slightly lower levels of deviation and asymmetry seen in the lower lip. The nasal regions remained unchanged.

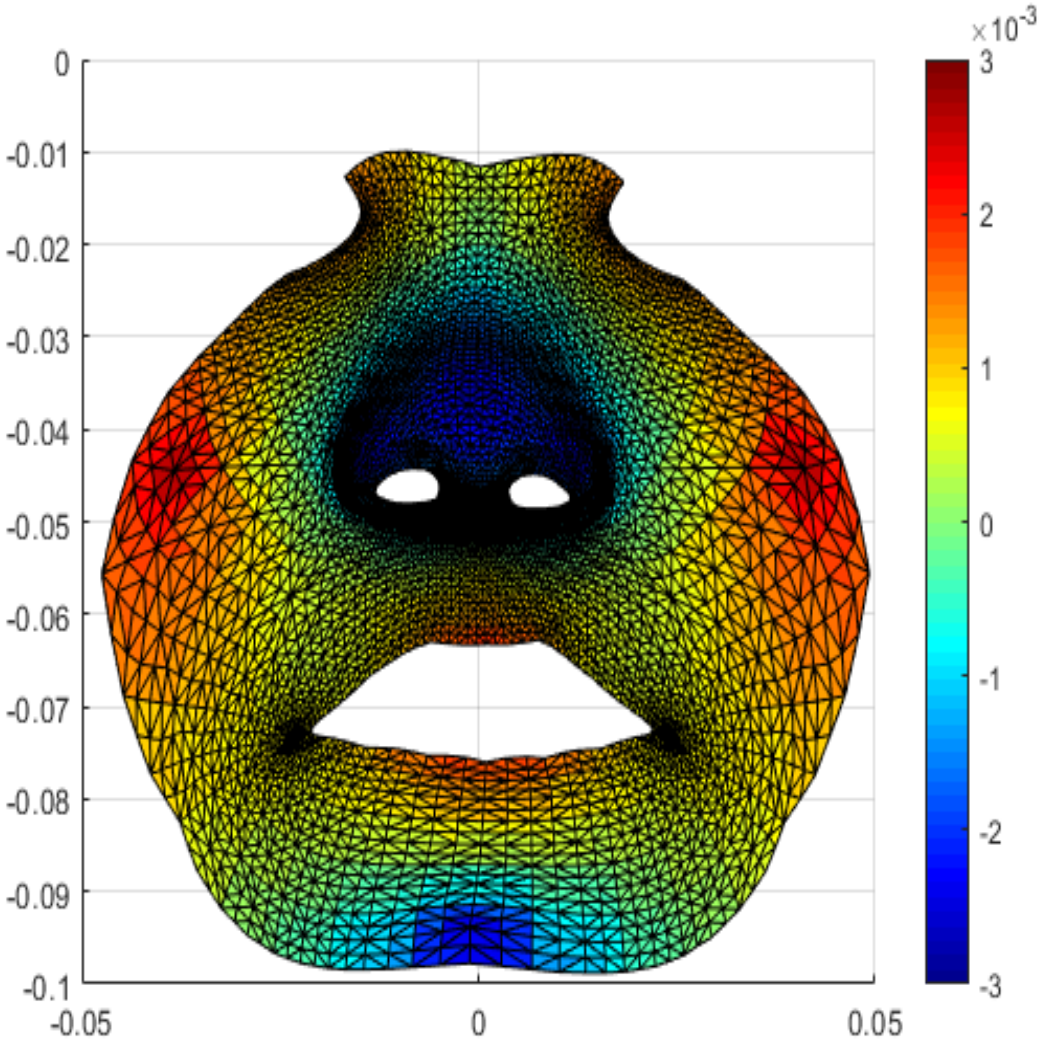

Figure 128: *FRAME 5* Color map of the average asymmetry in the X direction in frame 5 in UCL patients during grimace. The red color represents asymmetry towards the right. The blue color represents asymmetry to the left side.

Frame 5 (Figure 128) of the grimace showed similar but reduced asymmetry as compared to frame 4 with both upper and lower lips and the philtrum showing right side deviation and the nose and alar regions showing left or cleft side deviation.

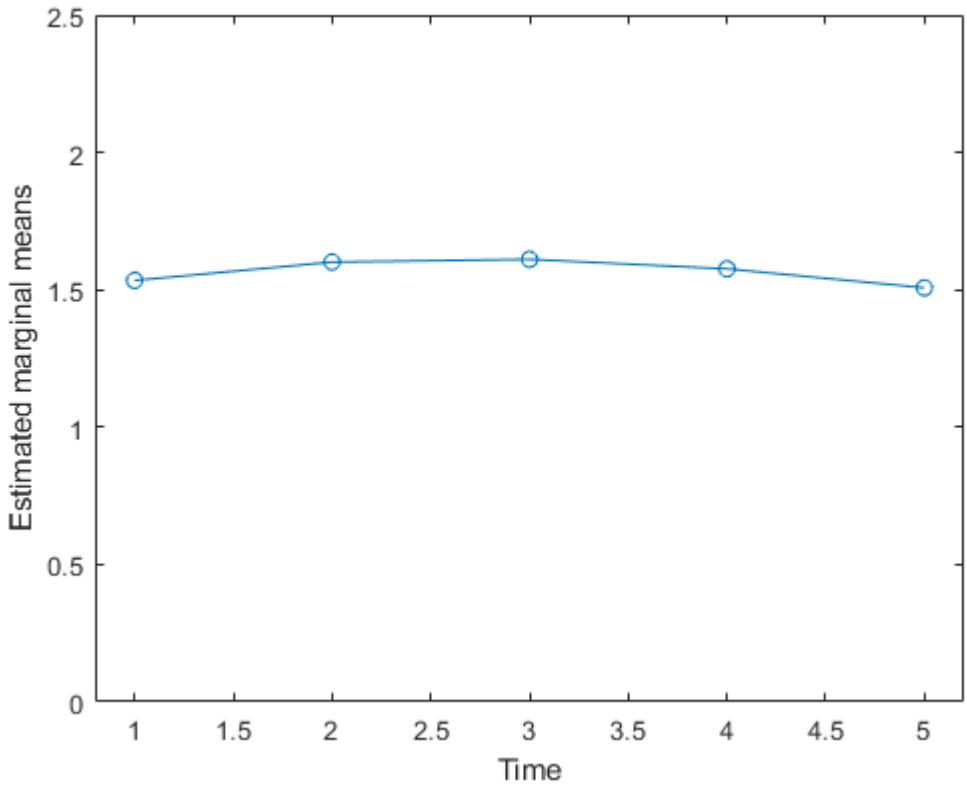

Figure 129: Asymmetry scores between the five frames during grimace in X direction

The graph for asymmetry scores (figure 129) showed highest asymmetry in frame 3. No significant difference was seen between frames in the UCL group in the X direction and changes seen were minimal due to asymmetry scores being small.

4.4.3. Asymmetry in the vertical (Y direction) during Grimace

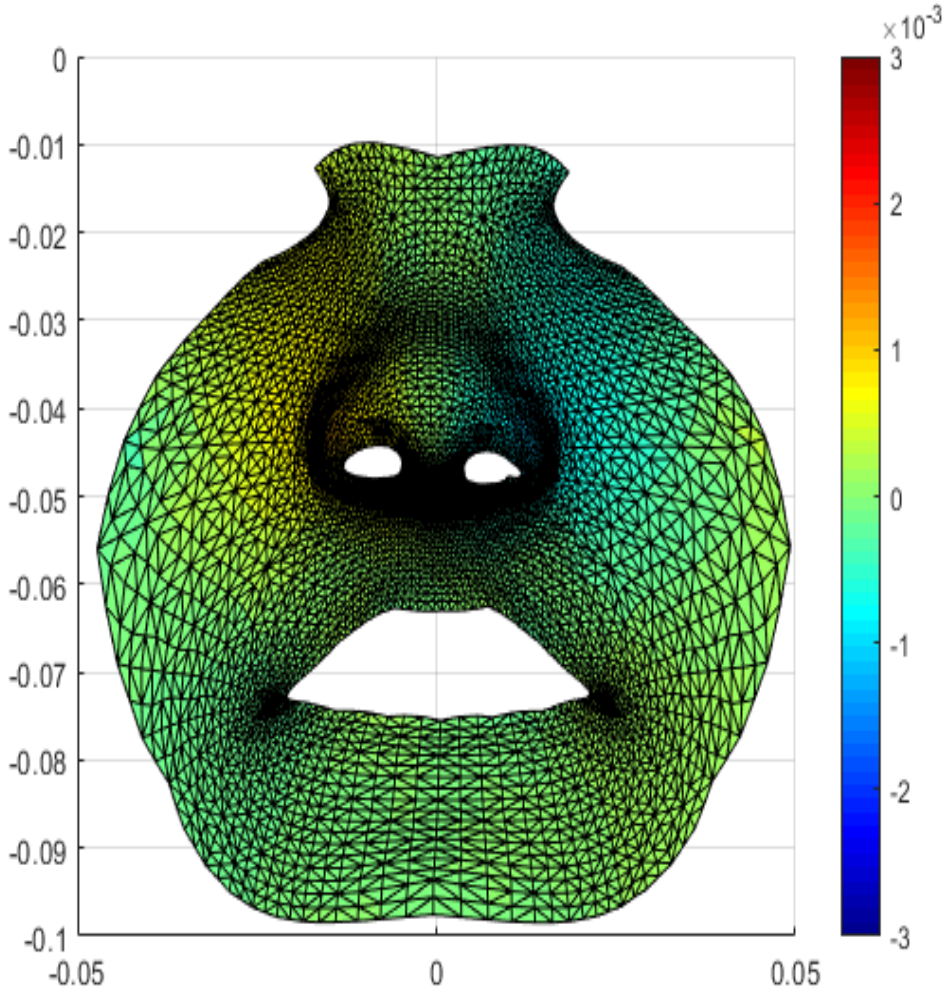

Figure 130: *FRAME 1* Color map of the asymmetry in the Y direction in frame 1 in UCL patients during grimace. The red color represents asymmetry in upward direction. The blue color represents asymmetry in a downward direction.

Figure 130 represents color map of asymmetry distribution in frame 1 in the vertical direction in UCL patients. Mostly areas of green and light green are seen in the nasolabial region indicative of minimal vertical changes occurring in frame 1. Frame 1 is the resting state of the face. The left ala of the nose shows slight blue patch indicating deviation in downward direction and the right ala shows mild yellowish red color indicating deviation in upwards direction.

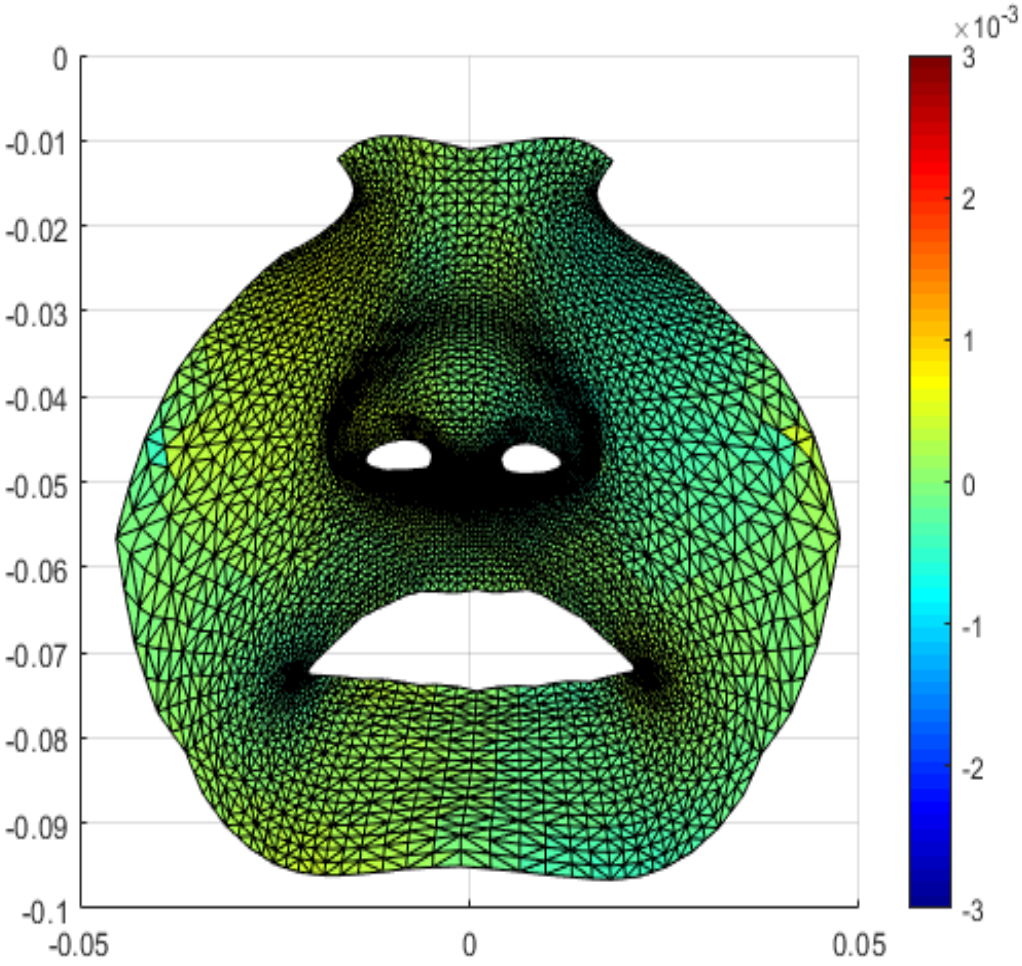

Figure 131: *FRAME 2* Color map of the asymmetry in the Y direction in frame 2 in UCL patients during grimace. The red color represents asymmetry in upward direction. The blue color represents asymmetry in a downward direction.

Frame 2 (figure 131) showed similar trend to frame 1 during the grimace. The left ala of the nose shows slight blue patch indicating deviation in downward direction and the right ala shows mild yellowish red color indicating deviation in upwards direction.

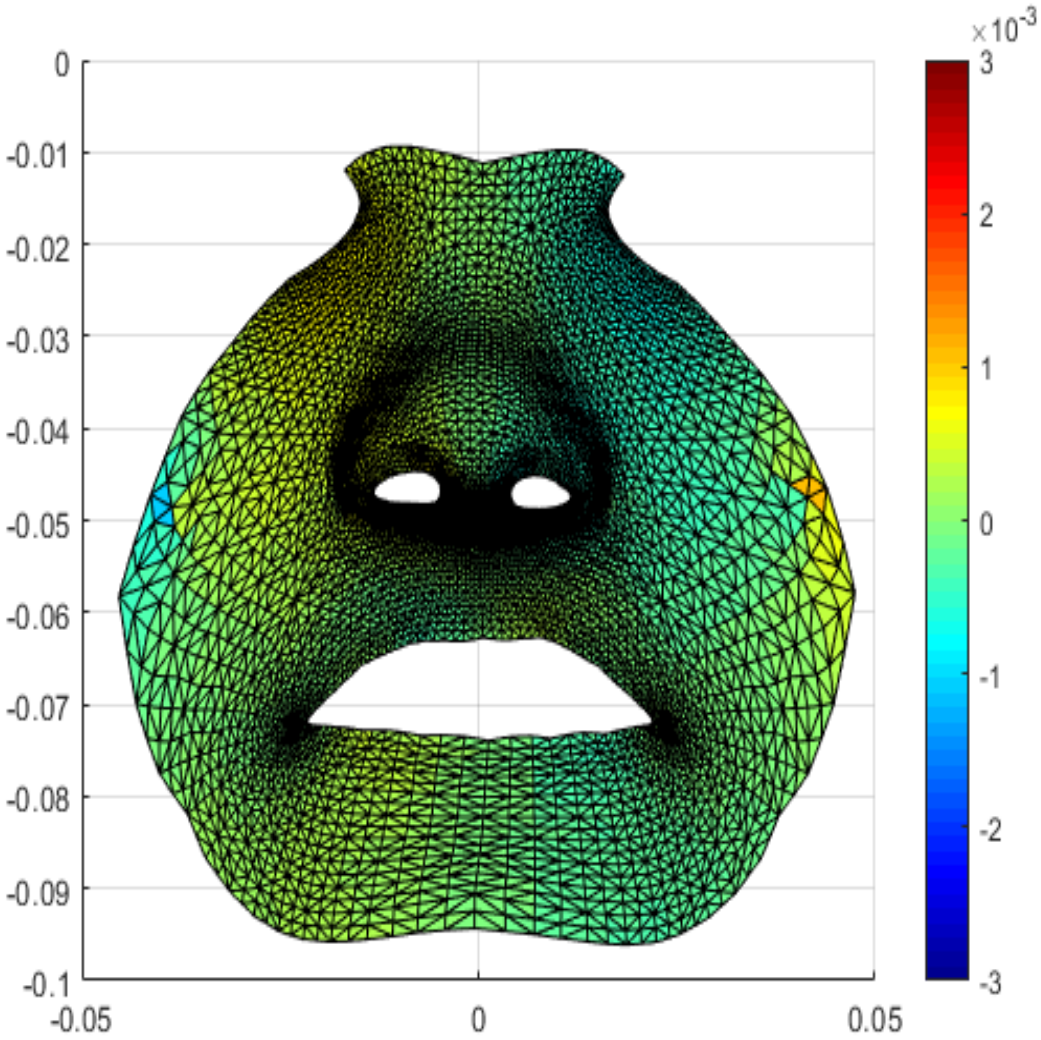

Figure 132: *FRAME 3* Color map of the asymmetry in the Y direction in frame 3 in UCL patients during grimace. The red color represents asymmetry in upward direction. The blue color represents asymmetry in a downward direction.

Frame 3 (figure 132) in the vertical direction shows minimum changes. The pattern of color distribution was same as frame 2 and 1 and showed minimum changes.

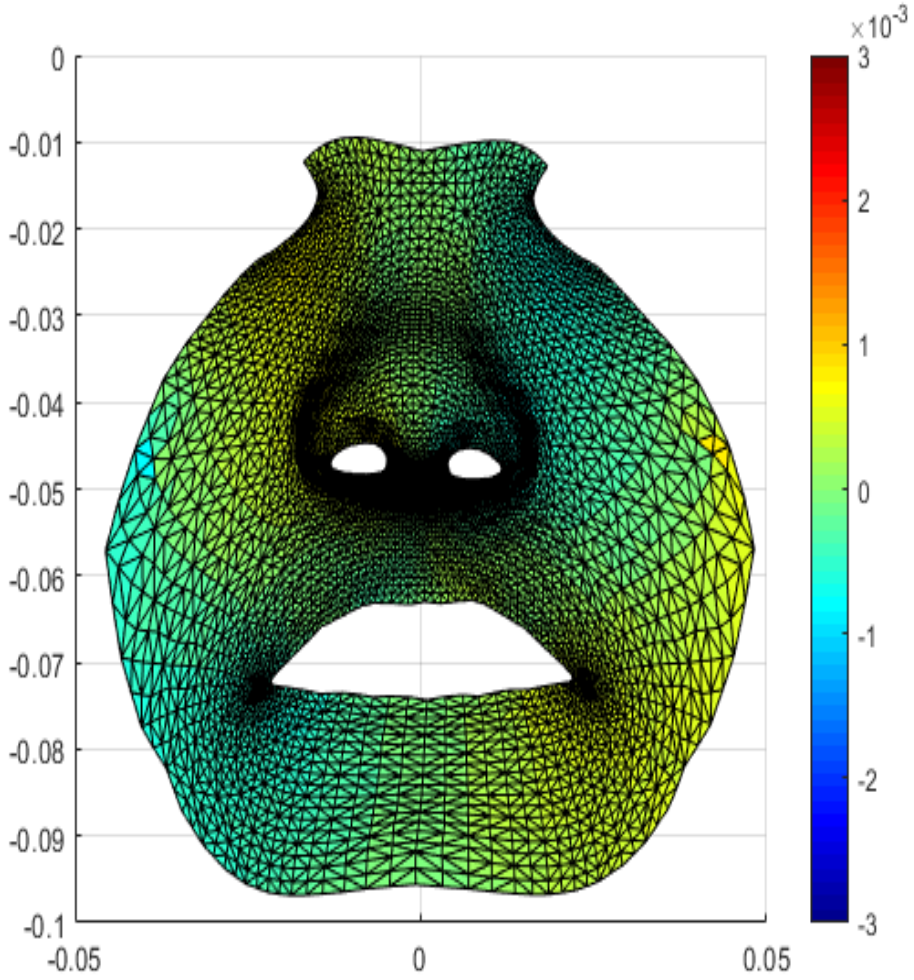

Figure 133: *FRAME 4* Color map of the asymmetry in the Y direction in frame 4 in UCL patients during grimace. The red color represents asymmetry in upward direction. The blue color represents asymmetry in a downward direction.

Frame 4 (figure 133) in the vertical direction showed no changes and minimum deviation and was seen similar to prior frames.

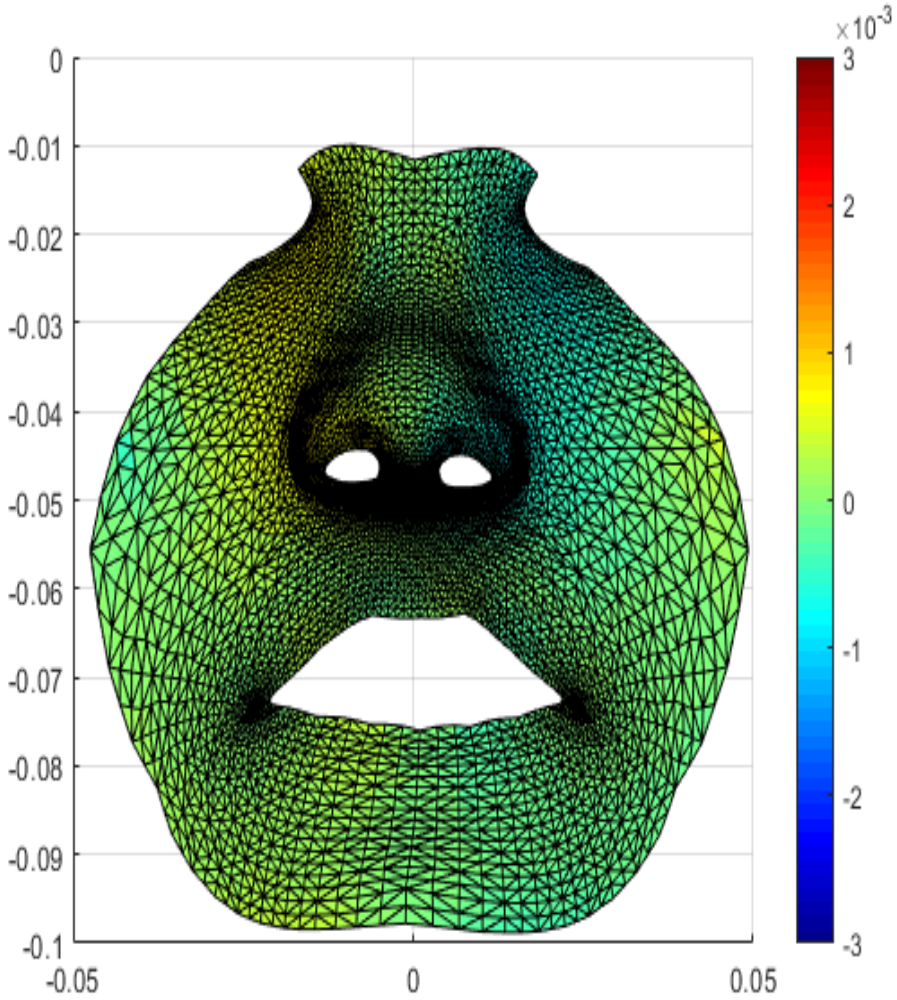

Figure 134: ***FRAME 5*** **Color map of the asymmetry in the Y direction in frame 5 in UCL patients during grimace. The red color represents asymmetry in upward direction. The blue color represents asymmetry in a downward direction.**

No changes were observed in frame 5 (figure 134) in the vertical direction.

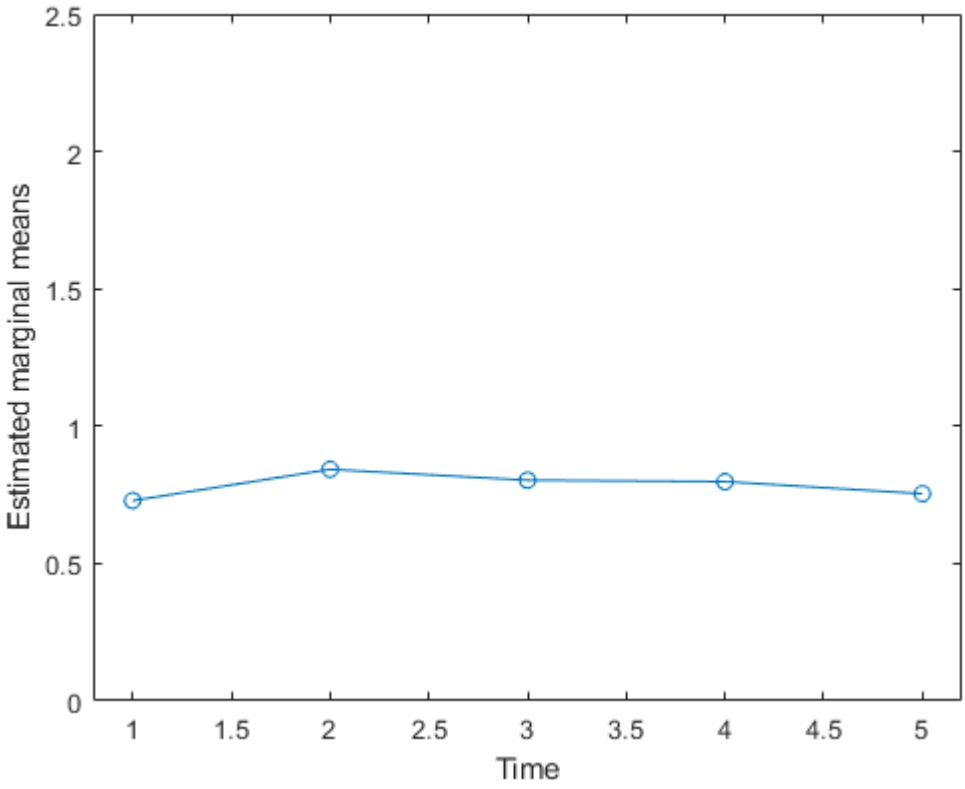

Figure 135: Asymmetry scores between 5 frames in the Y direction during grimace

In the marginal means asymmetry scores plot for grimace in the Y direction (figure 135), asymmetry was seen to be highest in frame 2. Significant differences existed in between all frames in vertical direction during grimace. Changes in asymmetry scores were minimum and indicated minimal vertical changes during grimace.

4.4.4. Asymmetry in antero-posterior (Z direction) during Grimace

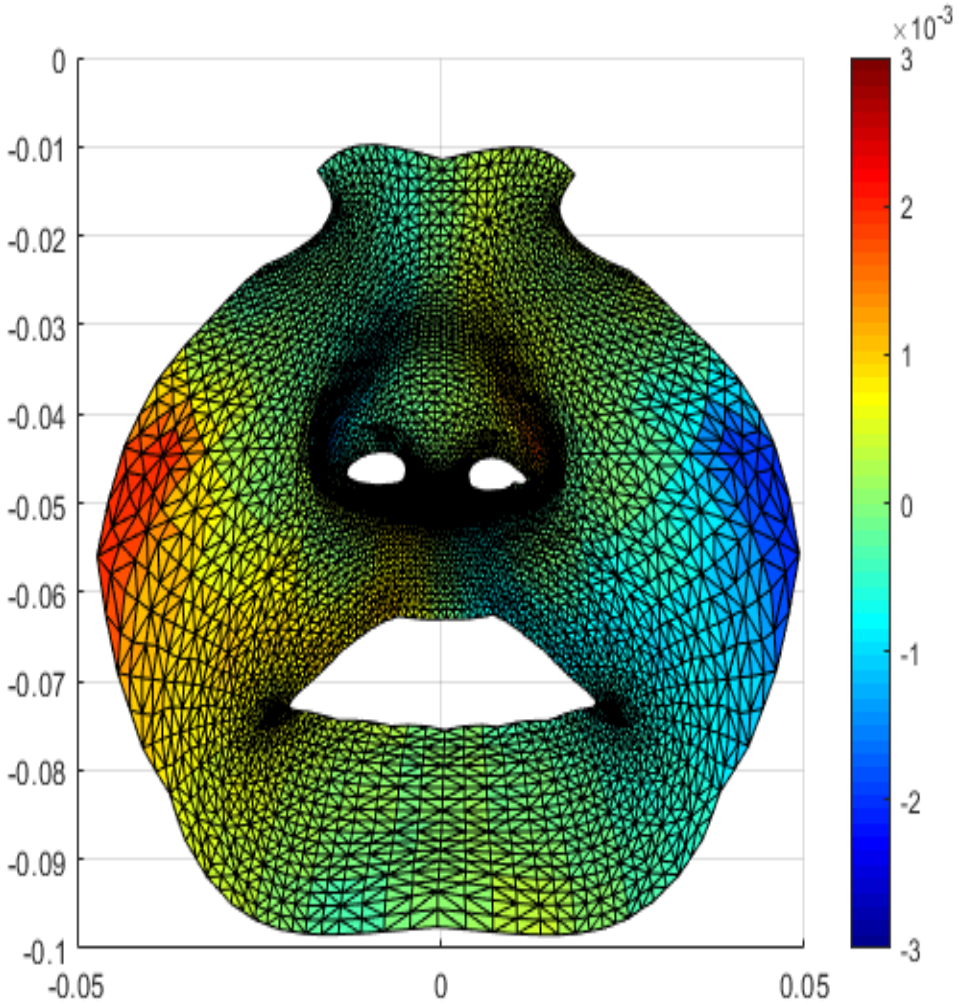

Figure 136: *Frame 1* Color map of the average asymmetry in the Z direction in frame 1 in UCL patients during grimace. The red color represents asymmetry in a forward (towards observer) direction. The blue color represents asymmetry in a backward direction (away from observer).

The left side vermillion border of the upper lip shows a patch of blue indicating posterior or backward deviation in frame 1 (figure 136). The right side of the vermillion border of the upper lip had a shade of yellow and light red which indicated anterior deviation towards the observer. The remaining areas showed minimal changes. The left ala of the nose showed deviation anteriorly whereas the right ala of the nose showed backward deviation.

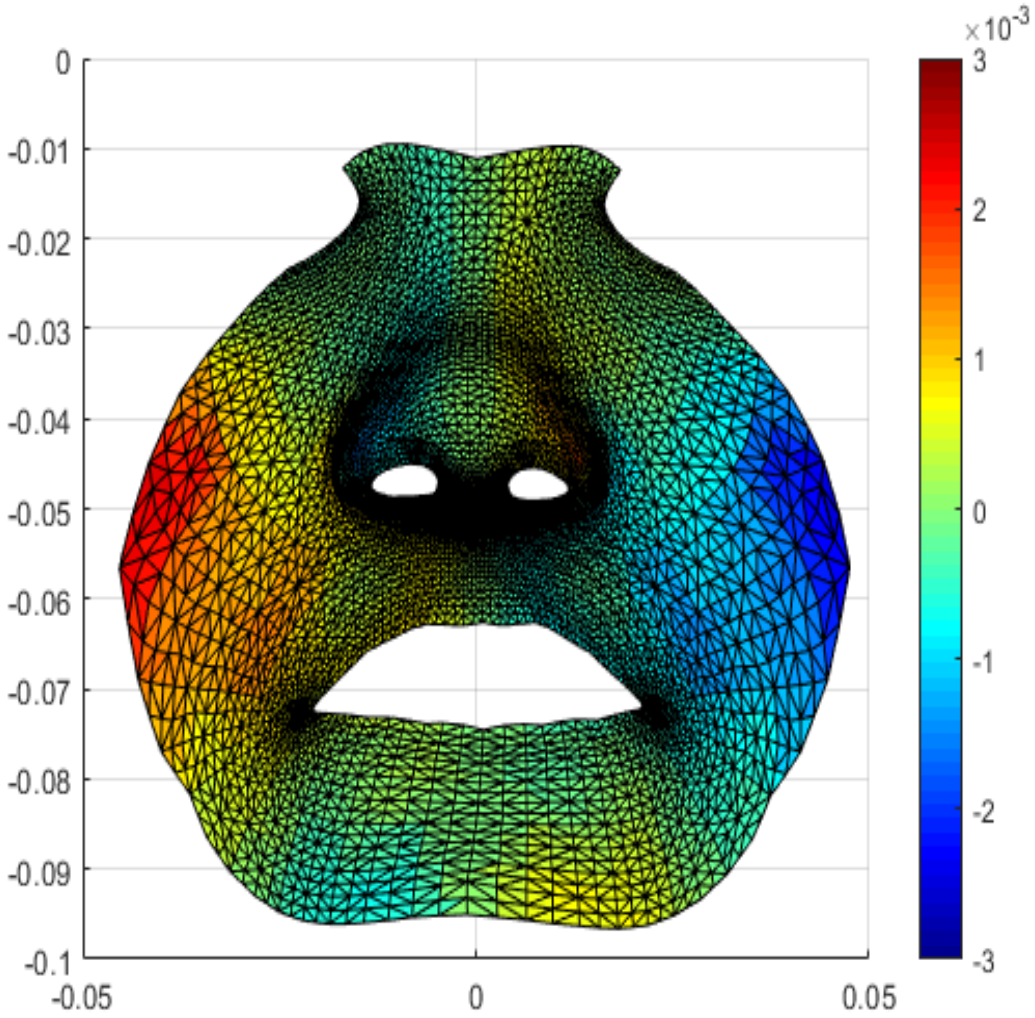

Figure 137: *Frame 2* Color map of the average asymmetry in the Z direction in frame 2 in UCL patients during grimace. The red color represents asymmetry in a forward (towards observer) direction. The blue color represents asymmetry in a backward direction (away from observer).

The left side vermillion border of the upper lip shows a patch of blue indicating posterior or backward deviation in frame 2 (Figure 137). The right side of the

vermillion border of the upper lip had a shade of yellow and light red which indicated anterior deviation towards the observer. The left nostril and surrounding alar regions showed slight yellowish coloration indicating mild anterior deviation as compared to the right sided nostril which showed backward deviation.

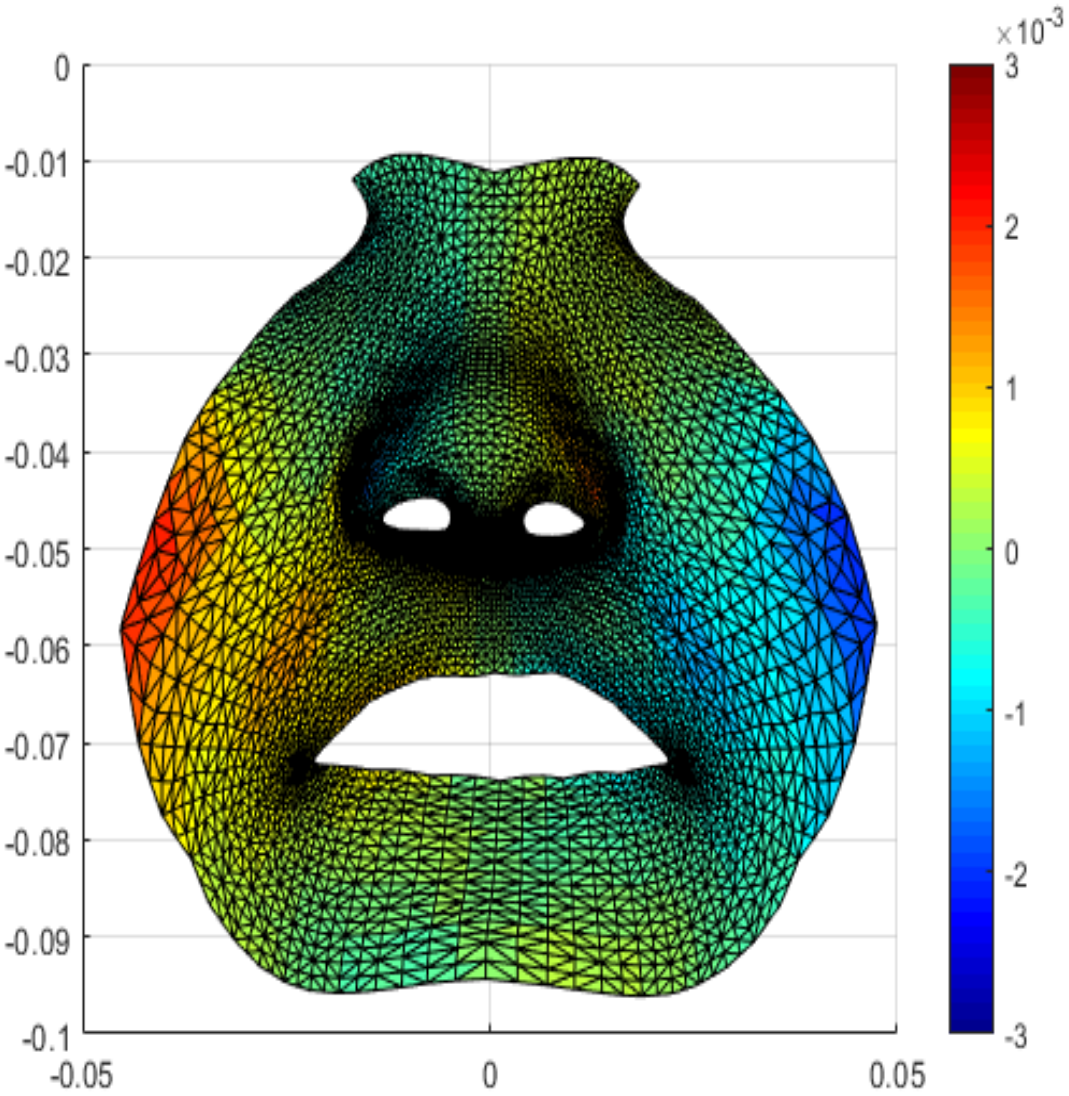

Figure 138: ***FRAME 3*** **Color map of the average asymmetry in the Z direction in frame 3 in UCL patients during grimace. The red color represents asymmetry in a forward (towards observer) direction. The blue color represents asymmetry in a backward direction (away from observer).**

Frame 3 (figure 138) of the grimace expression in the Z direction was similar to frame 2.

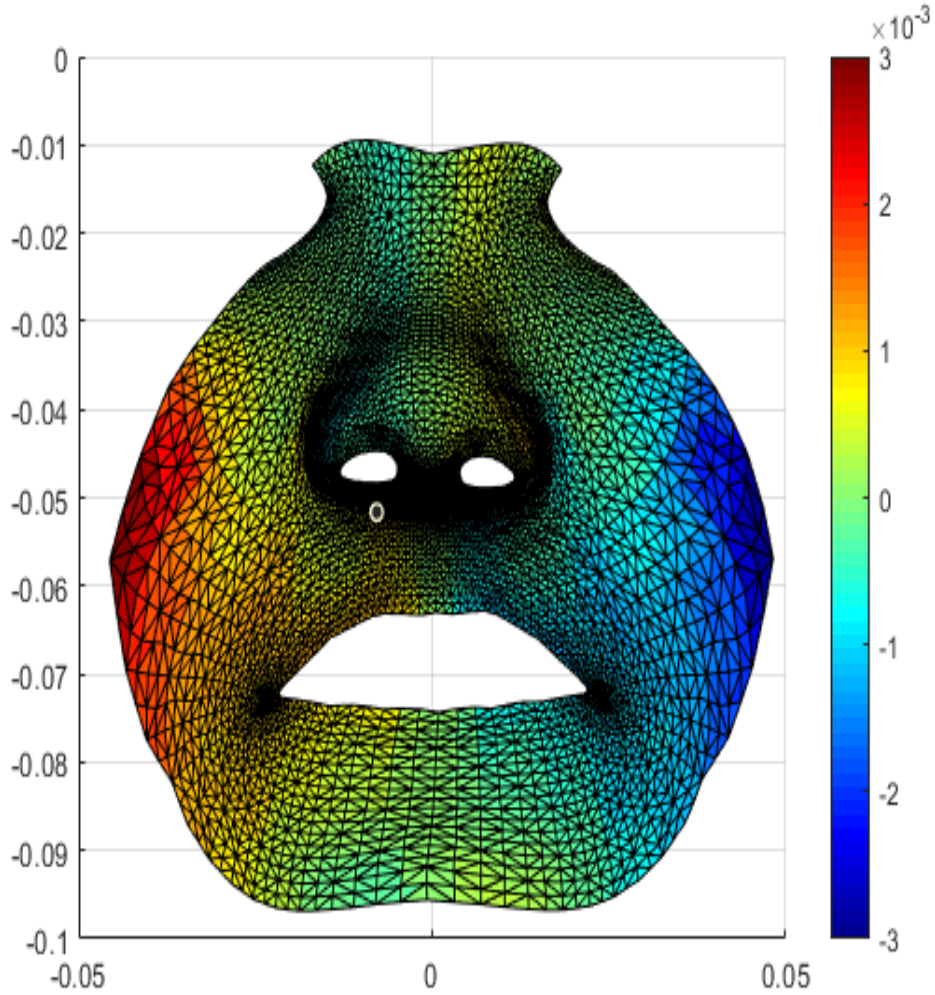

Figure 139: *FRAME 4* Color map of the average asymmetry in the Z direction in frame 4 in UCL patients during grimace. The red color represents asymmetry in a forward (towards observer) direction. The blue color represents asymmetry in a backward direction (away from observer).

In the Z direction, frame 4 (figure 139) showed higher asymmetry and greater deviation in the regions of the upper lip wherein the left upper lip showed deviation posteriorly and the right upper lip showed deviation anteriorly. The right ala region showed backward deviation and the left ala showed forward deviation.

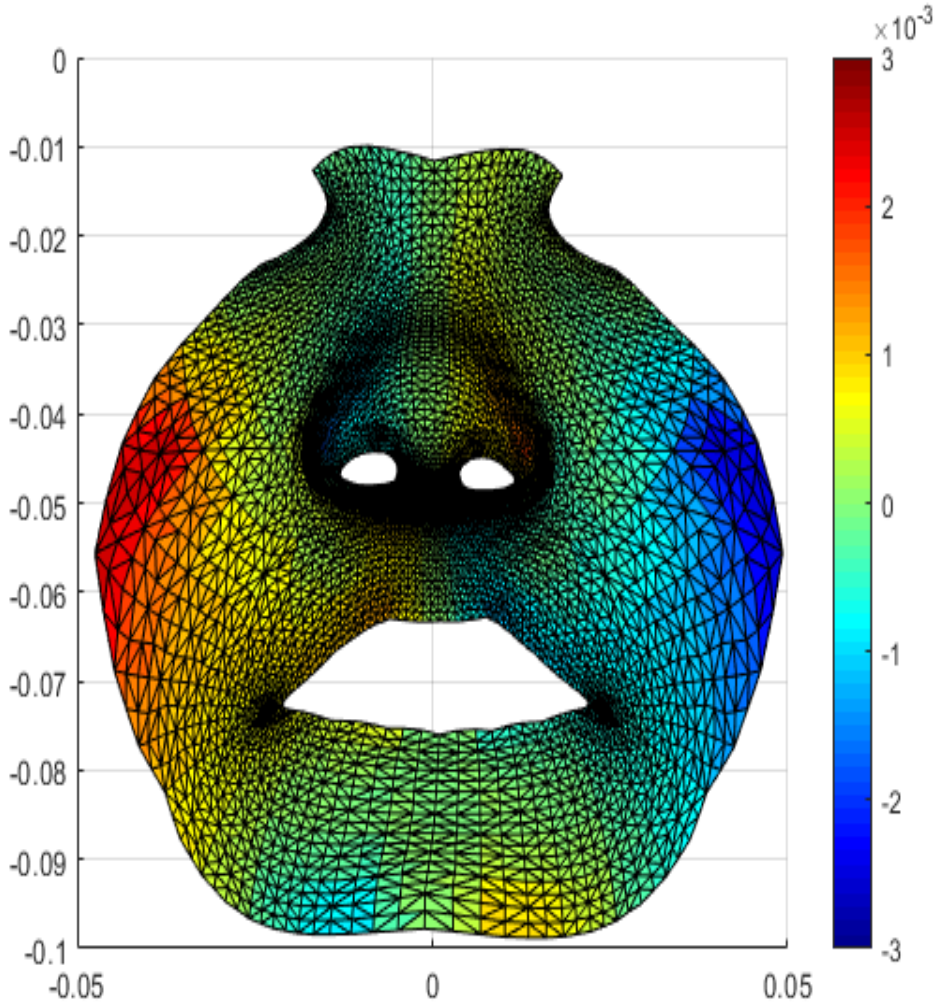

Figure 140: *FRAME 5* Color map of the average asymmetry in the Z direction in frame 5 in UCL patients during grimace. The red color represents asymmetry in a forward (towards observer) direction. The blue color represents asymmetry in a backward direction (away from observer).

Frame 5 (figure 140) or the resting frame remained unchanged as compared to frame 4 showing same directional trends as the prior frames.

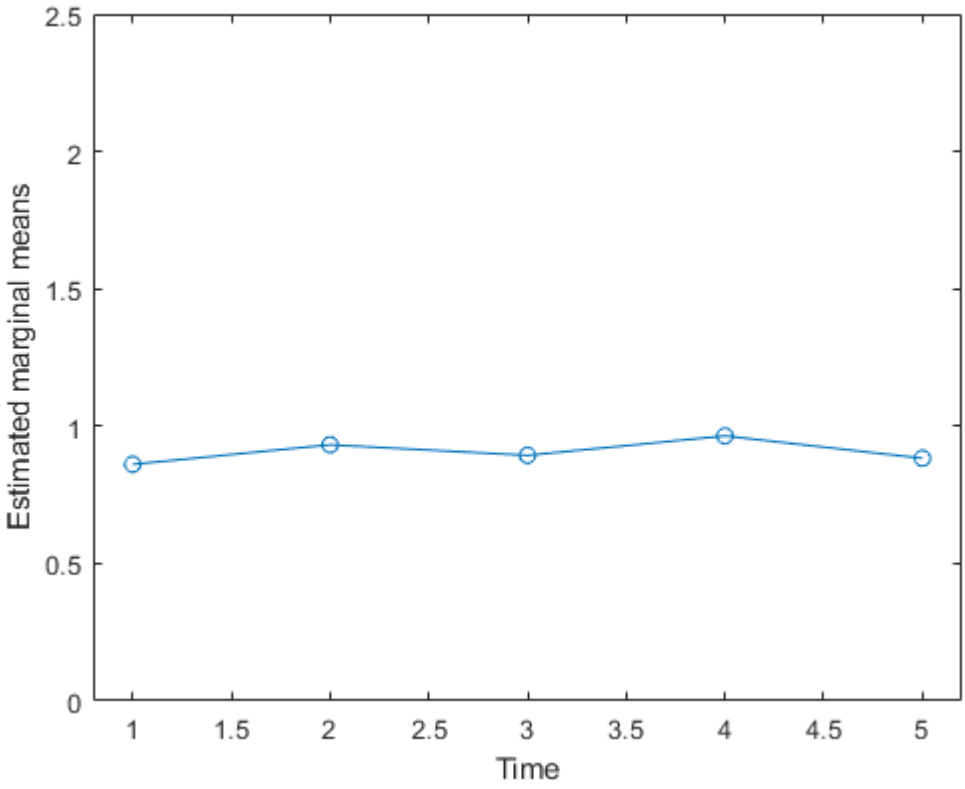

Figure 141: Asymmetry scores between 5 frames in Z direction during grimace

Asymmetry in the marginal means plot (Figure 141) was seen to be highest in frame 4 followed by frame 2 and 3 during grimace in the Z direction. Significant differences were seen in all the frames in the Z direction during grimace.

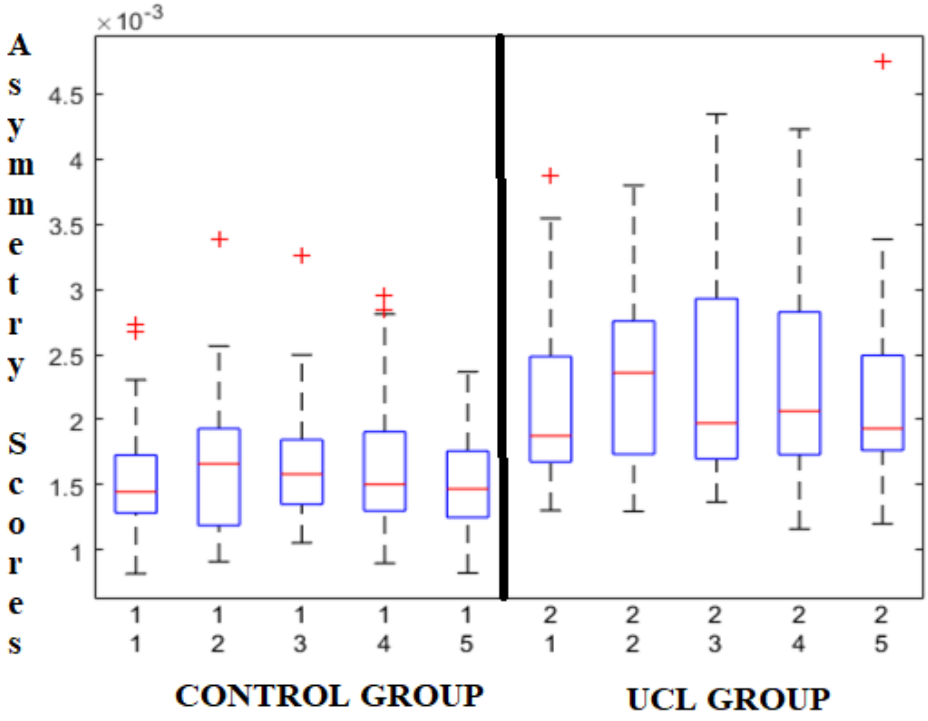

Figure 142: Box plot comparing asymmetry scores between controls (1-5 on the left) and the UCL group (1-5 on the right) during Grimace.

Significant differences were seen in all frames between the UCL group and the control group during performance of Grimace.

5 Interpretation of findings & Discussion

Contents

5.1. Interpretations of Findings

5.1.1. Cheek Puff

Performance of the cheek puff involves the activity of the peri-oral muscle group, starting with the contraction of the Orbicularis Oris muscle which assists in the initial embouchure and initial phase of puffing the cheek followed by the contraction of the Buccinator muscle, Risorius, Zygomaticus Major and Zygomaticus Minor muscles which helps the cheeks to puff maximally.

Maximum asymmetry in the total face was observed in frame 2 followed by frame 4 and frame 3.

As the first muscle group being involved in the cheek puff expression is the Pars Superficialis of the Orbicularis Oris muscle which tends to show abnormal insertion in cleft lip patients, this could be the reason why frame 2 tends to show higher asymmetry as compared to other frames during performance of the cheek puff. The incomplete surgical repair of the Orbicularis Oris muscle, the corresponding scarring and poor coordination of these muscles at the cleft site is the cause of the measured facial asymmetry in frame 2 of the cheek puff.

The peak expression frame (frame 3) also involves the contraction of the Buccinator muscle, Zygomaticus Major, the Zygomaticus Minor muscles and the Risorius muscles, which contribute to the cheeks puffing maximally. As these groups of muscles are untouched during the cleft lip repair surgery, asymmetry in frame 3 was seen to be comparatively less than in frame 2 and 4 in the UCL group. On the other hand, frame 3 in controls showed highest asymmetry among the five frames suggesting that facial expression at its peak accentuates facial asymmetry.

In frame 4, following the peak expression of cheek puff, high asymmetry scores could be attributed to the fact that the poorly approximated Orbicularis Oris muscles are in contraction to bring the upper and lower lips and cheeks back to the original resting position. Following maximum stretching of these muscles, instead of transitioning into a state of relaxation, muscles hold high tension/force prior to the final resting stage. Muscles may thus be acting in an increased energy expenditure environment occurring at the cost of reduced blood flow. This may be the cause of higher asymmetry scores in frame 4 as compared to frame 3 during performance of the cheek puff.

In the Y or vertical direction, the asymmetry scores were highest in frame 4 followed by frame 3 and frame 2. This is attributed to the fact that the superficial fibers of the Orbicularis Oris are attached to the vertically oriented Depressor Anguli Oris muscle. Asymmetry in the Z or anteroposterior direction was the only one that showed significant differences of asymmetry between the frames. This could be due to the fact that in the Z direction, both the horizontal and vertically oriented fibers of the Orbicularis Oris and Depressor Anguli Oris are involved in the anteroposterior movement of the nasolabial region. Since both superficial and deep fibers show anomalous origin and insertion in cleft patients and poor approximation post-surgery, this magnified the effects of asymmetry between frames, which accounted for the statistically significant differences between frames in the anteroposterior plane.

In the control group, the trend in asymmetry scores differed as frame 3 showed highest asymmetry followed by frame 2. Frame 3 involved the simultaneous contraction of major muscle groups including the Orbicularis Oris muscle, the Buccinator muscle, the Zygomaticus Major and Minor muscles and the Risorius muscle, this resulted in peak contraction of all these muscles accentuating facial asymmetry at frame 3. Frame 2 involves initial movement of the superficial fibers of the Orbicularis Oris muscle which are intact in the control group thus showing minimal asymmetry as compared to frame 3.

5.1.2. Lip Purse

The movement of lip purse involves the primary movement of the Orbicularis Oris muscle which is involved in the initial movement of the facial expression.

In UCL patients, the continuity of the Orbicularis Oris circumferentially is compromised, with abnormal insertions. In the lateral lip element, the upper part of cutaneous orbicularis (Pars Superficialis) inserts in the lateral aspect of the alar base and the nasolabial fold, while the lower part inserts into the nostril base periosteum of the pyriform rim. In the medial lip element, the cutaneous orbicularis (Pars Superficialis) inserts into the anterior nasal spine and columella. The deep Orbicularis muscle fibres (Pars Marginalis) is simply interrupted by the cleft deficiency and results in a diminished vermillion-cutaneous ridge at the cleft margin.

Reapproximating the Orbicularis muscle to circumferentially surround the opening of the oral cavity is important for long lasting cosmetic outcomes and lip and mouth function.

In the whole face average, as the first muscle group involved in the lip purse expression is the Pars Superficialis of the Orbicularis Oris muscle which tends to show abnormal insertion in cleft lip patients, this is the reason why frame 3 tends to show higher asymmetry as compared to other frames. Incomplete mobilization of the muscle bundles and the scar tissue around the surgical site is the reason why asymmetric movement and corresponding high asymmetry scores are seen in frame 3.

In the X direction during lip purse, Frame 3 shows highest asymmetry where the superficial and deep fibres of the Orbicularis Oris are at their maximum contraction. In the mediolateral direction, during performance of the lip purse the upper and lower fiber bundles of the superficial Orbicularis Oris are the only ones in a state of contraction. These muscles might show scarring following surgical intervention or poor approximation and reconstruction.

In the Y direction during lip purse, the asymmetry scores were highest in frame 2 followed by frame 4 and frame 3. The superficial fibres of the Orbicularis Oris muscle could have been poorly approximated and are undergoing movement to transition to a state of maximum contraction (frame 2). Frame 3 shows decreased asymmetry as compared to frame 2 due to involvement of the nasal bundles (Pars Marginalis) of the superficial Orbicularis Oris which show attachment to the Zygomaticus Major and Minor muscles (vertically oriented muscle fibres). The latter muscles are not surgically repositioned during cleft lip correction.

In the Z direction during lip purse, high asymmetry in frame 3 could be due to the fact that in the Z direction, both the fibers of the Orbicularis Oris muscle, the superficial Pars muscle bundles and the deep fibers respectively are involved in the anteroposterior movement. Since both superficial and deep fibers show anomalous origin and insertion in cleft patients and poor approximation post-surgery, this magnified the effects of asymmetry especially in frame 3, wherein movement is carried out by contraction of these sets of muscle fibers simultaneously.

The trend of asymmetry scores in the control group differed as frame 3 tended to show highest asymmetry during the lip purse. Frame 3 involves the maximum contraction of the superficial fibers of the Orbicularis Oris muscle thus suggesting that these fibres, even though intact in the controls contribute to asymmetry during lip purse.

5.1.3. Grimace

The perioral muscle groups can be considered as three distinct types based on their insertions. Group 1 includes the Buccinator muscles, Orbicularis Oris muscles, Levator Anguli Oris muscle, Depressor Anguli Oris muscle, Risorius muscle and Zygomaticus Major muscle, all of these inserting in the modiolus. Group 2 includes the Levator Labii Superioris and Levator Labii Superioris Alaeque Nasi muscles and the Zygomaticus Minor muscles, all of which insert into the upper lip and group 3 include the Depressor Labii Inferioris muscle, Mentalis and Platysma muscles, which insert in to the lower lip (Manjula et al., 2015).

In the X direction, during grimace, frame 3 shows highest asymmetry where the Depressor Anguli Oris and the Depressor Labii Inferioris are at their maximum contraction. The Depressor Anguli Oris has the largest muscle belly cross-sectional area and an intermediate muscle fibre size among the facial muscles. In the mediolateral direction, these are the only muscles in action during the grimace along with fibers of the Pars Peripheralis of the Orbicularis Oris, which are scarred following surgical intervention or poor approximation and reconstruction.

In the Y direction during grimace, frame 2 involves initial movements of the Depressor Anguli Oris and the Depressor Labii Inferioris to bring the lower lip downwards and laterally to carry out the grimace expression. The Platysma with its vertically oriented fibres becomes involved alongside these two muscle groups in frame 3. The platysma muscle is not surgically approximated in UCL patients, which correspondingly contributes to lower asymmetry scores as compared to frame 2.

In the Z direction during grimace, frame 4 shows highest asymmetry scores which could be because the Depressor Anguli Oris and the Depressor Labii Inferioris with its fibres intermingling with the Pars Peripheralis of the Orbicularis Oris are acting

to bring the lower lip to its original resting position. Frame 3 involves partly the action of the Platysma, an untouched muscle group that might explain lower asymmetry scores.

Significant differences in asymmetry between frames in the Y and Z directions could be attributed to the following reasons:

- In the Y direction, the primary muscles contributing to the vertical movements are the Depressor Anguli Oris whose fibers traverse vertically and obliquely. The reconstruction of the Orbicularis Oris muscles plays a major role in UCL repair. Failure to accurately reconstruct the muscular sling of the Orbicularis Oris muscle may result in abnormal insertion of the Depressor Anguli Oris, which in turn leads to asymmetric movements of the lower lip.

- In the Z direction, both the Depressor Anguli Oris and the Depressor Labii Inferioris act together to enable movement in the anteroposterior plane as their fibers run vertically and horizontally, respectively. The Depressor Labii Inferioris continues and becomes a part of the Pars Peripheralis of the upper Orbicularis Oris adjacent to the pars marginalis. The Depressor Labii Inferioris encircles the mouth; its contraction with the Orbicularis Oris muscle may make the lip protrude more by drawing the corner of the mouth medially. Both these muscles show an intimate relationship with what may be a poorly constructed and approximated Orbicularis Oris.

In the controls, it was seen that frame 2 showed highest asymmetry followed by frame 3 due to the movement and contraction of the Depressor Anguli Oris and the Depressor Labii Inferioris thus resulting in accentuated asymmetry as these muscles are entering a state of maximum contraction and contribute to the increased asymmetry when contracting together.

5.1.4. Maximum Smile

Performance of the maximum smile involves the activity of the peri-oral muscle group, starting with the contraction of the Levator muscles which assist in the movement of the upper lip towards the naso-labial fold followed by the contraction of the Risorius, Zygomaticus Major and Minor and the Buccinator which helps the lips to move further superiorly and laterally (Manjula et al., 2015). The first two muscles participating in the maximum smile are the Levator Labii Superiorus (LLS) and the Levator Labii Superiorus Alequae Nasi (LLSAN). Asymmetry during maximal smile was seen to be maximum in frame 4 or the mid-way frame between peak expression and the final resting position.

The restoration of the normal anatomy and the intricate relationships of the LLS and the LLSAN with the facial alar crease, the nasal vestibule and in particular, the Orbicularis Oris, is essential during primary repair of a cleft lip. The incomplete mobilization, rotation and the approximation of these group of muscles would contribute to asymmetry during maximum smile.

Additionally, scarring within and around the two muscles would compromise the range and speed of muscle movements and may contribute to the measured facial asymmetry in frame 3 or the peak expression in the UCL group. Maximum facial asymmetry was also observed in frame 3 in the non-cleft controls. Asymmetry at frame 3 (peak expression) of the maximum smile in the UCL and the control group indicates that facial expression accentuates facial asymmetry.

The peak smile frame also involves the contraction of the Zygomaticus Major, the Zygomaticus Minor and the Risorius muscles which help to raise the corner of the mouth producing the stretching of the lips during maximum smile. These groups

of muscles are untouched during surgical reconstruction of UCL and thus contribute to lesser asymmetry scores in frame 3.

In frame 4, following the peak expression of smile, high asymmetry scores (in the UCL group) could be because the Levator muscles that are poorly approximated during surgery, are acting to bring the upper lip back to its original resting position. High asymmetry scores are attributed to the "residual force enhancement theory" which states that the force of skeletal muscles immediately following eccentric or lengthening or stretching movement is higher than the force produced during isometric contraction (Campbell and Campbell, 2011). This seems to suggest that following contraction of muscles, instead of undergoing a relaxation phase, muscles hold high tension/force prior to the final resting stage or frame 4.

5.2. DISCUSSION

5.2.1. Facial Asymmetry

Presurgical care and surgical corrective procedures in the case of Unilateral Cleft Lip (UCL) patients is performed in the early years of life, between the ages of 3 months (cheilorhinoplasty) up to and until the age of 11 years. The fundamental goal of corrective surgery is to achieve a level of acceptable facial function and aesthetics (Al-Rudainy et al.,2018).

Facial aesthetics and asymmetry are crucial measurement references in understanding and evaluating the effectiveness of surgical intervention. Evaluation of facial asymmetry can be carried out both subjectively and objectively. Subjective interpretation of facial asymmetry has been conducted in various studies in the past (Asher McDade et al., 1991; Anastassov & Chipkov, 2003). However subjective evaluation of facial asymmetry is largely varied in its interpretation and therefore does not provide an accurate representation of facial asymmetry. The evaluation of facial beauty and symmetry by the human brain is a rapid cognitive process. However, this is far from accurate and is subject to various factors that affect subjective interpretation of symmetry. There have been a few studies in the past to correlate the subjective interpretation of attractiveness to the objective facial characteristics (Chatrath et al., 2007; Sim et al., 2000; Ueda et al., 2020). In a study by Kurkcuoglu et al. (2016) differences were found between subjective interpretation and objective measurement of facial symmetry. Chatrath et al. (2007) found that 38% of faces were seen as asymmetrical in subjective analysis as opposed to over 90% of faces seen as asymmetrical in objective measurements.

Thus far, many decisions on lip revision surgery following primary correction have been based on a subjective interpretation of a static nasolabial region by the surgeon (Trotman et al., 2010). These qualitative interpretations and assessments of facial asymmetry have demonstrated poor agreement between the surgeons and the assessors (Trotman et al., 2007). Therefore, the need arose to assess facial asymmetry in a more objective fashion. The objective assessment of residual facial asymmetry following primary corrective surgery is important in order to establish guidance and a surgical protocol on lip revision surgery in cleft lip and/or palate patients.

There have been a few studies carried out previously, which have objectively assessed facial asymmetry. Some of these studies focused on the post-operative assessment of facial asymmetry (Nkeke et al.,2006; Bilswatch,2006; Stauber et al., 2008; Meyer-Marcotty et al.,2011; Bughaigis et al.,2014; Bell et al., 2014; Kuijpers et al.,2015; Hallac et al.,2017) while a few others looked at assessing and comparing facial asymmetry pre-operatively and post-operatively (Tse at al., 2015; Al-Rudainy et al., 2018; Al-Rudainy et al., 2019; Hood et al., 2003; Schwenzer-Zimmerer et al.,2008).

In studies assessing asymmetry as pre and post-operative, there was no control group included and therefore no normative values of facial asymmetry to compare scores of the cleft group with. Inclusion of a control group to a study adds more quality to the data as there is a normal index of symmetry to compare scores of facial dysmorphology. Our study included a control group to compare asymmetry scores with the UCL population, which enabled a comprehensive assessment of how asymmetry due to specific muscle activity differs between the two groups.

5.2.2. The Objective evaluation of facial asymmetry

The evaluation of facial asymmetry can be carried out in an objective manner using 2D, 3D and 4D imaging modalities.

2D imaging modalities include methods such as orthopantomogram, photographic measurements, radiographic measurements, cephalograms and video-based measurements (Nagy & Mommaerts, 2007; Berlin et al.,2014; Coghlan,1987). 2D imaging techniques are unable to assess the depth of objects. 2D methods of measuring facial asymmetry therefore present with limitations such as the inability to assess the complete three-dimensional topography of the face. Three dimensional objects when displayed in two dimensions lose out on the depth feature and are presented as vertical and horizontal displacements only. There are a few other limitations associated with 2D methods of imaging and measurement such as landmark identification accuracy as the operator is required to accurately identify and manually place landmarks on the 2D image.

In order to overcome the limitations associated with 2D imaging and assessment of asymmetry, 3D methods of imaging were carried out which included laser scans and stereophotogrammetry. There is a paucity of 3D and 4D studies in relation to cleft lip and palate associated facial asymmetry in children.

3D methods of imaging have been considered advantageous and effective, more so in terms of accuracy of representation of objects as compared to 2D imaging methods as 3D systems can evaluate the complexity of the three-dimensional facial surface. These methods also offered the added advantages of being reliable, showing faster time of capture, being non-invasive and non-radiological (except CT scans and MRIs). Children exhibit a characteristic of decreased compliance especially when it comes to having an image taken requiring sitting for prolonged periods of time and over multiple sessions. Stereophotogrammetry offers the advantages of shorter imaging times of up to 1 to 3 seconds which therefore overcomes the limitation of prolonged imaging times as seen in systems such as laser scans. Techniques of assessment of facial asymmetry can be grouped into direct and indirect anthropometry. Direct anthropometry includes measurements obtained directly on the face of individuals using devices such as Sliding callipers and Vernier callipers. A significant drawback of direct methods of measurements is the lack of a digital co-ordinate record of individuals and therefore the inherent inability of direct anthropometric studies to repeatedly extract facial information

and data. There is also the drawback of the measuring instrument pressing and compressing the soft tissue and skin, and therefore affecting results and taking increased time.

Due to the major limitations posed by direct anthropometric studies, these were largely replaced by indirect methods of measurement. 3D stereophotogrammetry has been used in cleft lip and palate studies in adults (Ras et al., 1994a; Ras et al.,1994b; Othman et al., 2014), and cleft lip and palate studies in children (Duffy et al.,2000; Bughaigis et al.,2010; Van Loon et al., 2010; Zreakat et al., 2012; Bughaigis et al., 2014a; Bell et al., 2014; Bughaigis et al., 2014b; Djordevic et al.,

2014; Morioka et al., 2015; Hermann et al.,2016; Weinberg et al., 2009; Hoefert et al., 2010; Ayoub et al., 2011).

5.2.3. The decision between a landmark-based and surface-based analysis

Some studies used specific landmarks on the facial surface as part of their method to assess facial asymmetry by determining differences in landmarks as a displacement between the cleft and non-cleft sides and compared these displacements with controls. (Schwenzer-Zimmerer et al., 2008; Stauber et al.,2008; Ayoub et al.,2011). The disadvantage of using landmarks-based analysis is that these methods, although they show anatomical correspondence, are unable to comprehensively analyze the entire facial surface.

In order to overcome the limitations of landmarks-based analysis, surface-based analysis and measurements were carried out (Meyer-Marcotty et al., 2010; Djordevic et al., 2014; Nakamura et al., 2010) which used surface-based algorithms (ICP) and color maps of the facial surface to identify changes following corrective surgery. Although these surface-based methods of measuring facial asymmetry provide a global representation of the facial surface by using several thousand points on the face, algorithms like the ICP suffer from the distinct lack of anatomical correspondence between points. In a study comparing landmark and

surface-based methods (Kau et al., 2011), it was seen that when measuring pre and post-op asymmetry, surface-based measurements were more effective and account for more accurate quantification of changes following treatment.

3D studies show limitations which include the inability to assess the complexity of facial movement and facial expressions. These methods are unable to measure the magnitude and speed of asymmetry in the moving face. The human face is rarely static in normal day to day functioning and exhibits motion during activities such as speech, mastication and facial expressions. It is for this reason that 4D studies such as this one is more effective in analyzing facial asymmetry.

The 4D system (Di4D) used in this study for the imaging of the cleft patients and non-cleft volunteers was based on passive stereophotogrammetry and overcame the drawbacks of poor assessing abilities due to lack of complexity analysed in 2D systems as well as the static nature of images in 3D systems. The limitation of using specific landmarks was also overcome in our study as dense correspondence analysis using conformation of a generic mesh enabled the entire facial surface to be included for assessment of asymmetry. The analysis method is described in the section below and is the novelty of this study.

5.2.4. Dense Correspondence Analysis

As discussed above, surface-based measurements usually involve superimposing the original 3D image with its mirror image using algorithms which employ the entire surface such as ICP (iterative closest point) and correspondingly calculate the disparity between the surfaces being compared. These disparities are presented as a color map indicating in varying colors the amount of disparity present in specific areas. Although surface-based analysis possesses several advantages and is superior in terms of effectiveness of quantification, these methods also demonstrate limitations in their techniques of assessment. For example, the drawback of surface-based analysis using the ICP, as discussed above is the lack of any anatomical basis as the point clouds are created without following any anatomical considerations. Landmark based measurements offer the

advantage of being anatomically accurate but on the other hand lack comprehensiveness of measurement as these cannot cover the entire facial surface and instead only focus on specific landmark points.

This study offers a novel method to assess asymmetry of facial movement by overcoming the limitations of the landmarks-based method (lack of comprehensiveness) and the lack of anatomical correspondence in the ICP. This study utilises a facial mesh or face mask which consists of thousands of pre-indexed mathematical points or vertices. This face mesh can undergo elastic deformation or be "conformed" to take the shape of an individual's facial morphology. This method of dense correspondence offers the advantages of anatomical correspondence (due to each individual vertice point considered a landmark) as well as comprehensiveness of measurement (as it resembles the individual's facial surface and therefore takes into account the entire facial topography during analysis).

This method of dense correspondence between the facial images was used in a study on assessing facial asymmetry in UCLP patients (Al-Rudainy et al., 2018). This study utilized the facial mesh which underwent the conformation process and assessed and compared facial asymmetry pre and post-operatively using images at resting position (Static/3D).

Our study used the novelty of the comprehensiveness and the anatomic basis of the facial mesh and also assessed asymmetry in 4D by analyzing facial asymmetry along the axis of time (the fourth dimension). In other words, our study assessed the moving face during the performance of facial expressions. The assessment of facial asymmetry in Unilateral cleft lip patients using a dynamic approach or 4D imaging, whilst using the facial mesh for analysis has not been considered before. This provides the unique advantage of understanding asymmetry at certain crucial time points during the performance of the facial expression (rest, peak of expression, midway between rest and peak, midway between rest and end of expression and the final resting position). Each time point during the performance

of the facial expression has specific muscle groups undergoing contraction (depending on the facial movement at that time) and therefore, the analysis of asymmetry during these time points can help surgeons ascertain which group of muscles are compromised in activity and contribute to the asymmetry of movement.

Furthermore, similar to the 3D study by Al-Rudainy et al (2018), directionality of asymmetry was also considered. Asymmetry was measured in the mediolateral, vertical and antero-posterior directions thus providing an insight in to residual asymmetry in different directions. The directional basis of asymmetry measurement also accounts for the improper approximation of certain muscles oriented in that particular direction. It therefore provides the surgeon a quantitative measure of improvement of facial asymmetry following surgery in the global (total face), x, y and z directions thus highlighting areas of higher residual asymmetry which may require secondary surgery in order to improve facial form and function.

5.2.5. The Generic Mesh and the Conformation Process

Facial asymmetry presents an important feature in that, it is difficult to measure objectively especially since the human face is a three-dimensional structure and involving the whole facial surface based on anatomical correspondence would be considered the gold standard of asymmetry measurement. In order to overcome the limitations associated with the landmarks based and certain other surface-based techniques, dense correspondence analysis has been used in a few studies (Al-Anezi et al., 2016; Al-Mukhtar et al., 2017; Al Rudainy et al.,2018; Ekrami et al., 2018; Claes et al., 2011; Al Rudainy et al., 2019). These studies use an anthropometric face mask which consists of a number of vertices. Claes et al (2011) used a face mask consisting of points which were non-paired and non-symmetrical meaning that the number of points on one half of the face mask did not equal the points on the other half of the face mask. This could pose a problem when it comes to mirroring or creating a mirror image. Ekrami et al. (2018) used the mask developed by Claes as a reference point to prepare a symmetrised face mask with paired points (7160 paired points). The mapping algorithm used by

Ekrami et al. (2018) included the ICP wherein the template mesh was iteratively superimposed on the target face and asymmetry was calculated by superimposing the original and mirrored face masks by calculating the least squared distance between them. The study by Ekrami et al. (2018) was conducted to measure asymmetry using normal healthy faces in 3D. Asymmetry in both the Claes and Ekrami studies was assessed using color maps.

Al-Mukhtar et al. (2017) used a generic face mesh to test the accuracy of its conformation process. This generic face mask was a symmetrical face mask with a fixed number of pre-indexed points or vertices. Using the conformation process, the generic mesh can be wrapped around any facial image using landmarks as anchor points and the remaining vertices are elastically deformed to resemble the surface topography of the face. The accuracy of the conformation process was assessed in two studies (Al-Mukhtar et al.,2017; Cheung et al., 2016), one assessing the conformation process while focussing on the middle of the face and the second study did the same while focussing on the peripheries of the face.

Mao et al. (2006) conducted a study to construct dense correspondence using a face mesh which elastically deforms to analyze 3D facial morphology.

Al-Rudainy et al. (2018) assessed facial asymmetry before and after surgery in infants with UCLP. This study utilized a generic face mask, which was conformed, its mirror image obtained and the disparity between the original and mirror was a measure of asymmetry and displayed in the form of a color map. In the 2019 study, a longitudinal evaluation of improvement in facial asymmetry was carried out by assessing asymmetry before surgery, after surgery and at a 4-year follow up. Both her studies utilized 3D methods as these were carried out on static or still images of infants.

This generic face mask is used in our study, using a dynamic or four-dimensional approach to measure the asymmetry of facial expressions. No study has been conducted which assesses facial asymmetry in the moving face (4D) in Cleft

patients using dense correspondence analysis and use of the face mask, thereby utilizing the entire facial surface for analysis.

5.2.6. The Asymmetry of Facial Expressions

A study on the measurement of the asymmetry of facial expressions was conducted by Hallac et al. (2017), which used 4D imaging to record facial movement during the performance of two facial expressions- the smile and the lip purse. The imaging system used in that study was the Di4D imaging system- the system used in our study.

Asymmetry was analyzed using 13 specific facial landmarks. Asymmetry was assessed both geometrically and by using landmark speed and displacement from its position in the resting frame to the position of the landmark in subsequent frames. The difference in displacement of landmarks on each side of the face was considered as the measure of asymmetry. Maximum landmark displacement was seen during smiling and puckering at the oral commissures in the UCLP patients. It was seen in the Hallac et al. (2017) study (similar to our findings) that the cleft group had higher asymmetry than the control group during lip purse, but the differences were not significant during smiling. On the contrary our study showed that during maximum smile, asymmetry scores were significantly different between UCL patients and controls for all frames and in all directions. This could be attributed to the limitations in the study by Hallac et al. (2017) as only 13 landmarks were used and therefore could not account for the entire facial surface. It was further limited by a small sample size of 12 UCLP patients and 11 controls and the fact that only two facial expressions were recorded. Our 4D study included a sample size of 25 UCL patients and 75 controls. Furthermore, for each patient and control, 4 facial expressions were analyzed and recorded. Each 4D sequence correspondingly had 5 frames that were analyzed for asymmetry scores, thus generating a large sample size to work with.

Al-Rudainy et al. (2018) in a 3D study to assess asymmetry in UCLP patients aged 3-4 months of age, using the generic mesh as a tool to measure asymmetry,

identified the nasolabial region to be highly asymmetrical. Their study assessed facial asymmetry in static form and did not analyze facial movements or the muscles involved during facial expressions. Results were therefore limited to only the static nature of asymmetry in contrast to the dynamic form of asymmetry which is essential to be evaluated as this considers the complexities of facial movements associated with specific muscle groups that are surgically re-approximated. This provides a more in-depth approach to assessing symmetry as surgeons are then able to identify specific muscle groups contributing to the increased asymmetry in that specific frame of facial expression. Some 3D studies showed asymmetry being predominant near the nasal landmarks (Seidenstricker-Kink et al., 2008) while others showed that asymmetry was pronounced near the upper lip (Hood et al., 2003).

Both of these studies assessed asymmetry using landmarks which do not give a true representation of the facial surface and this could be the reason for contradictory results. Ayoub et al. (2011) showed that nasal base differences were not significant between UCL and controls (this was a 3D study using specific landmarks for analysis as well). Kuijpers et al. (2015) in their study showed that there was no significant difference between UCL and controls. The UCL subsample was however small (9 UCL patients) and therefore might have affected accuracy of findings. UCLP and controls on the other hand, showed significant differences in all areas. Their study was done on static images of the face and therefore did not assess the movements of the face and the activity of certain affected facial muscles during movement. Their study did however assess the facial surface by generating surface-based differences in the form of a color map between the original and the mirrored 3D surface and used absolute mean of the distance between the two facial surfaces as a record of facial asymmetry. While utilizing the entire facial surface was a strength, as was the case with our study, this study was limited in its findings as it utilized static images. The study by Kuijpers et al. (2015) showed the UCLP and UCLA group to have maximum asymmetry in the nose region followed by the lip and chin.

Our study measured facial asymmetry scores both in the whole face (globally) as well as directionally in the x, y and z directional planes. The nasolabial region was the region of interest as previous research on asymmetry in Cleft Lip and Palate in children indicated maximum asymmetry was seen in the nasolabial region pre-operatively (Bughaigis et al.,2014; Al-Rudainy et al., 2018). Post-op residual asymmetry was identified in the nasal tip, philtrum and cupids bow (Al-Rudainy et al.,2018; Garrahy et al., 2002) and in the mid face and lower face (Kuijpers et al.,2015).

Our study's findings in relation to the significant difference in asymmetry between UCL patients and controls were similar to a few other studies carried out previously (Meyer-Marcotty et al., 2010; Hood et al., 2003; Bell et al., 2014; Bughaigis et al., 2014). The study by Bell et al. (2014) assessed facial asymmetry in three-dimensions at rest and during maximum smile (static images) in UCL and UCLP patients and compared these to a control group. Their study used a combination of anatomical landmarks and facial curves to assess facial asymmetry. Asymmetry in their study was seen to be significantly higher in both the cleft groups compared to the controls. The upper lip and nasal region showed highest asymmetry in the cleft groups. This was a 3D study and only assessed asymmetry on a static face. Furthermore, it used limited landmarks to assess facial symmetry rather than the entire facial surface which was analysed in our study.

Contrary to our findings, a study by Kyrkanides (1996) showed that the difference in asymmetry between the UCL group and the controls decreased with time, and as compared to the controls, the asymmetry in CLP patients, post-operatively, in the nasal and upper lip regions was less than expected. These findings may be associated with the technique of asymmetry analysis conducted in this study. Kyrkanides et al. (1996) used 2D photographs on which they utilized six landmarks. The 2D visualization of an object like the human face, which is three-dimensional, greatly reduces the accuracy of the findings as the third dimension of depth is not assessed in 2D imaging. Wu et al. (2016) and Schwenzer-Zimmerer et al. (2008) also found that lip length in UCLP patients, post-operatively, approached closer

to the values of lip lengths in the normal population. These studies were also landmarks-based analysis and were limited in comprehensiveness during measurements as only specific landmarks were taken into consideration.

Our study assessed asymmetry scores for four facial expressions- maximum smile, cheek puff, lip purse and grimace. Each of these expressions were analyzed quantitatively with respect to the total face (global face), x, y and z directions. No other 4D study carried out previously on Cleft Lip patients utilizes the entire facial surface during facial movement and assesses the directionality of asymmetry as seen in this study. The novelty of our study lies in the fact that the entire facial surface was assessed by using a "conformed" generic mesh. By assessing facial asymmetry during individual frames during the facial movement, it was possible to highlight the specific muscle groups participating in the facial movement which contributed to increased asymmetry. Highlighting specific surgically corrected musculature of the face and assessing how this contributed to increased facial asymmetry helps surgeons understand how asymmetry can further be reduced in secondary corrective procedures.

In the maximum smile facial expression, the total face asymmetry in the UCL group according to the box plots obtained were seen to be highest in frame 4 (mid-way between peak expression and the final resting state) followed by frame 3 or the peak expression. The reason behind frame 3 being lesser in terms of asymmetry scores as compared to frame 4 is the involvement of the Risorius muscle, the Zygomaticus Major and the Zygomaticus Minor muscles which are relatively untouched during correction surgery in UCL patients. Frame 4 involves the different heads of the Levator Labii Superioris, which show scarring and possibly poor approximation, working to bring the upper lip back to its resting state. Maximum asymmetry was seen in the nasal regions and the upper lip vermillion similar to findings by Hallac et al. (2017) which showed asymmetry to be highest in the upper lip lateral to the cupids bow and the philtral ridge. Our findings in the maximum smile were also similar to findings by Bell et al. (2014) where it was seen that maximum smile increased asymmetry in the nasal rim and vermillion border of upper lip in the UCL, UCLP and control group. In the study by

Trotman et al. (2000), restricted movement during smiling was observed in the nasolabial fold in the cleft patients as compared to controls. Upper lip movement was also seen to be restricted during smiling in the cleft group as compared to control group in the study by Trotman et al. (2007). Similar to our study minimum changes in vertical direction were seen in the study by Trotman et al. (2007) and Al-Rudainy et al. (2018).

In the cheek puff expression, the total face asymmetry in the UCL group was seen to be highest in regions around the nasal tip and alar regions of the nose. Asymmetry was seen to be highest in frame 2 (the frame midway between rest and peak of the expression). This anatomical area consisting of the nasal tip, upper vermillion border and the alar regions were consistent in showing higher asymmetry than the other regions in all four facial expressions. High facial asymmetry in frame 2 could be attributed to the poorly approximated Orbicularis Oris muscle fibres contracting to bring about peak expression - puffing the cheeks. Frame 3 involves additional activity of the Buccinator, the Zygomaticus group of muscles and the Risorius muscle which are relatively untouched during surgery and thus show lesser asymmetry as compared to frame 2.

In the lip purse expression, total facial asymmetry was seen to be highest in the areas of the alar regions of the nose, upper lip vermillion border and the philtrum. Asymmetry was at its highest in frame 3 which was the peak expression. Frame 3 showed increased asymmetry as the Orbicularis Oris muscle fibres which are primarily involved in the lip purse facial expression are the first to bring about movement of the lips and enable the lip to stretch maximally during pursing movement. Cleft lip patients show abnormal insertions of the Orbicularis Oris and surgical correction may result in scarring around the muscle as well as poor approximation which would correspondingly result in an asymmetric peak expression due to these specific muscle fibres involved. Scarring around the Orbicularis muscle fibres can result in abnormal growth and correspondingly lead to asymmetries in specific directions. The 4D study by Hallac et al. (2017) quantified asymmetry during maximum smile and lip puckering. It was seen that maximum landmark displacement during lip puckering occurred at the oral

commissures, the mid philtral ridges and the cupid's peaks and upper lip. Increased asymmetry in the nasal rim and upper lip vermillion was seen in studies by Bell et al. (2014) and Ras et al. (1994). Contrary to our study these studies used landmarks to assess facial asymmetry which did not analyze the face in its entirety. The study by Bell et al. (2014) included assessment of facial curves to add to the landmarks-based analysis.

The grimace expression showed maximum asymmetry in the total face in frame 2 (mid-way between initial resting frame and peak expression). Asymmetry was seen to be accentuated in areas around the nasal tip, the upper lip vermillion, alar regions and philtrum, with the alar and nasal tip showing deviation to the left side. High asymmetry in frame 2 is associated with the Depressor Anguli Oris and the Depressor Labii Inferioris which contract to bring the lower lip downward and laterally to initiate the grimace movement. The fibres of the Depressor muscles intermingle with the Pars fibres of the Orbicularis Oris muscle and are therefore associated with asymmetric movement due to scarring and poor approximation. Frame 3 involves the contraction of the Platysma which is relatively untouched during cleft surgery and therefore shows lesser asymmetry than frame 2. A study by Trotman et al. (2000) assessed nasolabial displacement during four expressions in repaired cleft lip and palate patients. This study used the displacement of 14 specific landmarks as an outcome measure. It was seen in their study that movement of the nasolabial fold during the grimace expression was similar to that in controls. However, movement of alar regions was restricted during grimace in the cleft patients as compared to the controls. Our study showed similar results during grimace as the alar regions were highly asymmetric.

Ferrario et al. (2003) found higher nasal and alar base widths in CLP patients but found no significant difference in nasal surfaces between the clefts and control groups. Ferrario et al. (2003) used single landmarks and linear planes to analyze a three-dimensional surface such as the nose. Using individual landmarks instead of the entire nasal surface was also a limitation of this study.

Our study showed that the asymmetry in vertical or Y direction was minimal in all facial expressions except lip purse as compared to total face, x and z directions. The results of this study showed that lip repair and surgical treatment corrected the asymmetry in the vertical direction. Our results are consistent with the findings of Al-Rudainy et al. (2018) where vertical asymmetry postoperatively was seen to be minimal. Trotman et al. (2007) also found that lateral movements of the upper lip were more restricted than vertical movements of the upper lip in both the cleft revision and cleft non-revision group as compared to the controls.

Residual antero-posterior asymmetry in all four expressions was identified as being highest in the alar regions, philtrum regions and the upper lip. This was consistent with antero-posterior findings in the study by Al-Rudainy et al. (2018) where residual antero-posterior asymmetry was highlighted in the upper lip, alar regions and cheeks of the cleft side. Although the study by Al-Rudainy et al. (2018) studied static images or images at rest, it was a comprehensive analysis as it used the conformation of the generic mesh similar to our study for the analysis of facial asymmetry pre- and post-operatively. Emphasis should be laid on the dynamic approach to measuring facial asymmetry as the face is not static in day to day life and is always in motion. Further, every frame in the sequence of facial movement has specific muscles underlying that specific movement. By assessing asymmetry frame by frame during the movement sequence, specific muscle groups associated with accentuating asymmetry in that region can be highlighted and focused on by surgeons during revision surgery.

5.3. Impact of the Research

The main purpose of this study is to improve the quality of care and the treatment delivered to patients with Unilateral Cleft Lip. This study provides an objective assessment of asymmetry and facial dysmorphology at rest and with four facial expressions, during facial movement following the surgical repair of UCL at an age range of 8 to 10 years. This study uses 4D imaging and dense correspondence analysis and makes it possible to assess the entire facial surface for residual asymmetry. Color maps also make it possible to ascertain the direction, magnitude and location of residual asymmetry in the face, which may inform the decision of

lip revision surgery to deal with residual scarring and the associated abnormal facial muscle movement.

The primary objective of the primary cleft repair is to ensure optimum reconstruction and approximation of affected muscles both in terms of functionality and morphology. It was seen in previous work by Trotman et al. (2007) that cleft lip and palate patients had a more restricted upper lip movement as compared to non-cleft volunteers. This asymmetry of upper lip movement contributes to the limited lateral movements around the upper lip. The adequate mobilization of the disrupted nasolabial muscles in UCL is essential and the microscopic repair of these muscular bundles is paramount to improve lip function and to reduce the asymmetry of facial expressions.

This study provided for the first time, a sensitive instrument for the analysis of the dynamics of facial muscle movements which disclosed the mechanism of the asymmetry of facial expression during maximum smile, cheek puff, lip purse and grimacing. This is the first study documenting the asymmetry of the dynamics of facial expressions throughout the course of individual facial expressions (from the start to the peak to the end of the expression), which provides an insight into the anatomical basis of the residual asymmetry following cleft lip repair. The study presents an objective tool to evaluate and compare the outcomes following cleft lip repair, with a specific focus on the dynamics of the nasolabial muscle function. This could be used for comparative analysis of various surgical techniques and for the outcome measures of various cleft centers.

5.4. **Clinical recommendations of the study**

Following a detailed discussion on surgical techniques and scarring post-surgery in sections 1.11.2 and 1.12, following are the clinical recommendations of the study,

5.4.1. Growth Deficiency and scarring

Growth of patients with repaired orofacial clefts tend to be significantly different from healthy individuals in that there is seen to be a delay in the skeletal and

dental maturation in cleft patients. The maxilla of cleft patients also shows significant amounts of underdevelopment (Batwa et al., 2018).

Studies associated with growth patterns seen in cleft patients indicated a general mid-face hypoplasia and suggested that this hypoplasia could be due to the effect of scarring seen as a result of surgical intervention (Figueroa & Polley, 2007).

The altered craniofacial growth occurring in cleft patients may stem from the cleft anomaly itself in that the congenital abnormality may result in local tissue deficiency which may result in skeletal growth being affected (Venkatesh, 2009).

Furthermore, functional limitations in cleft patients such as nasal deviation or nasal mucosal hypertrophy and constriction of the alae might be responsible for growth deficiency in such patients (Mladina et al., 2015).

Bishara et al. (1976) found that intermaxillary relations in cleft patients were not much different from unaffected individuals but a maxillary protrusion was observed in Unilateral cleft lip and alveolus patients.

Patients with repaired Unilateral cleft lip and palates tend to show narrowing of their maxillary arch anteriorly (Mladina et al., 2015). Shi & Lossee (2015) also reported the effect of lip repair in UCLP patients regards mid-facial growth defects- a hypoplastic mandible and concave mid-face.

This study reveals an innovative technique in assessing residual facial asymmetry following surgical repair and guides surgeons regarding the need for lip revision procedures, thus reducing or eliminating the effects of scar tissue which may impede skeletal growth in cleft lip and palate patients. Growth deficiencies also stem from an important modifiable factor- surgical timing.

5.4.2. Surgical techniques and timing

Previous works on cleft lip and cleft lip and palate repair have reported skeletal (maxillary) growth defects arising as a result of the timing of lip repair (Wolford & Stevao, 2002). Some authors suggested that lip repair may have a significant effect on growth of the child when performed early (less than 2 months) as compared when performed late (3 months of age or older) (Hammoudeh et al., 2017).

Ross (1987) found that cleft alveolar repair resulted in reduced maxillary height and therefore recommended that alveolar repairs take place after 9 years of age as he proposed that the effect of procedures on growth is amplified when performed during a period of rapid growth.

In the 1960s Millard used a specific surgical timing wherein lip adhesion was performed at 3 months, lip revision or rotation-advancement was performed at 6-8 months, cleft closure was performed at 18-24 months and an alveolar bone graft 8-10 years of age. Berkowitz et al. (2005) also claimed that cleft palate surgery was best performed at 18-24 months or later if the ratio of the cleft space to the palatal soft tissue medial to the alveolar ridge was greater than 15%.

The timing of surgery and its effects remain a variable that is subject to change to this day and age. There are advantages and disadvantages of difference in timing of certain procedures as well as the type of surgical procedure employed in the treatment of cleft lip and palate. Surgical outcomes following primary lip repair using these procedures and variable timing as well as secondary corrections can be compared using this novel instrument used in assessing the dynamics of facial movements.

5.4.3. Muscle abnormalities and hypoplasia

In Unilateral cleft lip and palate patients, the continuity of the Orbicularis Oris muscle is compromised and shows abnormal insertions. Apart from this, muscles such as the Depressor Anguli Oris muscle and Depressor Labii Inferioris muscle show fibres that intermingle with the Orbicularis Oris muscle and due to improper continuation and insertions of these muscles, asymmetry of facial movement ensues. Re-approximation of the Orbicularis Oris muscle is necessary in order to ensure optimal muscle function and facial movement as several facial expressions including the lip purse are dependent on this muscle. Furthermore, scarring around these muscles following approximation of the bundles may result in the asymmetry of facial movement. This research study paves the path to guiding the surgeon on the asymmetry of facial movement post-surgery. In understanding the dynamics of facial muscle movement, identifying the specific muscle bundles and re-approximating these accurately, may contribute to reducing scar tissue and corresponding asymmetry and growth deficiencies.

5.5. Strengths and Limitations of the Research

Previous studies on the objective assessment of facial movement were conducted using surface-based analysis or analysis using a specific set of landmarks on the facial surface. Surface-based analysis was used in a few studies using the ICP and then calculating root mean square/least square distances as a measure of facial asymmetry. Surface-based algorithms such as the ICP suffer from a drawback in that there is no true anatomical correspondence between the surface meshes.

Landmark based approaches were also used in previous studies. This approach, although anatomically accurate, lacked in the fact that it could not analyze the entire facial surface.

The novelty in this study in assessing the facial asymmetry in the cleft group of patients was the use of dense correspondence analysis which utilizes a generic facial mesh which undergoes a conformation process to resemble the underlying 3D facial morphology of the patient. This approach combines the advantages of the comprehensiveness of surface-based analysis and the reliability of anatomical correspondence.

The main strengths of our research study could be summarized as follows:

1. The use of the generic facial mesh and dense correspondence analysis provided an accurate method of assessing facial asymmetry utilizing the strengths of both surface-based and landmarks-based analysis.

2. In addition to the total facial asymmetry, the directionality of asymmetry was considered in all three spatial planes (x, y and z planes) thus allowing the assessment of asymmetry and deficient movement of muscles in specific planes.

3. The dynamics of facial movement was assessed through five frames (from rest to maximum expression to final resting position) and facial asymmetry scores were obtained throughout the course of the expressions, thus overcoming the limitations of static capture of facial expressions or 3D techniques.

The weaknesses of the study can be summarized as follows:

1. There was the inclusion of one cohort (the UCL group) which was compared in terms of asymmetry with a control group. Including another cohort of UCLP patients could provide a richer database and help

understand better as to how asymmetry is distributed between the populations of cleft lip and palate.

2. Only the magnitude of facial asymmetry was measured. The pattern of facial movement and corresponding asymmetry of facial motion pattern is also important and could be an area of possible future investigation.

3. The nasolabial region was used as the key area of interest due to it being the region most affected in cleft lip and palate patients. Dividing the face into specific regions such as the nose, lips, chin, etc. could result in a more comprehensive assessment as this would cover regional facial asymmetry scores in addition to the nasolabial asymmetry scores.

5.6. Future Research

1. Automated computer-based processes can reduce the burden of manual image processing, landmarking and analysis to allow for convenient measurement of form, even with larger sample sizes.

2. An interesting future study may be the comparison of subjective and objective dynamic assessments of asymmetry in the face. The data obtained following the dynamic measurement of facial asymmetry during facial expressions could be compared to a panel of assessors giving their subjective interpretation of facial asymmetry and attractiveness. Subjective interpretation of symmetry alone can be carried out using facial movement videos of patients and controls performing various facial expressions. A rating score of symmetry can be given by a panel of skilled assessors which include surgeons. Objective measurement of facial movement and symmetry obtained using this novel instrument can then be compared to the rating scores given by the assessors using student t- tests or Mann Whitney tests based on the normality of the data.

3. Dynamic capture of facial movement and the assessment of facial motion pattern could be used to investigate how the symmetry of motion path differs between cleft lip and palate patients and control subjects.

6 Conclusions

A dynamic approach to assessment and quantification of facial asymmetry using 4D imaging is advantageous as the human face communicates in the social setting with a variety of verbal and non-verbal facial movements. The use of dense correspondence analysis and the conformation of the generic mesh to resemble the shape of the patient's facial morphology while assessing asymmetry of the face during facial movement was the novelty in this study.

Dense correspondence analysis amalgamates the strengths of the comprehensiveness of surface-based analysis and the anatomical accuracy of a landmarks-based analysis and thus gives more accuracy to the results obtained.

The use of this 4D imaging system and dense correspondence analysis to assess asymmetries associated with cleft lip and palate, facial paralysis and other craniofacial anomalies could be the way forward as this system offers the advantage of non-exposure to harmful radiation.

The 4D system used in this study is a reliable and fast method of capture of facial movements and its use in this study could pave the way for future research resulting in improved quality of care and treatment meted out to patients with unilateral cleft lip and palate. Surgical outcomes following primary lip repair and secondary corrections can be compared using this sensitive instrument used in the analysis of the dynamics of facial muscle movements.

The impact of this research study on the quality of treatment and its contribution towards ensuring that accurate and optimal reconstruction of muscle bundles during cleft repair surgery takes place, could go a long way in achieving high standards of surgical care associated with cleft lip and palate as well as other craniofacial anomalies.

7 References

Adams, L.P., 1974. Stereoscopic viewing of image pairs with the naked eyes. *Photogrammetric Record*. **8**,44, 229–30.

Adams, LP. & Spirakis, A., 1997. Stereophotogrammetry. Optical measurement methods in biomechanics. pp 17-38.

Al-Anezi, T., Khambay, B., Peng, MJ., O'Leary, E., Ju, X. & Ayoub, A., 2013. A new method for automatic tracking of facial landmarks in 3D motion captured images (4D). *Int J Oral Maxillofac Surg.* **42(1),**9-18.

Al-Hiyali, A., Ayoub, A., Ju, X., Almuzian, M. & Al-Anezi, T., 2015.The impact of orthognathic surgery on facial expressions. *J Oral Maxillofac Surg*. **1**,11.

Almukhtar, A., Khambay, B., Ju, X., McDonald, J. & Ayoub, A., 2017. Accuracy of generic mesh conformation: The future of facial morphological analysis. *JPRAS* Open.**14**, 39-48.

Al-Rudainy, D., Ju, X., Mehendale, F. & Ayoub, A., 2018. Assessment of facial asymmetry before andafter the surgical repair of cleft lip in unilateral cleft lip and palate cases. *International Journal of Oral and Maxillofacial Surgery*. **47**(3),411–419.

Al-Rudainy, D., Ju, X., Mehendale, F., Ayoub, A., 2019. Longitudinal 3D assessment of facial asymmetry in Unilateral Cleft Lip and Palate. *Cleft Palate Craniofac J*. **56**(4),495-501.

Anastassov ,Y. & Chipkov ,C., 2003. Analysis of nasal and labial deformities in cleft lip alveolus and palate patients by a new rating scale: preliminary report. *J Craniomaxillofac Surg*. **31**,299–303.

Asher-McDade, C. Roberts, Shaw, W.C. and Gallager, C., 1991. Development of a method for rating nasolabial appearance in patients with clefts of the lip and palate. *The Cleft Palate-Craniofacial Journal.* **28**, 4, 385–391.

Aung, S.C., Ngim, R.C.K. & Lee, S.T., 1995. Evaluation of the laser scanner as a surface measuring tool and its accuracy compared with direct facial anthropometric measurements. *Br. J. Plast. Surg*. **48**,551–558.

Ayoub, A., Garrahy, A., Hood, C., White, J., Bock, M., Siebert, J., Spencer, R. & Ray, A., 2003. Validation of a vision-based, three-dimensional facial imaging system. *The Cleft Palate-Craniofacial Journal*. **40**, 523-529.

Ayoub, A., Bell, A,. Simmons, D., Bowman, A., Brown, D., Lo ,T.W. & Xiao, Y., 2011a. 3D assessment of lip scarring and residual dysmorphology following surgical repair of

cleft lip and palate: a preliminary study. *Cleft Palate Craniofac J*. **48**, 379–387. 2010a Aug 17. [Epub ahead of print]

Ayoub, A., Garrahy, A., Millett, D., Bowman, A., Siebert, P., Miller, J. & Ray, A., 2011b. Three-dimensional assessment of early surgical outcome in repaired unilateral cleft lip and palate: part 1. Nasal changes. *Cleft Palate Craniofac J*. **48**,571–577.

Ayoub, A., Garrahy, A., Millett, D., Bowman, A., Siebert, P., Miller, J. & Ray, A., 2011c. Three-dimensional assessment of early surgical outcome in repaired unilateral cleft lip and palate: part 2. Lip changes. *Cleft Palate Craniofac J*.**48**,578–583.

Baghele, M.N., 2012. Buccinator muscle repositioning. *J Indian Soc Periodontol*. **16**(3), 456–460.

Barr, O. & McConkey, R., 2007. A different type of appointment:the experiences of parents who have children with intellectual disabilities. *Journal of Research in Nursing*.**12**, 637–652.

Batwa, W., Almoammar, K., Aljohar, A., Alhussein, A., Almujel, S. & Zawawi, K.H., 2018. The Difference in Cervical Vertebral Skeletal Maturation between Cleft Lip/Palate and Non-Cleft Lip/Palate Orthodontic Patients. *Biomed Res Int.*

Bauer, T.B., Trusler, H.M. & Glanz, S., 1946. Repair of unilateral cleft lip; advantages of LeMesurier technique use of mucous membrane flaps in maxillary clefts. *Plast Reconstr Surg.***11**(1),56-68.

Bell, A., Lo, T.W., Brown, D., Bowman, A.W., Siebert, J.P., Simmons, D.R., Millett, D.T. & Ayoub, A.F., 2014. Three-dimensional assessment of facial appearance following surgical repair of unilateral cleft lip and palate. *Cleft Palate Craniofac J*. **51**(4), 462-71.

Bergland, O. & Sidhu, S.S., 1974. Occlusal changes from the deciduous to the early mixed dentition in unilateral complete clefts. *Cleft Palate J.* **11**(0),317-26.

Berkowitz, S., Duncan, R. & Evans, C., 2005. Timing of cleft palate closure should be based on the ratio of the area of the cleft to that of the palatal segments and not on age alone. *Plast Reconstr Surg.**115***,1483–1499

Berlin, N., Berssenbrügge, P., Runte, C., Wermker, K., Jung, S., Kleinheinz, J. & Dirksen, D., 2014.Quantification of facial asymmetry by 2D analysis – A comparison of recent approaches. *Journal of Cranio-Crania-Maxillofacial Surgery*. **42**(3), 265-271.

Berssenbrügge, P., Lingemann-Koch, M., Abeler, A., Runte, C., Jung, S., Kleinheinz, J., Denz, C. & Dirksen, D. 2015. Measuring facial symmetry: a perception-based approach using 3D shape and color. *Biomed Tech (Berl).* **60**(1),39-47.

Bilwatsch, S., Kramer, M., Haeusler ,G., Schuster ,M., Wurm, J. & Vairaktaris,E., 2006. Nasolabial symmetry following Tennison-Randall lip repair: a three-dimensional approach in 10-year-old patients with unilateral clefts of lip, alveolus and palate. *J Craniomaxillofac Surg*. **34**(5),253-62.

Bishara, S.E., Krause, C.J., Olin, W.H., Weston, D., Ness, J.V. & Felling, C., 1976. Facial and dental relationships of individuals with unoperated clefts of the lip and/or palate. *Cleft Palate J.***13**, 238-52.

Bliss-Moreau, E., Moadab, G., Bauman, M. D., & Amaral, D. G., 2013. The impact of early amygdala damage on juvenile rhesus macaque social behavior. *J. Cogn. Neurosci.* **12**, 2124–2140.

Bloom, J. & Rayi, A. 2019., Anatomy, Head and Neck, Eye Levator Labii Superioris Muscle. [Updated 2019 May 5]. In: StatPearls [Internet]. Treasure Island (FL): StatPearls Publishing; 2019 Jan-. Available from: https://www.ncbi.nlm.nih.gov/books/NBK541031/

Bookstein F.L., 1991. Morphometric tools for landmark data: geometry and biology. *Cambridge University Press, Cambridge*

Bozic, M., Kau, C.H., Richmond, S., Hren ,N.I., Zhurov, A., Udovic, M., Melink, S. and Ovsenik, M., 2009. Facial morphology of Slovenian and Welsh white populations using 3-dimensional imaging. *Angle Orthod*. **79**(4), 640-645.

Bradbury, E., & Hewison, J., 1994. Early parental adjustment to visible congenital disfigurement. *Child: Care Health Dev*. **20**, 251–266.

Bradbury, E., 2012. Meeting the psychological needs of patients with facial disfigurement. *British Journal of Oral and Maxillofacial Surgery*. **50** ,193–196.

Brons, S, van Beusichem, M.E, Bronkhorst, E.M., Draaisma, J., Bergé, S.J., Maal,T.J. & Kuijpers-Jagtman, A.M., 2012. Methods to quantify soft-tissue based facial growth andtreatment outcomes in children: a systematic review. *PLOS ONE*. **7**(8).

Brown, L.G., 1992. A Survey of Image Registration Techniques. *ACM Computing Surveys*. **24**, 4.

Brugmann, SA., Kim, J. & Helms, JA., 2006. Looking different: understanding diversity in facial form. *Am J Med Genet A.* **140**(23), 2521-9.

Bugaighis, I. , O'Higgins, P., Tiddeman, B. , Mattick, C. , Ali, B. & Hobson, R., 2010. Three-dimensional geometric morphometrics applied to the study of children with cleft lip and/or palate from the North East of England. *Eur J Orthod.* **32**, 514-521.

Bugaighis, I., Mattick, C.R., Tiddeman, B. & Hobson, R., 2014. 3D asymmetry of operated children with oral clefts. *Orthod Craniofac Res.* **17**(1),27-37.

Bugaighis, I., Tiddeman, B. , Mattick, C. R. & Hobson, R., 2014. 3D comparison of average faces in subjects with oral clefts. *European Journal of Orthodontics*. **36**(4), 365–372.

Calzolari, E., Pierini, A., Astolfi, G., Bianchi, F., Neville, A.J. & Rivieri, F., 2007. Associated anomalies in multi-malformed infants with cleft lip and palate: An epidemiologic study of nearly 6 million births in 23 EUROCAT registries. *Am J Med Genet A.***143**A(6), 528-37.

Campbell, S. & Campbell, K., 2011. Mechanisms of residual force enhancement in skeletal muscle: insights from experiments and mathematical models. *Biophys Rev*. **3**(4),199–207.

Capelozza J. L., Taniguchi, S.M. & da Silva Júnior, O.G., 1993. Craniofacial morphology of adult unoperated complete unilateral cleft lip and palate patients. *Cleft Palate Craniofac J*. **30**(4),376-81.

Capelozza, F. L., Normando, A.D. & da Silva Filho OG., 1996. Isolated influences of lip and palate surgery on facial growth: comparison of operated and unoperated male adults with UCLP. *Cleft Palate Craniofac J*. **33**(1),51-6.

Chandak, R., Degwekar, S., Bhowte, R.R., Motwani, M., Banode, P. & Chandak, M., 2011. An evaluation of efficacy of ultrasonography in the diagnosis of head and neck swellings. *Dentomaxillofac Radiol*. **40**(4),213–21.

Chatrath, P., De Cordova, J., Nouraei, S., Ahmed, J. & Saleh H. 2007. Objective assessment of facial asymmetry in rhinoplasty patients. *Arch Facial Plast Surg* .**9**, 184-7

Cheung, M., Almukhtar, A., Keeling, A., Hsung, TC., Ju, X., McDonald, J., Ayoub, A. & Khambay, B. 2016. The accuracy of conformation of a generic surface mesh for the analysis of facial soft tissue changes. *PLoS ONE*. **11**(4).

Childrens Health. 2019. (online). Available at: https://www.childrens.com/specialties-services/conditions/cleft-lip. [Accessed on: 9/8/2019]

Ching, G.H.S. & Chung, C.S., 1974. A genetic study of cleft lip and palate in Hawaii. 1. Interracial crosses. *American Journal of Human Genetics*. **26**,162-172.

Choi, Y. K., Park, S. B., Kim, Y. I., & Son, W. S., 2013. Three-dimensional evaluation of midfacial asymmetry in patients with nonsyndromic unilateral cleft lip and palate by cone-beam computed tomography. *Korean journal of orthodontics*. ***43***(3), 113–119.

Chopan, M., Sayadi, L.R., & Laub, D.R., 2017. Surgical Techniques for Treatment of Unilateral Cleft Lip. *IntechOpen*. Available from: https://www.intechopen.com/books/designing-strategies-for-cleft-lip-and-palate-care/surgical-techniques-for-treatment-of-unilateral-cleft-lip [*Accessed on 20-11-2019]*

Christofides, E., Potgieter, A. & Chait, L., 2006. A long term subjective and objective assessment of the scar in unilateral cleft repairs using the Millard technique without revisional surgery. *J Plast Reconstr Aesthet Surg.* **59**, 380-386.

Claes, P., Walters, M. & John, C., 2011. Improved Facial Outcome Assessment using a 3D Anthropometric Mask. *International journal of oral and maxillofacial surgery*. **41**, 324-30.

Coghlan, B. A., Matthews, B. and Pigott, R. W., 1987. A computer- based method of measuring facial asymmetry. Results from an assessment of the repair of cleft lip deformities. *British Journal of Plastic Surgery.* **40**,37.

Cohn, J. & Schmidt, K.L., 2004. The timing of facial motion in posed and spontaneous smiles. *International journal of wavelets, multiresolution and information processing.* **2**,1-12.

Collett, B,R., Wehby, G.L., Barron, S., Romitti, P.A., Ansley, T.N. & Speltz, M.L., 2014. Academic achievement in children with oral clefts versus unaffected siblings. *J Pediatr Psychol.* **39(7),**743–751.

Correa, A., Gilboa, S.M., Besser, L.M., Botto, L.D., Moore, C.A. & Hobbs, C.A., 2008. Diabetes mellitus and birth defects. *American Journal of Obstetrics and Gynecology*.**199**,237.

Cutting, C.B.,2009. The extended Mohler unilateral cleft lip repair. In: Losee JE, Kirschner RE (ed): Comprehensive Cleft Care. New York: McGraw Hill Medical, 299-330.

Dahl, E., Hanusardóttir, B. & Bergland, O., 1981. A comparison of occlusions in two groups of children whose clefts were repaired by three different surgical procedures. *Cleft Palate J.* **17**,122.

Darby, LJ., Millett, DT., Kelly, N., McIntyre, GT. & Cronin, MS., 2015. The effect of smiling on facial asymmetry in adults: a 3D evaluation. *Aust Orthod J*. **31**(2),132-7.

Darwin, C., 1872. The expression of emotion in man and animals. New York: Oxford University Press

De Gelder, B., 2009. Why bodies? Twelve reasons for including bodily expressions in affective neuroscience. *Phil. Trans. R. Soc. B.* **364**, 3475–3484.

De Sousa, A., Devare, S. & Ghanshani, J., 2009. Psychological issues in cleft lip and cleft palate. *J Indian Assoc Pediatr Surg.* **14(2)**,55–58.

Dimensional Imaging. 2015. (online). Available at: https://www.di4d.com/. [Accessed on: 12/5/2018]

Dixon, M.J., Marazita, M.L., Beaty, T.H. & Murray, J.C., 2011. Cleft lip and palate: understanding genetic and environmental influences. *Nat Rev Genet.* **12**(3),167-78.

Djordjevic, J., Lewis, B., Donaghy, C., Zhurov, A., Knox, J.,Hunter, L. & Richmond, S., 2014. Facial shape and asymmetry in 5-year-old children with repaired unilateral cleft lip and/or palate: an exploratory study using laser scanning. *European Journal of Orthodontics.* **364**, 497–505.

Duffy, S., Noar ,JH., Evans, RD., Sanders ,R., 2000. Three-dimensional analysis of the child cleft face. *Cleft Palate Craniofac J*. **37**, 137–144.

Ekman, P., 1972. Universal and cultural differences in facial expression of emotion. Lincoln, NE: *Nebraska University Press.*

Ekman, P.,1973. Darwin and facial expression; a century of research in review. *New York: Academic Press.*

Ekman P. & Friesen, W. V.,1978. Facial action coding system: a technique for the measurement of facial movement. Palo Alto, CA: *Consulting Psychologists Press*

Ekman, P., 2009. Darwin's contributions to our understanding of emotional expressions. *Philosophical transactions of the Royal Society of London. Series B, Biological sciences.* **364** , 3449-51.

Ekrami, O.,Claes, P., White, J.D., Zaidi, A.A., Shriver, M.D. & Van Dongen, S., 2018. Measuring asymmetry from high-density 3D surface scans: An application to human faces. *PLoS One.*

Enemark, H., Bolund, S. & Jørgensen, I., 1990. Evaluation of Unilateral Cleft Lip and Palate Treatment: Long Term Results. *Cleft Palate Journal.* **27**(4), 354–361.

Endriga, M & Kapp-Simon, K., 1999. Psychological Issues in Craniofacial Care: State of the Art. *The Cleft palate-craniofacial journal*. **36**. 3-11.

Eubanks, RJ., 1957. Surgical correction of masseter muscle hypertrophy associated with unilateral prognathism: report of case. *J Oral Surg (Chic).***15**(1),66–9.

Farkas, L.G. & Cheung, G., 1981. Facial asymmetry in healthy North American caucasians. *Angle Orthod.* **51**:70–77

Farkas, L.G., 1994. Anthropometry of the head and face. 2nd ed Raven Press; New York, 405.

Ferrario, V.F., Sforza, C., Ciusa, V., Dellavia, C. & Tartaglia, G.M., 2001. The effect of sex and age on facial asymmetry in healthy subjects: a cross-sectional study from adolescence to mid-adulthood. *J Oral Maxillofac Surg.* **59**:382–388

Ferrario, V., Sforza, C. , Tartaglia, G. M. , Sozzi, D. & Car, A., 2003.Three- dimensional lip morphometry in adults operated on for cleft lip and palate. *Plast Reconstr Surg*.**111**,2149–2156.

Figueroa, A.A. & Polley, J.W., 2007. Management of the severe cleft and syndromic midface hypoplasia. *Orthod Craniofac Res.***10(3),**167-79.

Frank, M.G., Ekman, P. & Friesen, W.V., 1993. Behavioral markers and recognizability of the smile and enjoyment. *Journal of personality and social psychology*.**64**,83-93.

Fraser F.C., 1955. Thoughts on the etiology of clefts of the palate and lip. *Acta Genet Stat Med*.**5**(4),358–69.

Gauthier, I., Tarr, M.J., Anderson, A.W., Skudlarski, P. & Gore, J.C., 1999. Activation of the middle fusiform 'face area' increases with expertise in recognizing novel objects. *Nat. Neurosci.* **2**,568–73

GIS Resources. 2013. (online). Available at: http://www.gisresources.com/basic-of-photogrammetry_2/ . [Accessed on 6/10/2019]

Gower, J.C., 1975. Generalized procrustes analysis. *Psychometrika* .**40**, 33–51.

Grammer, K. & Thornhill, R., 1994. Human (Homo sapiens) facial attractiveness and sexual selection: the role of symmetry and averageness. *J Comp Psychol*. **108**(3),233-42.

Gray, H., 1977. Anatomy: Descriptive and surgical (American revision of 15th English edition of 1901). New York: Bounty Books.

Gray's Anatomy. 2008, p. 440.

Gregg, T., Boyd, D. & Richardson, A., 1994. The birth prevalence of cleft lip and palate in Northern Ireland from 1980-1990. *British Journal of Orthodontics.* **21**, 387-392.

Gross, M. M., Trotman, C. A., & Moffatt, K. S., 1996. A comparison of

three-dimensional and two-dimensional analyses of facial motion.
Angle Orthodontist. **66**, 189-194.

Gwilliam, J.R., Cunningham, S.J. and Hutton, T., 2006. Reproducibility of soft tissue landmarks on threedimensional facial scans. *Eur J Orthod.* **28**(5), 408- 415.

Hager, J.C. & Ekman, P., 1997. The asymmetry of facial actions is inconsistent with models of hemispheric specialization. In : Ekman P, Rosenberg E, editors. What the face reveals. New York: Oxford University Press, 40-62

Hajeer ,M.Y., Ayoub, A.F., Millett, D.T., Bock, M. and Siebert, J.P., 2002. Three-dimensional imaging in orthognathic surgery: the clinical application of a new method. *Int J Adult Orthodon Orthognath Surg*. **17**(4): 318-330.

Hallac, R., Feng, J., Kane, A.A. & Seaward, J.R., 2017. Dynamic facial asymmetry in patients with repaired cleft lip using 4D imaging (video stereophotogrammetry). *Journal of Cranio-Maxillofacial Surgery*. **45**(1), 8-12.

Hall, B.K. & Precious, D.S., 2013. Cleft lip, nose, and palate: the nasal septum as the pacemaker for midfacial growth. *Oral Surg Oral Med Oral Pathol Oral Radiol*.***115***(4),442-7.

Hammoudeh, J.A., Imahiyerobo, T.A. & Liang, F., 2017. Early Cleft Lip Repair Revisited: A Safe and Effective Approach Utilizing a Multidisciplinary Protocol. *Plast Reconstr Surg Glob Open*.**5(6).**

Heike, C.L., Upson, K., Stuhaug, E. & Weinberg, S.M., 2010. 3D digital stereophotogrammetry: a practical guide to facial image acquisition.
Head Face Med. **6**:18,36.

Hennessy, R.J. & Moss J.P., 2001. Facial growth:separating shape from size. *Eur. J. Orthod.,* **23**,275-285

Hennessy,RJ., McLearie, LJ., Kinsella, A. and Waddington, JL., 2005. Facial surface analysis by 3D laser scanning and geometric morphometrics in relation to sexual dimorphism in cerebral–craniofacial morphogenesis and cognitive function. *J Anat*. **3**,283–295.

Hermann, N. V. , Darvann, T. A. , Larsen. , Lindholm, P. , Anderson, M. & Kreiborg, S., 2016. A Pilot Study on the Influence of Facial Expression on Measurements in Three-Dimensional Digital Surfaces of the Face in Infants With Cleft Lip and Palate. *Cleft Palate Craniofac J*. **53**(1), 3-15.

Hess, U. & Kleck, R., 1997. Differentiating emotion elicted and deliberate emotional facial expressions. In: Ekman P, Rosenberg E, editors. What the face reveals. New York: Oxford University Press, 271-285.

Hodgkinson, P.D., Brown, S., Duncan, D., Grant, C., McNaughton, A., Thomas, P. and Mattick, R., 2005. Management of children with cleft lip and palate: A review describing the application of multidisciplinary team working in this condition based upon the experiences of a regional cleft lip and palate centre in the United Kingdom. *Fetal and Maternal Medicine Review.* **16**(1),1–27, 2005.

Hoefert, C. S. , Bacher, M. , Herberts, T. , Krimmel, M. & Reinert, S., 2010. 3D Soft Tissue Changes in Facial Morphology in Patients with Cleft Lip and Palate and Class III Malocclusion under Therapy with Rapid Maxillary Expansion and Delaire Facemask. *J Orofac Orthop*. **71**(2), 136–151.

Hoerter, J.E. & Patel, B.C. 2019. Anatomy, Head and Neck, Platysma. [Updated 2019 Aug 14]. In: StatPearls [Internet]. Treasure Island (FL): StatPearls Publishing; 2019 Jan-. Available from: https://www.ncbi.nlm.nih.gov/books/NBK545294/

Hood, C.A., Bock, M., Hosey, M.T., Bowman, A., Ayoub, A.F., 2003. Facial asymmetry - 3D assessment of infants with cleft lip & palate. *Int J Paediatr Dent*. **13,** 404–410.

Honrado, CP. & Larrabee, WF Jr., 2004. Update in three-dimensional imaging in facial plastic surgery. *Curr Opin Otolaryngol Head Neck Surg.* **12**,327-31.

Huffman, W. C., and Lierle, D.M., 1949. Studies of the pathologic anatomy of the unilateral harelip nose. *Plastic reconsir. Surg*. **4**, 225-234.

Hur, M.S., Hu, K.S., Park, J.T., Youn, K.H. & Kim, H.J., 2010. New anatomical insight of the levator labii superioris alaeque nasi and the transverse part of the nasalis. *Surgical and Radiologic Anatomy.* **3**, 753-756.

Izard, C. E., 1971. The face of emotion. East Norwalk, CT: Appleton-Century-Crofts.

Jack, R.E. & Schyns, P.G., 2017. Towards a social psychophysics of face communication. *Annual Review of Psychology.* **68**, 269-297.

Kawakami, S., Hiura, K.,Yokozeki, M., Takumi, T., Takuya, S. Hideki,N. & Keiji,M., 2003. Longitudinal Evaluation of Secondary Bone Grafting Into the Alveolar Cleft. *The Cleft palate-craniofacial journal* . **40**, 569-76.

Kau, C.H., Richmond, S., Zhurov, A.I., Knox,J., Chestnutt, I., Hartles, F. and Playle, R., 2005. Reliability of measuring facial morphology with a 3-dimensional laser scanning system. *Am J Orthod Dentofacial Orthop.* **128** (4), 424-430.

Kau, C.H., Zhurov, A., Richmond, S., Cronin, A., Savio, C., Mallorie, C., 2006. Facial templates: a new perspective in three dimensions. *Orthod Craniofac Res.* **9**(1),10–7.

Kau, C.H. and Richmond, S., 2008. Three-dimensional analysis of facial morphology surface changes in untreated children from 12 to 14 years of age. *Am J Orthod Dentofacial Orthop.* **134**(6), 751-760.

Kau, C.H., Richmond, S., Zhurov, A., Ovsenik, M., Tawfik, W., Borbely, P., English, J.D., 2010. Use of 3-dimensional surface acquisition to study facial morphology in 5 populations. *Am J Orthod Dentofac Orthop.* **137**(4), 56.

Kau, C. H. , Kamel, S. G. , Wilson, J. & Wong, M. E., 2011. New method for analysis of facial growth in a pediatric reconstructed mandible. *Am J Orthod Dentofacial Orthop*. **139**(4), e285–290.

Kenhub, 2019. Diagram: pictures- facial muscles. Kebhub [online]. Available at : https://www.kenhub.com/en/library/anatomy/the-facial-muscles [Accessed 20/08/2019]

Kernahan, D.A., 1971. The striped Y--a symbolic classification for cleft lip and palate. *Plast Reconstr Surg.* (**5),**469-70.

Kim, K.R., Kim, S. & Baek, S.H., 2008. Change in grafted secondary alveolar bone in patients with UCLP and UCLA. A three-dimensional computed tomography study. *Angle Orthod.* **78**,631–640.

Knight, J., Cassell, C., Meyer, R. & Strauss, R., 2015. Academic outcomes of children with isolated orofacial clefts compared with children without a major birth defect. *Cleft Palate Craniofac J.* **52(3),**259–268

Kuijper, A.M. & Long, R.E., 2000. The Influence of Surgery and Orthopedic Treatment on Maxillofacial Growth and Maxillary Arch Development in Patients Treated for Orofacial Clefts. *The Cleft Palate-Craniofacial Journal.* **37**(6), 512-543.

Kuijpers, M.A., Chiu, Y.T., Nada ,R.M., Carels, C.E, Fudalej, P.S., 2014. Three-dimensional imaging methods for quantitative analysis of facial soft tissues and skeletal morphology in patients with orofacial clefts: a systematic review. *PLoS One*. **9**(4).

Kurkcuoglu, A., Ozan, L., Deniz ,A., Rana, B., Ecem, D., Odul, O., Irmak, O. & Mert, S., 2016. Comparison of objective and subjective assessments for perception of facial symmetry. *Anatomy.* **10,** 2.

Kwong, R.Y. & Yucel, E.K., 2003. Computed tomography scan and magnetic resonance imaging. *Journal of American Heart Association*. **108**, e104–e106.

Kyrkanides, S., Bellohusen, R., & Subtelny, J. D. 1996. Asymmetries of the Upper Lip and Nose in Noncleft and Postsurgical Unilateral Cleft Lip and Palate Individuals. *The Cleft Palate-Craniofacial Journal*, **33**(4), 306–311.

Leite, I.C., Koifman, S., 2009. Oral clefts, consanguinity, parental tobacco and alcohol use: a case-control study in Rio de Janeiro, Brazil. *Braz Oral Res*. **23**(1),31-7.

Little, J., Cardy, A. & Munger, R.G., 2004. Tobacco smoking and oral clefts: a meta-analysis. *Bull World Health Organ*. **82**(3),213-8.

Maal, T.J., Verhamme, L.M., van Loon, B., Plooij, J.M., Rangel, F.A., Kho, A., Bronkhorst ,E.M. & Bergé, S.J., 2011. Variation of the face in rest using 3D stereophotogrammetry. *Int J Oral Maxillofac Surg*.**40**(11),1252–7.

MacLean, P. D., 1990. The Triune Brain in Evolution. London: Springer.

Majid, Z., Chong, A.K., Ahmad, A., Setan, H. and Samsudin, A.S., 2005. Photogrammetry and 3D laser scanning as spatial data capture techniques for a national craniofacial database. *Photogramm Rec*. **20**(109), 48-68.

Majid, Z., Chong, A.K., and Setan, H., 2007. Importamt considerations for craniofacial mapping using laser scanners. *Photogramm Rec*. **22**(120), 290-308.

Malek, R., 2001. Classification and anatomo-clinical forms. In: Cleft Lip and Palate: Lesions, Pathophysiology and Primary Treatment, pp. 17– 25. London: Martin Dunitz.

Manjula ,W., Sukumar, M., Kishorekumar ,S., Gnanashanmugam, K. & Mahalakshmi, K., 2015. Smile: A review. *J Pharm Bioallied Sci.* **7**(1), 271–275.

Manyama, M., Larson, J. R., Liberton, D. K., Rolian, C., Smith, F. J., Kimwaga, E., Gilyoma, J. Lukowiak, K.D., Spritz, R.A., Hallgrimsson, B., 2014. Facial morphometrics of children with non-syndromic orofacial clefts in Tanzania. *BMC oral health*, **14**, 93.

Marani, R., Renò, V., Nitti, M., D'Orazio, T. and Stella, E., 2016. A Modified Iterative Closest Point Algorithm for 3D Point Cloud Registration. *Computer-Aided Civil and Infrastructure Engineering*, **31**, 515–534.

Margulis, A.V., Mitchell, A.A., Gilboa, S.M., Werler, M.M., Mittleman, M.A., Glynn, R.J. & Hernandez-Diaz, S., 2012. Use of topiramate in pregnancy and risk of oral clefts. *Am J Obstet Gynecol.* **207**,405.

McComb, H., 1990. Primary repair of the bilateral cleft lip nose: a 15-year review and a new treatment plan. *Plast Reconstr Surg*. **86**(5),882-9.

McIntyre, G.T. & Mossey, P.A., 2002. Asymmetry of the parental craniofacial skeleton in orofacial clefting. *J Orthod*. **29**:299–305

Meyer-Marcotty., Alpers, G., Gerdes, A. & Stellzig-Eisenhauer, A., 2010. Impact of facial asymmetry in visual perception: a 3-dimensional data analysis. *Am J Orthod Dentofacial Orthop.* **137**(2),168.

Mette, A.R., Yu-Ting Chiu., Nada, R.M., Carels, E.L. & Fudalej, P.S., 2014. Three-dimensional Imaging Methods for Quantitative Analysis of Facial Soft Tissues and Skeletal Morphology in Patients with Orofacial Clefts: A Systematic Review. *PLoS One.* **9**(4).

Millar, K., Bell, A., Bowman, A., Brown,D ., Lo, T ., Siebert, P., Simmons, D. & Ayoub, A., 2013. Psychological Status as a Function of Residual Scarring and Facial Asymmetry After Surgical Repair of Cleft Lip and Palate. *The Cleft Palate-Craniofacial Journal.* **50**(2), 150.

Millard, D. R. Jr., 1958. A radical rotation in single harelip. *Am J Surg.* **95**(2),318–322.

Millard, D. Ralph Jr., 1976. Cleft Craft: The Evolution of Its Surgery—Volume I: The Unilateral Deformity. Cleft Craft: The Evolution of Its Surgery. 3. (online) Available at: https://scholarlyrepository.miami.edu/cleft_craft/ [Accessed on 12 November, 2019]

Mladina, R., Skitarelić, N., Poje, G. & Šubarić, M., 2015. Clinical Implications of Nasal Septal Deformities. *Balkan Med J.* **32(2),**137-146.

Mohler, L. R., 1987. Unilateral cleft lip repair. *Plast Reconstr Surg.* **80**(4):511–517.

Molina-Solana, R., Yáñez-Vico, R.M., Iglesias-Linares, A., Mendoza-Mendoza, A. & Solano-Reina, E., 2013. Current concepts on the effect of environmental factors on cleft lip and palate. *Int J Oral Maxillofac Surg*. **42**(2), 177-84.

Morecraft, R. J., Louie, J. L., Herrick, J. L., & Stilwell-Morecraft, K. S., 2001. Cortical innervation of the facial nucleus in the non-human primate A new interpretation of the effects of stroke and related subtotal brain trauma on the muscles of facial expression. *Brain* **124**, 176–208.

Morecraft, R. J., McNeal, D. W., Stilwell-Morecraft, K. S., Gedney, M., Ge, J. & Schroeder, C. M., 2007. Amygdala interconnections with the cingulate motor cortex in the rhesus monkey. *J. Comp. Neurol.* **500**, 134–165.

Mori, A., Nakajima, T., Kaneko, T., Sakuma, H. & Aoki, Y., 2005. Analysis of 109 Japanese children's lip and nose shapes using 3-dimensional digitizer. *Br J Plast Surg*. **58**,3,318-29.

Morioka, D., Sato, N., Kusano, T., Muramatsu, H., Tosa, Y., Ohkubo, F. & Yoshimoto, S., 2015. Difference in nasolabial features between awake and asleep infants with unilateral cleft lip: Anthropometric measurements using three-dimensional stereophotogrammetry. *J Craniomaxillofac Surg.* **43**(10),2093-9.

Mossey, P., Little, J., Munger, R.G., Dixon, M.J. & Shaw, W.C., 2009. Cleft lip and palate. *Lancet*. **374**., 1773–1785.

Mossey, P.A. & Modell, B., 2012. Epidemiology of oral clefts 2012: an international perspective. *Front Oral Biol.***16**:1, 18.

Murray, J.C., 2002. Gene/environment causes of cleft lip and/or palate. *Clin Genet*. **61**(4), 248-56.

Mushiake, H., Saito, N., Sakamoto, K., Itoyama, Y., & Tanji, J., 2006. Activity in the lateral prefrontal cortex reflects multiple steps of future events in action plans. *Neuron 50*, 631–641.

Nagy, K. & Mommaerts, M.Y. , 2007. Analysis of the cleft-lip nose in submental- vertical view, Part I—reliability of a new measurement instrument. *J Craniomaxillofac Surg.* **35**,265–277.

Nakamura, N. , Okawachi,., Nishihara, K. , Hirahara, N. & Nozoe, E., 2010.Surgical technique for secondary correction of unilateral cleft lip-nose deformity: clinical and 3-dimensional observations of preoperative and postoperative nasal forms.*J Oral Maxillofac Surg.* **68**(9),2248-57.

Narayanan, P.V. and Adenwalla, H.S., 2013. Unfavourable results in the repair of the cleft lip. *Indian J Plast Surg*. **46**(2), 171–182.

Nasr, M., Jabbour, S., Sidaoui, J., Haber, R. & Kechichian, E., 2015. Botulinum Toxin for the Treatment of Excessive Gingival Display: A Systematic Review. *Aesthetic surgery journal / the American Society for Aesthetic Plastic surgery*. **36**.

Nicholls, W., Selvey, L.A., Harper, C., Persson, M. & Robinson, S., 2019. The Psychosocial Impact of Cleft in a Western Australian Cohort Across 3 Age Groups. *The Cleft Palate-Craniofacial Journal.* **56(2),**210-221.

Nicolau, P. The orbicularis oris muscle: a functional approach to its repair in the cleft lip. 1983. *Br J Plast Surg.* **36**(2),141-53.

Nkenke, E., Lehner, B., Kramer, M., Kramer, M., Haeusler, G., Benz,.S., Schuster, M., Neukam, F.W., Vairaktaris, E.G., Wurm, J., 2006. Determination of facial symmetry in unilateral cleft lip and palate patients from three-dimensional data: technical report and assessment of measurement errors. *Cleft Palate Craniofac J.* **129**,137.

Noorollahian, M., Nematy, M., Dolatian, A., Ghesmati, H., Akhlaghi, S. & Khademi, G.R., 2015. Cleft lip and palate and related factors: A 10 years study in university hospitalised patients at Mashhad--Iran. *Afr J Paediatr Surg.* **12(**4), 286–290.

Normando AD, Capelozza Júnior L. & da Silva Júnior, O.G., 1992. Mandibular morphology and spatial position in patients with clefts: intrinsic or iatrogenic? *Cleft Palate Craniofac J.* **369**,75.

Oliver, R. G. & Jones, G. ,1997. Neonatal feeding of infants bornwith cleft lip and/or palate: parental perceptions of their experiences in South Wales. *The Cleft Palate-Craniofacial Journal*.**34,** 527–530.

O'Neill, J., 2008. Do folic acid supplements reduce facial clefts? *Evid Based Dent.* ***9****(3),82-3.*

Otero, L., Bermudez, L., Lizarraga,K., Tangco, I., Gannaban,R . & Meles,D.,2012. A Comparative Study of Facial Asymmetry in Philippine, Colombian, and Ethiopian Families with Nonsyndromic Cleft Lip Palate. *Plastic Surgery International*. **4,** 511.

Othman, S.A., Ahmad, R., Asi, S.M., Ismail, N.H. & Rahman, Z.A.A., 2014. Three dimensional quantitative evaluation of facial morphology in adults with unilateral cleft lip and palate, and patients without clefts. *Br J Oral Maxillofac Surg.* **52**,208–213.

Othman, S.A. & Aidil Koay, N., 2016. Three-dimensional facial analysis of Chinese children with repaired unilateral cleft lip and palate. *Sci Rep.* **6.**

Ouellette, E.M., Rosett, H.L., Rosman, N.P. & Weiner, L., 1977. Adverse effects on offspring of maternal alcohol abuse during pregnancy. *N. Engl. J. Med.* **297**, 528-530.

Patel, A., Islam, SMS., Murray, K. & Goonewardene, M., 2015. Facial asymmetry assessment in adults using three-dimensional surface imaging. *Prog Orthod.* **16**, 36.

Perrett, D.I., Lee, K.J., Penton-Voak, I., Rowland, D. & Yoshikawa S., 1998. Effects of sexual dimorphism on facial attractiveness. *Nature* .**394**,884–87.

Phillips, C., Tulloch, C. & Dann, C., 1992. Rating of facial attractiveness. *Community Dentistry and Oral Epidemiology.***20**(4), 214-220.

Pitkin, R.M., 2007. Folate and neural tube defects. *Am J Clin Nutr*. **85**,285S–288.

Pool, R. & Farnworth, T.K., 1994. Preoperative lip taping in the cleft lip. *Ann Plast Surg* . (3),243–249.

Pocketdentistry.com., 2019. (online). Available at: https://pocketdentistry.com/definitive-rhinoplasty-for-adult-cleft-lip-nasal-deformity/ [accessed on 5-10-2019]

Quan, W., Matuszewski, B. & Shark, L., 2012. Facial asymmetry analysis based on 3D Dynamic scans. IEEE International conference on system, man and cybernetics. Seoul.

Ramstad. T., Ottem, E. & Shaw, W.C., 1995a. Psychosocial adjustment in Norwegian adults who had undergone standardised treatment of complete cleft lip and palate. Part I. Education, employment and marriage. *Scandinavian Journal of Plastic and Reconstructive Surgery and Hand Surgery*. **29,** 251–257.

Randall, P., 1965. A lip adhesion operation in cleft surgery. *Plast Reconstr Surg*. **35,**371-6.

Ras, F., Habets, LLMF., Van Ginkel, F.C. & Prahl-Andersen B., 1994. Three-dimensional evaluation of facial asymmetry in cleft lip and palate. *Cleft Palate Craniofac J.* **31**,116–121.

Ras, F., Habets, LLMH., Vanginkel, FC. & Prahlandersen, B., 1994. Facial left- right dominance in cleft-lip and palate: three-dimension evaluation. *Cleft Palate Craniofac J.***31,**461–465.

Ras, F., Habets, L.L., van Ginkel, F.C., Prahl-Andersen, B., 1995. Longitudinal study on three-dimensional changes of facial asymmetry in children between 4 to 12 years of age with unilateral cleft lip and palate. *Cleft Palate Craniofac J.* **32**(6),463-8.

Reid, J., Reilly, S. & Kilpatrick, N., 2006. A prospective, longitudinal study of feeding skills in a cohort of babies with cleft conditions. *Cleft Palate Craniofac J.* **43**(6),702-9.

Reid, J., Reilly, S. & Kilpatrick, N., 2007. Sucking performance of babies with cleft conditions. *Cleft Palate Craniofac J.***44**(3),312-20.

Richman, L.C. & Nopoulos, P.,2008. Neuropsychological and neuroimaging aspects of cleft lip and palate. In: Losee J, Kirschner R, eds. Comprehensive Cleft Care. New York, NY: McGraw-Hill.

Rinn, W., 1984. The neuropsychology of facial expression: A review of the neurological and psychological mechanisms for producing facial expressions. *Psychological bulletin*. **95.** 52-77

Rogers, C.R., Mooney, M.P., Smith, T.D., Weinberg, S.M., Waller, B.M., Parr, L.A., Docherty, B.A., Bonar, C.J., Reinholt, L.E, Deleyiannis, F.W-B, Siegel, M.I., Marazita, M.L. & Burrows, A.M. 2009. Comparative microanatomy of the orbicularis oris muscle between chimpanzees and humans: evolutionary divergence of lip function. *J Anat* . **214**, 36– 44.

Rose W.,1891. London: H.K. Lewis. On harelip and cleft palate.

Ross, R. B. and Johnston, M. C., 1972. Cleft Lip and Palate, Baltimore: The Williams and Wilkins Co.

Rumsey, N. & Harcourt, D., 2005. The Psychology of Appearance. Maidenhead, UK: Open University Press.

Salyer, K., David, K., Chong, A.M., Joseph, M. 2019., Unilateral Cleft Lip and Nose Repair. Pocket Dentistry. (online). Available at https://pocketdentistry.com/unilateral-cleft-lip-and-nose-repair/ . *[Accessed on 8/9/2019]*

Seaward, J., Kane, A. & Hallac, R., 2015. Dynamic Facial Asymmetry in Patients with Cleft Lip and Palate - What 4D Video Stereophotogrammetry Can Tell Us About Motion of the Repaired Lip. *Plastic and Reconstructive Surg.* **135**, 130-131.

Seidenstricker-Kink, L. M. , Becker, D. B. , Govier, D.P., DeLeon, V.B. & Lo, L. J. 2008. Comparative osseous and soft tissue morphology following cleft lip repair. *Cleft Palate Craniofac J.* **45**(5), 511–517.

Senders, C.W., Peterson, E.C., Hendrickx, A.G. & Cukierski, M.A. 2003., Development of the upper lip. *Arch Facial Plast Surg.* **5**(1),16–25.

Schendel, S.A., 2000. Unilateral cleft lip repair--state of the art. *Cleft Palate Craniofac J* .**37**. (4),335-41.

Schwenzer-Zimmerer, K., Chaitidis, D., Berg-Boerner, I., Krol, Z., Kovacs,L., Schwenzer, N.F., Zimmerer, S., Holberg,C. & Zeilhofer, H.F., 2008. Quantitative 3D soft tissue analysis of symmetry prior to and after unilateral cleft lip repair compared with non-cleft persons (performed in Cambodia). *J Craniomaxillofac Surg*. **36,**431–438.

Sebire, N.J., Jolly, M., Harris, J.P., Wadsworth, J., Joffe, M., Beard, R.W., Regan, L. & Robinson, S., 2001. Maternal obesity and pregnancy outcome: a study of 287,213 pregnancies in London. *Int J Obes Relat Metab Disord.* **25**(8),1175-82.

Shaner, D.J., Peterson, A.E., Beattie, O.B. & Bamforth, J.S., 2000. Assessment of soft tissue facial asymmetry in medically normal and syndrome-affected individuals by analysis of landmarks and measurements. *Am J Med Genet*. **93**:143–154

Sharma, S., Rasila, D., Singh, M. & Mohan, M., 2014. Ultrasound as a diagnostic boon in Dentistry -A Review. *International Journal of Scientific Study*. **2**, 2.

Shaw, WC., Rees, G., Dawe, M. & Charles, CR., 1985. The influence of dentofacial appearance on the social attractiveness of young adults. *Am J Orthod.* **87**(1),21–6.

Shaw, W.C., Asher-McDade, C., Brattstrom, V., Dahl, E., McWilliam, J., Molsted, K., Plint ,D.A., Prahl-Andersen, B., Semb, G. & Sandy, JR., 1992. A six enter international

study of treatment outcome in patients with clefts of the lip and palate: part 1. Principles and study design. *Cleft Palate Craniofac J.* **29**,393–397.

Shaw, G.M., Wasserman, C.R., Lammer, E.J., O'Malley, C.D., Murray, J.C., Basart, A.M. & Tolarova, M.M., 1996. Orofacial clefts, parental cigarette smoking, and transforming growth factor-alpha gene variants. *Am J Hum Genet.* **58**(3),551-61.

Shaw, W. & Semb, G., 2017. The Scandcleft randomised trials of primary surgery for unilateral cleft lip and palate: 11. What next? *J Plast Surg Hand Surg.* **51**:88–93.

Shprintzen, R. J. & Bardach, J., 1995. Cleft palate speech management: A multidisciplinary approach. St. Louis, MO: Mosby.

Shujaat, S., Khambay, B., Ju, X., Devine, J., Macmohan, J., Wales, C. & Ayoub, A. 2014. Clinical application of 3d Motion capture (4D): A novel approach to quantify the dynamics of facial animations. *Int J Oral Maxillofac Surg.* **43,** 907-916.

Sim, R,S., Smith, J.D., &Chan, AS., 2000. Comparison of the esthetic facial proportions of southern Chinese and white women. *Arch Facial Plast Surg.* **2,** 113-120

Sperber, G.H., 2001. Craniofacial Development. Hamilton, Canada: B. C. Decker.

Stauber, I., Vairaktaris, E., Holst, A., Schuster, M., Hirschfelder, U., Neukam, F.W., Nkenke, E., 2008. Three-dimensional Analysis of Facial Symmetry in Cleft Lip and Palate Patients Using Optical Surface Data. *J. Orofac. Orthop. / Fortschritte der Kieferorthopädie* . ***69****,* 268–282.

Stone, D.H. & Dolk, H., 1994. High reported prevalence of congenital anomalies in a Scottish city. *Scottish Medical Journal.* **39,** 170-172.

Suzuki, H., Yamaguchi, T. & Furukawa, M., 1999 . Rhinologic computed tomographic evaluation in patients with cleft lip and palate. *Arch Otolaryngol Head Neck Surg* . **125,** 1000–1004.

Talmant, J.C., 2006. Evolution of the functional repair concept for cleft lip and palate patients. *Indian Journal of Plastic Surgery.* **39**, 196-209.

Tan, K.K. & Pigott, R.W., 1993. A morbidity review of children with complete unilateral cleft lip and nose at 10+- 1 years of age. *Br J Plast Surg.* **46**, 1-6.

Tennison, C. W., 1946. The repair of the unilateral cleft lip by the stencil method. *Plast Reconstr Surg.* **9**(2),115–120.

Thomason, H.A. & Dixon, M.J., 2009. Craniofacial defects and cleft lip and palate. Encyclopedia of Life Sciences (ELS) Chichester, UK: John Riley & Sons, Ltd.

Trepel, M., Weller, M., Dichgans, J., & Petersen, D., 1996. Voluntary facial palsy with a pontine lesion. *J. Neurol. Neurosurg. Psychiatry.* **61**, 531–533.

Trotman, C.A., Faraway, J.J, Essick, G.K., 2000. 3-D nasolabial displacement during movement in repaired cleft lip and palate patients. *J Plast Reconstr Surg***. 105,**1273–1283.

Trotman, C.A., Faraway, J.J. & Phillips, C., 2005. Visual and statistical modeling of facial movement in patients with cleft lip. *Cleft Palate Craniofac J.* **42,**245-254.

Trotman, CA., Phillips, C., Essick, GK., Faraway, JJ., Barlow, SM. & Losken, HW. 2007. Functional outcomes of cleft lip surgery. Part I: Study design and surgeon ratings of lip disability and the need for lip revision. *Cleft Palate Craniofac J.* **44,**598-606.

Trotman, CA., Faraway, JJ., Losken, HW. & van Aalst, J. 2007. Functional outcomes of cleft lip surgery. Part II: Quantification of nasolabial movement. *Cleft Palate Craniofac J.* **44**,607-616.

Trotman, C. A., Faraway, J. J., Phillips, C., & van Aalst, J., 2010. Effects of lip revision surgery in cleft lip/palate patients. *Journal of dental research.* **89**(7), 728–732.

Trotman, C.A., 2011. Faces in 4D—why do we care and why the 4th dimension? *Am J Orthod Dentofacial Orthop.* **140**,895–899.

Trotman, CA., Faraway, JJ., Soltmann, R., Hartman, T. & VanAalst, J., 2013. Facial soft tissue dynamics before and after primary lip repair. *Cleft Palate-Craniofac. J.* **50**(3),315-322.

Trotman, C.A., Faraway, J.J, Hadlock, T., Banks, C., Jowett, N. and Regan, D., 2018. Quantifying Soft Tissue Shape and Symmetry: Patients with Cleft Lip/Palate and Facial Paralysis. *Plast Reconstr Surg Glob Open.* **6**, 3.

Tyl, J., Dytrych, Z., Helclová, H., Scüller, V., Matějček, Z. & Beránková, A., 1990. Psychic and social stress of children with cleft lip and palate. C*eskoslovenska Pediatrie* .**45,** 532–536.

Tzou, C-HJ., Artner, NM., Pona, I., Hold, A., Placheta, E. & Kropatsch, WG. 2014. Comparison of three-dimensional surface-imaging systems. *J Plast Reconstr Aesthet Surg,* **67**(4), 489–97.

Ueda, N., Imai, Y., Yamakawa, N., Yagyu, T., Tamaki, S., Nakashima, S., Nakagawa, M. & Kirita, T., 2020. Assessment of facial symmetry by three dimensional stereophotogrammetry

after mandibular reconstruction: A comparison with subjective assessment. *Journal of Oral and Maxillofacial Surgery.* **4.**

Vanderas, A.P., 1987. Incidence of cleft lip, cleft palate and cleft lip and palate among races: a review. *Cleft Palate J.* **24,** 216-225.

Van Loon, B., Maal, TJ., Plooij, JM., Ingels, KJ., Borstlap, WA., Kuijpers-Jagtman, AM., Spauwen, PH. & Bergé, SJ., 2010. 3D Stereophotogrammetric assessment of pre- and postoperative volumetric changes in the cleft lip and palate nose. *Int J Oral Maxillofac Surg*. **39**,6, 534-40.

Venkatesh, R., 2009. Syndromes and anomalies associated with cleft. *Indian J Plast Surg*. **42**,S51-S55.

Verhoeven, T., Nolte, J., Maal, T., Bergé, S. & Becking, A., 2013. Unilateral Condylar Hyperplasia: A 3-Dimensional Quantification of Asymmetry. *PLoS One*. **8**(3).

Verzé, L., Nasi, A., Quaranta, F., Vasino, V., Prini, V., Ramieri, G., 2011. Quantification of facial movements by surface laser scanning. *J Craniofac Surg.* **22**(1),60–5.

Volker. 2018. Buccinator muscle. Available at : https://www.earthslab.com/anatomy/buccinator-muscle/ [Accessed on 12/9/2019]

Williams, A.C., Shaw, W.C. & Devlin, H.B.,1994. Provision of services for cleft lip and palate in England and Wales. *British Medical Journal.* **309**, 1552.

WHO Global registry and database on craniofacial anomalies. Human genetics programme. 2003. ISBN 92 4 1591102.

Wolford, L.M. & Stevao, E.L., 2002. Correction of jaw deformities in patients with cleft lip and palate. *Proc (Bayl Univ Med Cent).* **15(3),**250-254.

Wong, JY., Oh, AK, Ohta, E., Hunt, AT., Rogers, GF., Mulliken, JB. & Deutsch, CK., 2008. Validity and reliability of craniofacial anthropometric measurement of 3D digital photogrammetric images. *Cleft Palate Craniofac J.* **45**(3),232-9.

Wong, KWF., Keeling, A., Achal, K. & Khambay, B., 2019. Using three-dimensional average facial meshes to determine nasolabial soft tissue deformity in adult UCLP patients. *The Surgeon.* **17** (1). 19-27.

Wu, J. & Yin, N., 2016. Detailed Anatomy of the Nasolabial Muscle in Human Fetuses as Determined by Micro-CT Combined With Iodine Staining. *Ann Plast Surg.* **76**(1),111-6.

Wu, J., Liang, S., Shapiro, L. & Tse, R., 2016. Measuring symmetry in children with cleft lip. Part 2: quantification of nasolabial symmetry before and after cleft lip repair. *Cleft Palate-Craniofacial Journal*. **53**(6), 705–713.

Yamada, T., Mori, Y., Minami, K., Mishima, K., Sugahara, T., 2002. Three-dimensional facial morphology, following primary cleft lip repair using the triangular flap with or without rotation advancement. *Journal of Cranio-Maxillofacial Surgery.* **30**- 6, 337-342.

Yılmaz, R.B., & Cakan, D.G., 2018. Nasolabial Morphology Following Nasoalveolar Molding in Infants with Unilateral Cleft Lip and Palate. *J Craniofac Surg.* **4,**1012-1016.

Zaidel, D. & Cohen, J.A., 2005. The face, beauty, and symmetry: Perceiving asymmetry in beautiful faces. *The International journal of neuroscience.* **115**. 1165-73.

Zreaqat, M., Hassan, R. & Halim, A. S., 2012. Facial dimensions of Malay children with repaired unilateral cleft lip and palate: a three dimensional analysis. *Int. J. Oral Maxillofac. Surg*. **41**, 783–788

8 Appendices

Appendix 1. Presentations

1. Presented in the Scottish Oral Health Research Collaboration conference, Dundee, 2019.

2. Attended the European Association of Cranio-maxillofacial Surgery conference, London, 2016.

3. Regular seminar presentations- post-graduate seminars and journal club meetings 2016-2019 (Glasgow, UK)

Appendix 2 Publications

Accepted for publication:

"An innovative assessment of the dynamics of facial movements in surgically managed unilateral cleft lip and palate using 4D imaging." For the Cleft Palate-Craniofacial journal, 2020.

Authors: Gattani, S., Bell, A., Gillgrass, T., Ju, X. & Ayoub, A.

Ayoub, A., Gattani, S., Bell, A., Gillgrass, T. & Ju, X. 2019., 3D and 4D analysis of unilateral cleft lip. B J Oral Maxillofac Surg. 57, 10, 96-97.

British Journal of Oral and Maxillofacial Surgery

RSS Feeds

Login | Register | Claim Subscription | Subscribe

Articles & Issues | For Authors | Journal Info | Subscribe | BAOMS | JOMS | More Periodicals

All Content | Search | Advanced Search

Access provided by University of Glasgow

< Previous Article | December 2019 Volume 57, Issue 10, Pages e96–e97 | Next Article >

Access this article on ScienceDirect

3D and 4D analysis of unilateral cleft lip

Ashraf Ayoub, Shyam Gattani, Alieen Bell, Toby Gillgrass, Xiangyang Ju

Glasgow University Dental Hospital and School

DOI: https://doi.org/10.1016/j.bjoms.2019.10.280

Abstract | Full Text

Objective Assess facial asymmetry during maximal smile in patients with surgically managed Unilateral Cleft Lip (UCL), using a real time 3D imaging (4D) system.

Design Prospective two cohort comparative study

Methods 25 surgically managed UCL cases and 75 controls at 8-10 years of age were recruited. Facial movements during maximum smile were recorded using stereo-photogrammetry at a rate of 60 3D facial images per second. Maximum smile took approximately 3 seconds and generated 180 3D facial images for the analysis. A generic facial mesh which consists of about 7000 quasi landmarks, was used for the assessment of facial asymmetry. This was wrapped (conformed) on the 3D image, the conformed mesh was mirror imaged, the original and mirror images were superimposed and the distances between the two surfaces of five selected 3D frames quantified facial asymmetry

Results Statistically significant differences were seen regarding the magnitude of facial asymmetry between the UCL group and the non-cleft controls. Higher average asymmetry in the UCL group was seen in the 3D frame mid-way between maximal smile and rest (frame 4) followed by the frame at peak expression of maximal smile (frame 3).

Conclusion This study provided for the first time, a sensitive tool for analysis of the dynamics of muscle movements which provided an unprecedented insight into the anatomical basis of the residual dysmorphology. This demonstrates the limitations of the primary lip repair in achieving symmetrical function which could be attributed to the inadequate anatomical approximation of the naso-labial muscles and the residual scarring.

Article Tools

PDF (52 KB)

Email Article

Add to My Reading List

Export Citation

Create Citation Alert

Cited by in Scopus (0)

Request Permissions

Order Reprints (100 minimum order)

Related Articles

Preoperative nasoalveolar moulding in a patient with a unilateral cleft lip and palate using a modified nostril retainer: a technical note
British Journal of Oral and Maxillofacial Surgery, Vol. 57, Issue 4

Evaluation of lip force in patients with unilateral and bilateral cleft lip
British Journal of Oral and Maxillofacial Surgery, Vol. 55, Issue 4

Three-dimensional quantitative evaluation of facial morphology in adults with unilateral cleft lip and palate, and patients